THESIS

CHANNEL CHARACTERISTICS AND LARGE ORGANIC DEBRIS IN ADJACENT BURNED AND UNBURNED WATERSHEDS A DECADE AFTER WILDFIRE, PARK COUNTY, WYOMING

Submitted by

Ronald B. Zelt

Department of Earth Resources

In partial fulfillment of the requirements

for the Degree of Master of Science

Colorado State University

Fort Collins, Colorado

Spring 2002

COLORADO STATE UNIVERSITY

September 27, 2001

WE HEREBY RECOMMEND THAT THE THESIS PREPARED UNDER OUR SUPERVISION BY RONALD ZELT ENTITLED "CHANNEL CHARACTERISTICS AND LARGE ORGANIC DEBRIS IN ADJACENT BURNED AND UNBURNED WATERSHEDS A DECADE AFTER WILDFIRE, PARK COUNTY, WYOMING" BE ACCEPTED AS FULFILLING IN PART REQUIREMENTS FOR THE DEGREE OF MASTER OF SCIENCE.

Committee on Graduate Work

Adviser

Department Head

ABSTRACT OF THESIS

CHANNEL CHARACTERISTICS AND LARGE ORGANIC DEBRIS IN ADJACENT BURNED AND UNBURNED WATERSHEDS A DECADE AFTER WILDFIRE, PARK COUNTY, WYOMING

Relatively few studies of fire effects on streams have examined the period beyond the first few years following wildfire, particularly in the Middle Rocky Mountains. In 1988 the Clover-Mist Fire burned most of the 66.8-km^2 Jones Creek watershed, but less than 8 percent of the adjacent 49.5-km^2 watershed of Crow Creek. These two watersheds had very similar geologic and pre-fire hydrologic and vegetative characteristics, and few other human activities.

This study compared channel conditions between Jones Creek and Crow Creek. The objectives were to: (1) compare channel characteristics and channel stability; (2) compare large organic debris (LOD) characteristics and loading; and (3) identify processes that might explain the observed significant differences between the study streams. Ten reaches of each stream were studied, primarily during summer 1999.

On average, the bankfull channel was 1.2 m wider in the burned stream than the reference stream after accounting for differences in drainage area and number of debris jams. Drainage area was the most important factor for explaining mean riffle width. The direction and magnitude of channel-width differences are consistent with the increased duration of near-bankfull discharge in the burned stream and the likely bank erosion after

burning. After accounting for reach gradient, graphic mean size of riffle armor was 0.8ϕ units coarser on average in Jones Creek than in Crow Creek.

LOD frequency in forced-pool-riffle channels is less in Jones Creek than in Crow Creek. Small accumulations of LOD were more frequent along Crow Creek than Jones Creek. The frequency of debris jams was greater in Jones Creek after accounting for differences in either mean piece length or the frequency of pieces longer than channel width. Differences between streams in LOD frequency are consistent with continued greater mobility of debris in Jones Creek, leading to its rapid delivery to downstream reaches and export out of the watershed.

Pieces of LOD were smaller and less well anchored in the burned stream than in the reference stream. The combination of larger average piece size and narrower channels yielded a greater ratio of average piece length to channel width in the reference stream. LOD-associated fine-sediment deposits were thicker but less frequent along the burned stream than the reference stream.

Ronald B. Zelt
Department of Earth Resources
Colorado State University
Fort Collins, CO 80523
Spring 2002

ACKNOWLEDGMENTS

This study would not have been completed without the substantial contributions of many individuals. Major advisor, Ellen Wohl, provided excellent guidance at crucial points throughout the study, particularly when an initial study design proved to be intractable. The other members of my graduate committee, Lee MacDonald, Deborah Anthony, and Cathy Tate, gave encouragement and valuable technical comments that reflect the quality and breadth of their expertise.

Of equal importance to a successful field work component was the assistance provided by a cadre of field assistants. The following people, in alphabetical order, provided field assistance: Darin Brost, Merry Gamper, Ben Kamprath, Andy Massey, Jon Mason, Joe Pohl, Reuben Schaepe, Nathan Storey, Ellen Wohl, Bethany Zelt, and Marany Zelt. To each of you, I am grateful for patiently enduring foul weather, difficult living conditions, my impatience or insensitivity, and especially for helping to collect a large, quality data set for a rugged wilderness area. I also appreciate the consideration of Mr. and Mrs. Bob Coe and their able staff at Pahaska Tepee Resort. Additional thanks are due to the staff of Shoshone National Forest for permitting the wilderness research activities, and for maintaining the back-country trails.

I am grateful to Elizabeth Fasser, Colorado State University, Earth Resources Departmental Sediment Lab, who determined grain size distributions for bedload samples. The U.S. Geological Survey, Wyoming District, provided substantial assistance,

equipment loans, and encouragement. The Geological Society of America provided financial assistance through its student research grants program (grant no. 6172-97).

I also thank my wife, Cindy, parents, Ruth and the late Melvin Zelt, and parents-in-law, David and Jeanette Stewart, for their encouragement and confidence. Chief among those whose aid was indispensable is my heavenly Father, whose generous comfort and protection were discernible on numerous occasions.

TABLE OF CONTENTS

Chapter 1

INTRODUCTION

Fire influences the distribution and composition of vegetation communities in the Rocky Mountains, as well as geomorphic processes and resulting landforms. The geomorphic significance of fire in this region relates to the sensitivity of steep landscapes to fire-caused changes in vegetation and soils that can result in increased soil moisture levels and rates of streamflow and both surface and channel erosion following severe wildfire. For example, it is estimated that 30 percent of total sediment yield in the Pacific Northwest, as a long-term average, is induced by fire (Swanson, 1981). Also, fire-related deposits compose about 30 percent of the total thickness of 29 alluvial-fan sections examined along or near Soda Butte Creek in northeastern Yellowstone National Park (YNP) (Meyer et al. 1995).

Fire effects include onsite and offsite impacts. Reduced transpiration increases soil moisture levels and increased soil erosion from burned hillslopes can result in reduced soil productivity. In burned watersheds the altered hydrology, increased sediment inputs, or disturbance to riparian areas can affect channel erosion, sediment storage and transport and, in turn, aquatic life (cf. Berg et al., 1996). Debris torrents may dramatically alter stream channels and sediment loads (Meyer et al., 1995; Cannon et al., 1998b). Many fire-caused changes in watersheds have immediate and short-term (1-4 years) effects. Delayed or long-term effects result from processes such as root decay of

fire-killed trees, loading of stream channels with large organic debris (LOD), or recovery of channels scoured or widened by debris torrents. Current understanding of fire effects on stream-channel stability and LOD is limited by the large variability in effects caused by the multitude of affected processes and controls. Because of this variability and dependence on local site characteristics, the magnitude, extent, and duration of fire effects cannot be predicted accurately.

The 1988 wildfire season climaxed during the first 10 days of September (*Billings Gazette*, 1995, p. 67). The Clover-Mist Fire burned beyond the eastern boundary of YNP at Jones Pass on Sept. 6 and subsequently consumed most of the vegetation in the Jones Creek watershed and other headwater drainages of the North Fork Shoshone River in Shoshone National Forest (Greater Yellowstone Coordinating Committee, 1988). The headwater drainages of the North Fork Shoshone River, including Jones Creek, were the most severely burned in the Greater Yellowstone Area (GYA) fires of 1988 (Greater Yellowstone Coordinating Committee, 1989). However, less than 8 percent of the adjacent Crow Creek watershed was burned. The wilderness watersheds of Crow and Jones Creeks provide a rare opportunity to study fluvial processes following a severe wildfire disturbance in comparison with an undisturbed adjacent watershed with similar geologic and hydrologic characteristics. These two wilderness watersheds do not have the confounding influences of human activities such as timber harvest, roads, or mining.

Previous investigators (e.g., Bozek and Young, 1994; Young, 1994; King, 1995; Meyer et al., 1995; Ewing, 1996; McIntyre and Minshall, 1996; Troendle and Bevenger, 1996; Meyer and Wells, 1997) have quantitatively or qualitatively documented disturbances to the flow regime, suspended-sediment discharges, stability of woody debris, and channel morphology of severely burned watersheds after the Greater

Yellowstone fires of 1988. However, few of the previously reported GYA studies focused on channel processes or conditions beyond the first few post-fire years. In severely impacted watersheds with slow forest regrowth and heavy precipitation, recovery from fire disturbance may require 50 years or more (Albin, 1979; Minshall and Brock, 1991). For example, in the GYA, the input of fire-killed snags into streams may not produce general replacement of functioning debris dams until at least 10 years after wildfire (Minshall et al., 1989). Thereafter, a period of years may be required for the channels to adjust to the input of new debris (Keller et al., 1995).

Among the challenges and uncertainties faced by resource managers following the 1988 fires were (1) a lack of published information on the effects of fires on aquatic environments of the Middle and Northern Rocky Mountains, and (2) the delayed impacts and long-term recovery period that were expected (Minshall and Brock, 1991).

Long-term paired-watershed studies of channel response following a large-magnitude disturbance such as wildfire are scarce (cf. Madej and Ozaki, 1996). Although research conducted at this time cannot help GYA resource managers retroactively solve the impact-mitigation and stream-rehabilitation problems they faced in 1988, an improved understanding of the magnitude and duration of longer-term fire effects will provide the opportunity for science-based planning and management for future fires.

For example, in August 2000 a wildfire burned 497 ha in Crow Creek at an intensity and severity similar to the Clover-Mist fire in Jones Creek. The Shoshone National Forest plans to implement an aggressive program of prescribed fires, including stand-replacement fires. Other than the data collected for Jones Creek, the Shoshone National Forest has little information about what percentage of a watershed could be burned at one time under a prescribed-fire regime without producing adverse effects on

beneficial uses (G.S. Bevenger, U.S. Forest Service, written comm., 2000). Research on the effects of fires on channel characteristics and LOD also promotes increased understanding of the role of wildfire in landscape evolution in the Rocky Mountain region.

1.1 Study Objectives

This thesis is a case study comparing post-fire channel conditions of Jones Creek to the adjacent, undisturbed Crow Creek. The study occurred 11 years after the severe burning of Jones Creek watershed. The study focuses on indicators of channel instability and differences in LOD characteristics and loading that may be attributed to severe wildfire disturbance. However, observed differences between the streams cannot establish fire as the causal agent because no pre-fire data exist (see Troendle and Bevenger, 1996). Specific objectives of this study were to:

(1) Measure and compare channel characteristics of Crow and Jones Creeks, with particular focus on fine-sediment deposits in pools;

(2) Evaluate and compare channel stability in Crow and Jones Creeks;

(3) Measure and compare LOD loading and the characteristics of the LOD present in the two streams;

(4) Measure and compare accumulations of LOD and fine-sediment deposits associated with LOD in the two creeks; and

(5) Identify the fire-related or other hydro-geomorphic processes that could explain any significant differences between the two streams.

1.2 Report Organization

Chapter 2 presents a review of the literature concerning fire effects on streamflow, erosion, channel morphology, and LOD in streams. This chapter also describes and compares the watersheds of Crow and Jones Creeks.

Chapter 3 describes the selection of study segments and reaches, and the methods used to measure channel conditions and LOD characteristics. Data analysis procedures also are described in Chapter 3. Chapter 4 presents and discusses the results pertaining to channel characteristics, including channel geometry, substrate, and stability assessment. Chapter 5 reports the results and discussion of LOD characteristics and loadings in the two streams. The conclusions from this study, and recommendations for further study, are presented in Chapter 6.

Chapter 2

BACKGROUND

2.1 Literature Review

Severe fires can affect streamflow, sediment yields, channel morphology, LOD loading, channel stability, stream habitat quality, and aquatic biota through a complex set of interrelated processes (Robichaud and Waldrop, 1994). These affected characteristics and processes are reviewed in the following sections.

2.1.1 Forest Hydrology

Severe fires affect the timing and quantity of runoff through alteration of physical properties and hydrologic processes (cf., Wright, 1976; O'Loughlin et al., 1982; Shakesby et al., 1993; Robichaud et al., 2000). Fire severity refers to the condition of the forest floor after burning (Wells et al., 1979) and reflects the total amount of energy produced in the burning process (DeBano et al., 1998). In contrast, fire intensity describes the rate at which a fire produces thermal energy (DeBano et al., 1998), indicated by such parameters as flame height or rate of spread of the fire front (de Ronde, 1990). By removing or greatly reducing the vegetation, fires of moderate or greater severity reduce interception, transpiration, water adsorbancy of the litter layer, and surface roughness and increase soil exposure to rainsplash and surface sealing (Wright, 1976; Shakesby et al., 1993). By reducing transpiration losses, soil moisture content, and thereby streamflow, are enhanced, particularly at the end of the growing season and immediately afterward

(MacDonald et al., 1991; Cannon et al., 1998a). In some cases, extreme floods have been associated with storm events that followed closely after severe forest fires (e.g., Klock and Helvey, 1976; McCord, 1996; Moody 2001).

However, many instream or offsite effects of forest fires are detectable only when a large proportion of the drainage basin has been severely burned. In wildfires covering large areas, low-order watersheds (cf. Strahler, 1957) tend to burn extensively or not at all, whereas higher-order watersheds tend to burn partially (Minshall and Brock, 1991). For example, after the GYA fires of 1988, there were no watersheds above fourth order where essentially the entire watershed was burned (Minshall and Brock, 1991, p. 126).

Post-fire changes in watersheds of subalpine forests generally result in increases in (1) total runoff, primarily from decreased transpiration and decreased snow interception, (2) base flow rates, (3) duration of high flows (e.g., near bankfull stage), and (4) peak runoff rates (particularly for high-frequency events or while hydrophobic soils prevail). The pathways by which water moves downslope are an important control on the hydrology of mountain streams (Wohl, 2000). Overland flow is generally not the dominant flow pathway in forested watersheds (Dunne, 1978) because precipitation intensity rarely exceeds the infiltration capacity of the soil and duff layer found in most forests (Hewlett, 1982; MacDonald, 1989). However, in many mountainous settings Hortonian overland flow is common in zones of sparse vegetation and thin soil (Wohl, 2000). Also, saturation overland flow originating from areas of saturated soil (Dunne and Leopold, 1978) is fairly common in areas of convergent flow (i.e., topographic hollows).

Saturation overland flow clearly is dependent on soil-moisture conditions. Because a post-fire soil is more nearly saturated, enhanced runoff results from expanded areas of saturated overland flow (O'Loughlin et al., 1982) or subsurface flow from lower

slopes near channels (cf. Jones and Grant, 1996) during storm events and during the rising limb of the spring snowmelt hydrograph (Troendle and Bevenger, 1996).

Timber harvest has similar effects on the water balance and this affects the amount and timing of runoff. For example, Troendle and Olsen (1994) reported that the duration of flows in the range from 80 to 120 percent of bankfull discharge were most affected by timber harvest. Jones and Grant (1996) found that clear-cutting produced a pronounced increase in peak discharge following periods of evaporation and hillslope drainage, but a smaller response to larger events that are less sensitive to antecedent conditions.

In the GYA, it was expected that the 1988 fires would affect peak flows in the Absaroka Range (Greater Yellowstone Coordinating Committee, 1989), but not in other areas because of differences in basin morphology. Basins in the Absaroka Range have steep slopes and shallow soils, so streamflow response to intense thunderstorms is rapid, and burned areas could produce increased peak flows compared to pre-fire conditions (Greater Yellowstone Coordinating Committee, 1989, p. 45). In the Madison, Snake, and upper Yellowstone River drainages slopes are generally less steep, stream gradients milder, and valley floors wider than those of Absaroka Range streams, reducing the likelihood of fire effects on flooding (Greater Yellowstone Coordinating Committee, 1989).

Forest fires result in reduced snowpack shading that is most pronounced on south- and west-facing slopes. Snowpack albedo may also be reduced by dust from blackened timber (Minshall and Brock, 1991). Generally, these factors lead to earlier snowmelt and larger spring peak streamflows. However, air temperature and wind are more dominant controls for the timing of snowpack melting and the effect of forest fire may not be

detectable every year (Greater Yellowstone Coordinating Committee, 1989). Earlier snowmelt in burned subwatersheds may affect the synchronization of snowmelt peaks for larger, partially burned watersheds.

Additional impacts on runoff may result from changes in infiltration. When vegetation and litter are destroyed, infiltration rates can decrease due to losses of soil structure and porosity, soil compaction by raindrop impacts, sealing of the soil surface by ash or rainsplash-displaced particles, or hydrophobic soils (Debano et al., 1998). Moderate fire events do not generally cause changes in the infiltration capacity that persist beyond the first post-fire rain event (O'Loughlin et al., 1982). Some intense wildfires evidently produce little effect on infiltration capacity (e.g., Parks and Cundy, 1989). However, severe fires may induce a shallow, hydrophobic layer in the soil that can reduce infiltration and cause substantial surface runoff. As the organic surface layer of the soil is burned off, waxy organic substances vaporize and can be moved downward by the temperature gradient across the upper few centimeters of soil; they subsequently condense on the mineral soil particles, significantly reducing infiltration (DeBano, 1981). The amount of vegetation and litter consumed and the degree of soil heating determine the extent of soil-property alterations (Robichaud and Waldrop, 1994). The spatially discontinuous character of hydrophobicity, along with the presence of preferential flow paths into the deeper soil horizons, may result in a much smaller effect on infiltration than is often predicted (Booker et al., 1993). The persistence of fire-induced hydrophobicity may depend partly on the intensity of the fire (Dyrness, 1976), but plant roots, animal burrows, and chemical degradation all may contribute to breaking down the hydrophobic layer. Other investigators (Shakesby et al., 1993) found no clear relationship between time since burning and hydrophobicity.

Researchers have reported a large range in the persistence of post-fire effects on streamflow, from less than 2 years of detectable increase in base flow (O'Loughlin et al., 1982) to 16 years of elevated seasonal runoff (Anderson et al., 1976). Increases in peak discharges were substantial for the first 5 years after clear-cutting, but remained significant for 22 years for fall and winter events in the Cascades (Jones and Grant, 1996). Persistence of increases in peak flows is most important for channel stability and sediment transport.

2.1.2 Sediment Transport

2.1.2.1 The Sediment-Water Flow Continuum

Geomorphologists typically define several categories for different types of sediment transport, but in the natural environment there is a continuum of flow conditions and sediment concentrations (Costa, 1988). Pierson and Costa (1987) described four types of flow that are distinguished by ranges of sedimentologic and rheologic properties: (1) granular flow; (2) debris flow; (3) hyperconcentrated flow; and (4) normal water flow.

Granular flows occurs at very high sediment concentrations where the moving mass is not liquified, and particle interactions dominate flow behavior (Pierson and Costa, 1987). At the upper end of the range, these flows contain no water, requiring steep slopes or high inertia to maintain motion (Cannon et al., 1995). Dry ravel and debris avalanches are examples of granular flows that have been linked to fires. Channels may become loaded with sediment by dry ravel from steep, burned slopes where loose, noncohesive material was formerly stabilized by vegetation. Debris avalanches may occur partly because soil stability can decrease as roots of fire-killed trees decay. Water that has infiltrated into the hillslope soil or colluvium also facilitates such mass

movements both by lowering the resistance of the slope to motion and by increasing the downslope component of the weight of the mass potentially subject to failure. Depth of the soil piezometric surface is one of the principal influences on stability of steep mountain slopes with shallow, noncohesive soils (Gray and Megahan, 1981).

Debris flows are slurries in which the water-sediment mixture behaves in some respects as a homogeneous, viscoplastic material (i.e., the debris flows as a single phase when the yield strength is exceeded), but in other respects behave as a granular flow (Iverson and Denlinger, 1987). Debris flows are composed of poorly sorted sediments with 10-30% water content by weight (Costa, 1988). Debris flows occur most commonly in small, steep drainages but can flow on slopes of only a few degrees. Geomorphic evidence of a debris flow usually includes marginal levees of coarse, poorly sorted clasts; steep-fronted terminal lobe(s) on fans or in channels; and a cross-sectionally trapezoidal channel with a relatively small width-to-depth ratio in comparison to a water-formed channel (less than 10:1) (Costa, 1988).

Because of their immense power (Iverson, 1997) and the magnitude and longevity of the geomorphic work they accomplish, debris flows have been identified as the major channel-forming events in small, steep tributary catchments of Colorado (Costa and Jarrett, 1981), the Oregon Coast Range (Benda and Dunne, 1987), and mountains of southeastern Arizona, commonly scouring to bedrock and creating channels that are trapezoidal in cross-section (Wohl and Pearthree, 1991). In larger channels, the effects of moderate, high-frequency water floods become more important than debris flows, which generally perform little geomorphic work but do introduce coarse sediment that moderate floods may be unable to transport (Wohl and Pearthree, 1991).

If basin lithology is held constant, the chief controls on debris flows are climate, forest fires, and vegetation (cf. Wohl and Pearthree, 1991). Heavy rainfall on burned watersheds can produce effects ranging from slightly increased flooding to disastrous debris-flow activity (Cannon and Reneau, 2000). Among vegetation destruction (e.g., by fire), intense rainfall, and accumulation of sediment in headwater channels, the primary limiting control on debris-flow frequency in steep landscapes commonly is whichever process occurs least frequently. Where moderate amounts of material are introduced to channels by rilling (e.g., in mountains of southeastern Arizona) rather than by slope failure, accumulation of sediment in channels tends to be the limiting control (Wohl and Pearthree, 1991). However, debris flows in the GYA during 1989-91 appear to have been initiated by progressive sediment bulking of runoff, involving erosion by both surface runoff and channelized flow (Meyer and Wells, 1997). Debris-flow evidence typically appeared in the middle reaches of affected channels, indicating that channel erosion was required to produce debris-flow concentrations. The primary limiting control on the occurrence of debris flows in the GYA appears to be the vegetation destruction by fire, which exposed loose, silty soil on steep slopes and provided abundant fine sediment for entrainment by surface runoff (Meyer and Wells, 1997).

Hyperconcentrated flows are non-Newtonian flows with a smaller sediment concentration than a debris flow, but the sediments materially affect fluid properties and bed material transport (Julien, 1995, p. 187). The volumetric sediment concentration must exceed about 5 percent to affect the fluid properties. Only sand-dominated deposits have been described from documented hyperconcentrated flow (Pierson and Scott, 1985).

Sediment concentrations in normal streamflow are usually much less than 40% by weight, and the sediment has negligible effect on flow behavior, imparting no appreciable

shear strength to the flow (Costa, 1988). Turbulence is the primary mechanism for sediment support in such flows, although in slow-moving water electrostatic charges on tiny particles also are important (Costa, 1988). Water and sediment are distinct phases and the transport of sediment includes both a wash load and a bed-material load. Wash load moves almost entirely in suspension and is not correlated with discharge (Einstein et al., 1940, p. 632). In general, silt and clay compose the wash load, whereas sand and coarser particles are in frequent contact with the streambed, and transported by rolling or saltating (Julien, 1995). Schumm (1963) concluded that the proportions of wash load and bed-material load in a stream may be the critical factor upon which many stream characteristics depend.

The distinction between wash load and bed-material load has been succeeded in practice by the functional distinction between suspended load and bed load. Suspended load is operationally defined as the part of total sediment load that is subject to measurement using a suspended-sediment sampler. Therefore the suspended load does not include the sediment transported in the "unsampled zone" beneath and inaccessible to the suspended-sediment sampler (Edwards and Glysson, 1999). Bedload samplers provide information on the sediment transport in the layer extending 0.3 ft above the bed (Julien, 1995). The most commonly used bedload samplers collect both bed-material and suspended sediment being transported through the near-bed zone, and so are not true bedload samplers (Edwards and Glysson, 1999).

The stream energy available to transport sediment has been described in terms of stream power. Stream power per unit width of channel, ω, is defined as the product γqS, where γ is the specific weight of water, q is the unit discharge, and S is the stream gradient (Bagnold, 1977). The critical stream power is that required to transport the

sediment load supplied to a channel (Bull, 1979). Critical power increases proportionally to sediment load, particle size, and hydraulic roughness. Because critical stream power must be exceeded for sediment transport to occur, Bull (1979) defined the threshold of critical stream power as

(stream power) / (critical power) = 1.0 (1.1).

This geomorphic threshold (Grant, 1987) is a function of both sediment and flow characteristics. By assuming that channel cross-sectional geometry remains constant until scour of bed material begins, Grant (1987) demonstrated how empirical relations between discharge and the diameter of the largest particle moved (cf. Costa, 1983) can be combined with a particular streambed particle-size distribution to develop an estimate of the critical stream-power threshold. Bunte (2001) used empirical relations between fractional transport rating curves and a preset marginal transport rate (e.g., 0.0001 g m^{-1} s^{-1}) as a second line of evidence for estimating the threshold of motion.

2.1.2.2 Variability of Sediment Transport

The understanding of sediment transport is complicated by hysteresis, sediment availability, streambed morphology, bedform migration, interactions between individual clasts and the streambed, and other factors that are not well understood. Large spatial variability of sediment transport has been found in adjacent undisturbed watersheds in Colorado (Troendle and Olsen, 1994), and among adjacent, undisturbed basins from different areas of the U.S. (Bunte and MacDonald, 1996). Large variability is common across sampled cross-sections of individual streams (Horowitz et al., 1989), and in the downstream direction along individual streams (Lane et al., 1994; Olive et al., 1994). Experimental data have revealed a temporal pattern of sediment variability even under

controlled conditions (no change in precipitation intensity or duration) that reflects periodic storage and flushing of sediment from a drainage basin (Schumm and Rea, 1995). Short-term temporal variability of sediment transport in natural streams is great (Bunte, 1996; Horowitz et al., 1989) and is larger for bed load than for suspended load. Over moderate time periods, storm events are so variable that a single flood flow can account for 75 percent of a small basin's total yield in a 10-year period (Hewlett, 1982).

In natural stream systems, the inherent temporal variability is compounded by streamflow variation. Most of the annual sediment transport occurs during short periods of high flow, thus field measurement programs must cover flood periods to provide accurate information on total sediment loads (Julien, 1995). In Middle Rocky Mountain watersheds, the critical hydrologic period usually occurs during spring snowmelt runoff, and often occurs approximately simultaneously on many streams. Thus, mountain streams have critical sediment-transport periods that present substantial obstacles to successful sediment data collection programs.

Differences in channel slope can produce variable sediment transport. For example, variations in sediment yield during experimental studies (Schumm, 1977) and field studies (Trimble, 1975) were related to storage and flushing of sediment as slope thresholds were exceeded. Moody (2001) found that spatial variation in bed slope was a principal control on the spatial variability of deposits of bedload eroded from severely burned watersheds.

2.1.3 Sediment Yield

The effects of fire on sediment yield depend upon the severity of the fire, intensity and magnitude of subsequent precipitation events, the steepness of the watershed, and the

extent to which the vegetation, forest litter, and organic debris control the movement and storage of sediment in a particular watershed (MacDonald et al., 1991). Fire effects on erosion at the plot scale (Martin and Moody, 2001; Wohlgemuth, 2001) and sediment yield at the watershed scale (Laird and Harvey, 1986; Robichaud et al., 2000) have been documented.

2.1.3.1 Hillslope Processes

Fires can cause loss of forest floor cover, soil organic matter, and soil structure, producing a net increase of soil erodibility (Tiedemann et al., 1979). Increased exposure and vulnerability to rainsplash and overland flow, and enhanced rill and gully formation can result in large increases in hillslope erosion, particularly if intense rainfall events occur before the restoration of vegetative cover. Rainfall intensity seems more important than rainfall volume for increasing overland flow and erosion (Shakesby et al., 1993). Robichaud and Waldrop (1994) found that sediment yields in the Southern Appalachian Mountains, adjusted to a uniform slope of 30 percent, were 40 times greater from severely burned plots than from low-severity burned plots, and that sediment yield from a high-intensity thunderstorm exceeded 2,000 kg ha^{-1} from a severely burned plot. They also found that differences in runoff and sediment yield corresponded to differences in post-fire forest floor conditions. Loss of protective cover also leaves the soil surface more exposed to drying agents, and particles are more readily detached after drying. Soil losses following fires in pine and eucalyptus forests were two orders of magnitude higher than for areas that had not burned for at least 3 years (Shakesby et al., 1993).

The Greater Yellowstone fires in 1988 increased sediment yields from several watersheds (Minshall and Brock, 1991; Ewing, 1996; Troendle and Bevenger, 1996). In

the GYA, sheet erosion, rill and gully formation, mud slides, and debris flows all were observed during the summer of 1989, and suspended sediment levels increased considerably through 1991 for streams draining burned areas (Meyer and Wells, 1997; Minshall and Brock, 1991). During the first 2 years following the GYA fires, at least 82 debris flows occurred (Varley, 1991).

The amount of residual vegetation, including both trees and shrubs, is an important control on increased landslide incidence following fire or timber harvest. Vegetation removal from slopes tends both to increase soil moisture levels and to decrease root cohesion. On steep slopes, decreased stability caused by elevated soil moisture following vegetation removal may lead to mass movements such as landslides, debris flows (e.g., Helvey, 1980), or slumping (e.g., Klock and Helvey, 1976). However, the impact of vegetation removal on soil moisture appears to be most critical during the first year; and after 3 years, low vegetative regrowth is typically almost as effective as the removed forest in transpiring soil moisture (Gray and Megahan, 1981).

Live roots can provide a large part of the total cohesion present in the soil on a steep slope, particularly for granitic soils, but post-mortem root decay causes progressive loss of cohesion (Gray and Megahan, 1981). Previous investigations (e.g., O'Loughlin, 1974; Ziemer and Swanston, 1977; Megahan et al., 1978) indicate that a temporal "window" of greater landslide frequency typically occurs from about 4 to 10 years after a severe forest fire. Prior to this time, the residual strength of decaying roots of burned trees, tends to restrain mass movements (Ziemer and Swanston, 1977; Booker et al., 1993). Subsequent to this period, the root strength of forest regrowth increases slope stability towards pre-fire conditions.

Burroughs and Thomas (1977) found that the post-mortem decline in both number of roots and tensile strength of individual roots for Rocky Mountain Douglas-fir was more gradual than for Pacific Coast Douglas-fir, such that a 1-cm diameter root in the Rocky Mountain variety loses only 30 percent of its fresh tensile strength after 12 years. However, they concluded that finer roots are most important for slope stability, and that the tensile strength of fine roots decreases most rapidly during the first 2 to 3 years after harvest. However, a 1991 aerial reconnaissance of many of the drainages of northeastern YNP revealed only a few isolated debris slides (Meyer and Wells, 1997). In the spruce-fir forests of the GYA, it appears likely that landslides are most frequent 6 to 12 years after severe wildfire because rates of root decay and forest regrowth are slower.

Episodic events, such as landslides and debris flows, that release large quantities of sediment in a single location are likely to cause significant local increases in stream sediment (cf. Potyondy and Hardy, 1994). Commonly, a large part of the eroded mass is stored in the watershed before reaching its higher-order streams. Deposits in slope concavities or debris fans may remain active sources of sediment for an extended period. The storage of sediment within depositional areas of burned watersheds can prolong a fire's effect on sediment yield and channel habitat condition.

2.1.3.2 Riparian and Channel Processes

Fire-caused loss of riparian vegetation can increase sediment loads in streams because the vegetation normally filters sediments from overland flows and stabilizes stream banks (Greater Yellowstone Coordinating Committee, 1989). Increased sediment yields would tend to cause fining of the surface layer of bed material, increased sedimentation in pools, and channel aggradation (Madsen, 1995). However, effects of

increased sediment inputs from hillslopes to channels may be partly offset by increases in streamflow that would tend to cause coarsening in the surface layer of bed material, larger pools or more frequent steps, and increased channel cross-sectional area (Madsen, 1995). Moreover, several studies (Rich, 1962; Helvey, 1980; Laird and Harvey, 1986; Roby, 1989; Troendle and Bevenger, 1996) have attributed a majority of post-fire sediment yield increases to channel sources. Troendle and Olsen (1994) similarly found that increased post-harvest sediment loads were primarily from within-channel sources and appeared to be the result of increased runoff. The increased duration of higher streamflow rates, in particular, seems related to greater sediment transport from disturbed watersheds (Troendle and Olsen, 1994).

Potyondy and Hardy (1994) found increases in the fraction of sediment less than 6 mm in diameter in the bed surface during the first two years following wildfires in granitic watersheds. In two larger streams they found that the increase was significant during only the first post-fire year. Large streams may have sufficient sediment transport capacity to transmit the increased load, whereas headwater tributaries may store a larger proportion. Fine sediment in tributary channels may persist as a long-term source of fines to the larger streams (Potyondy and Hardy, 1994). Streamflow characteristics can influence the lag time between fire-increased sediment production and change in sediment yield from a basin, particularly in semi-arid regions with ephemeral streamflow (e.g., Laird and Harvey, 1986).

2.1.3.3 Magnitude and Duration of Post-fire Sediment Yields

Sediment yields from two small burned catchments in the Sierra Nevada averaged about 360 kg ha^{-1} during the first two post-fire years (Roby, 1989). Following wildfire

and subsequent salvage logging in three watersheds on the east slope of the Cascades, sediment yield averaged 261 kg ha^{-1} in the first post-fire year (Helvey, 1980).

Increased supplies of sediment may be the result of many interrelated factors, such as changes in precipitation, mass movements, and tectonic activity. Human structures and activities such as dams, roads, and mining also may have large effects on within-channel sediment conditions (Kondolf, 1997; Todd and Elmore, 1997). However, in most GYA watersheds such anthropogenic factors are not present or do not appear to be related to the increased sediment yields. Fire-fighting efforts, including bulldozing of fire breaks, may have increased local erosion in a few locations.

Only 38 percent of the 1,728 km^2 Lamar River basin was burned in 1988, and only 18 percent was affected by canopy burn. Nevertheless, Ewing (1996) found a post-fire increase of 627 percent in runoff-adjusted sediment discharge for the Lamar River during the summer months of 1989-92 as compared with 1985-87. However, during the snowmelt season, when most of the annual transport occurs, the increase of 2 percent in runoff-adjusted sediment discharge was not significant.

Burned watersheds generally are most vulnerable to erosion during the first two years following fire (Minshall and Brock, 1991). However, the persistence of fire effects on individual erosional processes appears quite variable. Burned watersheds are most vulnerable to rainsplash, sheet and rill erosion during the first few years following fire until vegetative cover is reestablished. Lyon (1984) reported that by the sixth post-fire year in western Montana, herbaceous cover averaged 20 to 25 percent by area. In northern Portugal, soil erosion rates declined to near background levels by 3 to 4 years after fire (Shakesby et al., 1993). However, many of the Greater Yellowstone burns of 1988 had not fully revegetated within the first three post-fire years (Lathrop, 1994), and

the fire effects on sediment load in the Yellowstone River persisted at least into the fourth post-fire year (Ewing, 1996). In severely impacted watersheds with shallow soils and little forest regrowth, the recovery to pre-fire conditions may take several decades (Heede et al., 1988; Minshall and Brock, 1991). Tiedemann et al. (1979) summarized that watershed erosion rates remain elevated for 10 years following a fire.

2.1.4 Bed Material

Bed material has been sampled for a variety of purposes, including assessment of land-use impacts (e.g., Potyondy and Hardy, 1994), the storage component of sediment budgets (Lambert and Walling, 1988), determination of grain roughness, and calculation of entrainment (Wiberg and Smith, 1987b), and bedload transport rates (Lisle, 1995; Kondolf, 1997). In coarse-bed streams, traditional methods of estimating incipient motion, such as the Shields diagram (Shields, 1936), do not work well because the effects of grain packing and hiding are substantial (Grant, 1987). Gravel-bed mountain streams typically transport a wide range of particle sizes, in part because steep channels enhance the competence of large, infrequent flows to transport very large clasts (Bunte, 1996). Also, gravel beds generally are vertically stratified with respect to particle size (Carling and Reader, 1982; Petrie and Diplas, 2000) and imbrication (Folk and Ward, 1957). The coarse top layer, or pavement, is generally imbricated and its roughness is hydraulically important. The poorly sorted but finer subpavement exerts significant influence on the stream's ecological characteristics (Diplas and Fripp, 1992).

Geomorphologists have long recognized the need for field methods specifically suited to coarse-bedded channels. Techniques should allow exclusive sampling of the vertical layer of interest in a stratified bed, and should accommodate the entire range of

particle sizes present (Petrie and Diplas, 2000). Moreover, methods should account for small-scale spatial variability of the streambed character, i.e., fine and coarse patches, produced by local variations in hydraulic conditions (Lambert and Walling, 1988). Compounding sedimentological considerations is the logistical difficulty of collecting the large bulk sample of coarse bed material that would be needed to produce reliable results.

Wolman (1954) developed a pebble count procedure to measure the grain size distribution of the surface layer of a streambed. Variations of the conventional random-walk sampling approach include transect and grid-sampling designs (Wohl et al., 1996). However, some workers conclude that pebble-count samples are unreliable for particles smaller than 10 or 15 mm because of the inability of the field technician's fingers to distinguish small particles when touched (Petrie and Diplas, 2000). The lower limit of reliability for pebble-count sampling is substantially different when wearing gloves (Bunte and Abt, 2001).

For a poorly sorted bed, the critical boundary shear stress required to initiate bedload transport is roughly proportional to the median grain size of the bed surface and inversely related to the relative protrusion of a particle into the flow (Wiberg and Smith, 1987b). The median grain size of the bed surface is chiefly controlled by the size of detritus supplied to the stream and by the velocity of the local flow field (Folk, 1974). If the size distribution of the subsurface bed material also is known, the ratio between surface and subsurface median grain size can be used as an indicator of surface fining in response to increased sediment supply (Dietrich et al., 1989). However, in streams with high initial bedload transport rates, only a limited adjustment in grain size is possible in response to increased sediment supply; in such cases net deposition might be expected to result in pool infilling and channel migration (Dietrich et al., 1989).

The fraction of pool volume filled with fine sediment (Lisle and Hilton, 1992; Hilton and Lisle, 1993) has been used as an index of supply of mobile sediment in gravel-bed streams with a pool-riffle morphology. During waning flows, fine sediment is selectively transported from zones of relatively high boundary shear stress, such as riffles, and deposited in zones of low shear stress, such as pools. Increases in the volume of pool infill can be caused either by an enrichment of the sediment load with fine material, or by an increase in sediment transport with no change in its grain size distribution (Lisle and Hilton, 1992).

2.1.5 Channel Stability

A stream in equilibrium is adjusted to carry the water and sediment supplied from upstream (Reid, 1991). Schumm (1963) observed that an excess of total sediment load causes deposition in a channel, a sediment-poor flow erodes its channel, and between these extremes lie stable channels. Natural channel stability is achieved as a stream develops a stable dimension, pattern, and profile such that, over time, channel features are maintained and the stream system neither aggrades nor degrades (Rosgen, 1996). Local scour and deposition occur as a channel adjusts to hydrologic variability, but the overall form of an undisturbed channel changes little through time (Reid, 1991). Hogan (1987) used changes in the distribution and amounts of stored sediment as an indication of instability.

Early studies of the stability of equilibrium channel dimensions were made by Kennedy (1895) and Lacey (1930). Channel width typically changes in the downstream direction in proportion to the square root of discharge (Leopold and Maddock, 1953; Leopold et al., 1964). Also, the collection of equations describing the changes of depth,

width, velocity, resistance, and gradient are conventionally known as the downstream hydraulic geometry (or channel geometry) of a stream system. A stream may migrate laterally, but maintain its bankfull width and width/depth ratio, thus achieving stability, although such a stream is considered to be an "active" and "dynamic" system (Rosgen, 1996).

In addition to discharge, other variables have been used to explain channel geometry. These "complicating" variables include sediment-load characteristics, bed and bank substrate characteristics, and various climate, vegetation, or other basin characteristics (Osterkamp and Hedman, 1982). However, for higher-gradient streams (e.g., gradient > 0.008 m/m), channel geometry may be less affected by complicating variables than for other types of alluvial channels (Osterkamp and Hedman, 1977). Recently, studies have concluded that LOD exerts considerable influence on the morphology and hydraulics of streams in forested watersheds (Keller and Swanson, 1979; Marston, 1982; Hogan, 1987; Bilby and Ward, 1989; Keller et al., 1995; Montgomery et al., 1995). The influence of LOD is discussed in more detail later in this chapter.

Channel adjustments to changes in the water and sediment loads may be immediate or temporally lag the disturbance (Madej and Ozaki, 1996). Adjustments may lag spatially as well. For example, increased erosion in headwaters can affect downstream reaches as the increased sediment loads are transported through the system (Madej and Ozaki, 1996). The response time and mechanisms of channel adjustments after disturbance depend on the magnitude of the imposed change and stream power available to effect changes (Knighton, 1984).

Channel recovery following disturbance has been defined in several ways by previous workers. Examples include the following definitions of recovery:

- Return to a former channel-bed elevation (Kelsey, 1980). Madej and Ozaki (1996) reported a range of recovery times from 8 to 15 years in upper reaches of a northern California basin, and longer recovery periods for downstream reaches, as a "wave" of aggradation progressed through the watershed.
- Return to pre-disturbance channel width (Osterkamp and Costa, 1987) or overall configuration of channel morphology (Hogan, 1987).
- Return to a pre-disturbance pool-riffle morphology (Madej and Ozaki, 1996).
- Return to previous sediment transport rates (Newson, 1980). Within 2 years after a catastrophic flood that deposited a great volume of sediment in and adjacent to its channel, the Fall River formed a channel where the bed material just began to move at the bankfull discharge, which was interpreted as a state of equilibrium (Pitlick, 1993).
- For channels where LOD functions as an independent control on channel morphology, a return to the pre-disturbance mass budget, size distribution, and instream arrangement of LOD (Hogan, 1987).

When the mean recurrence interval of disturbance events is shorter than the time required for the watershed to recover from those events, instability occurs because the watershed cannot adjust to new conditions before another disturbance occurs (Marston and Anderson, 1991). It is apparent that defining the recovery of disturbed streams remains somewhat ambiguous, but essentially involves the re-establishment of a quasi-equilibrium channel (Pitlick, 1993). Channel adjustments may lead to a recovery of previous channel conditions or to a new state of equilibrium. For example, a study of logging-altered LOD budgets in Pacific Northwest streams indicated that some channels would not return to pre-disturbance configuration unless the supply of LOD was maintained or re-established (Hogan, 1987).

To document channel recovery it is important to monitor areas of expected change, and to determine where the effects will become masked by local variations in hydro-geomorphic process controls (Madej and Ozaki, 1996). The documentation of long-term channel response to disturbance can be obscured by annual variations in scour and deposition. At longer temporal scales, Schumm (1980) notes that, particularly in areas of relatively rapid erosion and high sediment production, erosion and deposition may be episodic in nature, with relatively unstable periods of active adjustment separated by periods of stability. Thus, monitoring activities should reflect the time scale of the response to discriminate between annual variability and long-term trends in channel adjustments (Madej and Ozaki, 1996).

2.1.6 Large Organic Debris

Complex biological and physical processes control wood dynamics in most stream systems. Large organic debris (LOD), a term referring to the number of fallen or deposited trees or limbs in a stream channel, influences channel morphology and stability (Lisle, 1986; Montgomery et al., 1995), the storage and movement of sediment (Marston, 1982; Thompson, 1995), and the structure and ecological function of stream ecosystems (Richmond and Fausch, 1995). LOD occurrence ranges from isolated individual pieces through whole trees and small accumulations to massive debris jams (Keller and Swanson, 1979). When debris obstructs flow it creates habitat diversity for aquatic organisms. Even when not within the wetted section, LOD can provide shading and cover for aquatic residents. In the absence of LOD, streams would more rapidly transport their sediment load, fine-grained beds would have fewer stable substrates and depositional sites, and the stream's invertebrate community would be altered (Keller and

Swanson, 1979). Where LOD is a significant component of channel roughness, its removal has the potential to destabilize channel morphology (MacDonald and Keller, 1987). However, regional differences in LOD dynamics complicate the generalization and spatial extrapolation of findings (Richmond and Fausch, 1995; Berg et al., 1998). Though much has been learned about the role of wood in stream ecosystems, improved understanding of processes is needed. Additional knowledge of the quantity, distribution, and arrangement of LOD is needed, particularly for relatively unmanaged streams as a basis for comparison with managed systems (Gurnell et al., 2000).

2.1.6.1 LOD Loading

The quantity and distribution of LOD in a stream are the result of a complex set of input and output processes. The relative importance of each process changes from headwater to downstream reaches. In low-gradient, meandering streams, the prevalent input processes include bank failure, blowdown, flotation from upstream, and collapse resulting from ice loading. Of these, bank erosion caused by lateral migration of the channel probably delivers most of the LOD into low-gradient streams (Keller and Swanson, 1979). In steep, forested drainages, additional LOD is delivered to channels by snow avalanches, debris torrents, other mass movements (Keller and Swanson, 1979), and large-scale blowdowns (e.g., see Massey, 2000). Regional differences in climate and frequency of mass movements produce marked variation in the influence of mass movements on LOD dynamics (Berg et al., 1998).

LOD may be transported *en masse* by debris torrents in steep channels and by flotation at high flow in larger streams. Except for episodic events such as mass movement, fire, and blowdowns, maximum stream discharge is the best predictor of new

LOD input from upstream reaches and by bank erosion (Berg et al., 1998). LOD is removed from channels through biological decomposition or consumption and by physical processes (breakdown by abrasion and transport by flotation). During overbank flow, floatable LOD may leave the channel and be deposited on the floodplain (Keller and Swanson, 1979). In one third-order stream draining a forested GYA wilderness watershed, 24 percent of inventoried LOD had moved during one year (Young, 1994). Studies of similar-sized streams in other areas found that about 30 to 35 percent of the LOD moved each year when maximum flows were above normal (e.g., Berg et al., 1998).

Stream size is a key factor affecting LOD distribution in forested basins (Richmond and Fausch, 1995). LOD concentrations are large in small, headwater streams and generally decrease downstream (Keller and Swanson, 1979). In small streams, the LOD tends to remain where it initially fell, because flows are too small to transport most of the LOD. Flows in intermediate-sized channels can frequently redistribute LOD to form distinct accumulations that affect the entire channel width (Keller and Swanson, 1979).

2.1.6.2 Effects on Sediment

LOD can form or stabilize gravel bars, accumulate fine sediment behind steps or obstructions, and form pools by directing or concentrating flow such that bank or bed scouring occurs. By creating numerous sediment storage sites, LOD buffers or moderates the routing of sediment through the stream system (Keller et al., 1995). Steep channels often lack the bars, riffles, and floodplains that are important storage sites in meandering streams. LOD thus may account for a much larger portion of the total sediment storage in steeper channels (Keller and Swanson, 1979). Measurements of LOD and sediment

deposits in second- to fifth-order streams showed that increasing stream size decreases the importance of LOD in detaining sediment, and that the size of sediment accumulations was significantly related to the volume of associated LOD (Bilby and Ward, 1989). Even in streams where LOD stored relatively little sediment in general, the volume of LOD pieces was related to sediment storage (Berg et al., 1998).

The presence of a debris jam may cause adjacent scour and formation of a bar downstream (Keller and Swanson, 1979). Removal of LOD jams from a northwestern California stream resulted in local increases in flow velocity, bed material size, and pool depth in bends (MacDonald and Keller, 1987). Grain roughness increases partly compensated for the loss of LOD-caused channel roughness, and deepened bend pools offset the loss of numerous scour pools within the jams.

In smaller streams, log steps develop when LOD extends across the entire active channel (Marston, 1982). Log steps typically produce a sediment storage site upstream and a plunge pool downstream. The volume of sediment stored behind log steps in third- through fifth-order streams in Oregon was estimated to be slightly greater than the mean annual total sediment discharge (Marston, 1982). In many forested mountain streams, mobilization or decay of a key piece of LOD can transform stored sediment into a pulse of sediment transport (Wohl, 2000).

2.1.6.3 Effects on Channel Stability

Individual pieces of LOD may increase or decrease channel stability. LOD in channels tends to increase bank stability by forming zones of concentrated turbulence where stream energy is dissipated (Keller and Swanson, 1979) or by protecting banks from erosion where LOD is buried in or positioned against the bank. More than 20

percent of the LOD that exceeded 30 cm in diameter and 3 m in length shielded channel banks in six California streams (Berg et al., 1998). Fallen trees that form log steps dissipate potential energy that otherwise might cause bank erosion (Keller et al., 1995). In the Oregon Coast Range, the maximum concentration of log steps occurred in third-order streams, but the greatest dissipation of potential energy by log steps occurred in fourth-order streams where the average step height was greater (Marston, 1982).

LOD projecting from banks increases channel roughness, thus decreasing flow velocity along the stream banks (Keller and Swanson, 1979). Lisle (1986) proposed a model for channel stabilization by large obstructions such as LOD. Obstructions produce intense patterns of secondary flow which can alter local sediment-transport patterns and fix the positioning of bars in relation to the obstruction.

LOD contributes to bank instability where it deflects flow against banks (Keller et al., 1995). Also, during high flow, floating LOD may batter banks and riparian vegetation, thereby causing bank erosion during the flood and reducing the bank protection afforded by the surviving vegetation for several subsequent years (Keller and Swanson, 1979).

2.1.6.4 Fire Effects on LOD

The effect of a fire on LOD functions related to channel stability and sediment storage is complex. If the fire consumes the pre-fire LOD, there may be an increase in bed-material transport rates and pool filling. Loss of protective LOD, combined with increased peak flows or increased duration of bankfull flows, may dramatically increase boundary shear stresses and channel scour.

Eventually, fire-killed trees will replenish the pre-fire LOD loading (Greater Yellowstone Coordinating Committee, 1989). DeBano et al. (1998) stated that LOD

accumulations are usually larger in the first few years following wildfire than for pre-fire conditions, but typically decline to below pre-fire levels thereafter. A long-term study of fire-killed lodgepole pine found that 85 percent of the burned boles fell at an annual attrition rate of about 13 percent during post-fire years 3 to 15 (Lyon, 1984). Smaller-diameter trees (< 8 cm) fell at a much higher rate (28 percent annual attrition) than large-diameter (> 20 cm) trees (8.6 percent), with the attrition of larger boles characterized by sporadic blowdown rather than more regular annual losses.

In the longer term a shortage of LOD usually follows the decomposition or export of the burned mature trees (Greater Yellowstone Coordinating Committee, 1989). Berg et al. (1998) reported that LOD volume and frequency were significantly less in reaches of a watershed burned 35-40 years previously than in undisturbed basins. However, tree density variation caused by climatic differences complicated their assessment of the effects of fire on LOD. Nevertheless, it is reasonable to assume that forest regeneration usually cannot replace the LOD important to channel processes until after some period of diminished LOD loading.

2.2 Study Area

This comparative case study assumes that the physical, geologic, and hydrologic similarity of the watersheds of Crow and Jones Creeks makes plausible the assumption of negligible pre-fire differences between the streams. Characteristics of these two watersheds are compared in this section of the report. Troendle and Bevenger (1996) presented additional comparisons of watershed characteristics.

Crow and Jones Creeks drain steep terrain in the northern part of Wyoming's Absaroka Range (fig. 2.1). The confluences of Crow and Jones Creeks with the North Fork Shoshone River are about 1 km and 6 km, respectively, upstream from Pahaska

Tepee, a resort near the East Entrance to Yellowstone National Park (YNP). Both watersheds are located in Shoshone National Forest wilderness, adjacent to the eastern boundary of YNP. Many watersheds of the North Fork Shoshone River basin are important trout fisheries, supporting resident populations of Yellowstone cutthroat trout and serving as the spawning areas for valuable fish species that reside downstream.

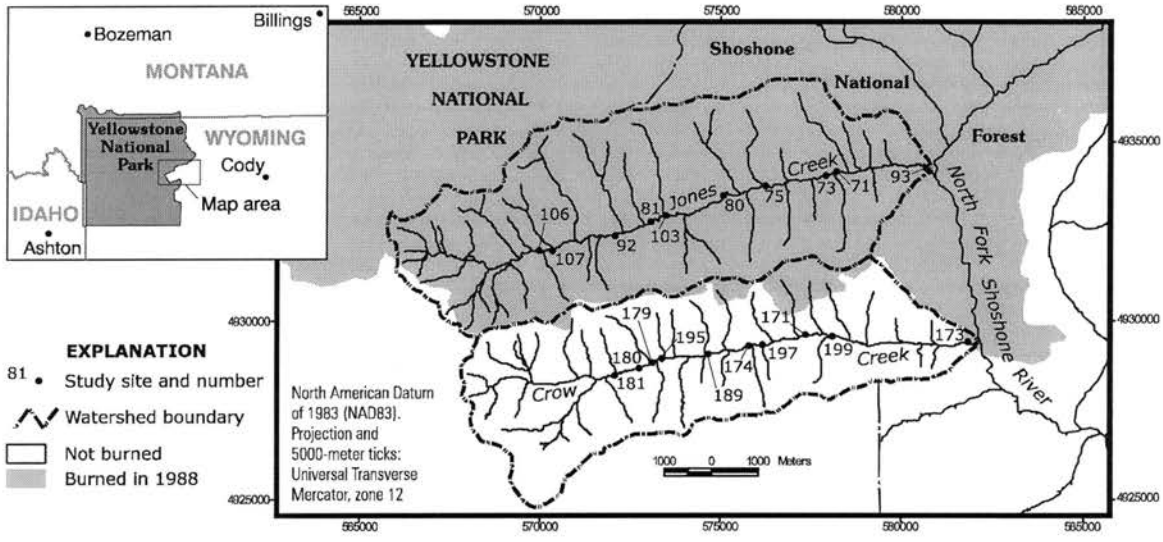

Figure 2.1. Location of study area in northwestern Wyoming.

Elevation ranges from 2030 to 3240 m (above MSL) in Crow Creek watershed (49.5-km^2), and from 2082 to 3280 m in Jones Creek's slightly larger (66.8-km^2) drainage (fig. 2.2). The axial streams are generally only 1.5 to 3.5 km (planimetric distance) from the crest of the ridges that bound the watersheds (fig. 2.3). Valley floors are rarely more than 300 m wide.

Terrain steepness is areally distributed very similarly in both watersheds, dominated by steep slopes averaging about 40 percent (fig. 2.4). Each watershed has more than 80 percent of its drainage area on slopes steeper than 20 percent grade. Terrain aspect is distributed bimodally in both watersheds (fig. 2.5), with south-southeast and north to north-northwest aspects being most common.

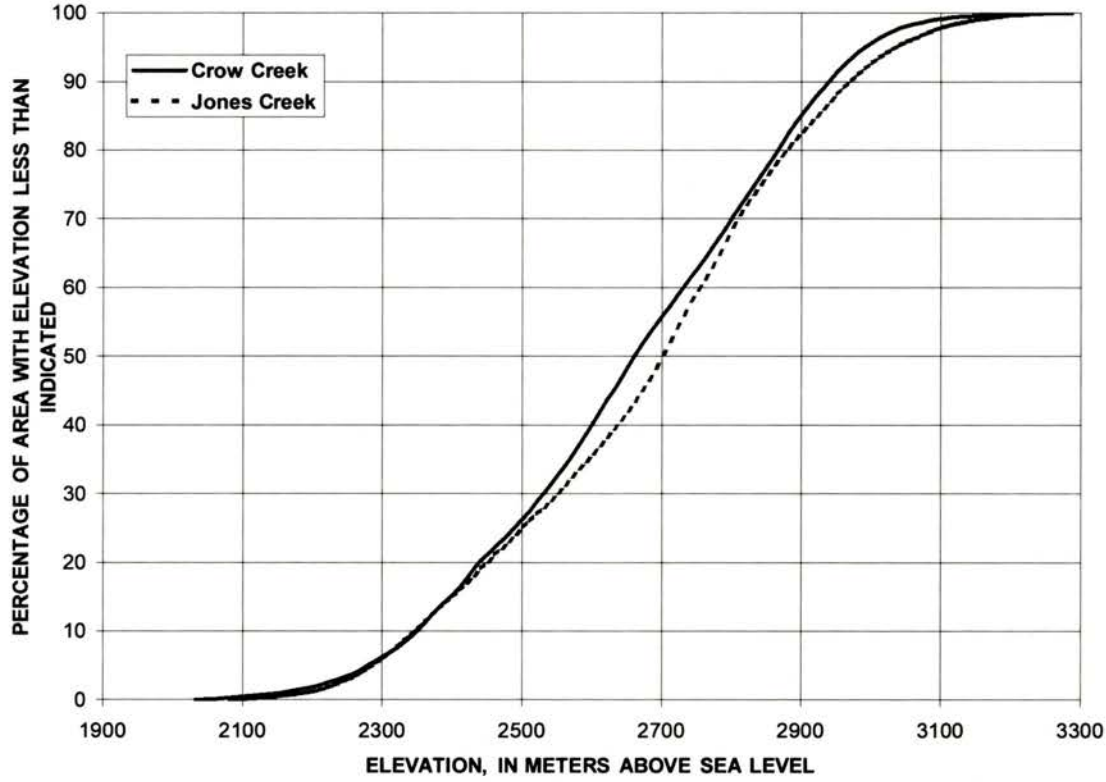

Figure 2.2. Hypsometric curves for drainage areas of Crow and Jones Creeks.

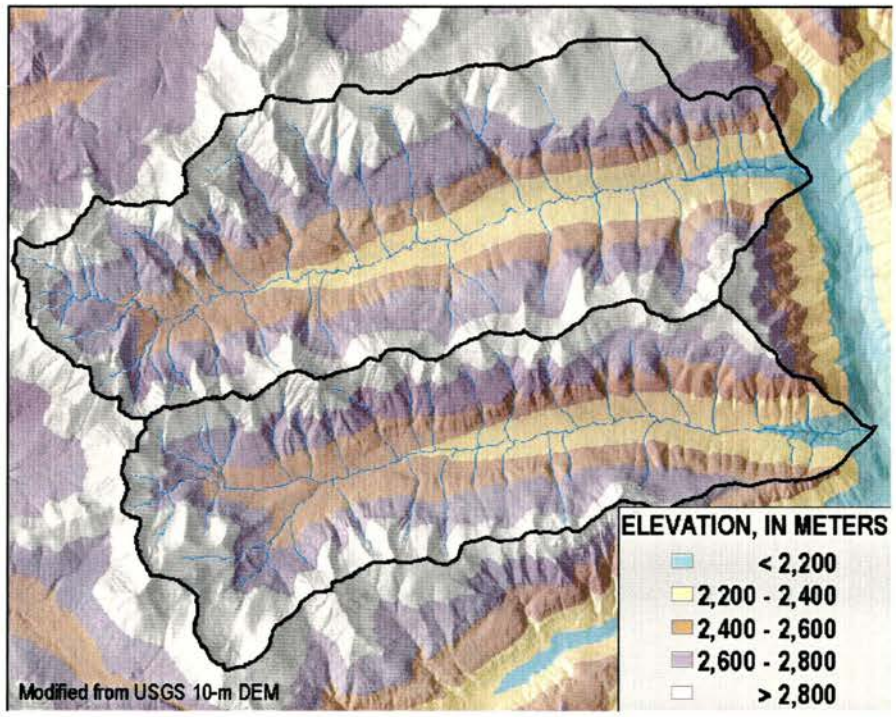

Figure 2.3. Physical relief of study area in northwestern Wyoming.

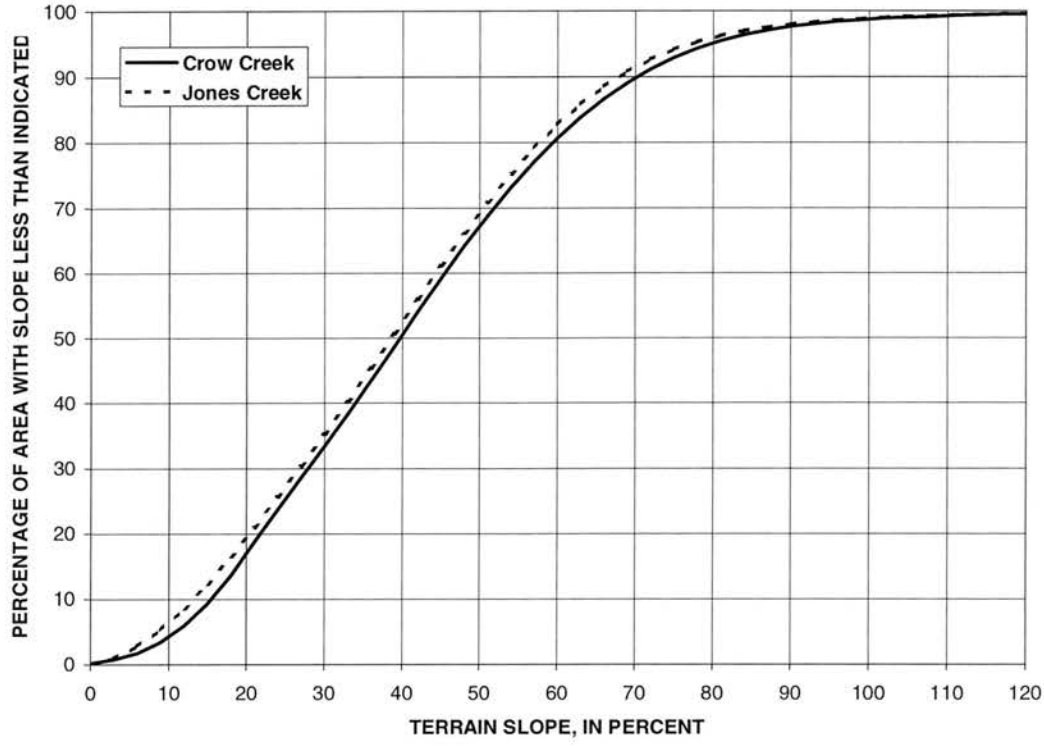

Figure 2.4. Cumulative frequency curves of terrain slope for drainage areas of Crow and Jones Creeks.

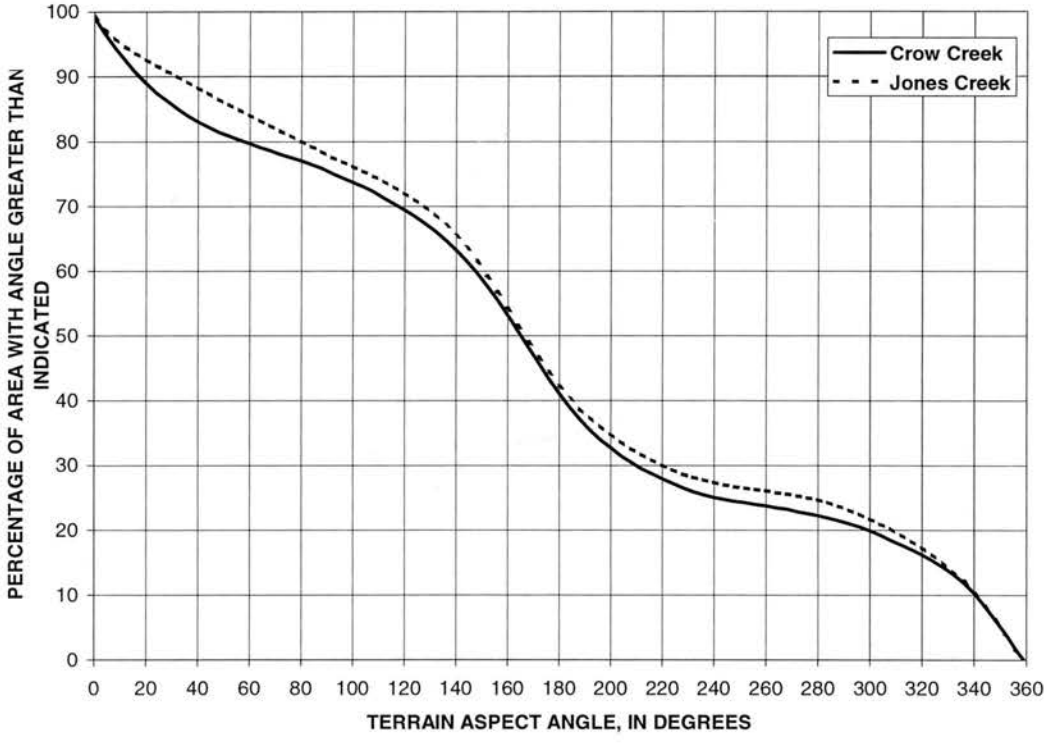

Figure 2.5. Cumulative frequency curves of terrain aspect for drainage areas of Crow and Jones Creeks.

2.2.1 Climate

In mountainous regions, climate is strongly controlled by elevation. Average air and soil temperatures in the study area decrease by about 0.6°C per 100 m increase in elevation (Despain, 1987). Mean annual temperature is about 0°C, with January mean daily minimum of -17°C and July mean daily maximum of about 22°C (Martner, 1986). The frost-free period averages less than 25 days, and in the alpine zone frost may come at any time.

Mean annual precipitation generally increases with elevation and tends to be greatest on the windward (west-facing) slopes. An unpublished regression analysis of precipitation data from USDA weather stations in and around the Shoshone National Forest (G.S. Bevenger, U.S. Forest Service, written comm., 1992) suggests that mean annual precipitation in the study area is about 1,350 mm on the ridgetops and decreases to about 450 mm at the watershed outlets. On average, there are more than 50 days per year on which thunderstorms occur in the vicinity of a given point in this area (Martner, 1986). Precipitation intensity during storms of moderate length (6 hr) very rarely averages more than 9 mm/hr (cf. Miller et al., 1973).

2.2.2 Geology

The northern Absaroka volcanic field consists of deeply eroded andesitic and basaltic lava flows and epiclastic deposits derived from them, some air-fall tuffs, and a variety of related intrusive rocks (Nelson and Pierce, 1968; Smedes and Prostka, 1972). The Eocene rocks of the Absaroka field were named the Absaroka Volcanic Supergroup (Smedes and Prostka, 1972) because three natural stratigraphic groups are included: in ascending order, the Washburn Group, Sunlight Group, and Thorofare Creek Group.

The Washburn Group is the oldest part of the volcanic deposits and composes much of the northern Absarokas, but in and near the study area it is overlain by rocks of the Sunlight Group. The Sunlight Group forms the stratigraphic middle of the Supergroup and is composed of a sequence of mainly dark colored pyroxene andesite lava flows and volcaniclastic rocks and potassic basalts. The Wapiti Formation and the Trout Peak Trachyandesite are units of the Sunlight Group that occur in the study area (fig. 2.6).

The Wapiti Formation, defined by Nelson and Pierce (1968), is a sequence of andesitic volcaniclastic rocks and sporadically interlayered lava flows of trachyandesite or, less commonly, dacite. Trachyandesites are fine-grained, intermediate rocks (silica percentage between 52 and 66) that differ from andesites and trachytes by having a ratio

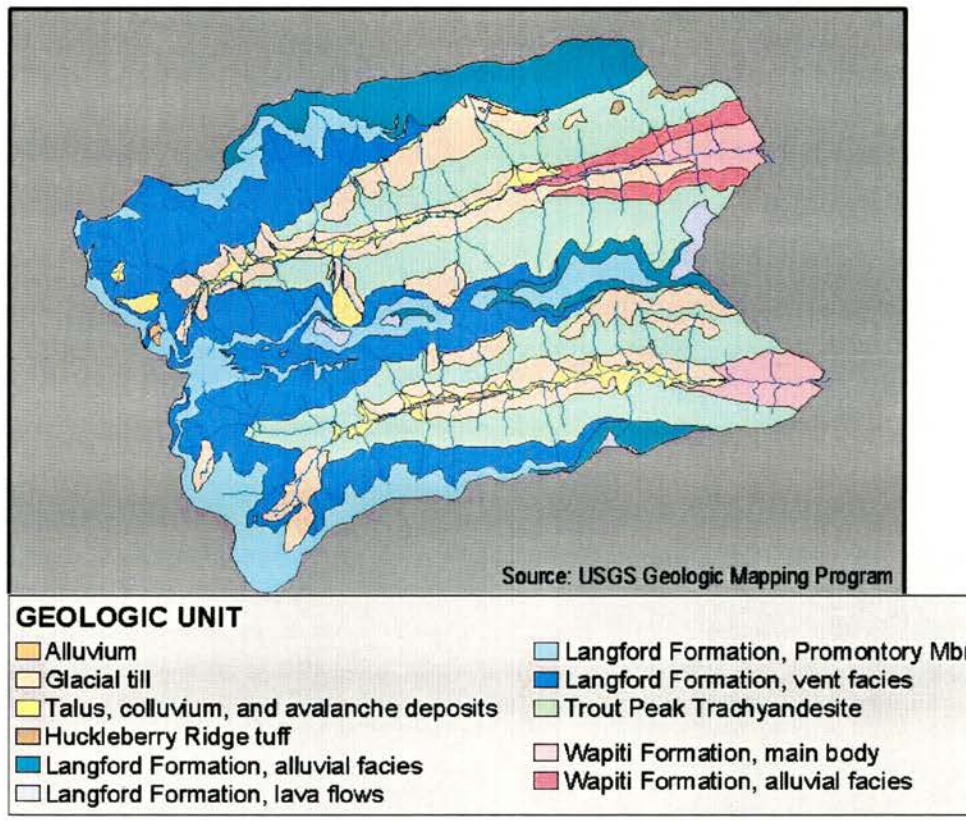

Figure 2.6. Geology of the study area in northwestern Wyoming.

of alkali feldspar to total feldspar between 1:9 and 2:3 (Williams et al., 1955). Volcanic breccia in this formation is mostly volcanic detritus and the matrix is chiefly silt- to coarse-sand-sized grains. Volcanic sandstone, siltstone, and conglomerate occur in sequences of variable thickness and bedded so as to suggest fluvial deposition (Nelson and Pierce, 1968). Near the study area, the Wapiti Formation is about 1200 m thick, overlies rocks of the Washburn Group, and consists of vent facies rocks cut by numerous dikes and other intrusives (Smedes and Prostka, 1972). The area of each watershed underlain by the Wapiti Formation is the most notable geologic difference between the study streams (fig. 2.7), but affects only a small, lower part of each catchment.

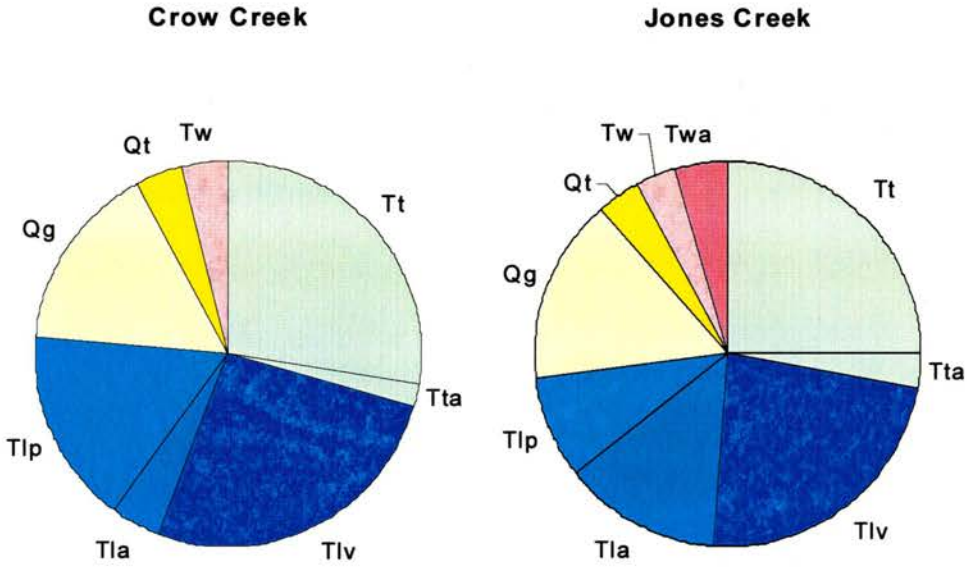

Figure 2.7. Relative areal extent of geologic units underlying Crow and Jones Creek watersheds. (Tw, Wapiti Fm., main body; Twa, Wapiti Fm., alluvial facies; Tt, Trout Peak Trachyandesite, main body; Tta, Trout Peak Trachyandesite, alluvial facies; Tlv, Langford Fm., vent facies; Tla, Langford Fm., alluvial facies; Tlp, Langford Fm., Promontory Mbr.; Qg, glacial till; Qt, talus and colluvium)

The Trout Peak Trachyandesite (Nelson and Pierce, 1968), uppermost formation of the Sunlight Group, is a massive sequence of dominantly mafic trachyandesite and

trachybasalt lava flows locally interbedded with minor amounts of volcaniclastic rocks. Individual lava flows have aphanitic groundmasses containing plagioclase and pyroxene phenocrysts (Nelson and Pierce, 1968). The Trout Peak Trachyandesite is about 240 to 360 m thick in east-central YNP (Smedes and Prostka, 1972). The source for both the Wapiti Formation and the overlying Trout Peak Trachyandesite was in the Sunlight-Crandall vent center to the northeast of the study area.

The Langford Formation (Smedes and Prostka, 1972), lowermost unit of the Thorofare Creek Group, is a thick section of dominantly light-colored andesitic volcaniclastic strata and lava flows. The volcaniclastic strata are composed of hornblende and pyroxene andesite fragments. The overall light color results largely from its light-gray ash-rich matrix. Near the study area, the lower part of the Langford Formation consists of vent facies deposits and the upper part is largely coarse alluvial facies deposits (Smedes and Prostka, 1972).

Drainage divides and upper slopes mostly are bedrock outcrops or talus composed chiefly of blocky deposits, but including some pebble screes and block streams. One small glacier occurs north of Avalanche Peak in the Crow Creek watershed. Pinedale till (and Bull Lake till at some eastern locations) dominates the lower hillslopes, but bedrock outcrops are common. Valley floor alluvium includes sand and gravel stream deposits, bouldery fan deposits, and avalanche debris. Deposits from landslides and debris flows are common (Nissen and Case, 1998; Bozek and Young, 1994).

2.2.3 Vegetation

The distribution of vegetation communities in these watersheds is strongly affected by elevation and, to a lesser degree, aspect (Marston and Anderson, 1991). At

the lowest elevations in the study area, riparian communities dominated by willows (*Salix* spp.) occur along the axial streams. Sagebrush (*Artemesia* spp.) dominates the few upland communities below about 2130 m elevation. Topography, vegetation, and geomorphic/hydrologic processes all exhibit notable changes at approximately the 2130-m contour (Marston and Anderson, 1991). Coniferous forest cover is dominant at elevations between 2130 m and the upper timberline, at about 3000 m.

Douglas fir (*Pseudotsuga menziesii*) is dominant in the lower-elevation forest community, particularly on north-facing slopes. At middle elevations, subalpine fir (*Abies lasiocarpa*) and Engelmann spruce (*Picea engelmannii*) are dominant on soils derived from andesites, in contrast to communities dominated by lodgepole pine (*Pinus contortis*) in nearby areas of YNP underlain by rhyolites (Despain, 1990). High elevation stands additionally feature whitebark pine (*Pinus albicaulis*). Scattered groves of stunted conifers are found at the timberline transition. The alpine zone lies above approximately 3000 m elevation (c.f. Thilenius and Smith, 1985; Barrett, 1994; Bunte, 1996) and the alpine community typically consists of a mix of perennial grasses, sedges, and forbs. Less than 10 percent of the study area is covered by alpine vegetation (Troendle and Bevenger, 1996).

At any time, the composition of a given patch of vegetation in this region reflects its disturbance history, with fire being the most widespread natural disturbance (Marston and Anderson, 1991). The climax forest vegetation for the prevailing climate is Engelmann spruce, subalpine fir, Douglas fir, and whitebark pine. In YNP lodgepole pine represents a fire climax; that is, a forest that burns periodically (300- to 400-year cycle in Yellowstone) and seldom attains the climatic climax community over extensive areas (Craighead, 1991).

2.2.4 Hydrology

Snowmelt generally composes the majority of runoff in the study streams. Because of the near permanence of the snowpack at the higher elevations and the contributions from soil drainage and groundwater, streamflow is sustained between periods of precipitation (Lowry and Smalley, 1993). The period of streamflow record for the North Fork Shoshone River near Wapiti (1921-26, 1979-89; and 1989-99 at Wapiti) is of sufficient length to provide relevant information on the streamflow characteristics of the upper basin in which the study watersheds are located. The seasonal pattern of streamflows for the North Fork Shoshone River and for Crow Creek were compared for their respective periods of record (1989-93 for Crow Creek). The pattern of streamflows in Crow Creek appears representative of that for the upper North Fork, in terms of the daily interquartile range of discharge for the mid-March through September season. In contrast, Jones Creek's post-fire streamflow record showed that a presumed increase in runoff has appeared during the spring rise of the snowmelt hydrograph as compared with Crow Creek. Also, comparison of seasonal flow duration curves for 1989-93 for Crow and Jones Creeks (fig. 2.8) indicates that streamflows exceeded about 5 percent of the time were 33 percent greater in Jones Creek. Assuming that such flows very rarely occur during the non-recorded season, they would correspond to mean annual duration of about 2.5 percent. The largest percentage increases in streamflow magnitude were associated with low flows. For example, the discharge exceeded 90 percent of the time was twice as large in Jones Creek (0.65 $ft^3 s^{-1} mi^{-2}$) as compared to Crow Creek (0.32 $ft^3 s^{-1} mi^{-2}$).

Hydrologic analysis of peak streamflows is essential to understanding flood hydrology and sediment transport. Jarrett (1990) has demonstrated that separating the peak flows on the basis of meteorologic cause provides an improved understanding of

flood hydrology in Colorado's mountain rivers. He concluded that rainfall floods are absent in channels above a latitude-dependent elevation threshold (2300 m in Colorado) where rainfall intensity does not exceed 50 mm per 6 hr. At lower elevations in Colorado, maximum rainfall intensity can exceed 250 mm per 6 hr.

In 1989, a cool, extended spring resulted in gradual early snowmelt and reduced spring peak flows in some GYA streams (Minshall and Brock, 1991), but flows in Crow

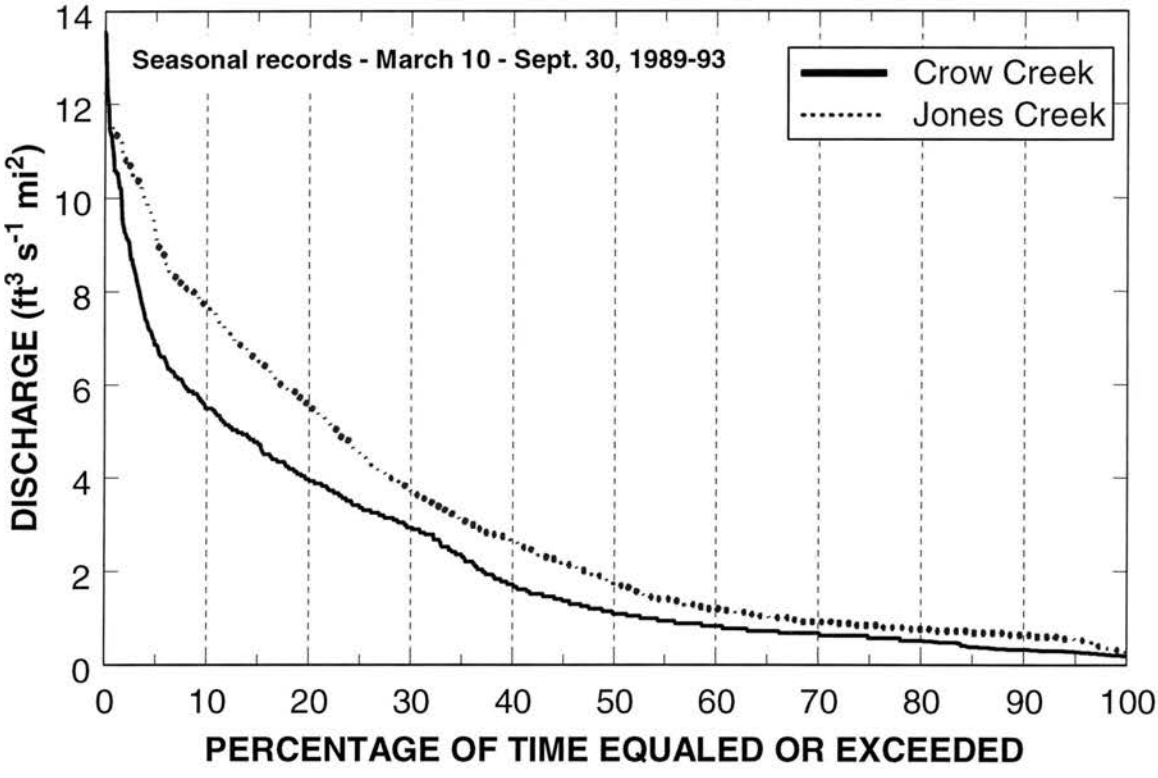

Figure 2.8. Seasonal flow-duration curves for Crow and Jones Creeks, 1989-93, for March 10 to Sept. 30 season.

Creek were above the median daily discharges for 1989-93 (fig. 2.9). For the week of June 14-20, 1989, streamflow in Crow Creek averaged about 80 percent above the 1989-93 median. Snowmelt runoff in 1990, 1992 (not shown), and 1993 (fig. 2.10) in Crow Creek was average to below normal. Flows in both streams were above normal in 1991, and Jones Creek streamflow in 1993 also was above average (fig. 2.10).

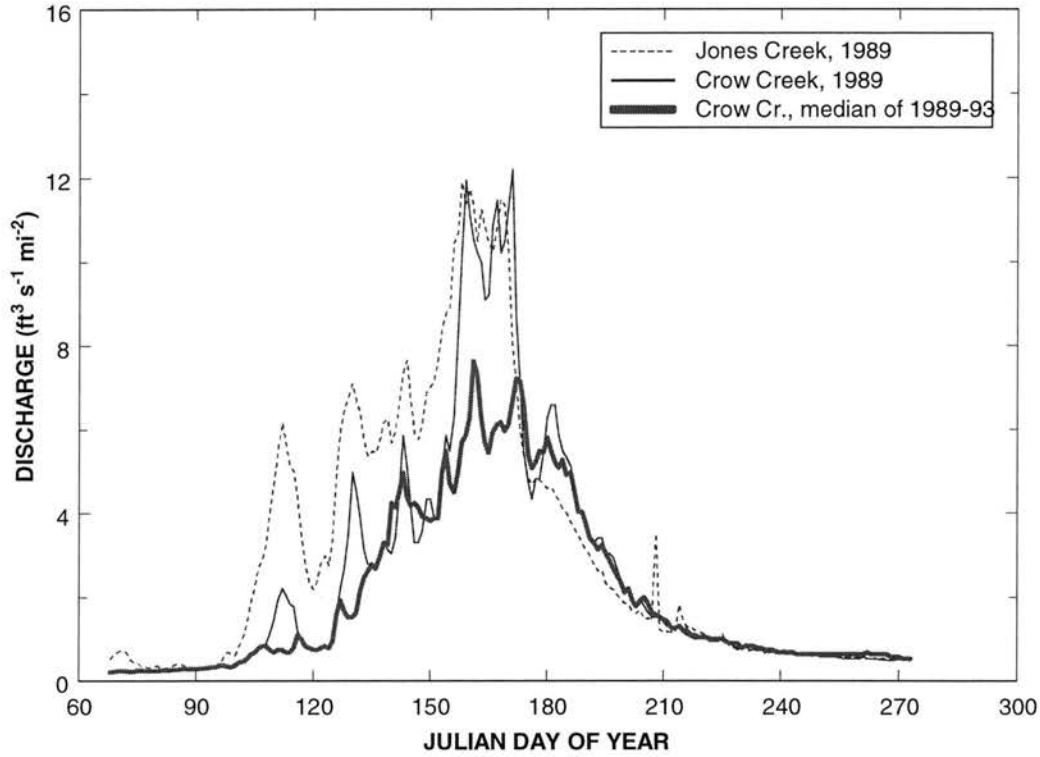

Figure 2.9. Hydrographs for Crow and Jones Creeks, Mar. 10 – Sept. 30, 1989.

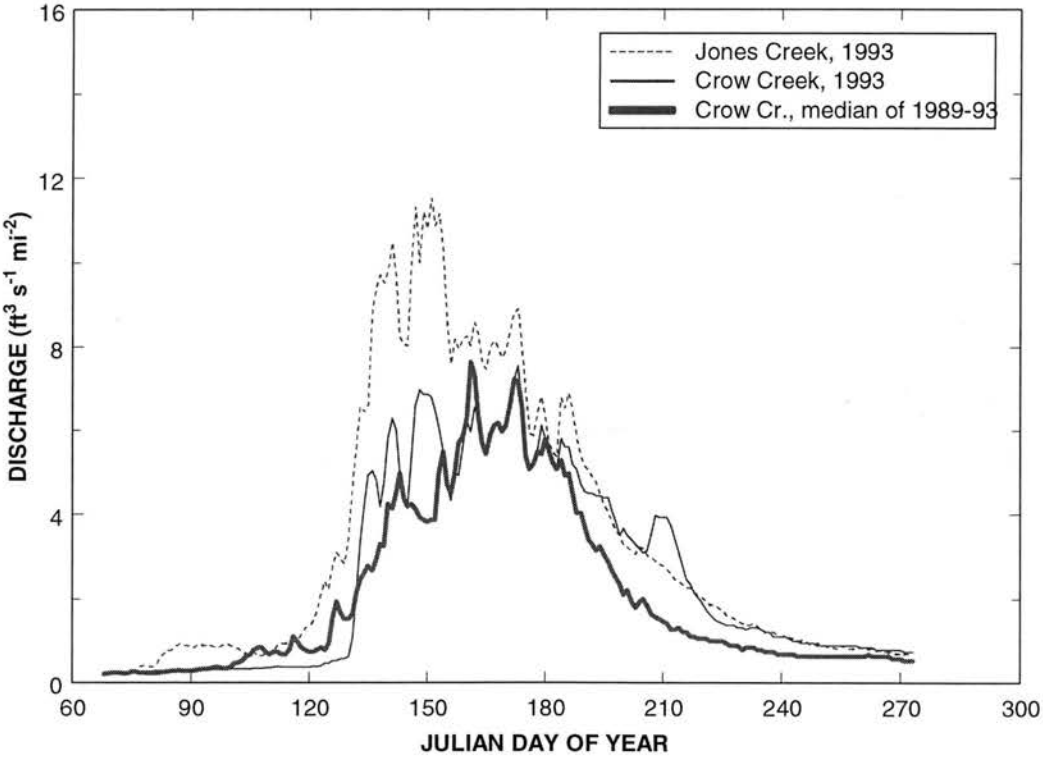

Figure 2.10. Hydrographs for Crow and Jones Creeks, Mar. 18 – Sept. 30, 1993.

2.2.5 Sediment Yield

Sediment yield data from the study area are limited to suspended sediment for the April through September season from 1989-93. These data indicate that, after 1989, most of the annual suspended-sediment yield was associated with high flows during snowmelt (Troendle and Bevenger, 1996). Peak sediment yields for the two streams were about 2100 kg day^{-1} km^{-2} in Crow Creek and 9400 kg day^{-1} km^{-2} in Jones Creek. The maximum sediment yield averaged over a sampling season was 1500 kg day^{-1} km^{-2} in Crow Creek in 1993 and 7200 kg day^{-1} km^{-2} in Jones Creek, also in 1993.

The largest concentrations of suspended sediment, which may pose the greatest potential threat to aquatic fauna, occurred in Jones Creek during intense summer storms. On July 28, 1989, the daily mean concentration was 3630 mg/L, and the maximum grab-sample concentration was 9680 mg/L on August 17, 1990 (Bozek and Young, 1994). However, large concentrations also occurred during snowmelt (e.g., 1230 mg/L in Jones Creek on May 15, 1993, and 294 mg/L in Crow Creek on May 20, 1993).

Sediment data collected from small watersheds in the Absaroka Range are relatively sparse. Bunte (1996) reported a maximum suspended-sediment concentration of 1600 mg/L during 2 years of monitoring at Squaw Creek, Montana, a 106 km^2 forested catchment mostly underlain by andesitic flows or reworked volcaniclastic materials. Reservoir-sedimentation data (Dendy and Champion, 1978) for the 3810 km^2 drainage area of Buffalo Bill Reservoir, which includes the study area, indicate that the mean sediment yield for 1910-1958 at the confluence of the forks of the Shoshone River was 230 m^3 yr^{-1} km^{-2}. By assuming a typical bulk density of 1,500 kg/m^3, an estimated mean sediment yield of 345 Mg yr^{-1} km^{-2} is obtained. However, bank erosion along the lower reaches of the North Fork Shoshone River is reported to contribute much of this yield.

2.2.6 Fire Impacts

During late summer 1988, wildfire severely burned essentially all of the watershed of Jones Creek. Assessment by the Shoshone National Forest (SNF) rehabilitation team indicated that Jones Creek was the most severely burned watershed in the Forest (Troendle and Bevenger, 1996). The adjacent watershed of Crow Creek is very similar to the Jones Creek watershed in most respects except the level of fire disturbance. Less than 8 percent of Crow Creek watershed was burned where fire crossed the divide from Jones Creek and burned some ridgetop and upper slope areas (Troendle and Bevenger, 1996).

Summer rainstorms appear responsible for much of the erosion and channel changes during the first post-fire year (cf. Minshall and Brock, 1991). Channel bed and banks appear to have been the primary sources of increased sediment load during the first several post-fire years (Troendle and Bevenger, 1996), partly because of the devastation of the riparian vegetation (Young, 1994). Also, a mud or debris flow from a tributary to Jones Creek in 1989 was noted (M. Smith, unpub. U.S. Geological Survey station records, Cheyenne, Wyo.). Sheet and rill erosion of burned hillslopes may have been localized secondary sources associated with summer storm events, especially where hydrophobic soils occurred. However, except on mostly barren landslide scars and deposits, few instances of rills or post-fire gullies were noted during 1997-2000 in the burned watershed.

Observations during July-August 1997 confirmed that several of the fire-related geomorphic processes reported in the literature appeared to be important and active. For example, several first-order channels in Jones Creek had post-fire channel-scouring debris flows and debris fans. One large mass movement in 1996 affected a hillslope area

of tens of hectares and deposited debris across the flood plain and directly into Jones Creek, reportedly causing the channel to shift laterally by tens of meters (Arlis Cook, Wapiti, Wyo., oral comm., 1998). Forest regrowth was in very early stages where present, but the general condition was that replacement trees had yet to germinate in the majority of the burned area. Locally vigorous stands of lodgepole pine saplings were observed, but almost no spruce or fir regeneration was noted. Many burned trees were still standing, but low root strength was evidenced by frequently falling trees, especially on windy days.

Most alluvial reaches are characterized as having adjustable boundaries. Both streams have some segments where bedrock control is substantial, but in many reaches upstream of the Wapiti Formation outcrops, bedrock impinges on the channel only sporadically.

Chapter 3

METHODS

This chapter first describes the methods used to select study sites. The following sections describe the field and laboratory methods used to measure channel characteristics and characterize LOD loading. The final section describes the methods used to analyze the data.

3.1 Site Characterization and Selection

Geographic data for the study area were compiled and stored in a computerized geographic information system (GIS) (ESRI, 1990) for use in analysis and characterization of watersheds and stream segments. Data sets included the watershed boundaries, stream channels, digital elevation models (DEMs), and surficial and bedrock geologic units. Sources of data were at 1:24,000 scale, or in some cases, the largest available source scale. Within the past few years, updated DEMs with 10-m horizontal resolution were produced for the study area by the U.S. Geological Survey (USGS). All of the study area was characterized using the newer, digitally interpolated DEMs (USGS Level 2 product).

3.1.1 Targeted Segments

Prior to dividing the fluvial channel network into analysis segments, the network must be defined. The ephemeral and perennial streams shown on 1:24,000-scale USGS topographic quadrangles comprised the population of stream channels. The fluvial

channels were divided into analysis segments, which were defined as channel lengths with fairly homogeneous flow and morphology (Gordon et al., 1992). Because flow changes most abruptly at tributary confluences, those were used as segment boundaries. Additional segment divisions were added where there were marked changes in geology, as indicated by the geologic maps.

Stream segments were characterized with respect to stream order, channel gradient, local geology, and segment length. The stream order of each segment was calculated using the Strahler (1957) method. Average segment gradient was estimated by determing the elevation at each end of the segment and dividing by segment length. Both the elevations and segment length were estimated from the DEMs.

Nine third-order stream segments from each stream were selected randomly as sampling targets from the segments with gradients ≤ 3 percent and lengths of at least 150 m. Such segments were most likely to have pool-riffle morphology (cf. Montgomery and Buffington, 1993). Two additional segments were selected randomly as alternate sampling targets in case primary target segments were unsuitable or inaccessible. Finally, the downstream segment of each stream was selected as a sampling target to allow comparisons with the previous LOD inventory data collected by Young (1994) for those segments. Thus, a total of 20 target segments were selected, ten of which were from Jones Creek.

Drainage areas of the selected stream segments were characterized using additional GIS processing. The evaluated characteristics included elevation, slope, aspect, geology, and area burned in 1988. Spatial overlays of thematic layers with drainage-area boundaries were analyzed to produce the summary characteristics for each drainage area.

3.1.2 Study Reaches

Nearly all the data for the study reaches (fig. 3.1) were collected during late July through September 1999. Four reaches also were visited in 1997 and 1998, when riffle substrate size distributions were sampled and reach gradients were surveyed at those sites. One reach was revisited in 2000 to measure two additional pools.

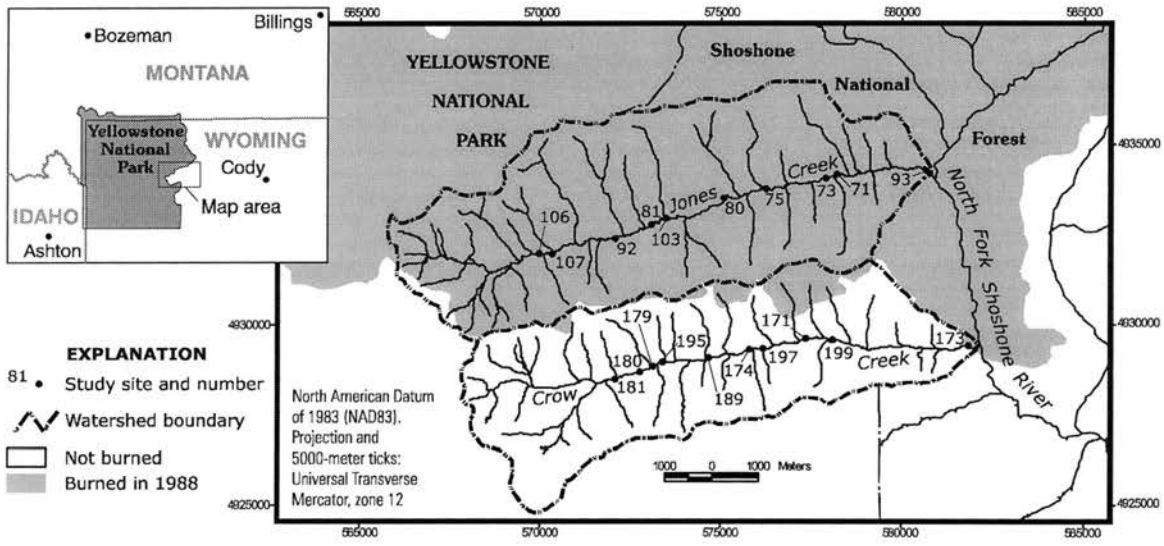

Figure 3.1. Location of study reaches of Crow and Jones Creeks.

At each selected stream segment, a primary study reach with a length equal to 20 average bankfull channel widths was defined after making 3 or 4 measurements of width. A study reach that appeared to have a gradient gentler than adjacent reaches was selected, thus targeting reaches assumed to be most sensitive to changes in sediment inputs (Lisle and Hilton, 1992). A couple of study reaches had some freely formed riffle-pool sequences (ideal for sensitivity to changes of interest), but most study reaches were forced-pool-riffle channels (e.g., Montgomery et al., 1995), and several segments had only plane-bed channels with infrequent pools.

3.2 Onsite Measurements and Laboratory Methods

The methods used for the various measurements and assessments made at each study reach are described in the following subsections. In addition, locational coordinates from global-positioning system receivers, photographs, and a diagrammatic sketch showing the principal fluvial forms and LOD accumulations were required for the documentation of each study site.

3.2.1 Channel Characteristics

Bankfull channel width was measured at 4 to 8 riffle locations per reach and at 4 to 6 pools. Although a minimum of 11 measurements equally spaced along a reach were reported by Simonson et al. (1994) as necessary to yield a mean width within 5 percent of the true mean (with 80 percent confidence), the stratification of width measurements by channel unit type reduces much of the random variability about the mean.

Residual water volume and fine-sediment volume were measured in six pools in each study reach, using methods of Lisle and Hilton (1992, 1999), except that only five pools were measured at two reaches. Pools were defined at low flow as areas of the channel with reduced velocity, little surface turbulence, deeper water than surrounding areas (Fitzpatrick et al., 1998), a distinct downstream terminus ("riffle crest"), and containing the channel thalweg (Lisle and Hilton, 1992). Several of the primary study reaches did not include six suitable pools. In such cases, a secondary study reach (the pool reach) was allowed whatever length necessary to include the set of measured pools, without crossing a stream segment boundary. All pools along the channel sequence were evaluated with respect to the described criteria, and those satisfying the criteria were included in the measured sample (i.e., no qualifying pools were skipped over).

Riffle-crest depth in the thalweg was the average of four to eight soundings on the downstream terminus of each pool. Reach length and downstream position of each pool were tape-measured approximately along the stream centerline. Eleven to 18 soundings were made along three or four transects across each pool, using a graduated steel rod 0.95 cm (0.375 in.) in diameter. Abrupt changes in resistance to penetration of the rod as it passed from sand or fine gravel to packed coarse gravel and cobbles indicated the base of the fine-sediment deposit.

Each measured pool also was classified as to pool type using five categories (c.f. Peck et al., 2000): lateral scour pools on channel bends, pools formed at a channel constriction, plunge pools formed at a channel step, vertical scour pools formed around a flow deflector, and pools freely formed by general fluvial processes (Keller and Melhorn, 1978). A sixth category, forced pools, is defined as pools formed by channel obstructions (Montgomery et al., 1995) and includes pools formed at channel constrictions, steps, and objects causing flow deflection against the bed. The pool types are not mutually exclusive, and each pool was assigned to all applicable categories. Based on these pool types, each reach was classified as either a forced-pool-riffle channel, defined as having more than half of its pools forced by channel obstructions, or a plane-bed channel, lacking freely formed bars and consisting primarily of riffles (Montgomery et al., 1995).

Three pools in each reach were selected randomly for bulk sampling of fine sediment. At each selected pool, a thin-walled piece of pipe (5-cm diameter) was inserted vertically into the residual-pool fines deposit(s) at a minimum of three different sampling points to collect subsamples. The sample was held in the pipe by covering the bottom by hand until it was emptied into a sample container. It is recognized that partial elutriation is a problem for this method, and resulting samples may be deficient in the

finer fractions (cf. Lambert and Walling, 1988). The subsamples were composited to produce a total sample volume of about 750 mL per pool. These samples were submitted to Inberg-Miller Engineers, Cheyenne, Wyo., for laboratory sieve analysis (ASTM D-1140 and D-422) to determine the grain-size distribution (GSD).

Bed-surface material (i.e., pavement or armor layer) was sampled from two riffles in each study reach by a Wolman (1954) pebble count of at least 100 clasts, using the half-largest clast grid sampling method (Wohl et al., 1996). The intermediate diameter of each clast was measured using a US SA-97 hand-held particle-size analyzer (template), except for a few samples collected prior to 1999, in which diameters were measured using a ruler. Marcus et al. (1995) found that the ability to detect differences between sites was enhanced by having only one observer collect pebble-count data at all sites, use of a template; and use of either a fixed grid or fixed points on a transect. For this study, the author conducted all pebble counts. Seven pairs of replicate samples were collected to document between-sample variability.

Reach-average water-surface gradient was computed as vertical drop, measured using a graduated rod and stabilized hand level with 5x magnification, divided by tape-measured distance along the channel. However, for four reaches visited during field reconnaissance in 1997 or 1998, water-surface gradient was surveyed using a surveyor's level and rod.

3.2.2 Channel Stability

Pfankuch (1975) developed a procedure for evaluating channel stability to: (1) systematize measurement and evaluation of the capacity of mountain stream channels to resist the detachment of bed and bank materials; and (2) provide information about the capacity of streams to adjust to and recover from changes in inputs of water or sediment.

Each study reach was rated subjectively using Pfankuch's (1975) system of 15 channel stability indicators that assesses upper banks (above the stage that fills the active channel), lower banks, and streambed. One reach was rated twice (in late July and mid-September) to provide a quality-control replicate pair.

3.2.3 Large Organic Debris Inventory

The organic debris of interest was defined as fallen or deposited pieces of wood having diameter of at least 10 cm for at least 2.0 m of length. The principal data set for LOD was collected by inventorying all pieces extending at least partially into or above the active channel in each primary study reach. The active channel is a geomorphic feature described by Osterkamp and Hedman (1977) as being of short-term duration because it is subject to modification by prevailing discharges. They defined its upper limit by an abrupt decrease in the relatively steep bank slope of the active channel to a more gentle slope on the surface beyond the active channel edge. These breaks in slope typically coincide with the lower limit of permanent vegetation (including herbaceous species), and bracket the portion of channel which is actively shaped by the present discharge regimes of water and sediment (Osterkamp and Hedman, 1977).

LOD piece size was estimated by measuring the length and diameter of all pieces in each study reach. The total piece length having diameter greater than 10 cm was tape measured, as was the partial length within or above the active channel. In a few cases, total length was estimated because reaching the end farthest from the stream involved hazards to worker safety. Diameter was measured once at the mid-length point, usually with a tree-caliper but in some cases using a tape or meter stick. Pieces with two trunks at the mid-length point had both trunks measured, and the equivalent diameter having the

same cross-sectional area was calculated and substituted for data analysis. In some reaches, LOD jams were too large and dense to access or reliably inventory every piece; in those cases, all principal pieces seen, together with a majority of other accessible pieces, were measured. In this fashion, an attempt was made to insure that the rank order of estimated LOD loadings among reaches reflected the actual loadings, despite the underestimation of magnitude of the largest loadings.

Several categorical variables were assessed for each piece of LOD. Debris position (fig. 3.2) was categorized as bridge, collapsed bridge, ramp, drift (Platts et al., 1987), or step. Bridges and steps span the channel whereas ramps rest on one bank only and drift rests on neither bank. Steps are distinguished by the wedge of stored sediment on the upstream side of the obstruction and plunging flow that scours a pool at its base (Wohl, 2000). The planimetric angle of orientation of each piece with respect to streamlines was visually estimated and categorized into one of four categories: parallel (within 22.5 degrees of streamlines), perpendicular (within 22.5 degrees of resting orthogonal to streamlines), angled downstream, or angled upstream (with vertex of angle at thicker end of piece, or at bank if piece is in contact with only one bank).

The volume of fine-sediment accumulation associated with each piece was measured by probing its depth with the graduated rod at about 6 to 12 distributed points (the number of points being proportional to surface area) and tape-measuring the axes of its areal extent. The degree to which each piece of LOD was anchored or stabilized was categorized as the number of ends or sides buried in banks or bed sediments (cf. Young, 1994). Well-anchored pieces were defined as those with more than one anchor. The channel-drop height over a piece of LOD functioning as a "step" was measured using the graduated rod.

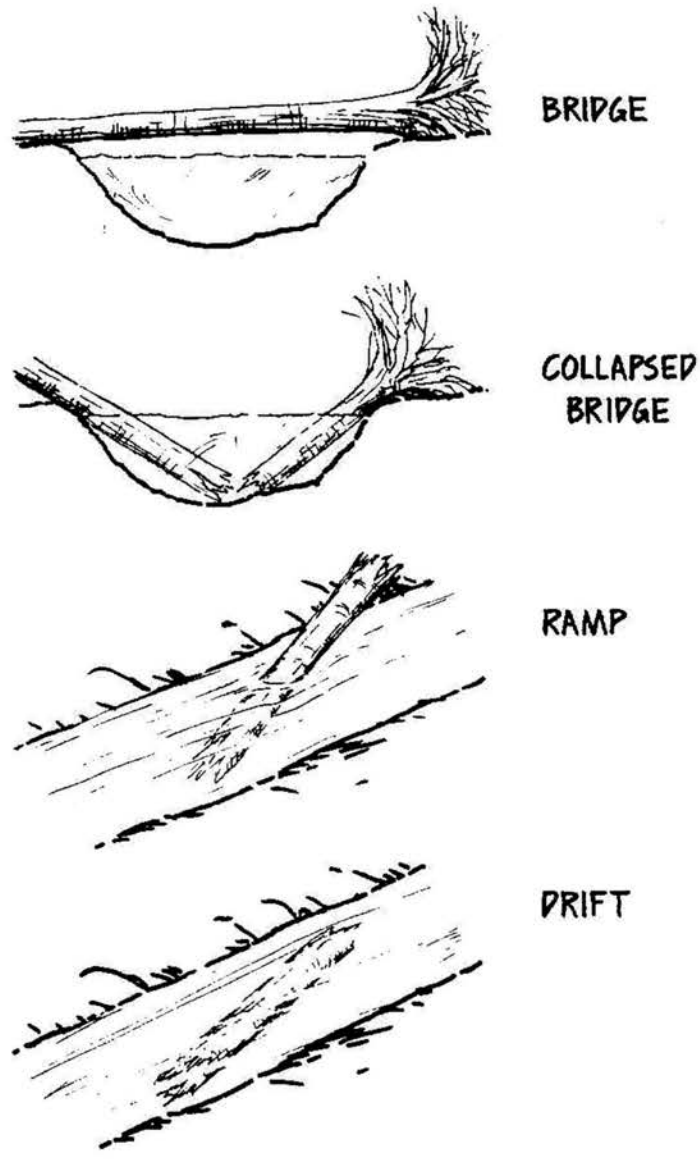

Figure 3.2. Four categories of organic debris position (Platts et al., 1987).

3.2.4 Bedload

Sparse bedload data were collected for two sampling sites on each creek during reconnaissance visits (U.S. Geological Survey, Cheyenne, Wyo., unpub. data, 1999). The bedload measurements were made in June 1998, at near-bankfull discharge conditions, using a hand-held Helley-Smith (1973) sampler with 7.6 cm (3 in.)-square nozzle, 3.22 expansion ratio, and 0.25-mm mesh size, polyester sample bag. The sampler was held on

the streambed for 60 s at each of 20 to 22 sampling stations equally spaced across the sampled section. Sample mass and particle-size distribution were determined by the Sedimentology Laboratory in the Earth Resources Department at Colorado State University.

These bedload data are included in this report to permit an examination of the ratios between selected measures of particle sizes of bedload and bed-surface material. Several such ratios have been postulated as indicators of selectivity of sediment transport or imbalance between sediment availability and sediment transport rate (cf. Parker et al., 1982; Dietrich et al., 1989; Lisle, 1995).

3.3 Data Analysis

The watershed-, channel-, and LOD-characteristics measured or calculated for the study reaches are listed in table 3.1. A number of statistical-summary variables and ratios between measured variables also were selected for analysis. Table C.1 of Appendix C gives the complete list of variables used for the study. For clarity, computations used for a number of calculated variables are explained in section 3.3.1. Statistical analysis methods are presented in section 3.3.2.

Table 3.1 – *Characteristics measured or computed for study reaches.*

[LOD, large organic debris; d_p, grain size at p^{th} percentile; -- (multiple symbols; see tables A.2 and C.1 in appendices)]

Characteristic	Symbol	Number of reaches
Upstream drainage area	A_d	20
Percent of drainage area burned in 1988	B%	20
Mean slope of drainage area	S_{basin}	20
Relative extent of geologic units across drainage area	--	20
Geologic unit containing stream segment	GU	20

Characteristic	Symbol	Number of reaches
Reach length	L_{rch}	20
Channel gradient	S_w	20
Mean bankfull channel width	W_{bf}	20
Mean pool spacing	SP	20
Percentage of reach length in pools	P%	20
Mean depth of residual pools	D_r	20
Mean volume of residual pools	V_r	20
Fraction of residual pool volume filled with fine sediment	V^*_w	20
Pool fines particle size distribution	$(d_p)_p$	20
Riffle armor particle size distribution	$(d_p)_R$	20
LOD frequency	LDF	20
LOD loading, volumetric	VL	20
LOD position, % of LOD count in i^{th} class	Π_i	20
LOD orientation, % of LOD count in $_i^{th}$ class	O_i	20
LOD anchoring, % of piece count	A%	20
Fine-sediment deposit volume associated with LOD	FDV	18
Channel stability index	CS_{tot}	20
Bedload particle size distribution	$(d_p)_L$	4
Instantaneous bedload transport rate	I_b	4

3.3.1 Computations for Specific Variables

Reach-average bankfull width was computed as the length-weighted average of mean riffle width and mean pool width. Most reach-average pool characteristics were computed using data from all pools (i.e., within the pool reach), but a few characteristics were averaged for the 20-channel-width reach (i.e., within the core reach). Reach-average pool spacing was computed for the pool reach at each study site. The percentage of reach length in pools was calculated for both the primary reach and pool reach at each study site. The percentage for the pool reach was used for analysis and interpretation

because it represents a reach that begins and ends at a riffle crest and should produce a more consistent result.

Laboratory results for size of pool fines were averaged by size fraction within each reach to compute a reach-average GSD for pool fines. For each study reach, the percentages by size fraction for each sampled riffle were averaged to compute a reach GSD for riffle armor. Estimates of average size, sorting, and other GSD parameters were determined graphically by reading selected percentile values from the cumulative curves (see Folk and Ward, 1957; Folk, 1974). Selected statistics were computed using percentile values in phi units, including graphic mean size $[(\phi_{16} + \phi_{50} + \phi_{84})/3]$, a modified inclusive sorting statistic $[(\phi_{84} - \phi_{16})/4] + [(\phi_{90} - \phi_{10})/5.13]$, and modified inclusive graphic skewness $[(\phi_{16} + \phi_{84} - 2\phi_{50})/(2\phi_{84} - 2\phi_{16})] + [(\phi_{10} + \phi_{90} - 2\phi_{50})/(2\phi_{90} - 2\phi_{10})]$. The modification of the statistics presented by Folk and Ward (1957) involves substitution of the 10th and 90th percentile values for the 5th and 95th percentiles, respectively, based on the following reasoning. Folk and Ward (1957) cited Inman (1952) in stating that percentile values beyond the 5th and 95th percentiles are seldom reliable. If that is true for the bulk samples they described, then, by extension, for pebble counts of less than 200 clasts it is likely that the 5th and 95th percentile values would be unreliable.

Previous workers have expressed LOD loading in various units, including pieces per unit channel length (i.e., piece frequency; e.g., Young, 1994; Madsen, 1995), pieces per unit channel area (Montgomery et al., 1995), and LOD volume per unit channel length (Hogan, 1987; Berg et al., 1998). For the present study, LOD piece volume was estimated from measured diameter and length by assuming cylindrical shape. The summed active-channel volume of LOD per reach was divided by inventoried reach

length to derive the LOD loading estimate expressed as volume per 100 m of channel length. The area of individual LOD-associated sediment deposits was estimated by assuming an elliptical shape unless otherwise noted in the field.

The number of inventoried pieces of LOD was multiplied by 100 and divided by the length of inventoried reach to derive a metric of LOD frequency as the number of pieces per 100 meters. In addition, the frequency of the largest pieces of LOD was analyzed separately because of its importance to channel morphology (cf. Montgomery et al., 1995). The most influential of these large pieces of LOD was expected to be those oriented obliquely or transversely to the flow, and extending down into the active channel rather than bridging above it. The data from the LOD inventory do not indicate whether a piece causes flow convergence nor whether it vertically intersects the active channel. Nevertheless, an *a posteriori* estimate of frequency of "most influential" LOD (LDF_{inf}) was calculated by including only pieces having diameter > 30 cm, orientation other than parallel to flow, active-channel length > 1.5 m, and position other than bridge.

To allow comparison of the 1999 LOD data from the present study with Young's (1994) results from surveys made in 1990, a subset of the 1999 data for the downstream study reach of each stream was prepared, including only LOD having diameter of at least 15 cm. This LOD data subset was compared with the 1990 data using reach-level summary statistics.

Several hydraulic and bedload-transport variables were calculated using the June 1998 measurements of streamflow discharge, bedload particle size, and estimated bedload transport. Average velocity and depth were computed from the measured streamflow discharge, cross-sectional area of flow, and top width. Total stream power was calculated using the local slope of bankfull-stage indicators in the vicinity of the

measured cross-section that were surveyed during late-summer reconnaissance visits. The average boundary shear stress calculation also used the reach-average median particle size of riffle armor.

Similar to the approach of Andrews (1983), boundary shear stress entraining the bedload (τ_L) was computed using the flow depth within the zone of maximum unit discharge (assumed to correspond to the zone of maximum bedload transport):

$$\tau_L = \gamma (D_L)(S_L) \qquad (3.1),$$

where γ is the specific weight of the fluid, D_L is the representative depth, and S_L is the local slope. Because larger particles were abundant on the streambed, it is reasonable that τ_L was near the critical value required to entrain the largest particles actively moving along the bed at the time of measurement. Thus, critical dimensionless shear stress (τ^*_c) was estimated for the particle diameter ($(d_{95})_L$) larger than that of 95 percent (by weight) of each bedload sample, as

$$\tau^*_c = \tau_L / [(\gamma_s - \gamma) (d_{95})_L] \qquad (3.2),$$

where γ_s is the specific weight of the sediment particles and $\gamma_s = 2.65\gamma$ was assumed.

Andrews (1983) found significant relations between τ^*_c and the ratios of the largest mobile particle to (1) median particle size of the streambed surface (d_i / d_{50}) and, more significantly, (2) median particle size of the subsurface ($d_i / (d_{50})_S$). No data were collected from Crow or Jones Creeks for bed subsurface particle size. However, if the equal mobility concept of bedload transport (Parker et al., 1982; Andrews, 1983) is applicable, then median particle diameter of the bedload may be substituted for subsurface $(d_{50})_S$. Also, Andrews' finding that τ^*_c for a specific particle size, d_i, is greater when the surrounding particles are larger than d_i than when they are smaller

suggests that the ratio of d_i to a parameter of the finest half of the bed surface such as d_{25} may be informative. Hence, the ratios $((d_{95})_L / (d_{50})_R)$, $((d_{95})_L / (d_{50})_L)$, and $((d_{95})_L / (d_{25})_R)$ were computed for this analysis as potential predictors of bedload parameters. Also, predicted critical dimensionless shear stress (τ^*_{cA}) was estimated using the following modification of Andrews' (1983) equation,

$$\tau^*_{cA} = 0.0834 \, ((d_{95})_L / (d_{50})_L)^{-0.872} \qquad (3.3).$$

3.3.2 Statistical Methods

Probability plots of the distribution of individual reach-level variables were used to determine the need for scale transformations and normality. Hypothesis tests of simple differences between the burned and reference streams were conducted for reach-level variables using the non-parametric Wilcoxon rank-sum test for independent samples (Ott, 1992), except for a few variables that had sample distributions that satisfied the assumptions for Student's t test. For $n_1 = n_2 = 10$ as the sizes of two independent samples, the critical values for the rank sum (W) are 83 and 127 using a significance level of $\alpha = 0.10$, and 79 and 131 using $\alpha = 0.05$. If W falls outside the interval within these critical values, the null hypothesis of identical populations is rejected.

Difference in variability between streams was tested using the F-test of equality of variances (Ott, 1992) if normality assumptions appeared to apply. Correlations among pairs of variables were tested using the large-sample approximation of significance for Spearman's rank correlation coefficient (R_s) when all or nearly all 20 study reaches were included. When the sample size was less than 17 reaches, correlations were tested using Kendall's tau (τ) (Kendall, 1962). Helsel and Hirsch (1992) indicate that Kendall's rank correlation procedure is superior to Spearman's for small samples ($n < 20$).

Many characteristics of stream reaches are highly variable in space or time, or both. Given the logistical difficulty of visiting a large number of sites in a remote study area, the large natural variance among sites reduces statistical power by increasing β, the likelihood of accepting the null hypothesis when it is false and the research hypothesis is true (Type II error; Ott, 1992). By increasing α, the probability of rejecting the null hypothesis when it is true (Type I error), the probability β is reduced. For this study, the significance level of statistical test results was indicated by reporting the p-value as marginally significant ($p < 0.10$), significant ($p < 0.05$), or highly significant ($p < 0.01$). Where a decision about significance of test results was required to proceed in one direction of analysis versus another, a Type I error tolerance of $\alpha = 0.05$ was used.

The bedload measurements are non-independent pairs of samples from each of four study sites collected within 3 days of each other. So p-values are not appropriately associated with correlation or linear regression coefficients for these data. Nevertheless, such statistics do provide insight into how well the measurements fit with expected relations and controls for bedload transport.

3.3.2.1 Multiple Linear Regression Models

In addition to using rank-sum tests for simple differences between streams, a linear-regression technique was used to test for such differences while simultaneously accounting for the effect of an independent variable besides stream identity. Such a linear model for a dependent variable, y, may take the form

$$y = \beta_0 + \beta_1 x_1 + \beta_2 x_2 + \varepsilon \qquad (3.4),$$

where β_0 is the unknown intercept term, x_1 is a quantitative independent variable, x_2 is the qualitative "dummy" independent variable representing stream identity, β_1 and β_2 are

unknown parameters, ε is unexplained random variation. Symbol WS was assigned to represent the dummy variable for stream identity, encoded as

WS = 0 if an observation was obtained from a Crow Creek reach, and

WS = 1 if an observation was obtained from a Jones Creek reach.

For observations from Crow Creek reaches, substituting x_2 = WS = 0 into equation 3.4 and simplifying, yields

$$y = \beta_0 + \beta_1 x_1 + \varepsilon \qquad (3.5).$$

In contrast, for observations from Jones Creek reaches, substituting x_2 = WS = 1 into equation 3.4, simplifying, and rearranging, yields

$$y = (\beta_0 + \beta_2) + \beta_1 x_1 + \varepsilon \qquad (3.6).$$

Comparison of equations 3.5 and 3.6 indicates that a single regression model (eq. 3.4) represents two parallel regression lines in (x_1, y) coordinate space, separated vertically by a distance β_2. So the coefficient, β_2, attached to the dummy variable, x_2 = WS, represents the difference between streams in the value of the dependent variable, y, after accounting for differences due to independent variable x_1.

Coefficients for linear models were estimated using least-squares regression (Ott, 1992) or robust least-trimmed-squares regression (Rousseeuw and Leroy, 1987). Standard diagnostic plots were used to check for gross violations of the assumptions underlying normal linear regression. Significance of linear regression models was tested using the F ratio of the explained variation to unexplained variation divided by their respective degrees of freedom (Ott, 1992). The significance of individual independent variables included in linear regression models was evaluated using the t statistic (the ratio of the estimated coefficient to the standard error) (Ott, 1992).

For robust least-trimmed-squares regression, the significance of a dummy variable was tested differently because such procedures do not estimate the standard errors. Residuals were computed from a simplified model excluding the dummy variable. These residuals were submitted to a test of difference between the groups represented by the settings of the dummy variable by using a rank-sum test. This procedure is less powerful statistically than least-squares regression using the dummy variable, but was used in cases where a valid parametric model could not be obtained.

3.3.2.2 Higher-Order Linear Regression Models

The foregoing section presented a hypothetical multiple linear regression model for dependent variable, y, (eq. 3.4) that contains the implicit assumption that the effects of the independent variables, x_i, are additive (Ott, 1992). This means the expected change in y per unit change in x_i is constant, i.e., does not depend on values of the other independent variables. Not all dependent variables are related to independent variables through additive effects, however. In such cases, higher-order multiple regression models may be appropriate.

Higher-order regression models are those which contain cross-product terms or powers of the independent variables (Ott, 1992). It is often more difficult to interpret the physical meaning of the coefficients in higher-order regression models. An exception applies to cross-product terms that contain dummy variables. Cross-product terms represent an interaction effect between two independent variables upon the dependent variable. Graphically, this means that regression lines of expected change in y per unit change in x_1 are nonparallel between different levels of x_2. The simplest model allowing for interaction between x_1 and x_2 is (from Ott, 1992)

$$y = \beta_0 + \beta_1 x_1 + \beta_2 x_2 + \beta_3 x_1 x_2 + \varepsilon \quad (3.7).$$

The expected value of y may be compared for different settings of a dummy variable, x_2, to illustrate the general interpretation of coefficients β_2 and β_3. Let x_2 = WS = 0 for Crow Creek observations. Then the expected value of equation 3.7 is

$$E(y) = \beta_0 + \beta_1 x_1 \quad (3.8).$$

Now let x_2 = WS = 1 for Jones Creek observations. Then simplifying and rearranging equation 3.7 yields the following expected value:

$$E(y) = (\beta_0 + \beta_2) + (\beta_1 + \beta_3) x_1 \quad (3.9).$$

Equations 3.8 and 3.9 represent two nonparallel regression lines in (x_1, y) coordinate space, with y-intercepts separated vertically by a distance β_2, with slopes differing by β_3 units per unit change in x_1. Hence, the coefficient, β_2, attached to the dummy variable, x_2 = WS, is interpreted as the difference between streams in y only when $x_1 = 0$. The coefficient, β_3, attached to the cross-product term, represents the slope difference between streams in the relation of the dependent variable, y, to independent variable x_1. The slope difference may represent a situation in which y is more sensitive to change in x_1 in one stream versus the other, or a situation in which y is positively related to x_1 in one stream but shows an inverse relation in the other stream.

Chapter 4

CHANNEL CHARACTERISTICS

In this chapter are presented data summaries and results of analyses of channel characteristics, including bankfull width, gradient, pool characteristics, and substrate characteristics. Except for the section dealing with the limited bedload data collected at four of the study reaches, and for a summary of pool characteristics, the analysis focuses on reach-average values of the studied characteristics.

Expressed in relation to average channel width, the set of study reaches ranged in length from 12.5 to 26.5 mean bankfull widths. Except for bedload-related data, the full set of variables was measured at each study reach. Data for channel characteristics are listed in tables A.4 through A.8 in Appendix A. Unless otherwise noted, significance levels (probability value, p) are reported for two-sided hypothesis tests.

4.1 Bankfull Width

In this section of the report, the results for weighted-average bankfull width are first presented, followed by those for widths of pools and riffles. Channel width typically is related to one or more parameters of stream discharge. For a watershed with homogeneous hydrologic-response characteristics, channel width usually is a function of drainage area. This is generally the case for Crow and Jones Creeks. However, Crow Creek is much narrower than expected near its mouth at site 173, which is downstream from where part of the flow is diverted into a supply ditch. (The diverted water is used for

stock watering outside the wilderness area.) Data for that reach were excluded from further analyses of channel width, including the statistical summaries (table 4.1).

4.1.1 Weighted-Average Channel Width

Weighted-average bankfull channel width (W_{bf}) ranges from 7.3 m at site 107 to 15.4 m at site 93 (table A.4 in Appendix A). W_{bf} is greater among Jones Creek reaches (median 11.2 m) than Crow Creek reaches (median 8.6 m), producing a statistically significant test result for the difference between streams ($W = 64$, $p = 0.035$). However, the rank-sum test results (table 4.1) for measures of channel width do not account for the general relation of width to drainage area.

Table 4.1 – *Summary of selected reach-average channel-geometry characteristics in study reaches.*

[CV, coefficient of variation; p-value, probability value; sample size is 10 reaches for each stream, except that for channel width variables sample size is 9 for Crow Creek and 10 for Jones Creek]

		Crow Creek			Jones Creek			p-value for rank-sum test of different medians
Channel characteristic	Variable name	Mean	Median	CV (%)	Mean	Median	CV (%)	
Bankfull width (m)	W_{bf}	8.9	8.6	16.3	11.2	11.2	21.3	0.035
Bankfull pool width (m)	W_p	9.8	9.8	14.5	12.4	12.6	22.7	.035
Bankfull riffle width (m)	W_r	8.7	8.2	14.4	10.6	9.7	20.3	.095
Gradient (m/m)	S_w	.022	.023	25.1	.016	.015	51.2	.105

The matrix of rank-correlation results for channel characteristics with other variables is listed in table B.1 in Appendix B. Variables highly rank-correlated with W_{bf} include drainage area ($R_s = 0.791$, $p = 0.0008$), percentage of LOD occurring in debris jams ($R_s = 0.654$, $p = 0.0056$), pieces of LOD per small accumulation ($R_s = 0.633$, $p = 0.0073$), and pieces of LOD per accumulation ($R_s = 0.613$, $p = 0.0095$). Other significant correlations with W_{bf} include reach gradient ($R_s = -0.553$, $p = 0.019$), percentage of LOD

loading occurring in debris jams ($R_s = 0.570$, $p = 0.016$), frequency of LOD in debris jams ($R_s = 0.564$, $p = 0.017$), and frequency of debris jams ($R_s = 0.484$, $p = 0.041$).

Simple linear regression of W_{bf} with drainage area (A_d, in km^2) explains 73.8 percent of the variability in bankfull width, with residual standard error (RSE; also known as the standard error of the estimate) of 1.19 m. Recognizing that in addition to the relation to drainage area, differences in channel width also might be related to runoff or gradient differences between watersheds or to LOD loadings and characteristics (see table 5.1 in Chapter 5), expanded linear models were examined using stepwise selection.

The best model with two independent variables,

$$W_{bf} = 7.95 + 0.119\ A_d - 94.3\ S_w \qquad (4.1),$$

is highly significant ($F = 36.4$, $p < 0.0001$) and achieves a coefficient of determination of 82 percent with RSE of 1.0 m. Water-surface gradient adds significant predictive ability ($t = -2.71$, $p = 0.016$) because gentler gradients correspond to wider channels through mass-conservation requirements. Adding the dummy variable, WS, for difference between streams does not improve this model ($F = 2.44$, $p = 0.139$).

The selected multiple-linear model for W_{bf} includes three independent variables: drainage area, the number of debris jams (N_{jam}), and the dummy variable, WS, for difference between streams. The least-squares fitted model,

$$W_{bf} = 5.39 + 0.094\ A_d + 0.37\ N_{jam} + 1.21\ WS \qquad (4.2),$$

explains 86.4 percent of the variability in average bankfull width with RSE of 0.91 m (see fig. 4.1), and is highly significant ($F = 31.8$, $p < 0.0001$). The estimated coefficients are significantly different from zero for A_d ($t = 5.32$, $p = 0.0001$), N_{jam} ($t = 2.82$, $p = 0.013$), and WS ($t = 2.69$, $p = 0.017$). The coefficient for WS indicates that bankfull

width of Jones Creek is 1.21 m (with 0.45 m standard error (SE)) greater than that of Crow Creek, after accounting for relations with drainage area and number of debris jams. The model coefficient for N_{jam} indicates that three additional debris jams per reach should produce an average effect on mean channel width about equal to the difference between burned and unburned watersheds a decade after wildfire.

A difference in average bankfull width between streams is consistent with the effects of greater runoff from Jones Creek than from Crow Creek during 1989-93

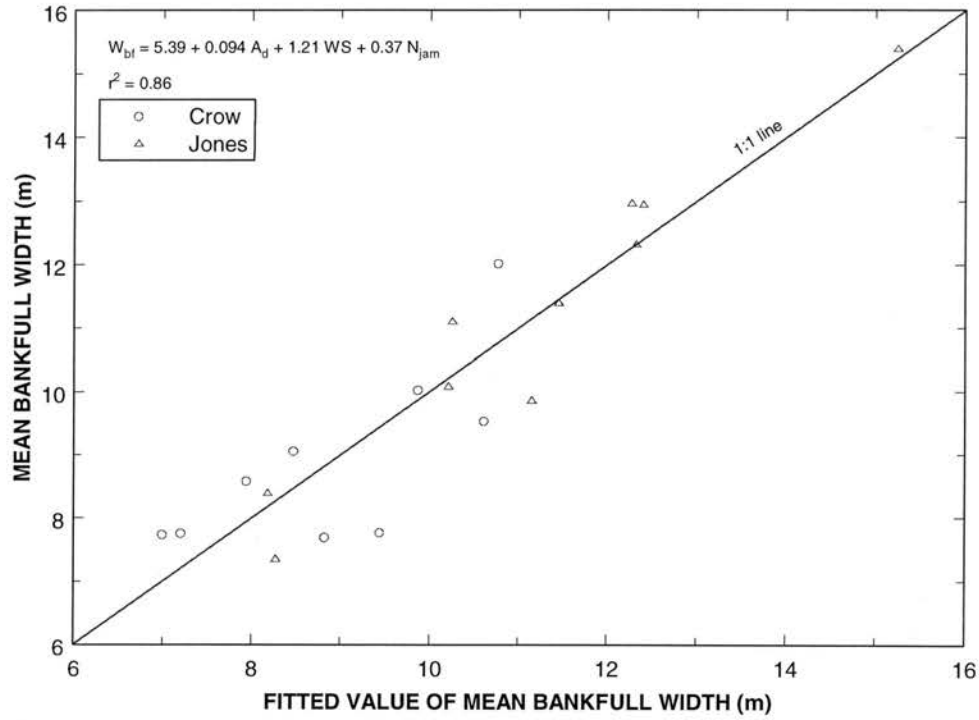

Figure 4.1. Fit of multiple linear regression model for reach-average bankfull channel width.

reported previously (U.S. Geological Survey, 1990-1994; Troendle and Bevenger, 1996). For example, a commonly accepted hydraulic-geometry exponent for discharge in the proportionality with W_{bf} of equilibrium channels is 0.5 (Leopold et al., 1964). Using this discharge exponent along with the average of 14 percent wider channels in Jones Creek

corresponds to a predicted increase of 30 percent in bankfull discharge. Analysis of the flow duration data for 1989-93 shows that the difference between streams in $Q_{2\%}$ was 16 percent (for the seasonal record of streamflow, which presumably corresponds to $Q_{1\%}$ for the entire period). The agreement between the percentage differences between streams in W_{bf} and predicted Q_{bf} is reasonably good, given uncertainties in the flow-duration curve caused by a short period of record, a 37 percent SE for the WS coefficient in the linear model, and some variability in hydraulic-geometry relations among streams.

The reach with the largest positive residual (1.24 m) from the model-predicted bankfull channel width is site 171. Site 171 has the lowest gradient among the study reaches on Crow Creek. It is part of an aggraded segment located upstream of a debris fan at the mouth of a steep right-bank tributary. The debris apparently blocked the channel of Crow Creek, which has formed a new channel shifted leftward from its previous course, evidenced by standing tree stumps in the present channel. The debris flow occurred sometime between 1958 and 1980, based on comparison of aerial photographs, but probably around 1975, judging from the size of the even-aged stand of lodgepole pines covering the fan at present.

The largest negative residual (-1.68 m) from the fitted bankfull channel width model is site 174 on Crow Creek. This reach had the least active-channel LOD loading, and second-least number of LOD accumulations, among Crow Creek reaches. Except for the single large jam that contained 46 percent of its inventoried pieces (and 56 percent of active-channel loading) of LOD in the reach, site 174 had a debris loading similar to those reaches with the lowest debris loadings. Relatively infrequent LOD would be expected to correspond to less flow deflection and narrower bankfull width (see Chap. 5).

4.1.2 Mean Width of Pools

The average of the reach-mean bankfull width of pools (W_p) is 2.6 m wider for Jones Creek than for Crow Creek (table 4.1). Drainage area explains 50.4 percent of the variability in W_p with RSE of 1.87 m. Mean pool width is strongly inversely correlated with reach gradient (R_s = -0.775, p = 0.0010) and positively correlated with pool length (R_s = 0.679, p = 0.0040) and pieces of LOD per small accumulation (R_s = 0.617, p = 0.0090). Mean pool width also is significantly correlated with percentage of LOD occurring in debris jams (R_s = 0.599, p = 0.0111), pieces of LOD per accumulation (R_s = 0.547, p = 0.021), number of large LOD jams (R_s = 0.518, p = 0.028), active-channel length per piece of LOD (R_s = 0.505, p = 0.032), and percentage of LOD loading occurring in debris jams (R_s = 0.466, p = 0.048).

Stepwise selection indicated that mean active-channel piece length (L_a), drainage area (A_d), and the dummy variable (WS) for difference between streams were the best set of independent variables for explaining mean pool width. The model for pool width,

$$W_p = 0.97 + 1.42\ L_a + 2.20\ WS + 0.055\ A_d \qquad (4.3),$$

explains 76.2 percent of the variability in reach-mean bankfull width of pools, with a RSE of 1.38 m (fig. 4.2), and is highly significant (F = 15.97, p < 0.0001). Both L_a and WS contribute significant explanatory power (t = 3.26, p = 0.0052; and t = 3.14, p = 0.0067, respectively). The increase in explanatory power from including drainage area in this model is only marginally significant (t = 1.99, p = 0.066), but its physical significance representing discharge is quite meaningful. The relatively high level of significance for the piece-length variable is interpreted to indicate that flow deflection and wedging against both channel banks are important functions of long pieces of LOD in these streams (see section 5.2). The significance of the dummy variable indicates that

pools in Jones Creek are 2.2 m wider (with SE of 0.35 m), on average, after accounting for differences in L_a and A_d. This difference is consistent with the expected increased duration of near-bankfull discharge in Jones Creek. Other possible sources of the difference between streams in pool width are suggested by correlations between W_p and measures of debris accumulations that differ between streams (Chap. 5) and between W_p and gradient. However, the strong correlation between W_p and mean pool length (PL_m) and between gradient and PL_m (R_s = -0.826, p = 0.0004, n = 19) suggest that gradient may be collinear with pool width and length. Therefore, linear models for W_p using gradient as an independent variable are not presented.

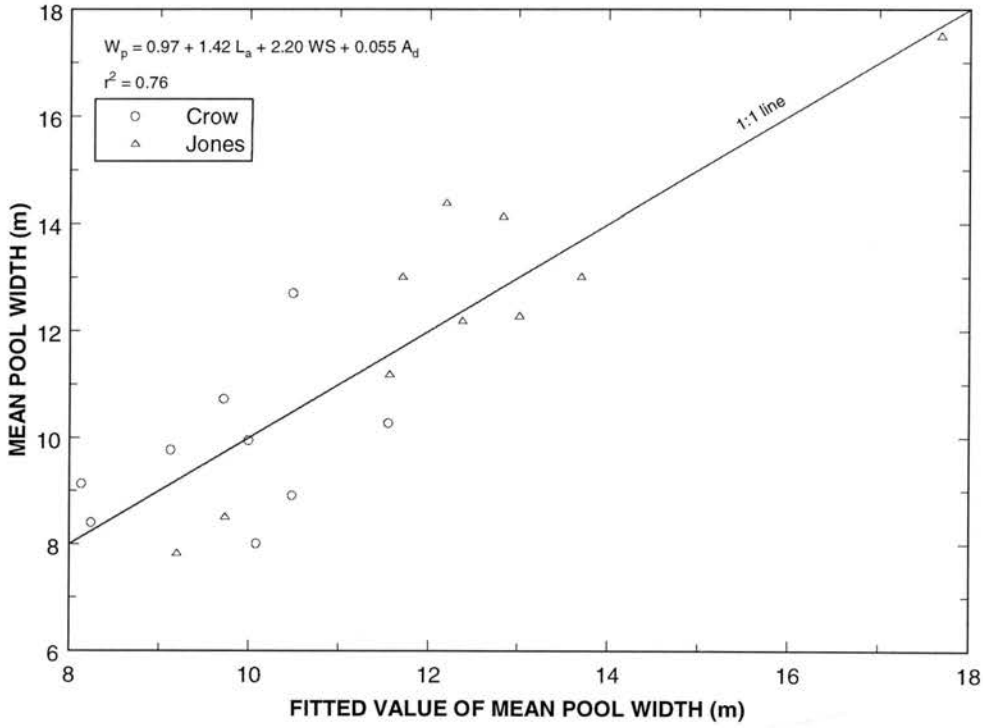

Figure 4.2. Fit of multiple linear regression model for reach-mean bankfull width of pools.

Another linear model for W_p that successfully explains 75.0 percent of the variability in mean pool width with RSE of 1.46 m uses A_d, the frequency of debris jams

(DJF), the dummy variable for difference between streams, and the interaction between A_d and WS as independent variables:

$$W_p = 10.00 + 1.08\ DJF - 2.93\ WS - 0.071\ A_d + 0.17\ A_d{:}WS \qquad (4.4).$$

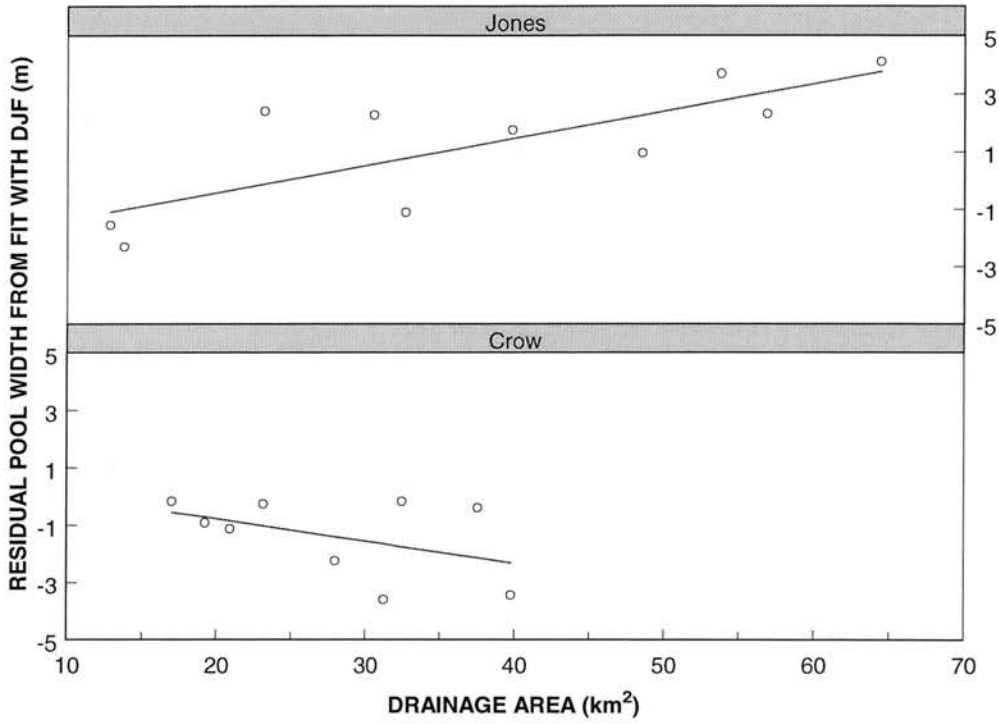

Figure 4.3. Marginally significant interaction between drainage area and stream (dummy variable) in multiple linear regression model for reach-mean bankfull width of pools. Ordinate is residual from regression of mean pool width with debris-jam frequency.

This model is not quite as satisfactory as equation 4.3 because neither A_d nor WS are significant on their own ($p > 0.22$ for each). However, the interaction term ($t = 2.14$, $p = 0.050$) indicates a significant positive correlation between W_p and A_d in Jones Creek, but not in Crow Creek (see fig. 4.3). This suggests that pool widths in Crow Creek are primarily a function of LOD effects, whereas those in Jones Creek reflect influences of both LOD and drainage area (i.e., discharge). Similarly, in relatively undisturbed streams in Washington (Bilby and Ward, 1989) and Colorado (Richmond and Fausch, 1995), pool width or size were found to be related to both LOD and stream size. However, equation

4.4 should be applied with caution because five degress of freedom are used in estimating the coefficients, which produces greater overall uncertainty in the model.

4.1.3 Mean Width of Riffles

Reach-mean bankfull width of riffles (W_r) ranged from 7.2 for site 107 (7.1 m for site 173) to 15.1 m for site 93. Although streamwise median W_r is 22 percent greater for Jones Creek than for Crow Creek, the difference is only marginally significant (table 4.1).

Drainage area explains 76.2 percent of the variability in W_r, with RSE of 1.12 m. Mean riffle width also is highly correlated with number of debris jams ($R_s = 0.656$, $p = 0.0054$) and percentage of LOD occurring in debris jams ($R_s = 0.624$, 0.0082). Other variables significantly rank-correlated with W_r include frequency of LOD in large jams ($R_s = 0.601$, $p = 0.0109$), pieces per LOD accumulation and percentage of LOD loading located in debris jams ($R_s = 0.585$, $p = 0.0131$, for both cases), pieces per small LOD accumulation ($R_s = 0.577$, $p = 0.0146$), and frequency of debris jams ($R_s = 0.559$, $p = 0.0179$).

The largest residual errors from the simple linear model for W_r were for sites 174 and 197 on Crow Creek, with average riffle widths 2.28 and 1.72 m narrower than predicted, respectively. Stepwise regression and correlation tests of residuals from simple and multiple regression models (e.g., fig. 4.4) were used to examine why these two reaches were outliers.

The model that significantly improved upon the simple linear regression without violating underlying assumptions uses drainage area, the dummy variable, WS, for difference between streams, and the interaction between percent pools (P%) and stream identity as the independent variables. This model,

$$W_r = 3.59 + 0.11\ A_d + 3.95\ WS + 0.085\ P\% - 0.13\ P\%:WS \quad (4.5),$$

explains 88.5 percent of the variability in mean riffle width with RSE of 0.86 m (fig.

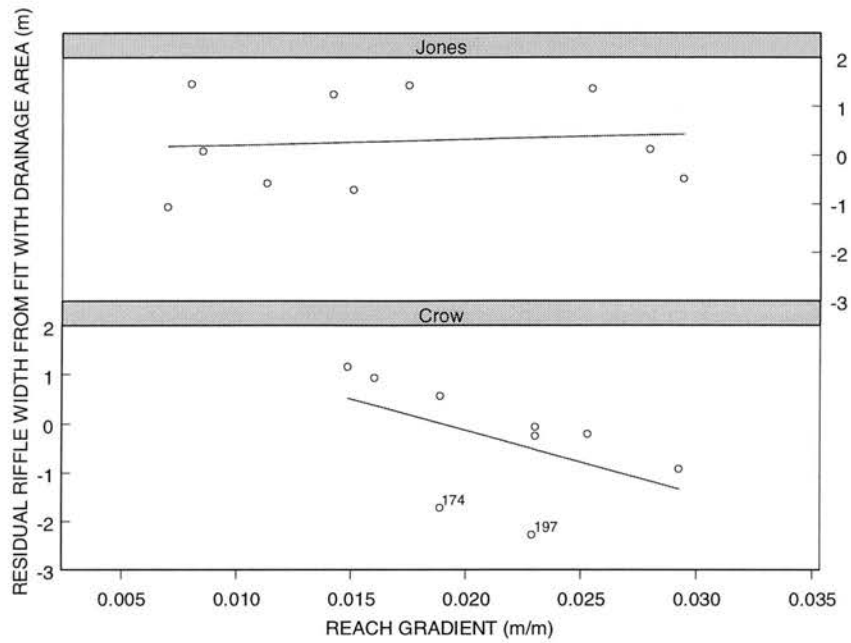

Figure 4.4. Interaction between reach gradient and stream in multiple-regression model for reach-mean bankfull width of riffles.

4.5). The significance of the independent variables in improving explanatory ability of the model is as follows: A_d is most important ($t = 7.69$, $p < 0.0001$), followed by the difference between streams ($t = 3.87$, $p = 0.0017$) and the interaction term ($t = -3.52$, $p = 0.0034$). Percent pools is not a significant explanatory variable ($p > 0.3$), but was retained in the model for completeness. The interaction term indicates that, after accounting for the relation with A_d, mean riffle width is more positively correlated with percentage of reach length in pools for Crow Creek than for Jones Creek (fig. 4.6).

It appears that shorter or less frequent riffles in Crow Creek tend to be wider than expected on the basis of drainage area alone. Long riffles were usually relatively narrow and more uniform in width. After accounting for the expected relation with drainage area

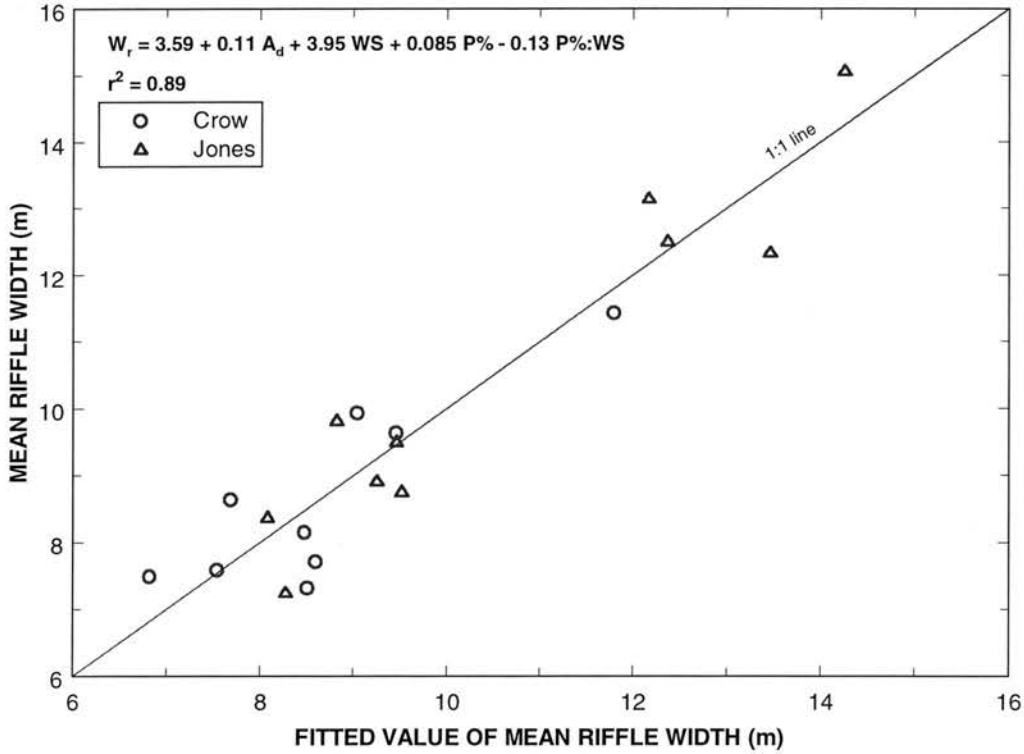

Figure 4.5. Fit of multiple linear regression model for reach-mean bankfull width of riffles.

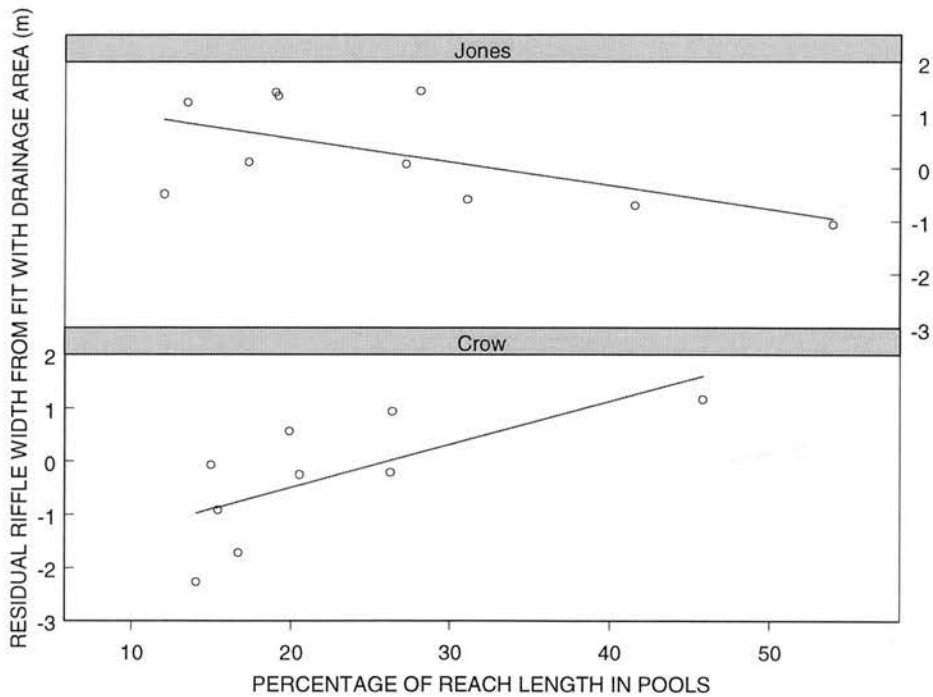

Figure 4.6. Interaction between stream and percentage of reach length in pools in multiple-regression model for reach-mean bankfull width of riffles.

and the relation with percent pools, the riffles of Jones Creek are significantly wider than those of Crow Creek ($p = 0.0017$). After accounting for A_d and P%, the 3.95 m average residual difference between streams in riffle width (with SE of 1.02 m) corresponds to 46 percent (SE of 12 percent) of mean Crow Creek riffle width. However, because of the interaction effect the 3.95 m difference between streams in riffle width applies only if a reach has no pools. The difference between streams in riffle width decreases as percent pools increases above that minimum value.

4.1.4 Summary

Although drainage area explains 73.8 percent of the variability in bankfull width, statistical significance increases by including the number of debris jams and the dummy variable for the difference between streams in an expanded linear model (eq. 4.2). The expanded model indicates that the mean bankfull channel is 1.21 m wider for the burned stream than for the reference stream after accounting for differences in drainage area and number of debris jams. Drainage area explains only 50 percent of the variability in mean pool width, but by including mean active-channel LOD piece length and the difference between streams in a multiple regression model (eq. 4.3), a 2.2 m greater mean width of pools is indicated in Jones Creek as compared with Crow Creek. Pool widths in Crow Creek are primarily a function of LOD effects, whereas those in Jones Creek reflect the influence of both LOD and drainage area. Drainage area is the most important factor for explaining mean riffle width.

The direction and magnitude of channel-width differences are consistent with typical hydraulic-geometry relations applied to the increased duration of near-bankfull discharge in Jones Creek as compared to Crow Creek. Bank erosion by increased

streamflow in Jones Creek during the early post-fire period (Troendle and Bevenger, 1996) is one process that may be responsible for the larger channel width of Jones Creek. Also, the importance of LOD deflecting flow against bed and banks appears to be greater in influencing the widths of pools than riffles, although widths of both were significantly correlated with the frequency and size of LOD accumulations. Differences in channel width imply that decreased channel stability followed the burning of Jones Creek, but any continued instability would be related to increases in streamflow deflection by channel obstructions.

4.2 Reach Gradient

The reach-average gradients are shown in figure 4.7. The mean channel gradient for Crow Creek reaches is 0.022 m/m versus 0.016 m/m for Jones Creek, a marginally significant difference ($t = -1.88$, $p = 0.077$). The third-order length of Crow Creek is 1.3 km shorter than that of Jones Creek, its mouth is 52 m lower, and Crow Creek enters its third-order valley at an elevation 60 m higher than does Jones Creek. GIS data for all third-order segments of each stream also indicate a steeper average channel gradient of 0.038 m/m for Crow Creek versus 0.027 m/m for Jones Creek.

The reach gradient data appear approximately normally distributed. Although the data for Jones Creek show more variability, a t test is applicable because the sample sizes are equal (Ott, 1992). Some of the variability among the reach-average gradients is likely caused by the measurement method. Gradients of 16 reaches were estimated from hand-level surveys, which have been shown by Isaak and others (1999) to be about 50 times more variable (but not significantly different from) gradients measured using surveying levels.

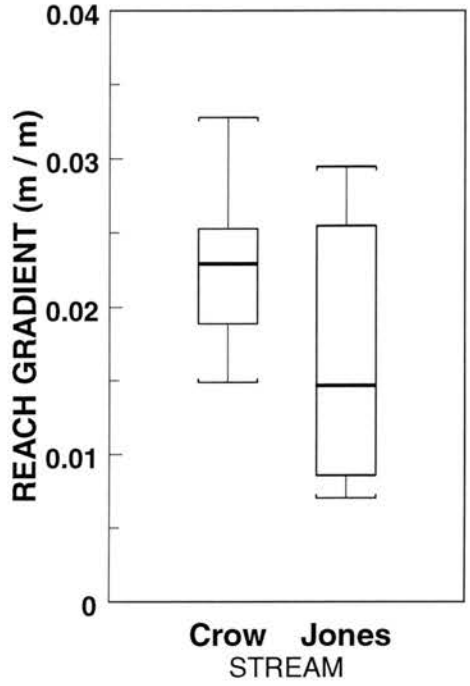

Figure 4.7. Boxplot diagrams by stream of frequency distribution of reach-average channel gradient.

The reach gradients of several sites (73, 80, 92, 171, 195, and 199) are influenced by local deposits of coarse sediment that produce a steep riffle or rapid on the downstream side of the deposit, and often a gently sloping reach on the upstream side. This type of channel-control feature also was reported in Arizona streams (Wohl and Pearthree, 1991).

4.3 Pool Characteristics

Sixty pools were measured in Crow Creek and 58 pools in Jones Creek. A comparison between streams based on all measured pools is presented in subsection 4.3.1. Pool characteristics also were averaged for each study reach, as were the variables discussed in other sections of the report. The summaries of reach-average pool characteristics are presented in the subsequent subsections.

4.3.1 Summary by Stream

Because an approximately equal number of pools was measured in each reach, and study segments had been selected randomly from reaches with gradients no greater than 3 percent, the measured pools from each stream are representative of all lower-gradient reaches of each stream. The pool data are summarized in table 4.2.

Table 4.2 – *Summary of pool characteristics in study streams.*

[Sample size is 60 pools for Crow Creek and 58 pools for Jones Creek; CV, coefficient of variation.]

Pool characteristic	Variable name	Crow Creek	Jones Creek
		Percentage of pools as type indicated[1]	
Lateral scour / bend	PT_{bend}	16.7	27.6
Channel constriction	PT_{const}	41.7	39.7
Plunge	PT_{plunge}	40.0	17.2
Vertical scour	PT_{vscour}	43.3	50.0
Fluvial (freely formed)	PT_{fluv}	1.7	6.9
Forced, by channel obstruction	PT_{forc}	98.3	89.7

		Crow Creek			Jones Creek		
		Mean	Median	CV (%)	Mean	Median	CV (%)
Pool Length (m)	L_{po}	7.1	6.0	54.6	8.6	8.2	58.4
Residual pool mean depth (cm)	D_r	16	14	47.1	18	17	45.3
Residual volume per pool (m^3)	V_r	4.2	2.1	127	6.2	3.1	128
Pool-fines volume per residual pool (m^3)	V_{rf}	1.11	.37	176	1.63	.52	176
Ratio of pool fines volume to residual pool volume	V*	.21	.17	68.0	.23	.19	61.6
Ratio of D_r to mean riffle-crest depth	D_r:D_c	.76	.54	122	.61	.49	63.6

[1]Percentages total more than 100 because categories are not mutually exclusive.

One of the largest differences between streams is that Crow Creek has more than twice as many plunge pools as Jones Creek. A majority of plunge pools in these lower-gradient reaches were associated with a step formed by LOD, though bedrock ledges and

lines of boulders also formed steps in study reaches and elsewhere. The frequency of LOD pieces positioned as steps is presented in Chapter 5, but noteworthy here is that 1.0 percent of the LOD in Crow Creek was positioned as a step, compared to 0.77 percent in Jones Creek. A change in the relative abundance of plunge pools is not necessarily an expected effect of severe forest fire, because most of the step-forming LOD remains intact during even hot fires (Minshall et al., 1989) and usually is among the most stable of LOD pieces. The channel widening and increased duration of near-bankfull flows in Jones Creek may have mobilized a number of step-forming pieces.

Forced pools, as opposed to freely formed pools, are the predominant class in these streams. Montgomery et al. (1995) concluded that freely formed pool-riffle channels are rare in forest streams. Although no specific data were collected in the present study to identify the type of obstruction causing each forced pool, a large percentage of these were caused by pieces of LOD. This was true of both streams, and underlines the importance of LOD to channel morphology in these two streams.

Although table 4.2 provides some insight into differences between streams, hypothesis tests must satisfy the assumption that each sampled unit is independent. Therefore, reach-average values for each pool characteristic were calculated, summarized (table 4.3), and used to test the significance of differences between streams.

4.3.2 Forced Pools and Channel Types

At least half of the measured pools in each study reach were forced pools formed by scour around an obstruction (table A.7 in Appendix A). Only four reaches had measured pools that were not forced pools, and three of these reaches were in Jones Creek. Site 80 had the most freely formed pools, and this reach could be classified as a

short reach of pool-riffle channel type. However, if all pools in reach 80 are considered (i.e., those measured and those unsuitable for residual-pool measurement) a majority of its pools are forced by obstructions. Fifteen of the study reaches are forced pool-riffle (FPR) channels (table A.4 in Appendix A). The remaining five reaches are plane-bed channels.

Table 4.3 – *Summary of reach-average pool characteristics in study reaches.*

[CV, coefficient of variation; p-value, probability value; sample size is 10 reaches for each stream]

Pool characteristic	Variable name	Crow Creek			Jones Creek			p-value for rank-sum test of different medians
		Mean	Median	CV (%)	Mean	Median	CV (%)	
Forced pools (percentage)	F%	98.3	100	5.4	90.0	100	19.9	0.26
Length (m)	PL_m	7.1	6.4	37.4	8.8	8.7	37.9	.22
Length (channel widths)	PL	.80	.76	24.1	.79	.76	28.7	> .5
Spacing (m)	SP_m	33	31	25.1	41	31	49.8	.91
Spacing (channel widths)	SP	3.9	3.7	31.6	3.5	3.5	32.7	> .5
Percentage of reach length	P%	23	20	41.9	26	23	50.4	> .5
Residual pool mean depth (cm)	D_r	16	16	28.2	18	18	29.2	.48
Residual volume per pool (m^3)	V_r	4.2	3.4	82.7	6.4	5.8	82.3	.35
Pool-fines volume per residual pool (m^3)	V_{rf}	1.11	.49	144	1.67	.87	108	.18
Ratio of pool fines volume to residual volume	V^*_w	.20	.17	58.6	.23	.23	33.2	.16

4.3.3 Pool Length

On average, reach-mean pool length (PL_m) was 1.7 m longer in Jones Creek than in Crow Creek, but this difference is not significant ($W = 88$, $p = 0.22$). Pool length is significantly correlated with reach-average bankfull width ($R_s = 0.686$, $p = 0.0037$), as might be expected for any pool characteristic that scales with channel size. Reach-mean pool length (PL) expressed as a ratio with reach-average bankfull channel width was very

similar for both streams, averaging about 0.8 channel widths. The similarity of these ratios implies that if the larger channel width of Jones Creek is an effect of post-fire changes in runoff and LOD characteristics, then pool geometry also has responded through a proportional increase in average pool length.

Pool length (PL) is rank correlated with reach-average gradient (R_s = -0.456, p = 0.047). Although the monotonic association is significant, the weakness of the linear relation is illustrated by a coefficient of determination of 23.6 percent for simple linear regression of pool length with reach gradient (S_w). Adding the dummy variable for stream identity does not improve the linear model significantly (F = 1.44, p = 0.25), confirming that pool length does not differ between streams even after accounting for differences in channel width and gradient.

4.3.4 Pool Spacing

Reach-mean pool spacing (SP_m) ranged from 21 m in one reach of each stream (sites 103 and 180) to 80 m in reach 93 of Jones Creek. The median pool spacing for both streams is 31 m. Although the streamwise mean of SP_m is 8 m longer in Jones Creek than in Crow Creek (table 4.3), the distribution of SP_m is positively skewed for Jones Creek.

SP_m is significantly correlated with mean riffle width (W_r) (R_s = 0.470, p = 0.046), but not correlated with any of the LOD variables. The positive correlation of SP_m with channel width follows a pattern previously noted for channels of varying types in a wide range of locations (e.g., Keller and Melhorn, 1978; Montgomery et al., 1995). The amount of variability in SP_m explained by channel width in the present study (54.4 percent using simple linear regression) is substantially less than that reported by Keller

and Melhorn (1978) in their study of freely formed pools in 11 streams. This suggests that the predominance of forced-pool-riffle channel types may be important for understanding pool spacing in Crow and Jones Creeks.

For the 15 FPR reaches, pool spacing is strongly related to mean riffle width (W_r) ($R_s = 0.589$, $p = 0.028$). The linear regression model for SP_m includes W_r, the dummy variable, CT, for channel type (CT = 1 for FPR, 0 otherwise), and LOD frequency (LDF):

$$SP_m = 13.8 + 5.2\ W_r - 21.3\ CT - 16.3\ LDF \qquad (4.6).$$

This model ($F = 40.93$, $p < 0.0001$) and the coefficients for each independent variable are highly significant ($t = 7.89$, $p < 0.0001$ for W_r; $t = -6.83$, $p < 0.0001$ for CT; and $t = -2.47$, $p = 0.025$ for LDF). The model explains 88.5 percent of the variation in SP_m with a RSE of 5.8 m (fig. 4.8). The coefficient for W_r indicates that average pool spacing is about 5.2 channel widths (of riffles, with SE of 0.65 W_r). The coefficient for CT represents an average difference of 21.3 m (with 3.1 m SE) in pool spacing between the two channel types, with plane-bed channels having greater pool spacing.

Montgomery et al. (1995) found a simple inverse proportionality between pool spacing and LOD frequency in forest stream reaches of mixed types. Although the inverse relation between pool spacing and LDF (fig. 4.9) is represented in equation 4.6, the correlation differs in sign between plane-bed channels ($R_s = 0.20$) and FPR channels ($R_s = -0.52$). However, the interaction between LOD frequency and channel type is not quite marginally significant ($p = 0.12$) when added to the model. Montgomery et al. (1995) reported that the channels with the largest percentage of forced pools also had the smallest percentage of freely formed pools, and that FPR channels had greater LOD loading and smaller pool spacing than other channels. Hogan (1987) found that in

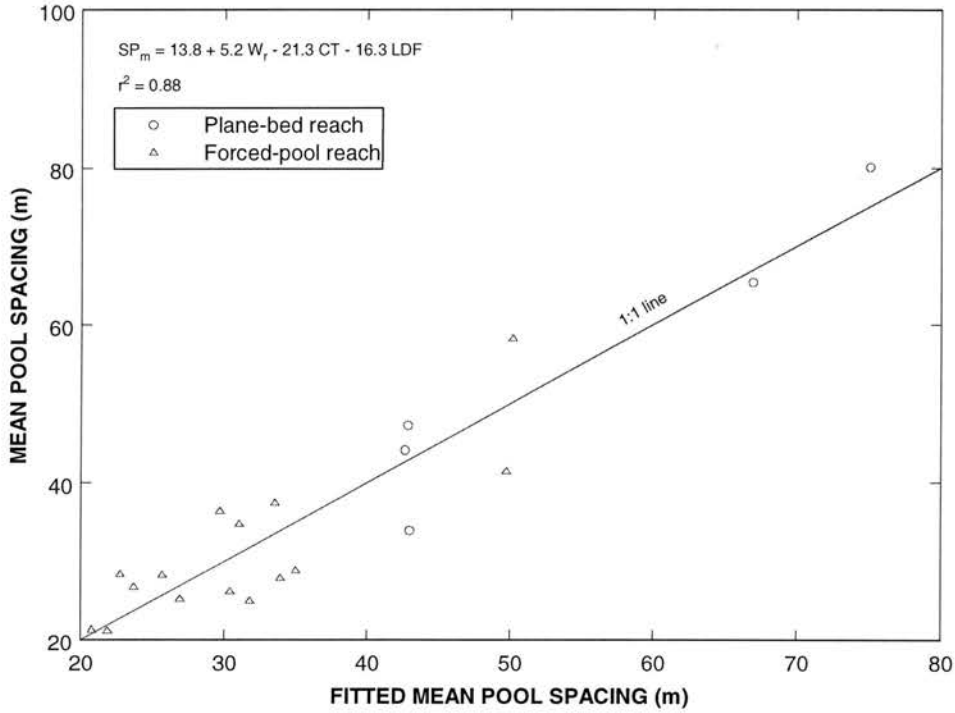

Figure 4.8. Fit of multiple linear regression model for mean pool spacing.

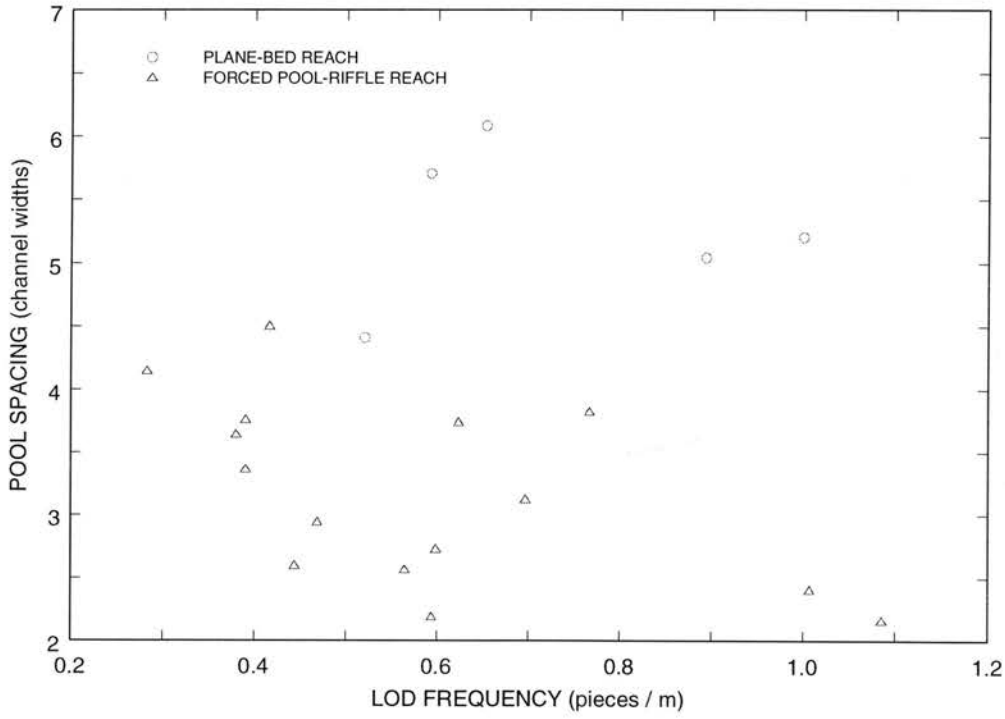

Figure 4.9. Relation between mean pool spacing and mean frequency of large organic debris.

channels draining watersheds of 6.9 to 45 km^2, LOD loading paralleled channel bed irregularity (i.e., large bed irregularity indicated greater pool frequency).

Expansion of equation 4.6 to include a dummy variable for stream identity does not improve the model ($F = 0.41$, $p > 0.5$). There is no difference between streams in average pool spacing after accounting for relations with channel width, channel type, and LOD frequency.

Expressed in units of channel widths, reach-mean pool spacing (SP) ranged from 2.2 channel widths for site 103 to 6.1 channel widths for site 174. The fraction of a channel width greater average SP in Crow Creek is not significantly different from Jones Creek ($W = 96$, $p > 0.5$). Pool spacing for 65 percent of the study reaches ranged from 2.5 to 4.5 channel widths. This is less than the 5- to 7-channel-width spacing commonly expected for freely formed pool-riffle morphology (Leopold et al., 1964). However, for mountain streams, Wohl (2000) summarizes that pool-riffle streams, even with low LOD loading, typically feature pool spacing of 2 to 4 channel widths. Montgomery et al. (1995) reported mean pool spacing of 2 to 4 channel widths for pool-riffle channels, 2.3 to > 13 channel widths for plane-bed channels, and 0.2 to 3 channel widths for forced pool-riffle channels.

Among plane-bed reaches, the two reaches having smallest mean pool spacing (sites 75 and 197) have the largest average size of debris jams (both sites averaging at least 34 pieces per jam) and lowest percentage of LOD being anchored (40 and 46 percent, respectively). Sites 174 and 181 have the largest mean pool spacing (> 5.7 channel widths) and largest percentage of anchored LOD (> 52 percent). Site 174 has the smallest average size of debris jams (19 pieces) and site 181 had no debris jams present. For plane-bed channels, these results suggest an inverse relation between SP and average

woody debris-jam size. This is consistent with Montgomery et al. (1995), who stated that the influence of LOD on channel morphology depends on its size relative to channel size and its height above the bed. Debris jams thus may function as pool-forming obstructions similar to very large pieces of LOD but rising farther above the bed.

4.3.5 Percent Pools

The percentage of reach length in pools (P%) integrates pool length and spacing in a single metric. The values of P% for the primary reach and pool reach were highly correlated ($R_s = 0.865$, $p = 0.0002$), and only the values for pool reaches are summarized in table 4.3 because they usually include a larger number of pool-riffle sequences. Average P% is not significantly different between streams ($W = 97$, $p > 0.5$). This result is consistent with the lack of significant differences between streams in either mean pool length or spacing. The CV of P% was somewhat greater for the reaches of Jones Creek. Moreover, excluding the previously noted anomalous, aggraded reach (site 171), the maximum P% for any Crow Creek reach was only 26 percent whereas half of the Jones Creek reaches had P% greater than 26 percent.

Percent pools is significantly correlated with the percentage, F%, of pools that were forced-pools ($R_s = -0.653$, $p = 0.0044$) and with reach gradient ($R_s = -0.582$, $p = 0.0111$). Freely formed pools were found only in reaches that had P% greater than 28 percent. Simple linear regression of P% with reach gradient (S_w) does not yield a valid model using least-squares regression because residuals are positively skewed. Estimation using robust least-trimmed squares regression visually appears to better represent most of the study reaches (fig. 4.10). But this simple model,

$$P\% = 31.3 - 475\, S_w \qquad (4.7)$$

has an estimated coefficient of determination of only 21.4 percent and a scale estimate of residuals (analogous to RSE for least-squares) of 6.9 percent of reach length. Residuals from the LTS regression are not different between streams (rank-sum test $p > 0.5$).

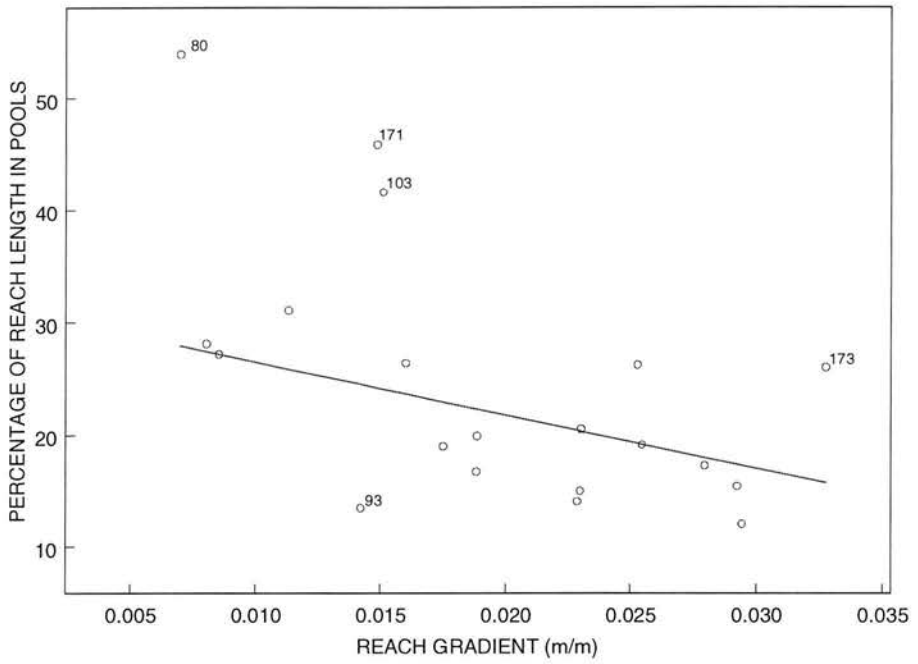

Figure 4.10. Fit of robust linear regression model for percentage of reach length in pools (eq. 4.7).

4.3.6 Mean Depth of Residual Pools

The reach-average residual-pool mean depth (D_r) ranged from 0.10 m for site 107 to 0.27 m for site 171. Average D_r does not significantly differ between the study streams (table 4.3). D_r was significantly correlated with such other reach-average characteristics as percent pools ($R_s = 0.817$, $p = 0.0004$), reach gradient ($R_s = -0.802$, $p = 0.0005$), percentage of pools as forced-pools ($R_s = -0.619$, $p = 0.0069$), mean size of small LOD contact groups (P_{scg}; $R_s = 0.474$, $p = 0.039$), number of LOD jams ($R_s = 0.464$, $p = 0.043$), and measures of pool width and length.

Linear regression models for D_r using all 20 study reaches produced invalid results (non-normal residuals) because of the anomalously large value of D_r for site 171.

With site 171 excluded, reach gradient explains 74.8 percent of the variability in D_r with a residual standard error of 0.02 m (fig. 4.11).

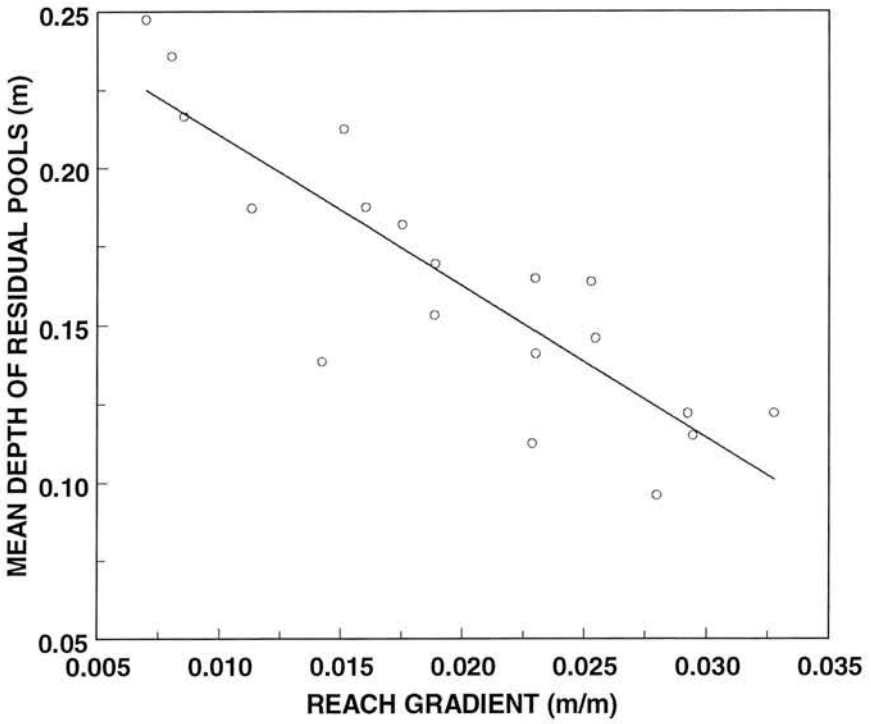

Figure 4.11. Fit of linear regression model for mean depth of residual pools. Equation of fitted regression line shown is: $D_r = 0.26 - 4.80\ S_w$.

4.3.7 Mean Volume of Residual Pools

The reach-average residual volume per pool (V_r) ranged from 0.95 m^3 for site 107 to 16.6 m^3 for site 73. Average V_r for Jones Creek was 2.2 to 2.4 m^3 greater than for Crow Creek (table 4.3), but the difference between streams was not significant ($W = 92$, $p = 0.35$) due to large variability among reaches.

Variables highly correlated with V_r include reach gradient ($R_s = -0.811$, $p = 0.0004$), percent pools ($R_s = 0.708$, $p = 0.0020$), percentage of LOD occurring in jams ($R_s = 0.602$, $p = 0.0087$), pieces per LOD accumulation ($R_s = 0.598$, $p = 0.0092$), pieces per small accumulation ($R_s = 0.595$, $p = 0.0096$), and the ratio, L_t:W_{bf}, between mean piece

length and channel width (R_s = -0.595, p = 0.0094). Other variables significantly correlated with V_r include the percentage of LOD loading occurring in jams (R_s = 0.554, p = 0.016), number of LOD jams (R_s = 0.531, p = 0.021), and LOD frequency in jams (R_s = 0.524, p = 0.022).

The residuals from linear regression suggested that logarithmic transformation of V_r would improve the normality of the residuals. Simple linear regression of $\log(V_r)$ with reach gradient as the independent variable explains 64.2 percent of the variation with a RSE of 0.23 log units. Stepwise selection indicated that the ratio, L_t:W_{bf}, should be added to an expanded linear model for $\log(V_r)$, along with the dummy variable, WS, for stream identity. The resultant multiple-regression model,

$$\log(V_r) = 2.49 - 42.2\, S_w - 1.33\, (L_t{:}W_{bf}) - 0.33\, WS \qquad (4.8),$$

was fit to a data set trimmed by the exclusion of data for site 173, which caused residuals to be non-normally distributed. The fitted model (fig. 4.12) explains 86.4 percent of the variability in $\log(V_r)$ with a RSE of 0.155 log units. Tests of the independent variables' coefficients indicate very significant improvement in explanatory power for each variable: S_w (t = -7.57, p < 0.0001), L_t:W_{bf} (t = -4.18, p = 0.0008), and WS (t = -3.46, p = 0.0035). Milder reach gradients are positively associated with larger pool volumes. As the length of pieces of LOD increases relative to channel width, pool volumes decrease, probably because individual pieces are more stable (e.g., wedged against both banks) and are associated with small forced pools. After accounting for these relations, $\log(V_r)$ averaged 0.33 log units smaller (with 0.094 SE) in Jones Creek than in Crow Creek. Most of the variability in residual-pool mean volume is correlated with reach gradient, whereas residual differences may be caused by LOD dynamics.

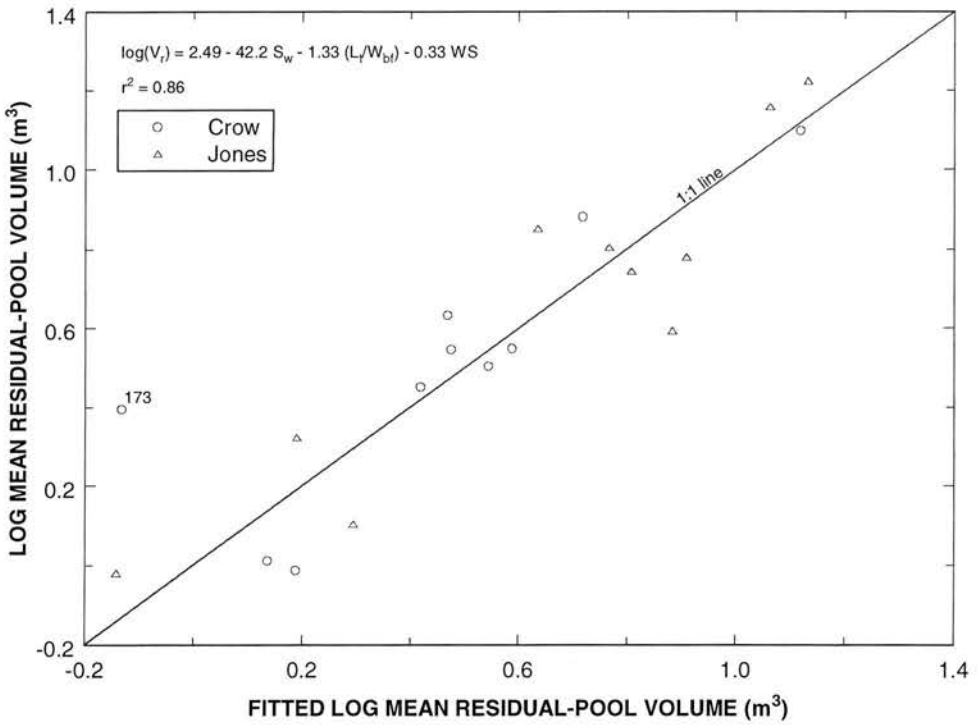

Figure 4.12. Fit of multiple regression model for mean volume of residual pools. Model was fit to trimmed data set excluding reach 173.

Crow Creek reach 173 is poorly described by equation 4.8. As noted in section 4.1, site 173 has an anomalously narrow channel, probably due to the flow diversion just upstream. Its small value of W_{bf} causes an inflated value of L_t:W_{bf} that in equation 4.8 produces a much smaller estimate of $\log(V_r)$ than would otherwise be the case (fig. 4.12). Hence, reach 173 was excluded from model parameterization.

These results demonstrate the importance of channel gradient to both D_r and V_r. This is consistent with results reported by other workers (Phillips and Harlin, 1984; Frissell and others, 1986) who found that variations of slope within a stream segment were so large that channel form could not be explained without primary reference to complex local profiles at the reach scale.

4.3.8 Fine Sediment in Residual Pools

The reach-average volume of fine sediment per residual pool (V_{rf}) ranged from 0.12 m^3 for site 197 to 5.40 m^3 for site 171. Median V_{rf} for Crow Creek reaches is 0.49 m^3 versus 0.87 m^3 for Jones Creek. Variability in V_{rf} among the reaches of both streams is quite large (CV > 100 percent) and makes the difference between streams statistically insignificant ($W = 92$, $p = 0.18$). Some variability in V_{rf} likely results from the measurement of pools of different types, some of which are not as likely to be sites of fine-sediment storage.

Several reach characteristics were highly correlated with V_{rf}, including median particle size of pool fines ($R_s = -0.870$, $p = 0.0002$), percent pools ($R_s = 0.811$, $p = 0.0004$), reach gradient ($R_s = -0.776$, $p = 0.0007$), the ratio of mean residual-pool depth to riffle-crest depth ($R_s = 0.734$, $p = 0.0014$), and mean thickness of LOD-associated fine-sediment deposits ($R_s = 0.784$, $p = 0.0017$). Also significantly rank-correlated with V_{rf} were mean pool width ($R_s = 0.579$, $p = 0.0117$), mean LOD-associated fine-sediment volume per 100 m ($R_s = 0.639$, $p = 0.0085$), pieces per small LOD accumulation ($R_s = 0.550$, $p = 0.017$), median particle size of riffle armor ($R_s = -0.538$, $p = 0.019$), forced-pools as a percentage of pools ($R_s = -0.506$, $p = 0.027$), and percentage of LOD occurring in jams ($R_s = 0.500$, $p = 0.029$).

Simple linear regression of the logarithms of V_{rf} with reach gradient explains 64 percent of the variability in $\log(V_{rf})$ with a RSE of 0.31 log units (fig. 4.13). This was the best linear model found, and it was not improved by adding a dummy variable for a difference between streams ($F = 0.539$, $p > 0.5$).

For each study reach, the weighted-average ratio of residual-pool fine sediment volume to residual-pool volume (V^*_w) was calculated following Hilton and Lisle (1993).

V^*_w values range from 0.09 for site 173 to 0.43 for site 171 (fig. 4.14). The difference between streams is not significant (W = 91, one-sided p = 0.16). Except for two positive outliers (Crow Creek reaches 171 and 179), the difference between streams in V^*_w would be significant. Outliers are discussed at greater length following the consideration of correlations and linear models.

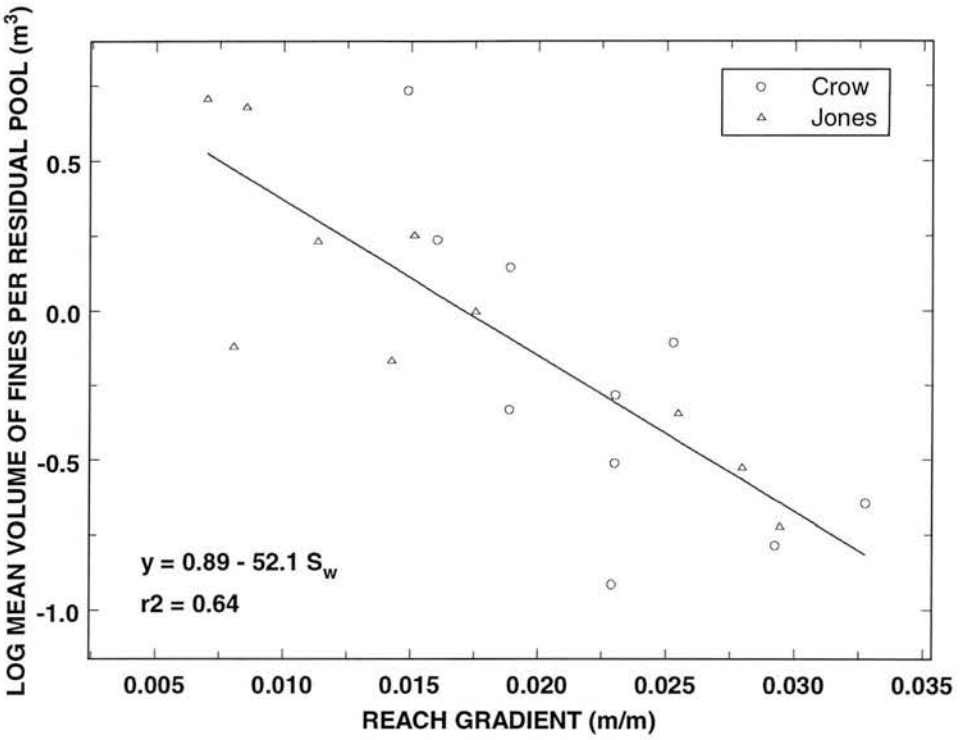

Figure 4.13. Fit of linear regression model for mean volume of fine sediment per residual pool.

Variables highly rank correlated with V^*_w include percent pools (R_s = 0.683, p = 0.0030), pool spacing (SP; R_s = -0.636, p = 0.0055), and pool-fines d_{50} particle size (R_s = -0.617, p = (0.0072). Other reach characteristics significantly correlated with V^*_w include mean LOD volume per piece (R_s = -0.570, p = 0.013), D_r (R_s = 0.565, p = 0.014), ratio of residual-pool mean depth to riffle-crest depth (R_s = 0.483, p = 0.036), riffle-surface d_{50} particle size (R_s = -0.504, p = 0.028), percentage of pools forced by obstructions (R_s = -0.481, p = 0.036), and V_r (R_s = 0.459, p = 0.046).

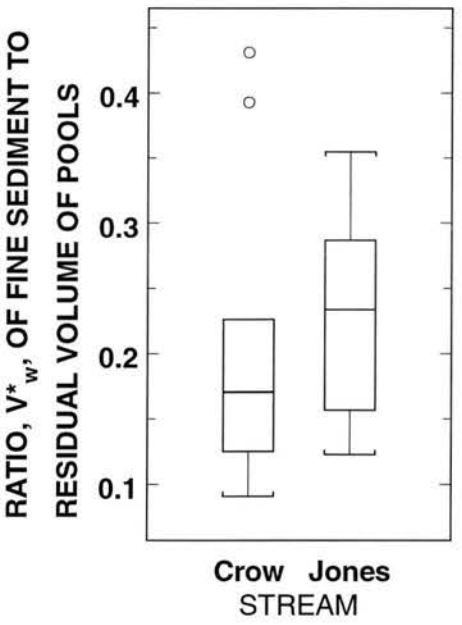

Figure 4.14. Boxplot diagrams of frequency distributions of ratio, V^*_w, of volume of residual-pool fine sediment to total volume of residual pools.

Residuals from linear regression indicated that linear models would benefit from a logarithmic transformation of V^*_w. Also, site 179 consistently caused a non-normal distribution of residuals and was excluded from the final model analysis. Simple linear regression of $\log(V^*_w)$ with pool spacing (SP) explains 39.5 percent of the variability in the dependent variable with a RSE of 0.16 log units. Stepwise selection suggested that LOD volume per piece (V_a) and residual pool volume also might be included in a multiple linear regression model for V^*_w, and the preferred model includes their interaction as a fourth independent variable. The fitted model,

$$\log(V^*_w) = -0.166 - 0.059\ SP - 2.23\ V_a - 0.036\ V_r + 0.297\ V_a{:}\ V_r \qquad (4.9),$$

explains 86.8 percent of the variation in $\log(V^*_w)$ with a RSE of 0.078 log units (fig. 4.15). Adding WS as an additional independent variable does not improve this model ($F = 0.0016$, $p > 0.5$). The results indicate a high level of significance ($t = -3.61$, $p = 0.0028$) for the inverse relation between V^*_w and pool spacing. Pools in mountain forest

streams are most widely spaced in plane-bed and other channels having relatively few obstructions. Such channels also are associated with smaller V^*_w ratios.

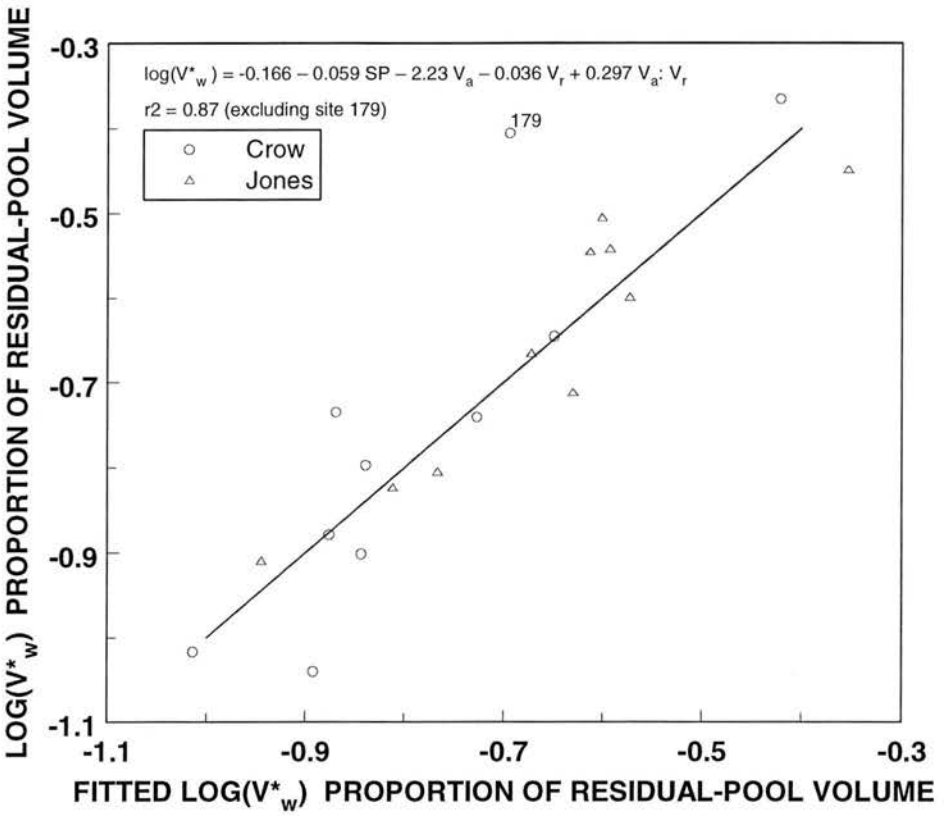

Figure 4.15. Fit of multiple linear regression model for ratio, V^*_w, of volume of residual-pool fine sediment to total volume of residual pools. Model was fitted to trimmed data set excluding reach 179.

The interaction between V_a and V_r also is very significant ($t = 3.40$, $p = 0.0043$) in improving the explanatory ability of equation 4.9. For small pools, when mean LOD piece size is large, V^*_w tends to be smaller, presumably because the flow deflection by large debris continues to keep pools scoured free of fine sediment deposits, even during low-flow conditions. However, for reaches with relatively large pools there is no relation between mean LOD piece size and V^*_w. Based on graphical analysis, the interaction only appears to be significant when residual pools are less than about 9 m^3 in volume.

Excluded site 179 is immediately downstream from an incised tributary that features actively headcutting channels within a few hundred meters of its mouth, possibly delivering anomalously large sediment loads to Crow Creek. Alternatively, the outlier value of V^*_w might have resulted from a poor measurement in pool 2, where bank failure connected with an undercut tree along the outer bank of a sharp bend made it difficult to identify a boundary between fine bed material and bank material. Pool 2 of reach 179 had the third largest V* ratio among all pools measured. Among the six pools with V* > 0.5, pool 2 of reach 179 had the smallest pool volume. Among the 19 pools of Crow Creek with $V_r < 1.3$ m^3, pool 2 of reach 179 was the only one with V* greater than 0.40, so the value of V* for pool 2 (0.63) is much greater than any similar-sized pool in Crow Creek. However, if the V* ratio for pool 2 were changed to 0.40, the V^*_w ratio for reach 179 would only decrease from 0.39 to 0.38 versus the prediction of 0.20 (eq. 4.9).

4.3.9 Summary

Study reaches are predominantly forced-pool-riffle channels, but 5 of the 20 reaches are plane-bed channels consisting primarily of riffles. Freely formed pools were found only in reaches that had more than 28 percent of the reach length in pools. Reach-mean pool length expressed as a ratio with mean bankfull channel width is similar for both streams, averaging about 0.8 channel widths. The ratio of pool spacing to mean channel width is similar in magnitude and variability among the reaches of both streams. Pool spacing for 65 percent of study reaches ranges between 2.5 and 4.5 channel widths. A linear regression model for pool spacing indicates that average pool spacing is 5.2 channel widths (measured at riffles) after accounting for differences in channel type and LOD frequency.

A comparison of pool characteristics reveals no differences for percent pools, pool spacing, residual-pool mean depth, or pool length. The similarity of mean pool length for both streams implies that Jones Creek pool geometry, like channel width, has responded to the post-fire increase in streamflow through a proportional increase in size. The inverse relation between pool volume (V_r) and reach gradient explains most of the simple difference between streams in V_r. After accounting for differences in reach gradient and the ratio of mean LOD piece length to channel width, residual-pool mean volume is smaller in the burned stream than in the reference stream. Most of the variability in residual-pool mean volume is correlated with reach gradient, whereas residual differences may be caused by LOD dynamics. The difference between streams in the fraction, V^*_w, of residual volume occupied by fine sediment is not significant.

4.4 Channel Substrate

The spatial variability of streambed materials (e.g., between riffles and pools) must be addressed in understanding sediment processes of gravel-bed channels (Wohl, 2000). Subsequent sections address substrate size distributions of riffles and pool fines.

4.4.1 Bed-surface Material in Riffles

This section summarizes the size distribution of the bed surface, or armor layer, on riffles of the study streams. Quality assurance results are first discussed to provide perspective on the accuracy and precision of the size-distribution data.

4.4.1.1 Quality Assurance Results

Pairs of within-riffle replicate pebble-count samples were collected at seven riffles in six study reaches. RMS difference between replicate sample proportions in four

size fractions ranged from 5.8 to 8.1 percent for samples collected in 1999, and from 4.9 to 12.1 percent for all seven replicate pairs. Replicates had smaller RMS differences in the finer and coarser fractions than in the fractions between 8 and 128 mm in size. Differences between replicates in the grain-size distribution (GSD) were not significant ($\alpha = 0.05$) for the five reaches where both samples were collected in 1999, as measured by the chi-square test of heterogeneity. Two riffles (both in reach 171) did have significant heterogeneity between the replicate samples within a single riffle, but the samples composing both of these pairs were collected in different years. Particle diameters in the 1998 samples were measured using a ruler, whereas the 1999 samples were measured using a template. Interestingly, the size distributions of the two riffles in 1999 were more homogeneous ($\chi^2 = 9.18$, $p = 0.057$) than were the within-riffle across-years replicates. It appears that either the difference in measurement method or in substrate condition between the two field seasons is a more significant source of variability in the GSD data than is spatial variability within an individual riffle. Presuming the method difference to be the more likely source of extraneous variability (cf. Bunte and Abt, 2001), subsequent comparisons were made using template-measured GSDs whenever possible.

GSD data for 17 of the 20 study reaches were collected from two different riffles using identical methods. Of these, six pairs of between-riffle replicates showed significant differences ($\alpha = 0.05$) in GSD when compared using the chi-square test of heterogeneity. Chi-square tests of independence for binomial data were used to examine whether specific grain-size categories might be associated with differences in the between-riffle replicate samples. Three pairs of between-riffle samples differed in the percentage of particles less than 8 mm in diameter, four pairs differed in the 8 to 32-mm

fraction, and three pairs differed in the 32 to 128-mm fraction. Of 12 pairs of samples having expected counts of at least five in the 128 to 512-mm fraction, four pairs differed significantly in the sample proportion falling into that size category. Although the coarser fraction was especially prone to showing between-riffle differences, these results indicate that representative reach-scale grain-size data for any size fraction in coarse-bedded streams should include sampling from multiple riffle areas within a reach. Channel gradients of individual riffles were not measured, but probably are one factor contributing to this variability.

4.4.1.2 Reach-Average Grain Size

For each study reach, percentages by size category were averaged over the sampled riffles to produce a reach-mean grain-size distribution. Streamwise mean GSD for riffle armor is summarized graphically in figure 4.16. The 90-percent confidence intervals shown were computed pointwise for the mean percentage finer than each grain-size class limit, not as a simultaneous confidence interval (cf. Petrie and Diplas, 2000). Median grain sizes indicate that both streams' riffles typically are armored with gravel.

Reach-average grain-size distributions of riffle armor as summarized for five size fractions (table 4.4) only showed a significant difference ($\alpha = 0.05$) between streams for the fraction less than 8 mm, with Jones Creek being deficient in the fine fraction relative to Crow Creek. Although not summarized in the table, each one-phi-unit interval from 8 to 256 mm also was tested for potential difference between streams, but none were found. For the fraction finer than 8 mm, Crow Creek reaches averaged 12.3 percent and Jones Creek reaches averaged 8.4 percent, or 68 percent of the mean for Crow Creek. However, other workers have noted that the pebble-count method becomes increasingly

difficult to apply reliably as grain sizes decrease below about 8 to 15 mm (Fripp and Diplas, 1993; Kondolf, 1997).

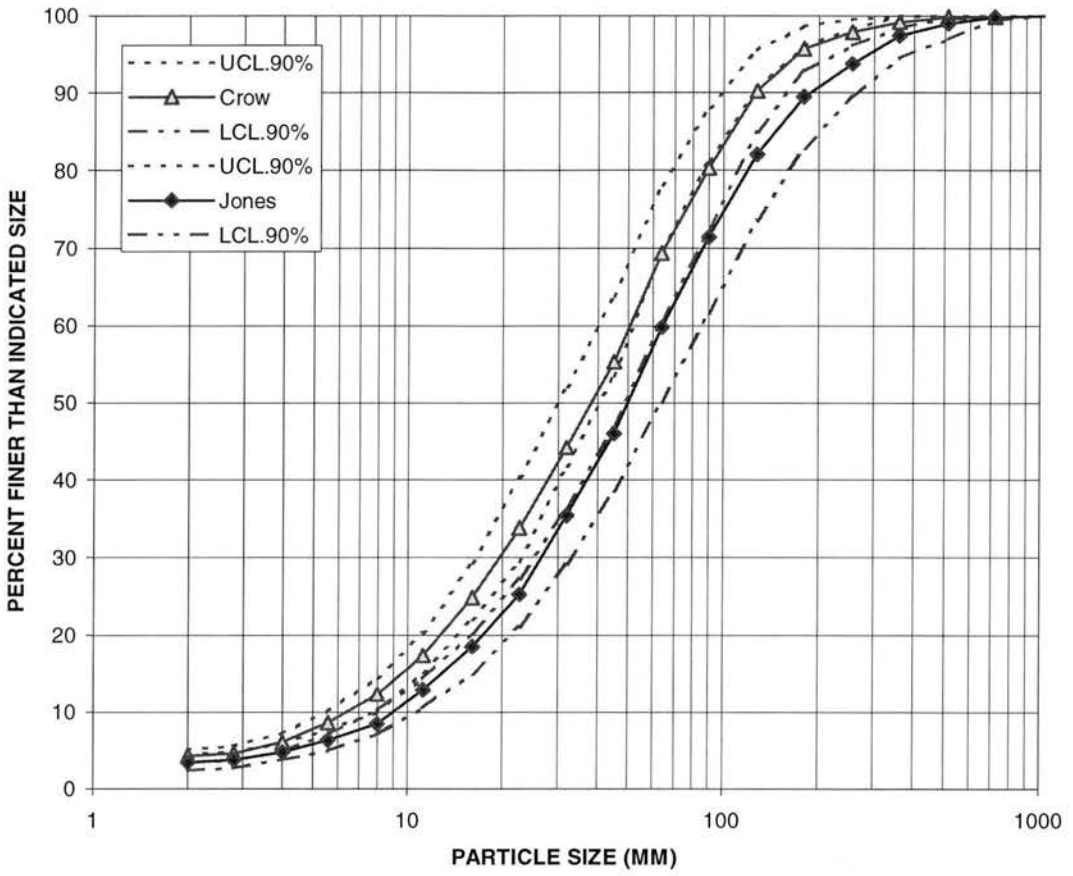

Figure 4.16. Mean grain-size distributions of riffle armor of study reaches. Limits of 90-percent confidence intervals are shown.

The next largest difference, in terms of significance level, was for the percentage in the 128 to 256 mm fraction, followed by the fraction coarser than 256 mm. For the fraction coarser than 256 mm, the frequency distribution for the reach-average percentages was right-skewed, so the median is a more reliable average than the mean. Jones Creek reaches averaged 4.0 percent boulders in their riffle armor, compared with only 0.7 percent for Crow Creek, but large variability among reaches within each stream causes the difference between stream averages to be insignificant.

Table 4.4 – *Summary of reach-average riffle-armor characteristics.*

[CV, coefficient of variation; p-value, probability value; sample size is 10 reaches for each stream (2 riffles per reach); pct, percent; ϕ, phi units.]

Riffle-armor characteristic	Variable name	Crow Creek			Jones Creek			p-value for rank-sum test of different medians
		Mean	Median	CV (%)	Mean	Median	CV (%)	
Grain size, pct finer than 8 mm	$(G\%_{fg})_R$	12.3	12.1	29.5	8.4	8.1	28.5	.0115
Grain size, pct in 8 to 32 mm fraction	$(G\%_{mcg})_R$	31.9	30.6	36.9	27.0	26.1	34.5	.39
Grain size, pct in 32 to 64 mm fraction	$(G\%_{vcg})_R$	25.2	24.4	20.8	24.4	26.2	28.9	> .5
Grain size, pct in 64 - 256 mm fraction	$(G\%_{cbl})_R$	28.5	26.7	45.0	34.0	33.5	36.1	.35
Grain size, pct coarser than 256 mm	$(G\%_{bld})_R$	2.1	0.7	136	6.2	4.0	123	.25
Grain size, 10th percentile (mm)	$(d_{10})_R$	7.2	6.6	34.1	9.6	9.9	29.1	.063
Grain size, 16th percentile (mm)	$(d_{16})_R$	11.3	10.0	37.4	15.2	14.3	30.7	.026
Grain size, 25th percentile (mm)	$(d_{25})_R$	18.5	16.7	38.8	23.9	23.2	34.4	.069
Grain size, 50th percentile (median) (mm)	$(d_{50})_R$	41.6	37.6	41.9	57.9	50.3	45.0	.105
Grain size, 75th percentile (mm)	$(d_{75})_R$	80.2	74.8	39.3	113	102	53.2	.22
Grain size, 84th percentile (mm)	$(d_{84})_R$	101	95.6	38.6	150	132	59.2	.20
Grain size, 90th percentile (mm)	$(d_{90})_R$	124	115	41.5	196	169	67.0	.19
Grain size, graphic mean (ϕ)	$(M_\phi)_R$	-5.09	-5.03	9.7	-5.54	-5.52	10.0	.075
Sorting, inclusive graphic standard deviation (ϕ)	$(s_\phi)_R$	1.58	1.52	14.6	1.60	1.44	20.0	> .5
Skewness, inclusive graphic (dimensionless ratio)	$(\alpha_\phi)_R$	- .19	- .21	52.5	- .20	- .20	38.5	> .5

Of the determined percentiles of the riffle-armor GSD for each reach, only the $(d_{16})_R$ size differed significantly between streams (W = 75.5, p = 0.026), with Crow Creek having the finer size (fig. 4.17). The range of reach-average median size $(d_{50})_R$ for Crow Creek riffles was 24 to 75 mm, with one study reach having small cobbles as its

median size (fig. 4.17). For Jones Creek, the range was 31 to 118 mm and four reaches had medians in the small cobble class. Streamwise average $(d_{50})_R$ was insignificantly coarser in Jones Creek than Crow Creek (50 mm versus 38 mm, W = 127, p = 0.105). Folk and Ward (1957) consider the graphic mean grain size to be a better overall statistic than the median for comparing the coarseness of multiple sediment samples. This statistic, $(M_\phi)_R$, is coarser among Jones Creek reaches than Crow Creek reaches, with marginal significance (W = 81, p = 0.075).

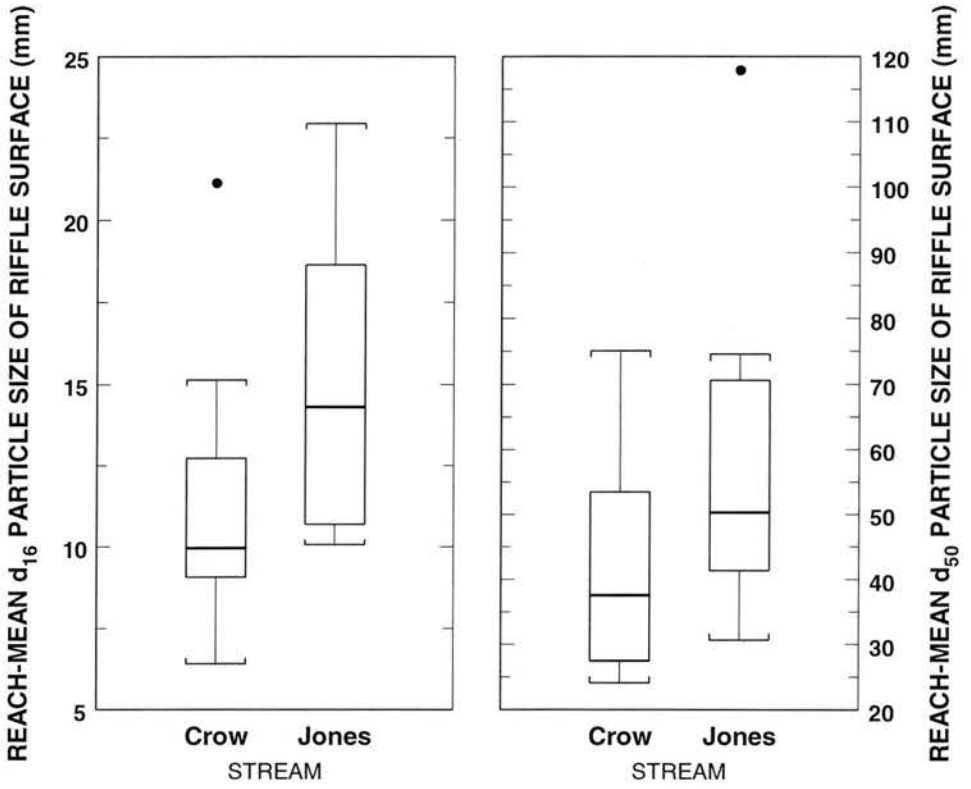

Figure 4.17. Boxplot diagrams of frequency distribution by stream of reach-mean d_{16} and d_{50} sizes of riffle armor.

Riffle-armor median size is rank correlated significantly with such reach characteristics as percentage of LOD being well-anchored (R_s = -0.605, p = 0.0085), number of anchors per piece of LOD (R_s = -0.579, p = 0.0117), mean depth of residual pools (R_s = -0.553, p = 0.016), fine-sediment volume in residual pools (V_{rf}; R_s = -0.538,

$p = 0.019$), percentage of reach length in pools ($R_s = -0.534$, $p = 0.020$), V^*_w ratio ($R_s = -0.504$, $p = 0.028$), volume of LOD-associated fine sediment (FDV_l; $R_s = -0.525$, $p = 0.031$), and percentage of LOD associated with fine-sediment deposits (FS%; $R_s = -0.468$, $p = 0.042$). Graphic-mean size, $(M_\phi)_R$, is correlated with reach gradient ($R_s = -0.453$, $p = 0.048$) as expected. Also, $(M_\phi)_R$ is similarly correlated with many of the same reach-average variables as is $(d_{50})_R$ (e.g., D_r, V_{rf}, P%, FDV_l, and LOD anchoring), but the correlation with active-channel length of LOD is more significant ($R_s = 0.529$, $p = 0.021$).

Negative correlations between average riffle grain size and residual-pool mean depth, active-channel piece length, and LOD anchoring might be related to the effect these factors exert on flow resistance, current velocity, and consequent stream power. Greater unit stream power in steeper reaches would tend to enhance selective entrainment of fine particles from riffles and deposition in pools and other slack-water zones during waning flows. This may explain the correlations between average grain size on riffles and indicators of sedimentation in pools (V_{rf}, V^*_w) and deposition near LOD (FDV_l, FS%).

Linear regression models for $(M_\phi)_R$ were fitted to test for significance of differences between streams after accounting for differences in gradient and other independent variables. The simple regression of graphic mean size with reach gradient (S_w) is significant ($F = 5.42$, $p = 0.032$), but explains only 23 percent of the variability in $(M_\phi)_R$, and has a RSE of 0.51ϕ. Adding the dummy variable for stream identity to the simple model dramatically increases model significance ($F = 17.97$, $p < 0.0001$) and the coefficient of determination (0.68), and decreases the RSE to 0.34ϕ. In this model,

$$(M_\phi)_R = -3.80 - 57.1\ S_w - 0.80\ WS \qquad (4.10),$$

coefficients for both independent variables are highly significant ($p = 0.0001$), and the coefficient for WS indicates that $(M_\phi)_R$ is 0.80ϕ coarser (with 0.16ϕ SE) on average for Jones Creek than for Crow Creek, after accounting for differences in reach gradient (fig. 4.18).

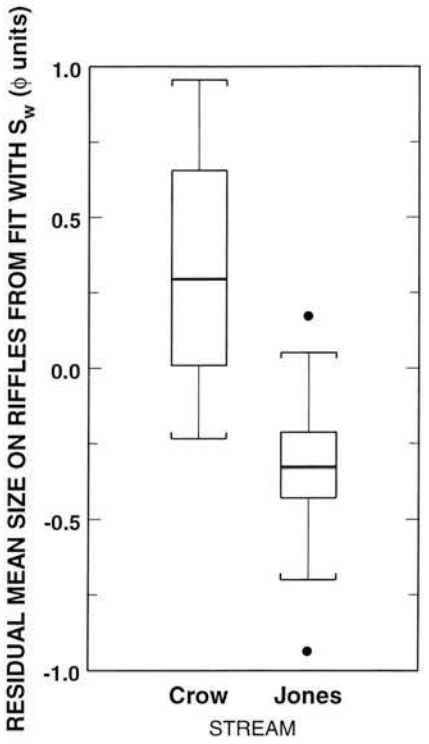

Figure 4.18. Boxplot diagrams by stream of residuals from simple linear regression of graphic mean size of riffle armor with reach gradient.

The selected regression model indicates that fining of riffles (i.e., increased $(M_\phi)_R$) accompanies decreases in both gradient and pool spacing. The model,

$$(M_\phi)_R = -3.32 - 53.0\ S_w - 0.15\ SP - 0.83\ WS \qquad (4.11),$$

explains 77.0 percent of the variance in $(M_\phi)_R$ with a RSE of 0.29ϕ (fig. 4.19). The model ($F = 17.8$, $p < 0.0001$), and coefficients for WS ($t = -5.74$, $p < 0.0001$), S_w ($t =$

-5.42, p = 0.0001), and SP (t = -2.52, p = 0.023) are each significant. This model indicates that $(M_\phi)_R$ is 0.83ϕ units coarser (with 0.14ϕ SE) on average for Jones Creek than for Crow Creek after accounting for effects of reach gradient and pool spacing. Similarly, the coefficient for SP indicates a 0.15ϕ fining in $(M_\phi)_R$ (with 0.06ϕ SE) for each channel-width decrease in mean pool spacing.

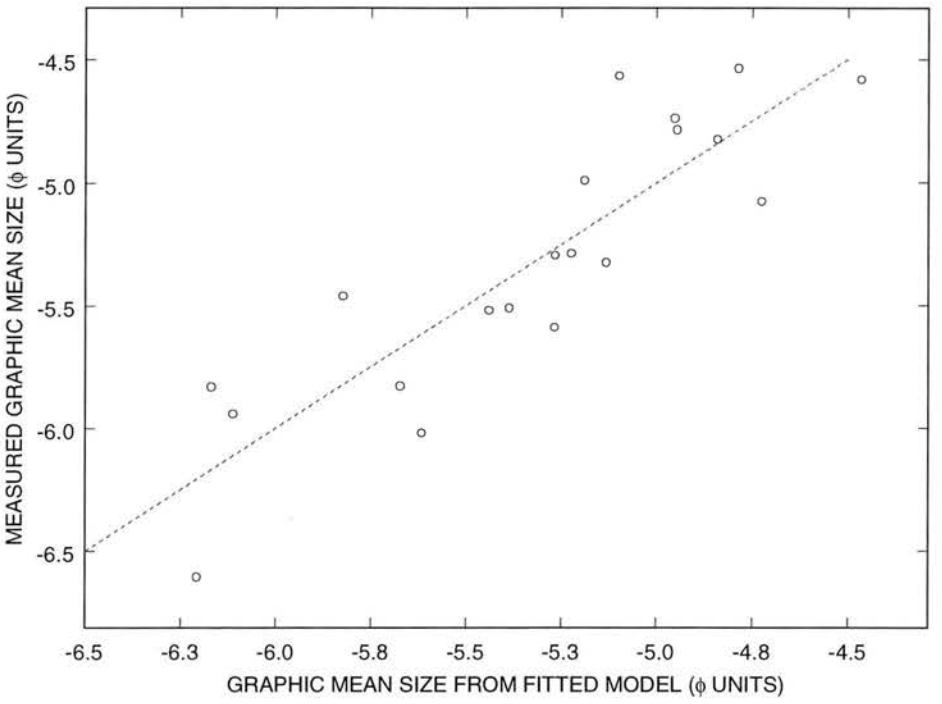

Figure 4.19. Fit of multiple linear regression model for graphic mean size of riffle armor (eq. 4.11).

The difference between streams indicated by these models is somewhat larger than the nearly 0.5ϕ difference in $(M_\phi)_R$ averages shown in table 4.4. Because much of the within-stream variability is accounted for by the other independent variables in the regression models, the t-test of the WS coefficient is significant whereas the rank-sum test result is not. The coefficient for gradient indicates a coarsening of the grain size by about 0.53ϕ per 1 percent increase in channel gradient. The model results reflect effects

of decreased stream power in lower-gradient reaches, especially those with more frequent pool-riffle sequences and consequently greater resistance to flow by these bedforms.

4.4.1.3 Sorting

Reach-average values of the inclusive graphic standard deviation, $(s_\phi)_R$, ranged from 1.24 for site 179 to 2.08 for site 71. Site 75 is the only other site with average sorting greater than 2.00 and hence categorized as very poorly sorted (Folk and Ward, 1957). Stream averages of $(s_\phi)_R$ are similar for both streams (table 4.4), indicating that both streams' riffles are characterized by poorly sorted beds (cf. Folk and Ward, 1957).

Average sorting of riffle armor is correlated significantly with mean grain size of pool fines ($R_s = 0.732$, $p = 0.0014$), mean depth of residual pools ($R_s = -0.699$, $p = 0.0023$), percentage of reach length in pools ($R_s = -0.693$, $p = 0.0025$), mean volume of fines deposited in residual pool ($R_s = -0.632$, $p = 0.0058$), volume of fines associated with LOD (FDV_l; $R_s = -0.591$, $p = 0.0146$), reach gradient ($R_s = 0.561$, $p = 0.015$), V^*_w ($R_s = -0.558$, $p = 0.015$), V_r ($R_s = -0.508$, $p = 0.027$), and mean size of LOD jam (P_{jam}; $R_s = 0.536$, $p = 0.027$). The signs of these rank-correlation coefficients are negative, except for size of pool fines, reach gradient, and LOD jam size. Smaller values of $(s_\phi)_R$ indicate better sorting, so the negative correlations indicate a positive association with improved sorting of riffle armor.

The correlations of riffle-armor sorting with pool depth and storage of fines in pools may reflect improved trapping efficiency by deeper pools for the finest fraction winnowed from riffles during hydrograph recession. As this process becomes increasingly effective, the sediment populations of riffle armor and pool fines could become more segregated, and better sorted riffle armor may result. The correlation of

sorting with the volume of fine deposits associated with LOD might indicate a similar storage process acting to effectively segregate fine sediment winnowed from riffles and store this sediment during low-flow periods. However, a second interpretation stems from associating two sets of results. First, deeper pools are associated with lower-gradient reaches (R_s = -0.802, p = 0.0005). Second, reach gradient is significantly correlated with the particle-size percentiles on the coarse limb of the riffle-armor GSD (p < 0.015 for $(d_{75})_R$ through $(d_{90})_R$), but is not correlated with the percentiles on the fine limb. The improved sorting of riffle armor in reaches with deeper pools (lower-gradient reaches) may be the result chiefly of decreased size of the coarse fraction in the riffle armor.

4.4.2 Deposits of Fine Sediment in Pools

Of the 30 Crow Creek pools where fine sediment was sampled, 47 percent were associated with scour around an obstruction, 40 percent were formed at a channel constriction, 40 percent were plunge pools, and 27 percent were formed on a channel bend. Of the 30 Jones Creek pools sampled, 57 percent were scour-related, 43 percent were at channel constrictions, 23 percent were plunge pools, and 13 percent were on channel bends. To permit a more rigorous analysis of relations between grain-size of pool fines and pool characteristics, several pool variables were summarized using data only from the 60 sampled pools. The data for sampled pools are summarized in table 4.5.

The reach-average grain-size data for fine sediment in pools are summarized in table 4.5, both for percentages in each of four size fractions, and for percentiles and other selected parameters of the size distribution. Both streams' pool fines are predominantly coarse sand to very fine gravel, with 80 percent of reaches having from 25 to 45 percent of pool fines material in the 0.6 to 4.75 mm fraction. Only four study reaches had more

Table 4.5 – *Summary of reach-average characteristics of pools in which fine-sediment was sampled.*

[CV, coefficient of variation; p-value, probability value; sample size is 10 reaches for each stream (3 pools per reach); pct, percent; ϕ, phi units; --, not tested.]

Pool characteristic	Variable name	Crow Creek			Jones Creek			p-value for rank-sum test of different medians
		Mean	Median	CV (%)	Mean	Median	CV (%)	
Residual pool mean depth (m)	$(D_r)_{sp}$	0.16	0.16	29.1	0.17	0.18	31.4	--
Pool length (m)	$(L)_{sp}$	7.4	6.3	39.0	8.3	8.3	38.8	--
Residual volume per pool (m^3)	$(V_r)_{sp}$	4.0	3.0	89.6	6.1	5.8	89.6	--
Fine-sediment volume per residual pool (m^3)	$(V_{rf})_{sp}$	.98	.44	126	1.60	1.12	124	--
Ratio of pool fines volume to residual volume	$(V^*_w)_{sp}$	.22	.18	63.0	.22	.22	30.2	--
Grain size of pool fines, pct finer than 0.6 mm	$(G\%_{0.6})_p$	24.2	18.3	48.9	27.4	29.6	52.4	> 0.5
Grain size of pool fines, pct from 0.6 to 1.18 mm	$(G\%_{1.18})_p$	13.7	11.3	39.8	13.9	13.8	35.3	.48
Grain size of pool fines, pct from 1.18 to 2.36 mm	$(G\%_{2.36})_p$	11.3	9.8	45.0	12.0	11.5	14.5	.34
Grain size of pool fines, pct coarser than 2.36 mm	$(G\%_{>2.36})_p$	50.8	54.4	36.3	46.7	45.8	33.9	.25
Pool fines, 10th percentile of grain size (mm)	$(d_{10})_p$	.34	.38	38.6	.37	.27	83.1	.26
Pool fines, 16th percentile of grain size (mm)	$(d_{16})_p$	.49	.52	39.0	.54	.35	87.5	.35
Pool fines, 25th percentile of grain size (mm)	$(d_{25})_p$	.82	.91	50.1	.80	.49	89.9	.28
Pool fines, 50th percentile of grain size (mm)	$(d_{50})_p$	3.5	3.0	59.9	2.2	1.8	69.3	.072
Pool fines, 75th percentile of grain size (mm)	$(d_{75})_p$	8.1	8.0	49.0	6.8	6.8	36.1	.083
Pool fines, 84th percentile of grain size (mm)	$(d_{84})_p$	11.1	11.2	45.5	10.6	10.5	27.8	.27
Pool fines, 90th percentile of grain size (mm)	$(d_{90})_p$	14.0	14.0	30.8	13.6	13.0	21.2	.38
Pool fines, graphic mean grain size (ϕ)	$(M_\phi)_p$	-1.21	-1.40	68.1	-.99	-.83	75.7	.28
Sorting, inclusive graphic standard deviation (ϕ)	$(s_\phi)_p$	2.15	2.11	10.6	2.20	2.30	13.0	.39
Skewness, inclusive graphic (dimensionless ratio)	$(\alpha_\phi)_p$	- .17	- .24	153	.07	- .03	338	.043

than 33 percent of sampled material finer than 0.6 mm (medium sand or finer). This may reflect partial elutriation of the finest fraction caused by the sampling method of using the hand to seal the bottom of the sampling pipe. Another contributing factor is the current strength in many of the sampled pools, even at low flow, resulting from the upstream riffle gradient and small size of many pools. Sufficient energy appeared available to transport finer sands either into shallow pool-margin deposits beyond the residual pool or downstream out of the pool.

There were no significant differences between streams for any of the percentages by size fraction. However, the 50th and 75th percentiles of the reach-average GSD were finer in Jones Creek on average, with marginal significance ($p = 0.072$ and $p = 0.083$, respectively), but differences between streams for percentiles outside the central half of the grain-size distributions were not significant (see table 4.5 for $(d_{10})_p$, $(d_{16})_p$, $(d_{84})_p$, $(d_{90})_p$). Site 107 on Jones Creek had the coarsest GSD among Jones Creek reaches, particularly on the fine tail of the distribution where it was the coarsest of all 20 study reaches, contributing to the large CV statistics for the lower percentiles. Results for the broadly based graphic mean size statistic, $(M_\phi)_p$, show that fine deposits in pools in both streams are near the class boundary between very coarse sand and very fine gravel, on average. Expressed in phi units, summary statistics for $(M_\phi)_p$ indicate that pool fines tend to be coarser in Crow Creek than in Jones Creek, but the difference is not significant.

Values of the sorting statistic, $(s_\phi)_p$, are not significantly different between streams. Among Crow Creek reaches, 40 percent of study sites have sorting statistics interpreted as poorly sorted (Folk and Ward, 1957), whereas 20 percent of Jones Creek sites are so classified, with the remainder of sites from both streams having very poorly sorted pool fines with $(s_\phi)_p$ values ranging up to nearly 2.5ϕ. The graph of reach-mean

values of graphic mean grain size versus sorting, shown together with lowess-smooth line in figure 4.20, shows a high frequency of poor sorting for sites having mean grain size between –0.5ϕ and –1.0ϕ, consistent with the general pattern for fluvial sediments shown by Folk (1974, p. 6). The substantial improvement in sorting for most sites having mean grain size finer than 0.0ϕ or coarser than -2.0ϕ also is consistent with that general pattern.

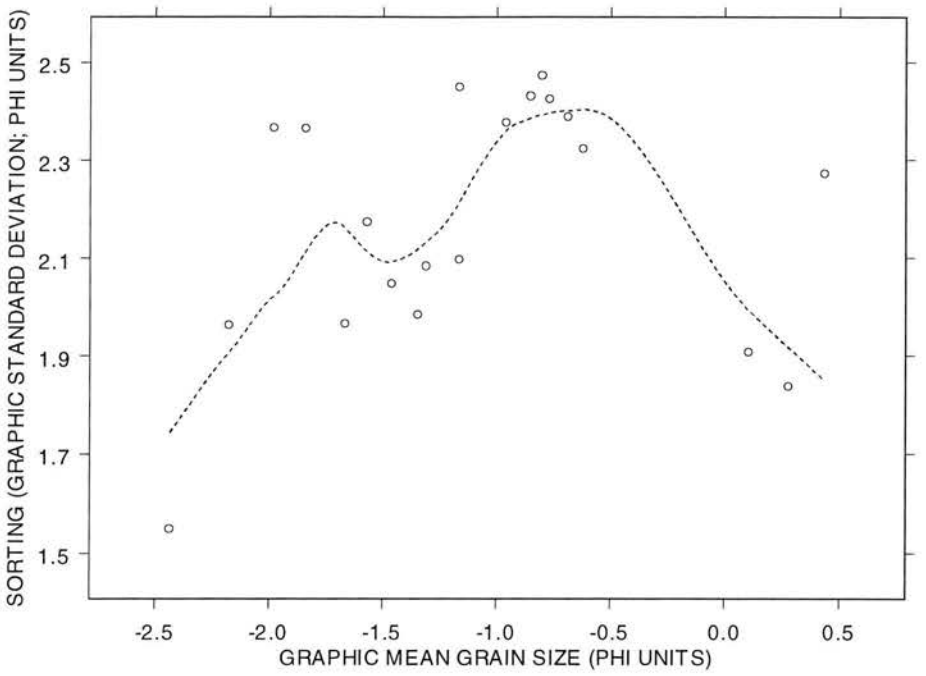

Figure 4.20 Relation between graphic mean grain size and sorting of fine sediment in residual pools. Lowess-smooth line highlights robust curvilinear trend.

Skewness of pool fines is significantly more negative ($p = 0.043$) for Crow Creek reaches than for Jones Creek. A negative value of $(\alpha_\phi)_p$ indicates a GSD having a tail of coarser grains. Using the general classification of grain-size skewness values suggested by Folk and Ward (1957), half of Jones Creek reaches and 20 percent of Crow Creek reaches have nearly symmetrical GSDs ($-0.1 < (\alpha_\phi)_p < +0.1$). Forty percent of Jones Creek reaches have positively skewed GSDs, with half of those falling into the very positively skewed category ($(\alpha_\phi)_p > +0.3$), whereas only site 71 has a negatively skewed

GSD. Among Crow Creek reaches, 70 percent have negatively skewed GSDs, with 50 percent of reaches classed as very negatively skewed ($(\alpha_\phi)_p < -0.3$), and only site 171 has a GSD skewed toward fine sizes ($(\alpha_\phi)_p = +0.39$). The aggraded site 171 appears to be a preferred location for deposition of fines.

The graph of $(M_\phi)_p$ versus skewness (fig. 4.21) shows that most sites with nearly symmetrical GSDs have mean size between -1.5ϕ and -0.7ϕ (very fine gravel to very coarse sand). This may be inferred to represent relatively pure deposits of the dominant grain size transported by these streams during waning flows. For pools having mean grain size finer than about -0.7ϕ the pattern of positively skewed GSDs reflects inclusion of small quantities of fine sand into the mixture. Reaches with mean size coarser than about -1.5ϕ had negatively skewed GSDs that indicate addition of increasing quantities of gravel in the pool fines deposits. Insight into the general correspondence between skewness and mean grain size is found in the strong correlation between mean grain size of pool fines and mean volume per pool-fines deposit ($(V_{rf}$; $R_s = -0.832$, $p = 0.0003$). In pools with more extensive fine deposition, the sampled core often did not reach the base of the deposit, whereas in pools where fines are sparse the relatively coarse base of the deposit typically was included in the sample.

Graphic mean grain size of pool fines (in phi units) also is significantly correlated with reach gradient ($R_s = -0.848$, $p = 0.0002$), mean depth of residual pools ($(D_r)_{sp}$; $R_s = 0.808$, $p = 0.0004$), mean volume of residual pools ($(V_r)_{sp}$; $R_s = 0.806$, $p = 0.0004$), mean pool length ($(PL_m)_{sp}$; $R_s = 0.753$, $p = 0.0010$), mean bankfull pool width ($R_s = 0.682$, $p = 0.0038$), weighted-mean V* ratio ($(V^*_w)_{sp}$, $R_s = 0.678$, $p = 0.0031$), percentage of LOD occurring in large jams ($R_s = 0.569$, $p = 0.0132$), mean active-channel piece length of

LOD (R_s = 0.552, p = 0.0163), and number of LOD jams per 100 meters of channel (R_s = 0.526, p = 0.022).

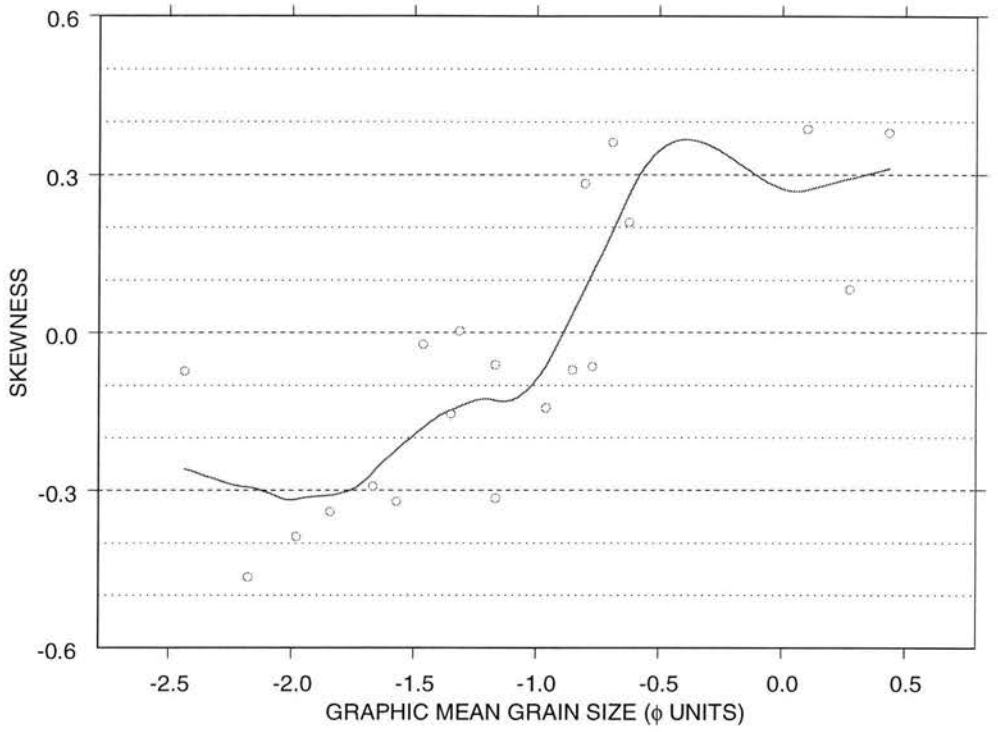

Figure 4.21. Relation between graphic mean grain size and skewness of fine sediment in residual pools. Lowess-smooth line highlights robust curvilinear trend.

Stepwise regression-model selection indicated that a multiple linear model for graphic mean grain size (in phi units) that uses mean volume of sampled residual pools, V^*_w ratio for sampled pools, and active-channel LOD loading (VL_a) as the independent variables was most appropriate. The model,

$$(M_\phi)_p = -2.59 + 0.104\ (V_r)_{sp} + 3.1\ (V^*_w)_{sp} + 0.019\ VL_a \qquad (4.12),$$

explains 86.2 percent of the variability in $(M_\phi)_p$ with a residual standard error of 0.31 phi units (fig. 4.22). Coefficients for $(V_r)_{sp}$ (SE = 0.017, p < 0.0001), $(V^*_w)_{sp}$ (SE = 0.76, p = 0.0009), and VL_a (SE = 0.0079, p = 0.031) were significant in improving the explanatory

power of the model. Moreover, including the dummy variable for difference between streams did not improve the model ($F = 0.0007$, $p > 0.5$).

The largest residuals from the fitted model were about 0.5ϕ from the line of agreement (fig 4.22). Two of the independent variables in the model represent factors associated with reduced current velocity (during low flows) in large pools, producing an environment favorable to deposition of fine sediment. The third independent variable, $(V^*_w)_{sp}$, is interpreted to reflect a relative abundance of mobile fine sediment.

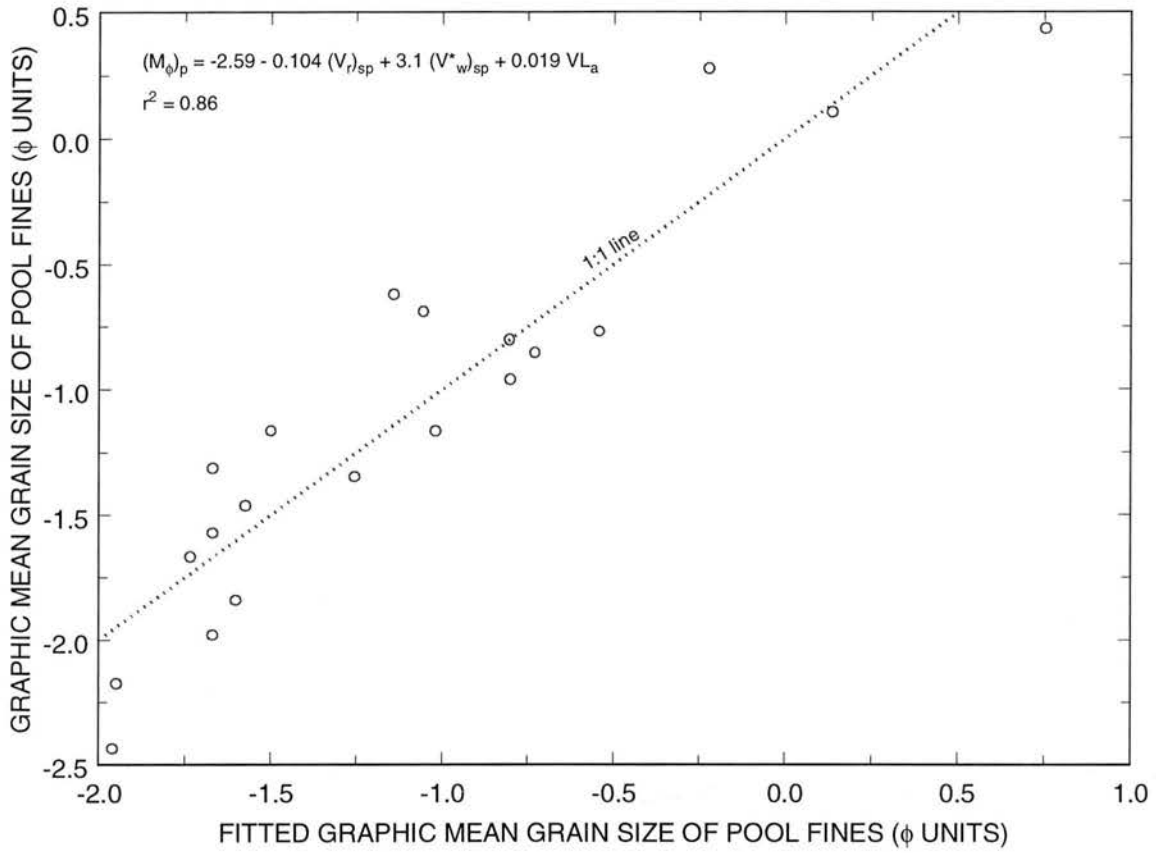

Figure 4.22. Fit of multiple linear regression model for graphic mean size of residual-pool fine sediment (eq. 4.12).

4.4.3 Summary

Graphic mean size of riffle armor $(M_\phi)_R$ is 0.83ϕ units coarser on average for Jones Creek than for Crow Creek after accounting for effects of reach gradient and pool

spacing. The multiple-regression results indicate that graphic mean size coarsens by about 0.53ϕ per 1 percent increase in channel gradient. The high level of significance for the difference between streams (even when pool spacing differences are neglected) suggests strongly that riffle coarsening is a fire-related effect, presumably caused by the increased duration of near-bankfull streamflow.

Sorting of riffle armor is similar for both streams and indicates that poor sorting characterizes riffles of nearly all reaches. Correlations of riffle-armor sorting with pool depth and storage of fines in pools might indicate improved trapping efficiency in deeper pools for the finest fraction winnowed from riffles during hydrograph recession. However, the improved sorting of riffle armor in lower-gradient reaches with deeper pools may result from the decreased size of the coarse fraction in the riffle armor.

Fine deposits in pools of both streams are predominantly coarse sand to very fine gravel, with 80 percent of reaches having from 25 to 45 percent of pool fines material in the 0.6 to 4.75 mm fraction. Mean grain size of pool fines can be explained largely by factors associated with an environment favorable to deposition of fine sediment (reduced current velocity during low flows in large pools) and relative abundance of mobile fine sediment.

Sorting of pool fines is not significantly different between streams, with a majority of study reaches having very poorly sorted deposits. The relation between reach-mean grain size and sorting is consistent with the typical pattern for fluvial sediments. Forty percent of Jones Creek reaches have size distributions of pool fines skewed toward finer sizes, with only one site showing coarse skewness, whereas 70 percent of Crow Creek reaches have size distributions skewed toward coarse sizes.

Skewness differences between streams appear to be related to differences in mean grain size and mean volume per pool-fines deposit, and may be related to sampling methods.

4.5 Channel Stability

The Pfankuch (1975) channel stability rating is composed of three groups of factors, each of which is rated individually, and may then be subtotaled. Lower ratings correspond to more stable channels. Assigned ratings are listed by reach in table A.8 in appendix A. Summaries for the individual factors (CS_n) and for the subtotals for upper banks (CS_{ub}), lower banks (CS_{lb}), and streambed (CS_{sb}) are listed in table 4.6, along with the summary for the overall channel stability index (CS_{tot}). As a caveat, it is readily acknowledged that the author's limited experience with this rating system undoubtedly affects the reliability of the channel-stability ratings. These were the first pair of streams where the author has used the Pfankuch (1975) assessment methods.

4.5.1 Channel Stability Index

Scores for CS_{tot} ranged from 74.5 at site 173 to 113 at site 171 among Crow Creek reaches and from 74 at site 107 to 103 at site 80 along Jones Creek. Streamwise averages (table 4.6) were not significantly different between streams ($W = 124.5$, $p = 0.15$). Ten percent of Crow Creek reaches had CS_{tot} ratings falling into the "good" range of channel stability, as proposed by Pfankuch (1975), and 20 percent of Jones Creek reaches would be so classified. The remaining reaches had CS_{tot} ratings falling into the "fair" range. However, Myers and Swanson (1992) correctly noted that the range of ratings in each qualitative category is skewed. For example, if a reach is rated at the excellent end of the scale on every factor, it just barely falls into the "excellent" range, and the same is true for the "good" and "fair" ranges. If each range is shifted upward by

one-half the range width (i.e., a 19-point shift) to correct for this skew, a different description of overall channel stability results. Interpreted using these adjusted ranges, 60 percent of Crow Creek reaches and 90 percent of Jones Creek reaches received ratings in the "good" stability range (ratings of 58 – 95), with the remainder of reaches in the "fair" range (96 – 133).

Table 4.6 – *Summary of channel-stability characteristics.*

[CV, coefficient of variation; p-value, probability value; U.B., upper bank; L.B., lower bank; S.B., streambed; sample size is 10 reaches for each stream.]

Channel-stability characteristic	Variable name	Crow Creek			Jones Creek			p-value for rank-sum test of different medians
		Mean	Median	CV (%)	Mean	Median	CV (%)	
U.B. slope	CS_1	7.8	8.0	8.1	7.8	8.0	8.1	> 0.5
U.B. mass-wasting potential	CS_2	8.2	8.0	23.6	7.5	8.0	22.9	.44
U.B. floatable objects	CS_3	6.6	6.8	16.3	6.4	6.0	16.8	> .5
U.B. vegetation density	CS_4	6.4	6.5	19.8	6.0	6.0	30.4	> .5
L.B. channel capacity	CS_5	2.4	2.0	29.1	2.0	2.0	0.0	.28
L.B. rock content	CS_6	3.1	3.0	28.2	4.0	3.5	42.5	.26
L.B. flow deflectors	CS_7	4.4	4.0	25.4	4.1	4.0	21.3	> .5
L.B. cut banks	CS_8	11.7	12.0	19.3	10.7	10.5	28.6	> .5
L.B. bar enlargement	CS_9	8.1	8.0	25.7	7.3	7.0	26.7	.44
S.B. angularity	CS_{10}	2.0	2.0	26.4	2.1	2.0	15.1	> .5
S.B. brightness	CS_{11}	2.7	3.0	17.9	1.9	2.0	38.8	.026
S.B. packing	CS_{12}	4.9	5.0	19.5	4.6	4.5	27.5	> .5
S.B. size distribution	CS_{13}	10.6	11.0	20.5	9.6	10.0	27.4	.39
S.B. scour and deposition	CS_{14}	12.0	12.0	27.6	9.0	8.5	28.7	.035
S.B. clinging flora	CS_{15}	2.8	3.0	22.6	1.7	1.5	48.4	.0102
Upper bank stability index	CS_{ub}	29.0	28.5	9.0	27.7	29.0	13.3	> .5
Lower bank stability index	CS_{lb}	29.6	29.0	15.1	28.1	27.0	18.0	.37
Streambed stability index	CS_{sb}	35.0	36.0	18.7	28.9	28.5	22.5	.058
Channel stability index	CS_{tot}	93.6	94.5	13.0	84.7	80.0	11.8	.15

Another modification to Pfankuch's (1975) classification of overall ratings was proposed by Rosgen (1996), who urged comparison among streams of the same type.

Most of the study reaches are in colluvial or confined alluvial valley segments (cf. Montgomery and Buffington, 1993) with consequently narrow flood-prone areas. Though detailed classification is beyond the scope of this study, the reaches would probably be classed as type B3 (cobble dominant) or B4 (gravel dominant) streams in Rosgen's system. For type B4 streams, Rosgen (1996) proposed that the "good" range of channel stability include ratings from 40 to 64, "fair" stability from 65 to 84, and "poor" channel stability as 85 or greater. For type B3 streams, stability ratings from 40 to 60 correspond to "good" conditions, from 61 to 78 indicate "fair" stability, and 79 or greater are generally in "poor" condition (Rosgen, 1996). Using these classes, 20 percent of Crow Creek reaches and 50 percent of Jones Creek reaches fall into the "fair" range, and the remainder are rated as being in "poor" condition.

A number of rank correlations between CS_{tot} ratings and other reach-average characteristics are significant. The 25th through 90th percentiles of riffle armor GSD are correlated with better CS_{tot} ratings ($-0.739 < R_s < -0.622$, $0.0013 < p < 0.0067$). Coarseness and relative immobility of the streambed may indicate greater channel stability, but few of the 15 rated characteristics would be expected to strongly reflect it and affect the total score. Poorer CS_{tot} ratings are correlated with indicators of fine-sediment deposition, including percent of LOD associated with sediment deposits ($R_s = 0.628$, $p = 0.0063$), frequency and volume of LOD-associated sediment deposits per unit channel length ($R_s = 0.580$, $p = 0.0116$ and $R_s = 0.619$, $p = 0.0108$, respectively), and V_{rf} ($R_s = 0.659$, $p = 0.0041$). For similar streams, differences in fine-sediment deposition would affect multiple rated characteristics of the lower banks and streambed.

Factor ratings for each of the three groups of rated characteristics were summed (i.e., variables CS_{ub}, CS_{lb} and CS_{sb}; table 4.6). The only significant correlation among the

three factor-group subtotals is between CS_{lb} and CS_{sb} ($R_s = 0.557$, $p = 0.015$). These two factor groups are more affected by differences in fine-sediment deposition than are upper-bank ratings.

Crow Creek's lower banks were rated as slightly more stable than those of Jones Creek, but the difference was not significant. The tendency toward more unstable banks in Jones Creek, while not significant statistically, is what would be expected in adjustable, coarse-bedded channels that experience post-fire increases in the duration of near-bankfull flows. Channel capacity (CS_5) and rock content (CS_6) were the lower-bank factors for which Crow Creek reaches were rated most stable in comparison with Jones Creek reaches. However, no individual bank-stability factors showed statistically significant differences between streams. Evidence of bank erosion and erodibility was abundant along most reaches of both streams.

Streambed stability (CS_{sb}) was the only factor group with an even marginally significant difference between streams ($W = 130.5$, $p = 0.058$), as the streambed of Jones Creek was more stable than Crow Creek on average. Ratings for individual factors composing CS_{sb} showed three streambed-stability factors for which Jones Creek scored significantly lower (more stable): brightness (median of 2.0 versus 3.0; $W = 134.5$; $p = 0.026$), scour and deposition (median of 8.5 versus 12.0; $W = 133$; $p = 0.035$), and clinging flora (median 1.5 versus 3.0; $W = 138.5$; $p = 0.0102$). However, the scour and deposition factor was critiqued by Myers and Swanson (1992) as not being useful as a visual indicator of stability due to seasonality of scour and difficulty of identifying new deposition. When the scour and deposition factor (CS_{14}) is excluded and the sum of remaining streambed-stability factors is calculated, streamwise median scores are more similar (23 for Crow Creek versus 19.5 for Jones Creek). The difference between

streams for this modified streambed-stability subtotal is barely marginal in statistical significance ($W = 127.5$, $p = 0.097$).

The results provide inconclusive evidence for a difference between streams in overall streambed stability. The slightly better rating for streambed stability in Jones Creek may reflect differences in geology along study segments. The streambed-factors subtotal for reaches adjacent to talus or alluvium (table A.3 in appendix A; median = 35) indicates significantly less stability ($W = 28$, $p = 0.033$) than for reaches adjacent to landslide deposits or the Wapiti Formation (median = 27). Four of the five reaches in the latter group are on Jones Creek.

The single streambed-stability factor that differed most between streams was clinging flora. Post-fire decreases in canopy cover and shading probably improved the habitat for filamentous algae and other clinging flora. Forest regrowth is in early stages where present, but germination of replacement trees has yet to occur in much of the burned area. Shading of Jones Creek will likely remain sparse for years. There were locally vigorous stands of lodgepole pine saplings, but almost no young spruce or fir.

4.5.2 Quality Assurance Results

The pattern of correlations with quantitatively measured variables presented in the previous section lends some credibility to the subjective ratings in Pfankuch (1975). The results from replicate evaluations of one reach (site 173) by the author on July 20 and Sept. 20, 1999, yielded the following differences in assigned ratings: upper-bank vegetation density increased by 2; lower-bank rock content decreased by 2; flow deflectors decreased by 3; and cut banks decreased by 2. The subtotal for upper banks increased by 1 unit, but for lower banks decreased by 7 units, and for streambed

decreased by 3 units. The net decrease of 9 units in overall channel-stability rating represents a change of 11.4 percent from the first evaluation.

4.5.3 Summary

Using the stream-type-specific classification of overall channel-stability ratings (Rosgen, 1996), 20 percent of Crow Creek reaches and 50 percent of Jones Creek reaches fall into the "fair" range, and the remainder are rated as being in "poor" condition. Neither overall channel-stability ratings nor bank-stability ratings were significantly different between streams. The difference between streams in the modified streambed-stability summary rating is only marginal in statistical significance, and appears to reflect geologic differences among stream segments rather than a fire-related difference between streams.

The single streambed-stability factor that differed most between streams was clinging flora. Post-fire decreases in canopy cover and shading probably improved the habitat for filamentous algae and other clinging flora.

4.6 Bedload Reconnaissance

A summary of the eight bedload measurements from study sites made in 1998 is presented along with associated discharge and hydraulic data in table 4.7. The estimated critical dimensionless shear stress, τ^*_{cA} (from eq. 3.3), for three-fourths of the samples is below the range that Andrews (1983) found was hydraulically necessary to entrain the largest mobile particles. If the median particle size of bedload is less than that of the subsurface bed material, then the modification of Andrews (1983) equation for τ^*_c used herein would result in underestimation, which it apparently did. Hence, the τ^*_{cA} values were not used in further analyses. These results do suggest that conditions at the time of

bedload sampling do not reflect equal mobility in that the sampled bedload likely is finer than the subsurface bed material.

Table 4.7 – *Summary of bedload measurements and ancillary data, June 1998.*

[Each sample represents the average of two traverses of the sampled section; time on bottom was 60 s at each sampling point; Q_s, sediment discharge; Q, streamflow discharge, twz, thalweg zone]

Variable	Variable name	Site 80	Site 80	Site 92	Site 92	Site 171	Site 171	Site 181	Site 181
Surface width (m)	W_w	9.14	9.30	6.86	6.86	12.19	11.95	6.52	6.55
Sampled width (m)	W_s	1.52	1.52	1.68	1.68	1.52	1.52	1.60	1.60
Instantaneous bedload Q_s (kg s^{-1})	Q_b	.035	.057	.025	.028	.089	.061	.014	.010
Normalized bedload Q_s (g s^{-1} km^{-2})	Q_{bn}	.89	1.43	1.07	1.22	2.4	1.6	.83	.58
Bedload transport rate (g m^{-1} s^{-1})	I_b	3.85	6.11	3.61	4.11	7.33	5.08	2.16	1.51
Discharge (m^3 s^{-1})	Q	2.53	2.83	1.64	1.62	3.72	3.04	1.68	1.76
Normalized Q (m^3 s^{-1} km^{-2})	Q_n	.064	.071	.071	.070	.099	.081	.099	.103
Mean velocity (m/s)	V_m	.91	.96	.74	.76	.99	.87	.92	.92
Mean depth (m)	D_m	.30	.32	.32	.31	.33	.30	.28	.29
Bankfull slope (m/m)	S_L	.011	.011	.015	.015	.012	.012	.015	.015
Average boundary shear stress (Pa)	τ_0	32.7	34.1	47.4	46.0	38.6	35.9	41.5	43.0
Shields shear stress	τ^*	.065	.068	.095	.093	.094	.088	.048	.050
Mean depth in twz (m)	D_L	.43	.45	.60	.59	.51	.47	.34	.33
Boundary shear stress in twz (Pa)	τ_L	46.7	48.3	87.9	87.0	59.6	55.6	50.2	48.4
Total stream power (W/m^2)	Ω	273	305	243	239	437	359	248	258
Stream power per unit width in twz (W/m)	ω_L	52.4	55.9	89.5	86.4	70.6	59.1	52.1	51.5
25^{th} percentile of particle size (mm)	$(d_{25})_L$	< 1	< 1	3.5	1.85	< 1	< 1	< 1	< 1
Median particle size (mm)	$(d_{50})_L$	1.48	[E] .82	22	10.8	2.1	2.1	2.6	2.2
84^{th} percentile of particle size (mm)	$(d_{84})_L$	11.3	5.5	47	37	20	25	12.0	20
90^{th} percentile of particle size (mm)	$(d_{90})_L$	17.0	23	53	46	32	38	35	24

Variable	Variable name	Site 80	Site 80	Site 92	Site 92	Site 171	Site 171	Site 181	Site 181
95th[th] percentile of particle size (mm)	$(d_{95})_L$	23	42	58	55	45	49	46	28
Sorting, graphic (ϕ)	$(s_\phi)_L$	[E] 2.9	[E] 2.7	2.6	2.6	[E] 3.2	[E] 3.5	[E] 2.2	[E] 3.2
Relative submergence	$\frac{(d_{95})_R}{D_m}$	.29	.28	.22	.22	.23	.24	.48	.46
Mobility ratio 1	$\frac{(d_{95})_L}{(d_{50})_R}$	.76	1.37	1.91	1.78	1.79	1.95	.87	.52
Mobility ratio 2	$\frac{(d_{95})_L}{(d_{50})_L}$	15.8	51	2.6	5.1	21	23	17.9	12.7
Mobility ratio 3	$\frac{(d_{95})_L}{(d_{25})_R}$	1.43	2.6	4.1	3.8	3.4	3.7	1.79	1.07
Critical Shields stress for $(d_{95})_L$ particle size	τ^*_c	.123	.071	.093	.098	.081	.070	.067	.108
Predicted critical Shields stress for $(d_{95})_L$ particle size	τ^*_{cA}	.008	.003	.045	.024	.006	.006	.007	.011

[E] estimated value. For $(s_\phi)_L$, values were estimated as $[(d_{84})_L - (d_{50})_L]$, in ϕ units, because $(d_{16})_L$ is below analysis limit.

4.6.1 Bedload Transport Rate

Bedload transport rates (I_b) ranged from 1.5 to 7.3 g m^{-1} s^{-1} for the measured stream discharges that ranged from 1.62 to 3.72 m^3 s^{-1} (table 4.7). Normalized per unit drainage area, stream discharges ranged from 0.064 m^3 s^{-1} km^{-2} to 0.103 m^3 s^{-1} km^{-2} and generally increased during the sampling period that fell between the snowmelt runoff peaks for 1988 (at North Fork Shoshone River at Wapiti; fig. 4.23). The sampled discharges generally were near, but slightly less than, bankfull stage. At site 171, banks were filled just to where bankfull level would be for an equilibrium channel, but as noted previously this reach has apparently aggraded in recent decades. General mobilization of the coarse surface layer was not observed, although gravel movement was obvious.

Variables significantly rank-correlated with I_b include two pool fines variables, V^*_w ($\tau = 0.714$, $p = 0.011$) and $(s_\phi)_p$ ($\tau = -0.714$, $p = 0.011$), and at weaker correlation

levels median particle sizes of riffle armor and pool fines (τ = -0.571, p = 0.048 for both). The inverse relations to bed material sizes are indicative of the greater mobility of the finer fraction of the bed surface (cf. Lisle, 1995). These fines would be expected to be deposited in low-velocity areas during waning stages of the snowmelt hydrograph. Reach-average sorting of pool fines, $(s_\phi)_p$, was greater than 2 for three sites, and was 1.9 for site 171. In 13 natural gravel-bed streams studied by other workers, Lisle (1995) reported that equal mobility of bed material was generally maintained for sorting (s_ϕ) values up to roughly 2, but that high values of s_ϕ were common among channels with bedloads finer than bed material. The observed correlations of bedload transport rates with V^*_w and $(s_\phi)_p$ is consistent with previous studies.

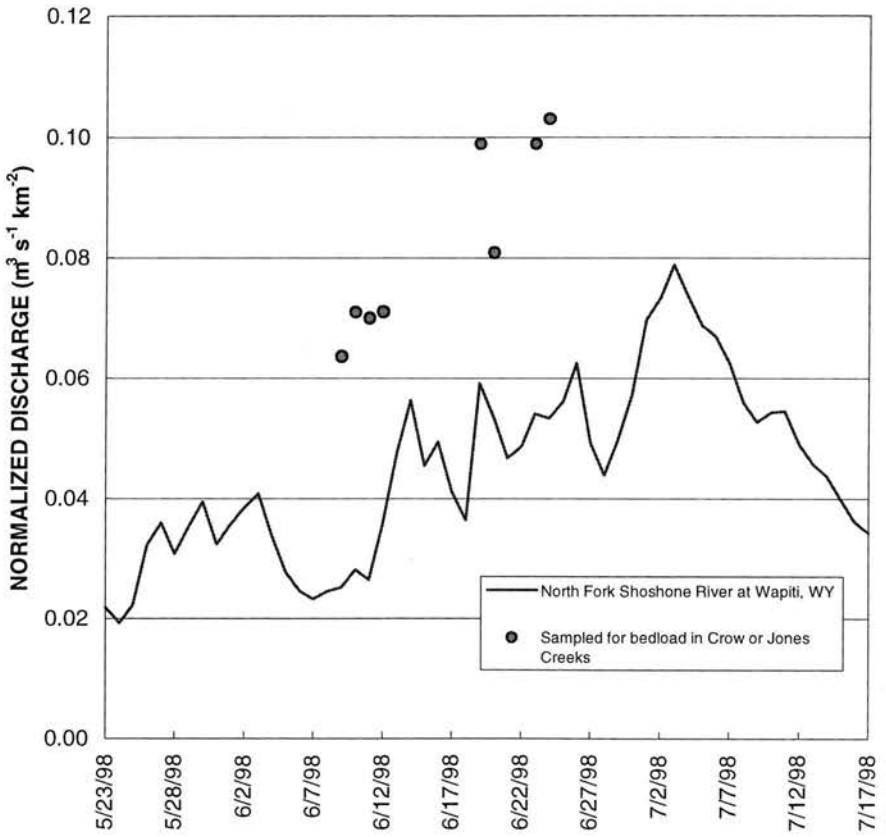

Figure 4.23. Normalized streamflow discharges sampled for bedload of study streams in reference to normalized streamflow of North Fork Shoshone River, June 1998.

The logarithms of I_b were found more linearly associated with many potential explanatory variables than were untransformed values. Correlations with median particle size of riffle armor and pool fines are the strongest (Pearson's R = -0.92 and –0.90, respectively), but scatter plots indicated that much of the total variance was contributed by a single site having median particle size much coarser than the other three sites. The correlation with V^*_w was nearly as strong and figure 4.24 shows that the distribution of samples is relatively uniform along the V^*_w scale. Linear correlation of $\log(I_b)$ with V^*_w is significant ($R = 0.874$, $p = 0.0045$). These limited data lend some support to Lisle's (1995) summarization that patches of fine sediment stored in pools during low flow can account for most of the volume of unarmored fine sediment on streambeds and, being readily entrained at high flows, contribute disproportionately more to annual bedload than their small volume would imply.

The relative sampling intensity (Bunte, 2001) is the employed sampling intensity divided by the potential sampling intensity, where employed sampling intensity is the sampled width (nozzle width times number of sampling points) times sampling time (e.g., 60 s on bottom). Bedload sampling intensity for this study averaged 0.93 percent of potential sampling intensity, ranging from 0.62 to 1.2 percent among the eight samples. K.I. Bunte (oral comm., 2001) described the typical range of sampling intensity using a Helley-Smith-type sampler as 0.06 to 1.0 percent. Although the instantaneous bedload data reported herein reflect a mostly interpolated estimate, they represent a relatively high sampling intensity during a small part of one year's runoff. Except for the brevity of the sampling season, the collected data are about the best that can be obtained from cobble-bed streams without installation of either a smooth sill or bedload trap.

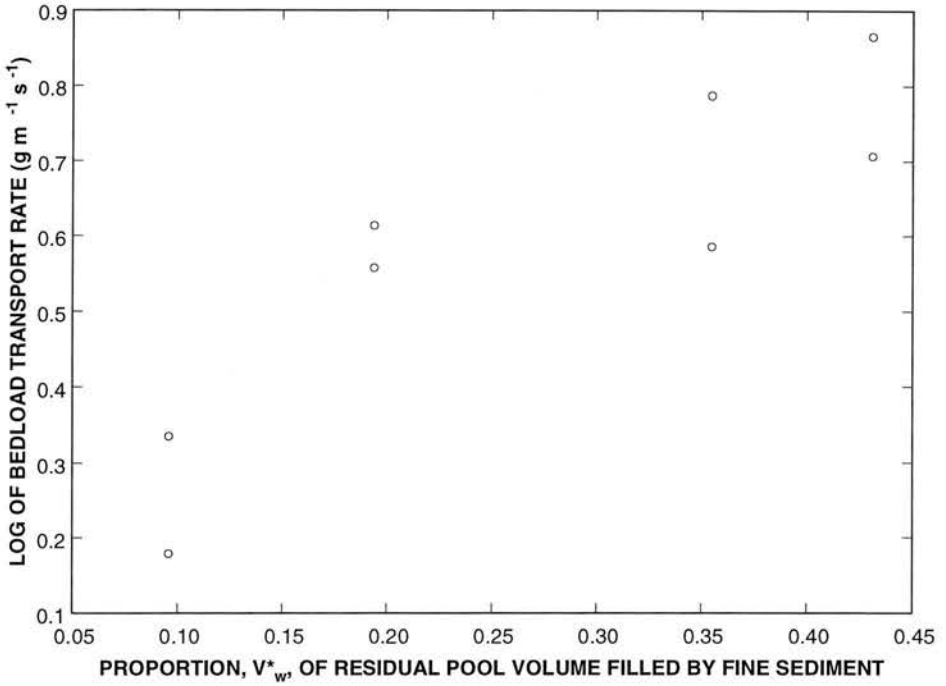

Figure 4.24. Scatter plot of bedload transport rate versus ratio, V^*_w, of residual-pool fine sediment to pool volume.

4.6.2 Bedload Particle-Size Distribution

Bedload transported at less than bankfull discharge generally is finer than that transported at higher flows (Lisle, 1995). The particle-size data from the eight bedload measurements are insufficient to characterize either stream's bedload, but may suggest patterns with limited applicability to conditions matching those of June 1998. Median particle size of bedload, $(d_{50})_L$, ranged from 1.5 to 22 mm in the eight samples. The two coarsest samples were collected at site 92, where the cross-section was located near the downstream end of a riffle and locally convergent flow may have increased bed mobility.

Values of $(d_{50})_L$ are significantly rank correlated with average boundary shear stress ($\tau = 0.786$, $p = 0.0065$). The $(d_{25})_L$ of bedload particle-size distribution was greater than the 1 mm censoring limit only for the samples from site 92 (table 4.7). The range in $(d_{84})_L$ of bedload was 5.5 to 47 mm, and was 17 to 53 mm for $(d_{90})_L$. Rank correlations

with bedload $(d_{90})_L$ were most significant for mean boundary shear stress in the bedload zone ($\tau = 0.857$, $p = 0.003$), the mobility ratio $(d_{95})_L / (d_{25})_R$ ($\tau = 0.714$, $p = 0.013$), and average boundary shear stress ($\tau = 0.643$, $p = 0.026$). None of the particle-size percentiles were significantly correlated with the product of V_m and S_L ($p > 0.2$ in each case tested). The rank correlations with boundary shear stress in the bedload zone (τ_L) increase monotonically for successively larger percentiles of the bedload GSD, from a Kendall's $\tau = 0.464$ for $(d_{25})_L$ to $\tau = 0.857$ for $(d_{90})_L$. This pattern is consistent with the accepted concept that when shear stress exceeds a critical value, sediment motion will be initiated (cf. Wiberg and Smith, 1987a and 1987b). Thus it is the largest fraction of the bedload that is most near its threshold of motion, and therefore is the size parameter most highly correlated with prevailing shear stress at the channel boundary.

Bedload sorting, indicated by the graphic sorting statistic, $(s_\phi)_L$, ranged from 2.6ϕ to 3.5ϕ among the eight samples. All samples were very poorly sorted (cf. Folk and Ward, 1957), suggesting that the bedload is a mixture of two sources: fine-grained surface patches and coarse streambed armor (cf. Lisle, 1995). The sorting statistic was inversely rank-correlated with the sorting statistic for pool fines ($\tau = -0.571$, $p = 0.041$), but not correlated with sorting of riffle armor ($p > 0.5$). The fraction, V^*_w, of residual pool volume filled by fines (at low flow) also was rank correlated with $(s_\phi)_L$ ($\tau = 0.571$, $p = 0.041$). Reaches where pool fines are more abundant might be expected to contribute a disproportionally large volume to bedload at less-than-bankfull flows, thereby increasing the heterogeneity of sampled bedload relative to reaches where pool fines are rare.

Lisle (1995) investigated relative transport velocities of bedload sediment from two types of streambed patches of differing coarseness through iterative application of

mixing ratios in a rough model. He found that selective transport of fine patches in pools decreased with a stream's increasing potential for scouring subsurface bed material.

For the four reaches of Crow and Jones Creeks where bedload was sampled, graphical comparison of GSDs for bedload, riffle armor, and pool fines (figs. 4.25 to 4.28) can provide some insight into relative contributions to bedload composition for the sampled conditions (near, but less than, bankfull discharge). However, confidence in specific values along the GSD curve is limited due to sample sizes, particularly for bedload.

In two reaches (80 and 181), the size distribution of sampled bedload is more similar to the pool fines than to the riffle armor. Site 181 on Crow Creek is the lone plane-bed channel among the four, and has a riffle-armor median size 0.8ϕ coarser than, and V_{rf} , V^*_w, and drainage area less than half those of site 80. Site 80 on Jones Creek has abundant pool fines (V^* values of 0.29 to 0.44 for four of six measured pools, and $V^*_w = 0.35$) and a reach gradient less than one-third that of site 181. Given the lower normalized discharges for the samples at site 80 compared with those for site 181, it appears that the GSD for site 80 chiefly reflects entrainment of pool fines along with some gravels from other patches that were susceptible to mobilization at less than bankfull flows. In contrast, the bedload GSD for site 181, where bedload transport rates were lowest despite streamflow being most nearly at bankfull discharge, probably reflects supply-limited conditions and channel armor better able to resist entrainment and consequent scour of subsurface material.

Results for site 92 show a bedload size distribution more similar to riffle armor than to pool fines. As noted above, local hydraulics at the sampling section may contribute to the coarseness of the bedload samples from this reach. The sampled section

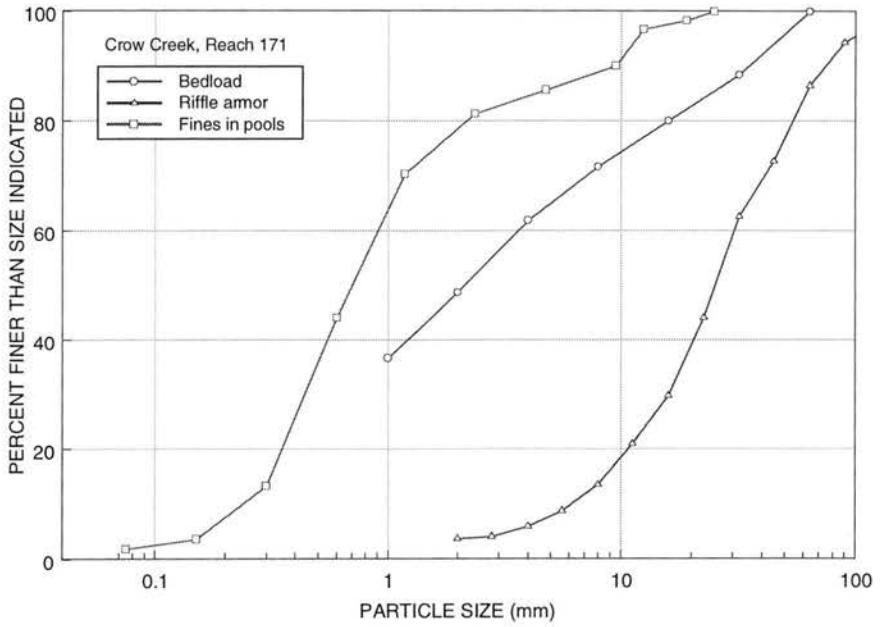

Figure 4.25. Particle-size distributions of sample bedload, riffle armor, and residual-pool fine sediments from reach 171, Crow Creek.

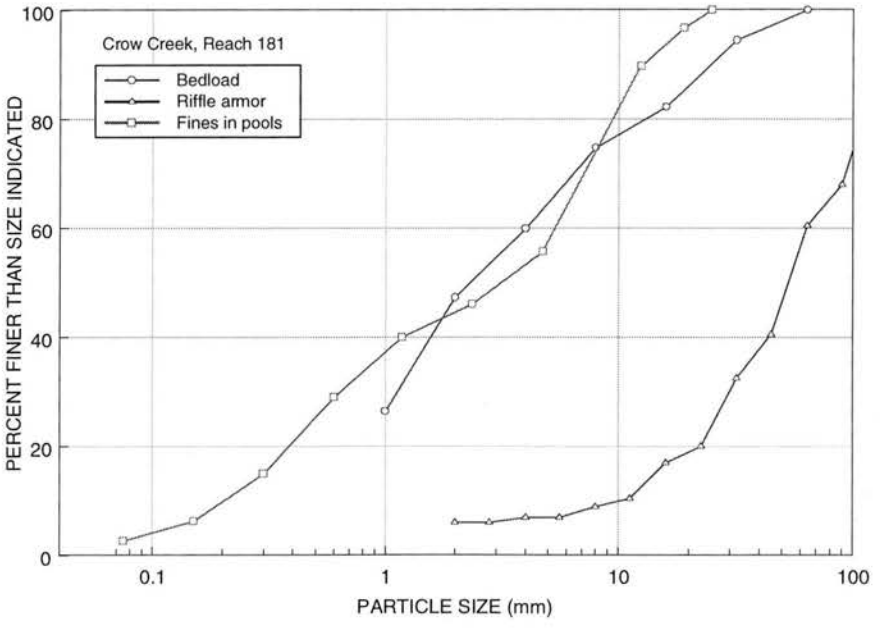

Figure 4.26. Particle-size distributions of sample bedload, riffle armor, and residual-pool fine sediments from reach 181, Crow Creek.

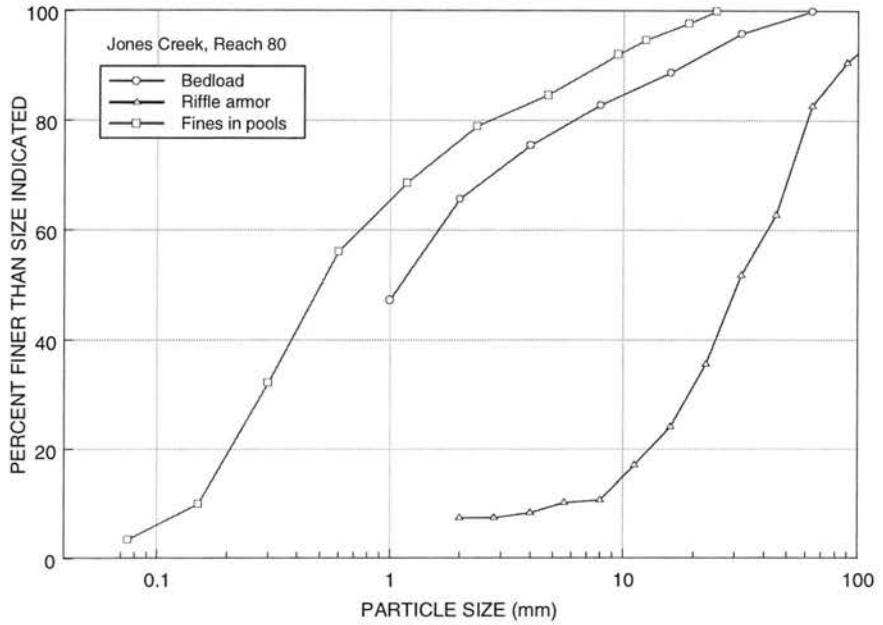

Figure 4.27. Particle-size distributions of sample bedload, riffle armor, and residual-pool fine sediments from reach 80, Jones Creek.

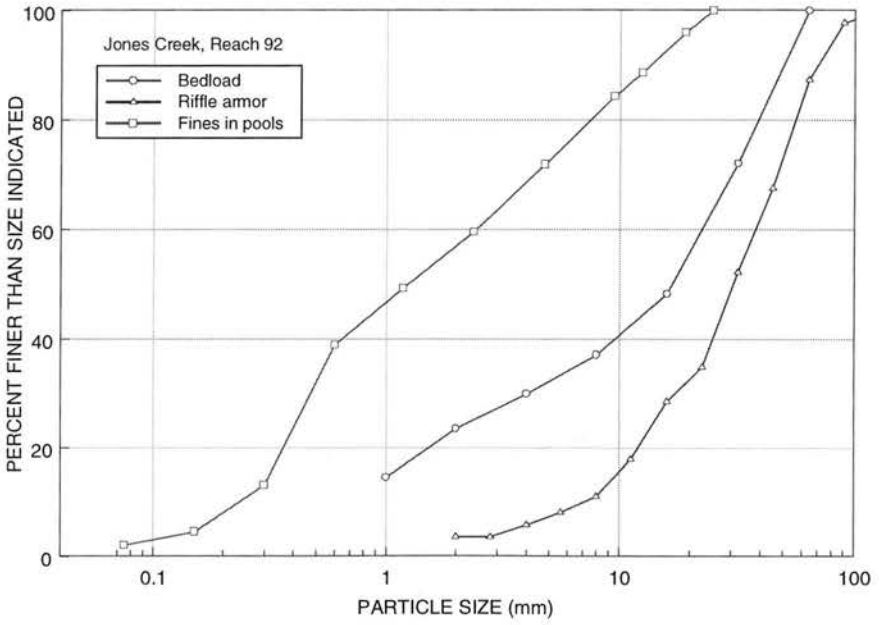

Figure 4.28. Particle-size distributions of sample bedload, riffle armor, and residual-pool fine sediments from reach 92, Jones Creek.

geometry was less trapezoidal than those for the other three sites, resulting in greater depth in the thalweg (bedload transport) zone (table 4.7). This flow geometry allows greater boundary shear stress and stream power per unit width in the thalweg zone, relative to the other sampled sections, and explains the entrainment of a coarser bedload.

Bedload coarseness for site 171 is intermediate between the size distributions for pool fines and riffle armor. For the finest two thirds of bedload, the size percentiles are closer to those of the pool fines. But for the coarsest third of bedload, the size-distribution curve lies about midway between those of the two sources. Streamflow was near bankfull and site 171 had the largest V^*_w fraction and second-finest riffle armor among all 20 study reaches. For such conditions, local mobilization of channel framework material in zones of greatest shear stress is likely. These results are consistent with Lisle's (1995) findings that greater mobility of much of the streambed leads to domination of bedload by sources that represent the streambed in general rather than by localized patches of fine material.

4.6.3 Summary

Based on only 8 measurements of highly variable bedload, all findings reported in this section must be qualified as tentative. Bedload transport rates did not exceed 7.3 g m^{-1} s^{-1} for the measured stream discharges that were less than 3.8 m^3 s^{-1}. Both the bedload transport rate and bedload sorting statistic are significantly correlated with V^*_w, a finding consistent with previous work indicating that patches of fine sediment stored in pools contribute disproportionately to annual bedload, thereby increasing the heterogeneity of sampled bedload relative to reaches where pool fines are rare. The sampled bedload was very poorly sorted, suggesting that it is a mixture of fine-grained surface patches and coarse streambed armor.

Rank correlations with boundary shear stress in the bedload zone increase monotonically for successively larger percentiles of the bedload size distribution to a maximum Kendall's $\tau = 0.857$ for $(d_{90})_L$. This pattern reflects the concept that when shear stress exceeds a critical value, sediment motion is initiated and bedload transport rates increase rapidly with additional shear stress.

4.7 Chapter Summary

There were several significant differences between the burned and reference streams. Mean bankfull channel width was 1.2 m wider for the burned stream than for the reference stream after accounting for differences in drainage area and number of debris jams. Mean width of pools was 2.2-m greater for the burned stream than for the reference stream after accounting for relations with drainage area and mean active-channel LOD piece length. Graphic mean size of riffle armor was 0.83ϕ units coarser on average for Jones Creek than for Crow Creek after accounting for reach gradient and pool spacing. The fraction, V^*_w, of residual pool volume occupied by fine sediment was not significantly different between streams.

There were no significant differences between streams in percent pools, pool spacing, residual-pool mean depth, or pool length. The riffle armor for both streams was poorly sorted in nearly all reaches. Fine-sediment deposits in pools of both streams were predominantly coarse sand to very fine gravel, and typically very poorly sorted.

Bank-stability ratings were not different between streams. The difference between streams in the modified streambed-stability summary rating is only marginal in statistical significance, and appears to reflect differences in stream-segment geology rather than fire-related effects.

Process-based explanations were proposed to explain the observed differences between streams in channel width, riffle-armor particle size, and streambed stability. Pool widths in Crow Creek appear to be primarily a function of LOD effects, whereas pool widths in Jones Creek reflect influences of both LOD and drainage area, which is a surrogate for discharge. Bank erosion by increased streamflow in Jones Creek during the early post-fire period may be responsible for the greater channel width of the burned stream. The importance of LOD in deflecting flow against bed and banks appears to have a greater influence on pool widths than riffle widths. Riffle-armor coarsening in Jones Creek was probably caused by increased duration of near-bankfull streamflow.

Chapter 5

LARGE ORGANIC DEBRIS

Inventories of LOD were analyzed chiefly using reach-average characteristics to determine whether frequency, loading, or piece characteristics differed between streams in ways that may reflect long-term effects of severe wildfire.

5.1 LOD Frequency

LOD frequency per some standard length of channel indicates LOD abundance by effectively normalizing LOD loading with respect to channel width (Montgomery et al., 1995). Reach-mean LOD frequency may be partitioned among three different types of accumulations: isolated pieces, small contact groups (< 10 pieces in mutual contact), and debris jams (10 or more pieces in mutual contact). The total frequency of LOD is discussed first. The frequencies of isolated pieces and most influential pieces are discussed in sections 5.1.2 and 5.1.3, respectively. The frequency of pieces occurring in small contact groups and debris jams is discussed in section 5.1.4.

5.1.1 Total LOD Frequency

The reach-average frequency of all LOD (LDF) ranged from 28 pieces per 100 m for site 106 to 108 pieces per 100 m for site 103. In figure 5.1, LDF corresponds to the total height of the stacked bars. LDF is slightly greater among Crow Creek reaches than for Jones Creek (table 5.1), but the difference is not statistically significant ($p = 0.37$).

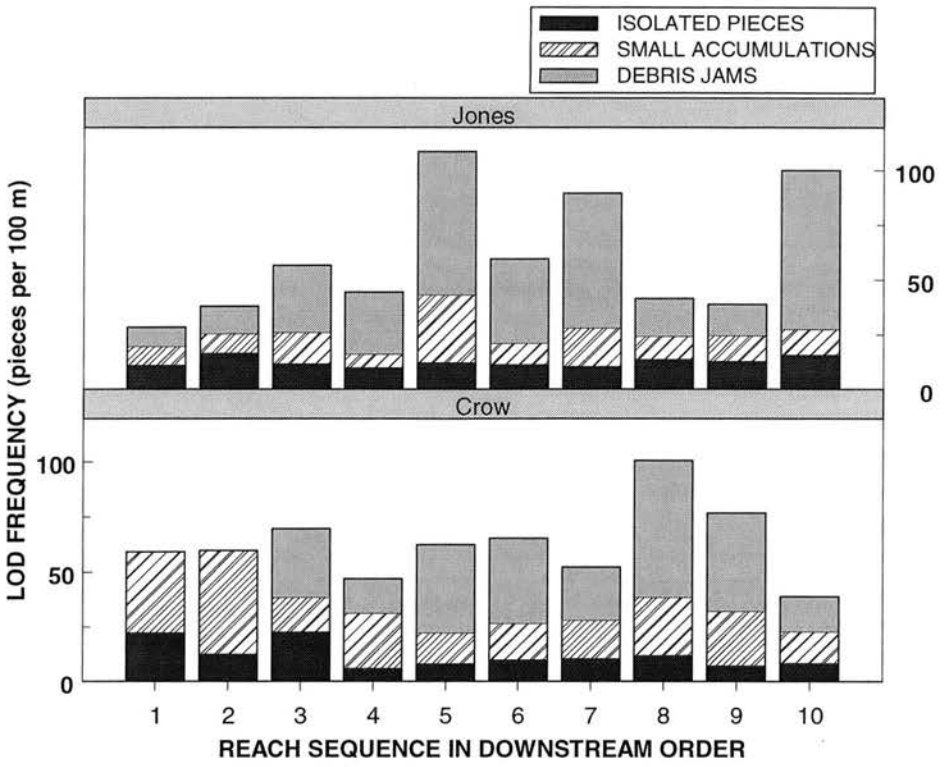

Figure 5.1. Reach-mean frequency of LOD by type of accumulation, in downstream order.

Montgomery et al. (1995) summarized LOD frequencies for their 52 study reaches in southeastern Alaska and central Washington, but included pieces as short as 1 m. In undisturbed old-growth forest streams nearly all reaches had LOD frequency greater than 40 pieces per 100 m, which is very similar to the minimum LDF value for Crow Creek of 39 pieces per 100 m. In 73 percent of the Alaska/Washington reaches flowing through areas of clear-cut forests with no riparian buffer strip, LOD frequency was less than 20 pieces per 100 m. However, burned areas are very different from clear-cut areas with respect to the density of standing trees remaining after the disturbance. Berg et al. (1998) reported LOD data from two central Sierra Nevada streams that had been burned at least 35 years previously. LOD frequency in reaches with gradients less than 3 percent averaged 22.6 and 26.2 pieces per 100 m for the two streams, although

Table 5.1 – *Summary of large organic debris characteristics in study reaches.*

[LOD, large organic debris; CV, coefficient of variation; p-value, probability value; sample size is 10 reaches for each stream, except that for P_{jam} and V_{jam} sample size is 8 Crow Creek reaches and 10 Jones Creek reaches; W_{bf}, bankfull width]

LOD characteristic	Variable name	Crow Creek			Jones Creek			p-value for rank-sum test of different medians
		Mean	Median	CV (%)	Mean	Median	CV (%)	
Pieces per 100 m of channel	LDF	63.2	61.1	27	60.5	50.4	47	0.37
Isolated pieces per 100 m of channel	LDF_{iso}	12.1	10.3	49	12.7	12.1	18	.20
Influential pieces per 100 m of channel	LDF_{inf}	5.4	6.1	66	4.1	3.0	107	.34
Frequency of pieces occurring in contact groups (per 100 m)	LDF_{acc}	51	47	34	48	40	60	.44
Frequency of pieces in small contact groups (per 100 m)	LDF_{scg}	23	21	46	12.9	11.0	54	.0052
Frequency of pieces occurring in debris jams (per 100 m)	LDF_{jam}	27	28	73	35	29	68	> .5
Mean piece diameter (cm)	D_{LD}	22	21	10	20	19	10	.022
Mean piece length (m)	L_t	7.1	7.1	12	6.7	6.5	14	.14
Ratio of L_t to W_{bf}	L_t:W_{bf}	.82	.83	15	.62	.60	19	.0039
Mean active-channel piece length (m)	L_a	5.1	5.1	11	5.0	4.75	22	.24
Total volume per piece (m^3)	V_t	.36	.33	22	.28	.26	37	.026
Active-channel volume per piece (m^3)	V_a	.25	.23	23	.21	.20	50	.032
Total volume per 100-m channel length (m^3)	VL_t	22.4	21.6	25	18.6	13.8	79	.105
Active-channel volume per 100-m channel length (m^3)	VL_a	15.5	14.6	29	14.2	8.9	92	.22
Number of anchors per piece	N_a	.76	.77	30	.59	.57	31	.026
Percentage anchored	a%	54.5	54.5	25	45.7	47.5	22	.062
Percentage with > 1 anchor	A_W%	16.2	14.9	50	10.5	8.6	68	.062
Contact groups per 100 m	DAF	8.3	8.9	31	5.7	4.5	36	.0115
Pieces per contact group	P_{acc}	6.5	6.5	34	8.0	7.4	33	.109
Percentage of pieces occurring in contact groups	DA%	80.2	82.2	12	74.8	78.3	16	.31
Small contact groups per 100 m	SAF	6.7	7.0	45	4.1	3.6	34	.0185
Pieces per small contact group	P_{scg}	2.4	2.6	41	3.8	3.1	45	.123
Debris jams per 100 m	DJF	1.5	1.5	79	1.6	1.5	61	> .5

LOD characteristic	Variable name	Crow Creek Mean	Crow Creek Median	Crow Creek CV (%)	Jones Creek Mean	Jones Creek Median	Jones Creek CV (%)	p-value for rank-sum test of different medians
Pieces per debris jam	P_{jam}	19.7	17.7	34	21.4	21.3	32	.27
Active-channel volume per debris jam (m^3)	V_{jam}	5.6	4.9	38	5.1	4.3	62	> .5
Percentage of pieces occurring in debris jams	DJ%	40.8	45.3	58	52.5	57.2	30	.154

their definition of LOD included some smaller pieces than in this study. In Jones Creek, 50 percent of reaches had LDF less than 45 pieces per 100 m and abundant supplies of burned boles still remained along most reaches of this stream in 1999. Conditions may be quite different in another 25 years.

Young (1994) reported 1990 piece counts of 32 and 15 pieces per 100 m for downstream-most Crow and Jones Creeks, respectively. Those results contrast with LDF values of 31 and 77 pieces per 100 m in 1999 for same debris-size definition (diameter > 15 cm). However, Young included only LOD in or above the wetted channel, whereas the 1999 data included nonwetted active-channel areas. This difference in methods undoubtedly accounts for much of the large difference in piece frequency for Jones Creek's widened downstream reach. Young (1994) reported the channel of Jones Creek shifted laterally more than 100 m at some locations between 1990 and 1991. But increased LOD inputs since 1990 also appear likely, given that the minimum frequency of 15-cm or larger LOD among Jones Creek reaches was 21 pieces per 100 m in 1999.

Berg et al. (1998) concluded that channel type may have little effect on LOD recruitment factors and they found only a few significant differences among channel types for LOD frequencies. In the present study, LDF did not differ significantly ($p > 0.8$) between forced-pool-riffle (FPR) reaches ($n = 15$, median 56 pieces per 100 m) and

plane-bed reaches (n = 5, median 65 pieces per 100 m). However, among 14 FPR reaches, LDF is significantly different between streams (W = 34.5, p = 0.022) with high outlier site 103 (fig. 5.2) excluded. The frequency of debris in FPR reaches is greater in Crow Creek (median 62.4 pieces per 100 m) than in Jones Creek (median 41.6 pieces). Site 103 is adjacent to landslide runout debris and one lobe of debris extended into the stream channel just upstream of the study reach. With the highest overall LDF among all study reaches, site 103 is atypical of Jones Creek conditions overall. Among FPR reaches, LDF is very highly correlated with frequency of LOD contact groups (R_s = 0.810, p = 0.0025).

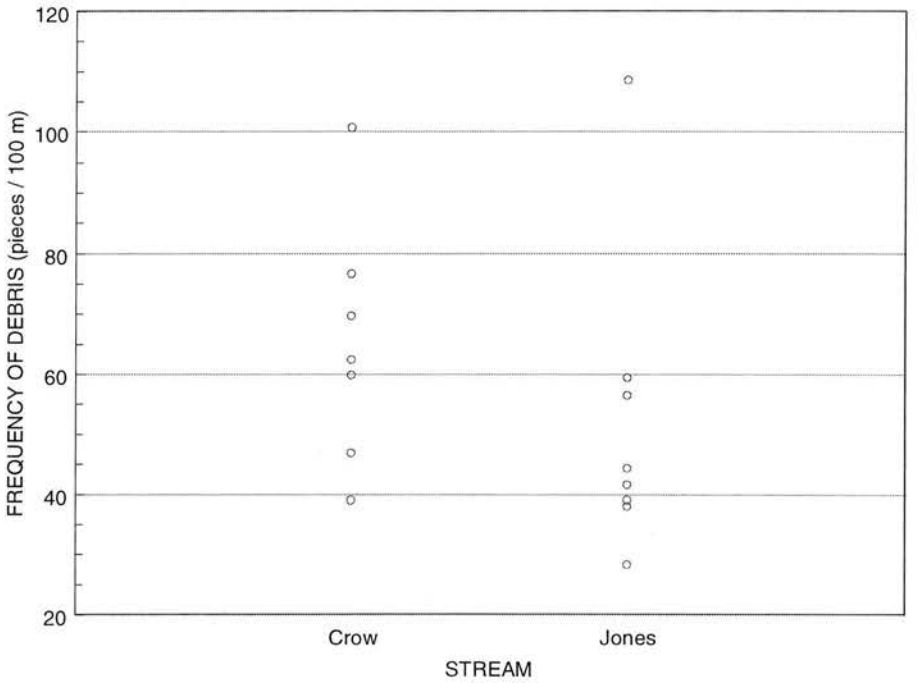

Figure 5.2. Reach-mean frequency of LOD in forced-pool-riffle reaches of Crow and Jones Creeks.

LDF is significantly correlated with the frequency and percentage of pieces occurring in LOD jams (R_s = 0.805 and 0.618, p = 0.0005 and 0.0072, respectively), the

frequency and percentage of pieces occurring in contact groups (R_s = 0.972 and 0.769, p < 0.0001 and p = 0.0008, respectively), the frequency of contact groups and jams (R_s = 0.703 and 0.698, p = 0.0022 and 0.0024, respectively), and the active-channel- and total length per piece (R_s = 0.581 and 0.520, p = 0.0115 and 0.023, respectively). Because LDF is one measure of LOD loading, it is not surprising that it is also highly correlated with volumetric LOD loading (VL_a; R_s = 0.899). The correlations with debris-jam measures and mean piece length are interpreted to reflect generally that where LOD frequency is high, a number of whole trees have fallen into the channel and contribute to or anchor debris accumulations, which contribute a large proportion of the total piece count in most reaches. Also, among the forced-pool reaches the negative correlation between LDF and pool spacing (SP) is much stronger (R_s = -0.520, p = 0.0508) than it is for the full set of reaches (R_s = -0.086). This suggests that the closer spacing of pools in FPR reaches is primarily caused by effects of LOD on pool-formation processes.

Variability in LOD frequency is greater among Jones Creek reaches (CV = 47.2%, IQR = 42.3) than Crow Creek reaches (CV = 27.1%, IQR = 14.6). A high outlier is Crow Creek reach 171, where aggradation has expanded the frequently flooded or saturated area and killed numerous riparian trees that are now falling into the channel. Variability in LDF is significantly greater among Jones Creek reaches than those of Crow Creek (F = 6.09, p = 0.018) when reach 171 is excluded.

The linear model for LOD frequency includes frequency of debris jams (DJF), the dummy variable, WS, for difference between streams, and the DJF:WS interaction:

$$\log(LDF) = 1.69 + 0.065\ DJF - 0.23\ WS + 0.109\ DJF{:}WS \qquad (5.1).$$

The fitted model explains 69.3 percent of the variability in log(LDF) with RSE of 0.096 log units (fig. 5.3). All three independent terms significantly improve the model (t =

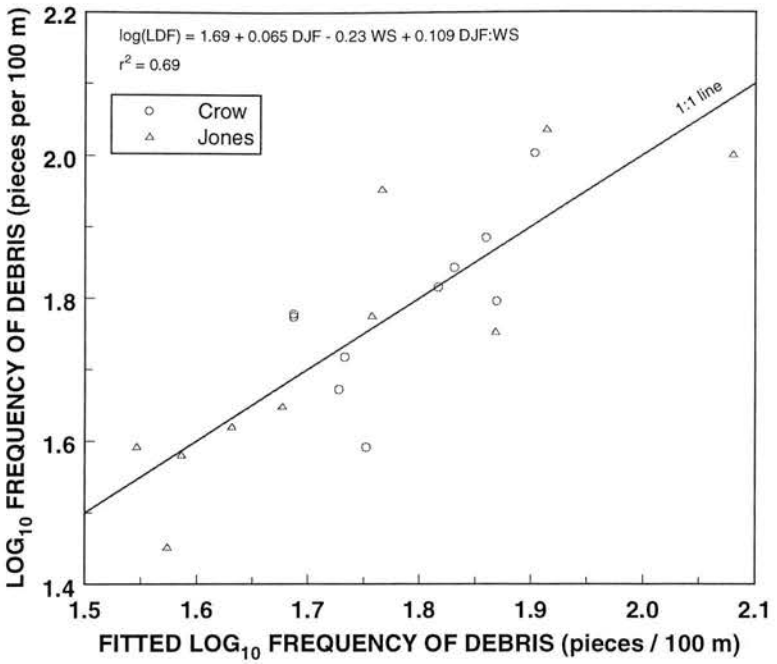

Figure 5.3. Fit of multiple linear regression model for reach-mean frequency of LOD.

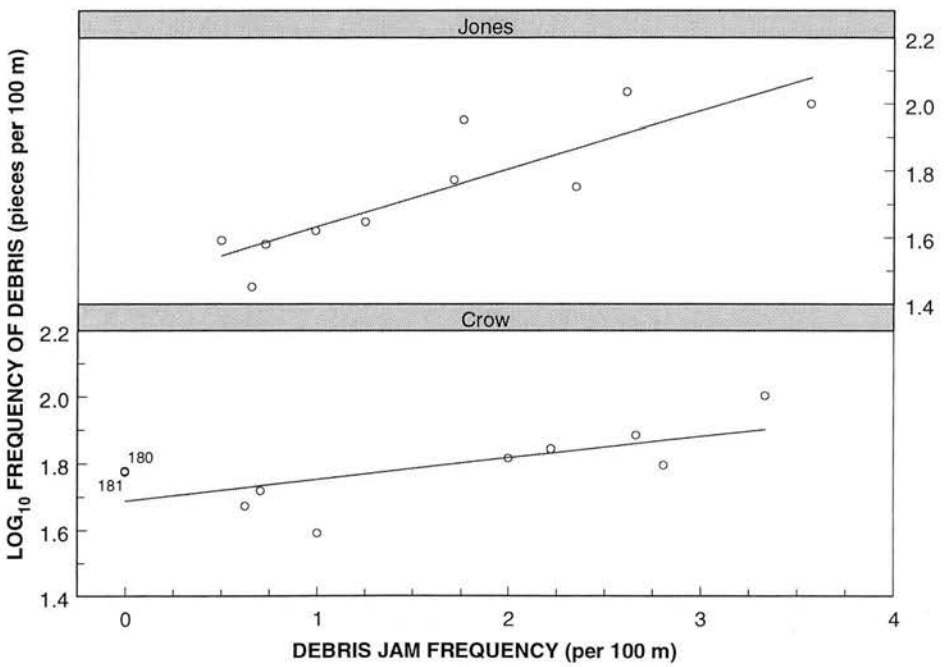

Figure 5.4. Interaction between debris-jam frequency and stream in multiple-regression model for reach-mean LOD frequency (eq. 5.1).

2.46, p = 0.026 for DJF; t = -2.89, p = 0.0107 for WS; and t = 2.61, p = 0.019 for the interaction). The model indicates that LDF in Jones Creek is less than that in Crow

Creek on average, after accounting for the effect of debris-jam frequency. Also, overall LDF in Jones Creek is more sensitive to the frequency of debris jams (steeper slope coefficient; see fig. 5.4) than in Crow Creek. This is consistent with the overall visual impressions of these streams, including all observed segments, not just the study reaches.

5.1.2 Frequency of Isolated Pieces

The frequency of LOD pieces not in contact with another piece ranged from 6.2 pieces per 100 m in reach 195 to 23 pieces per 100 m in reaches 179 and 181. The reach-mean frequency of isolated pieces (LDF_{iso}) is quite similar, in terms of the streamwise means (table 5.1), and the median among Jones Creek reaches was insignificantly greater ($W = 87$, $p = 0.20$) than that for Crow Creek. A much larger CV of LDF_{iso} among Crow Creek reaches (table 5.1) results from the presence of two outlier values (sites 179 and 181). Thus the difference between streams in residual LDF after accounting for the relation with DJF is not caused by a greater frequency of isolated pieces, but instead must be found in a greater frequency of small contact groups in Crow Creek (see section 5.1.4.1 of this report).

5.1.3 Frequency of Influential Pieces

A total of 160 "most influential" pieces of LOD were inventoried, comprising 8 percent of inventoried pieces. Influential pieces as a percentage of the total ranged from 0 for sites 106 and 107 to 17.9 percent for site 173. Both reaches that had no influential pieces are in Jones Creek upstream from the middle valley section that has numerous debris-torrent scoured channels among its right-bank tributaries. However, other (non-study) reaches in upstream segments did contain debris jams and isolated occurrences of pieces that would qualify as "influential" LOD.

When all 20 study reaches are summarized together (table 5.1), the larger average frequency of influential pieces (LDF_{inf}) in Crow Creek is not significantly different from Jones Creek, as large CVs characterize the sampling distribution of both streams. When the forced-pool-riffle reaches are considered separately, the difference between streams becomes more pronounced. Though the difference remains insignificant ($W = 69$, $p = 0.12$), median LDF_{inf} among forced-pool-riffle reaches in Crow Creek is more than triple that in Jones Creek (7.0 versus 2.1 pieces per 100 m). Also, among the forced-pool reaches the inverse relation between LDF_{inf} and pool spacing (SP) is much stronger ($R_s = -0.425$) than it is for the full set of reaches ($R_s = -0.159$), suggesting that influential pieces may affect forced-pool formation and spacing. But contrary evidence is found in lower median LDF_{inf} in FPR reaches than plane-bed reaches (3.8 versus 4.2 pieces per 100 m).

5.1.4 Frequency of Pieces in Contact Groups

A total of 786 pieces of LOD in Crow Creek and 824 pieces in Jones Creek occurred in physical contact with other LOD. Streamwise median counts per reach of pieces in contact groups were 66 pieces for both streams. Reach total pieces in contact groups was divided by reach length to derive the mean frequency of pieces in contact groups (LDF_{acc}).

Reach-mean LDF_{acc} ranged from 17.1 pieces per 100 m for site 106 to 96 pieces per 100 m for site 103. Streamwise median LDF_{acc} was 47 pieces for Crow Creek versus 40 pieces per 100 m for Jones Creek, an insignificant difference (table 5.1). The IQR of LDF_{acc} among Jones Creek reaches was three times as large as that for Crow Creek. Average frequency of LOD in contact groups is more evenly distributed along Crow Creek as compared with Jones Creek.

5.1.4.1 Frequency of Pieces in Small Contact Groups

Reach-mean frequency of LOD in small contact groups (LDF_{scg}) ranged from 6.2 pieces per 100 m for site 81 to 47 pieces per 100 m for site 180. Stream median LDF_{scg} is significantly greater ($W = 141$, $p = 0.0052$) for Crow Creek (21 pieces per 100 m) than for Jones Creek (11 pieces per 100 m). Also, the rank correlation of LDF_{scg} with residuals from simple linear regression of LDF with DJF is highly significant ($R_s = 0.773$, $p = 0.0008$). These results indicate that the greater overall frequency of LOD (LDF) in Crow Creek (after accounting for the effect of debris-jam frequency) occurs chiefly in contact groups of less than 10 pieces.

Rank correlations of LDF_{scg} with LOD loading, i.e., VL_t ($R_s = 0.665$, $p = 0.0038$) and VL_a ($R_s = 0.630$), and mean piece diameter ($R_s = 0.600$, $p = 0.0090$) are highly significant. At less significant levels, total and active-channel volume per piece ($R_s = 0.529$, $p = 0.021$; and $R_s = 0.486$, $p = 0.034$, respectively), and frequency of influential pieces ($R_s = 0.474$, $p = 0.039$) also are correlated with LDF_{scg}. The correlations with LOD size may indicate the importance of stable pieces in creating small accumulations, or it may simply reflect that both piece size and LDF_{scg} are greater in the reference stream than in the burned watershed.

5.1.4.2 Frequency of Pieces in Debris Jams

Reach-mean frequency of LOD in debris jams (LDF_{jam}) ranged from 0 (sites 180 and 181 had no debris jams) to 72 pieces per 100 m (site 93). Streamwise median LDF_{jam} values were nearly the same: 28 and 29 pieces per 100 m for Crow and Jones Creeks, respectively, an insignificant difference ($W = 100$, $p > 0.5$).

Mean debris-jam piece frequency is highly rank correlated with mean piece length ($R_s = 0.718$, $p = 0.0018$ for L_a; $R_s = 0.667$ for L_t) and riffle width ($R_s = 0.601$, $p =$

0.0087). Debris-jam piece frequency is also significantly correlated with mean residual-pool volume ($R_s = 0.524$, $p = 0.022$) and reach gradient ($R_s = -0.515$, $p = 0.025$).

When considering only forced-pool-riffle channels, two additional reach characteristics are correlated with LDF_{jam}: mean residual-pool depth ($R_s = 0.600$), and percent pools (P%; $R_s = 0.550$). This result suggests that scour around debris jams may influence forced-pool formation. Comparison of plots of LDF_{jam} versus pool spacing by stream (fig. 5.5) shows that an inverse correlation between SP and LDF_{jam} among Jones Creek reaches (Kendall's $\tau = -0.786$, $p = 0.0065$) contrasts with the situation in Crow Creek, where SP does not appear related to LDF_{jam} ($\tau = 0.238$, $p = 0.45$).

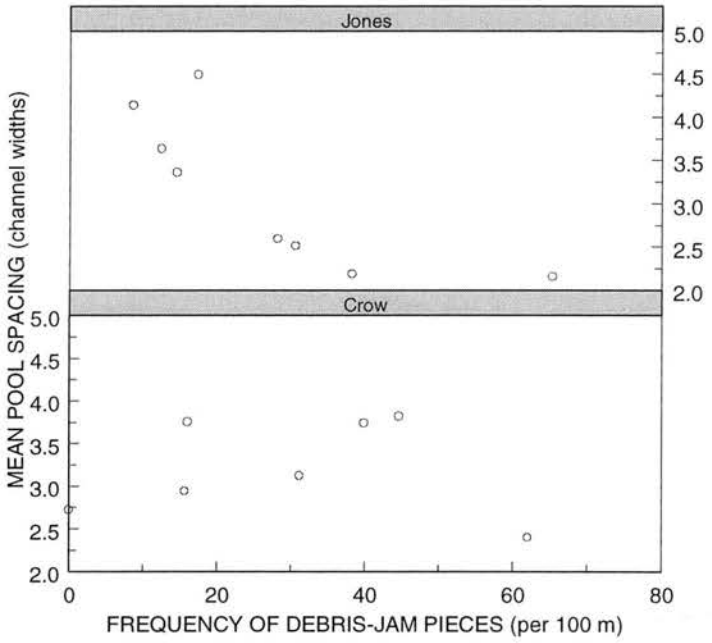

Figure 5.5. Plots by stream of reach-mean pool spacing versus reach-mean LOD frequency in debris jams, for forced-pool-riffle reaches.

This result, when considered together with results for overall LOD frequency and for influential LOD in relation to channel type, suggests that different pool-forming mechanisms are dominant for each stream. In Crow Creek, the data suggest that scour

around influential pieces of LOD is the important mechanism forcing pool formation. In contrast, in Jones Creek the frequency of debris jams (see section 5.7.3) and LOD frequency in debris jams are highly correlated with pool spacing, suggesting that flow deflection around debris jams is the dominant pool-forming mechanism.

The ratio of LDF_{jam} to LDF_{scg} ranged from 0 (sites 180 and 181) to 6.2 (site 93), and streamwise median values of the ratio were 1.6 and 2.1 for Crow and Jones Creeks, respectively. The ratio did not differ significantly between streams ($W = 84$, $p = 0.1230$), nor was there a significant correlation between LDF_{jam} to LDF_{scg}.

5.1.5 Summary

The frequency of LOD in forced-pool-riffle channels is greater in Crow Creek than in Jones Creek after excluding site 103. Variability in LOD frequency is greater in Jones Creek than in Crow Creek. A regression model explains 69 percent of the variability in LOD frequency and indicates that average LDF is less in Jones Creek than in Crow Creek after accounting for debris-jam frequency. This difference is found chiefly in the frequency of LOD in small contact groups.

There was an inverse correlation between pool spacing and the frequency of LOD in debris jams in Jones Creek, but not in Crow Creek. These results suggest that different pool-forming mechanisms are dominant for each stream. In Crow Creek, scour around influential pieces of LOD is the chief mechanism for pool formation. In Jones Creek, flow deflection around debris jams appears to be the dominant pool-forming mechanism.

5.2 Average Piece Size

Data were collected for two measures of piece size, midpoint diameter and piece length. A third measure, estimated piece volume, was calculated.

5.2.1 Mean Diameter and Length

Reach-average LOD diameter (D_{LD}; table 5.1) is significantly larger (t = -2.284; one-sided p-value = 0.017) for Crow Creek reaches (mean = 22 cm) than for Jones Creek (mean = 20 cm). The difference between streams in mean diameter is 2.2 cm $\pm$ 2.0 cm (95-percent confidence interval). With CVs of about 10 percent, variability of D_{LD} values among study reaches (fig. 5.6) is small relative to most other variables measured.

Mean piece diameters of 24 and 27 cm for Crow and Jones Creek's downstream-most reaches, respectively, measured in 1990 (Young and Bozek, 1996) are similar to the 27 and 25 cm mean diameters, respectively, measured in 1999. The difference between these reaches in 1999 is only marginally significant (p = 0.073). Although having a significantly larger mean diameter in 1990, Jones Creek LOD was less frequently in younger apparent-age categories and was more commonly in a decayed or rotted condition than Crow Creek debris (Young, 1994). This suggests that much of the Jones Creek LOD measured in 1990 was older, pre-fire debris.

Reach-average LOD piece length for Crow Creek (median L_t = 7.10 m) is not significantly greater than that for Jones Creek (6.50 m). Site 93 above the mouth of Jones Creek has the longest pieces on average (8.78 m), apparently as a result of bank undercutting and channel widening that felled a number of exceptionally large fire-killed trees that were growing on the floodplain of the North Fork Shoshone River. Sites 106 and 181 have the shortest L_t (5.70 m) and are the upstream-most reaches studied on each stream. L_t is significantly correlated with downstream sequence (R_s = 0.465, p = 0.043), but not with elevation (R_s > -0.3, p > 0.12). When sites 93, 106, and 181 are excluded, however, L_t and downstream sequence are not correlated (R_s = 0.13), so perhaps local riparian community history is behind the average piece lengths in those three reaches.

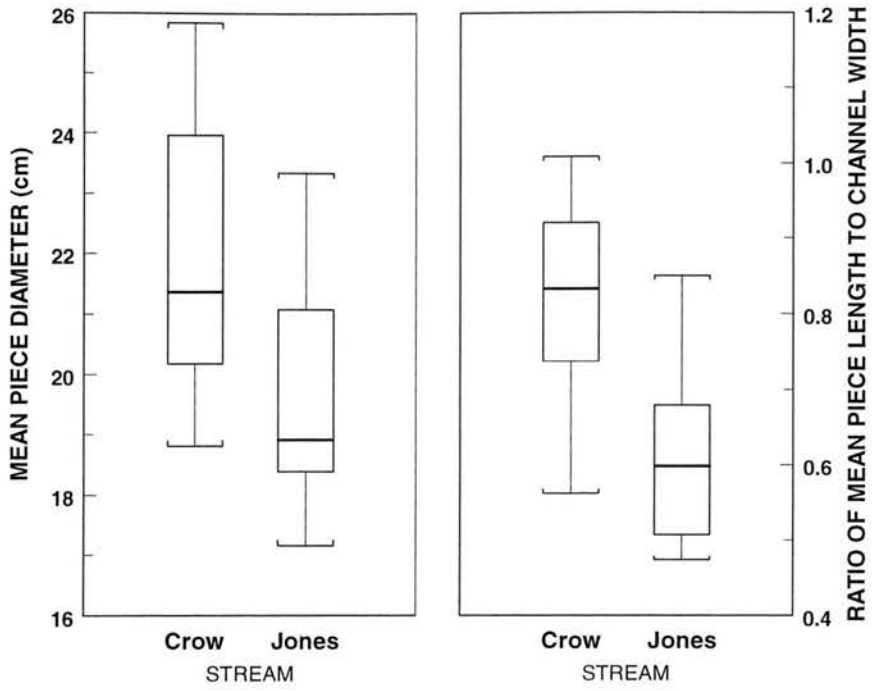

Figure 5.6. Boxplot diagrams by stream of frequency distribution of reach-mean LOD diameter and ratio of mean piece length to mean channel width.

In 1990, mean piece length in downstream Crow Creek (8.5 m) was significantly longer than that for Jones Creek (7.5 m) (Young and Bozek, 1996). Mean piece lengths for these reaches in 1999 are in the opposite rank order: 7.9 m for Crow Creek and 10.0 m for Jones Creek (with pieces less than 15 cm in diameter excluded from the inventories of both reaches). The large change in L_t for downstream-most Jones Creek supports the interpretation of visual evidence for post-1990 undercutting of many very large trees along the left bank of reach 93.

When mean piece length was summarized separately for pieces composing debris jams versus all other pieces (fig 5.7), average length of debris-jam pieces was shorter by a median difference of 0.70 m. This difference is marginally significant (signed ranks V = 45, p = 0.081) and reflects the fact that short, highly mobile pieces of LOD are detained in and comprise a sizable component of most debris jams. However, L_t is positively

correlated with several reach measures of debris jams, including debris jam frequency (R_s = 0.754, p = 0.0010) and percentage of LOD occurring in jams (R_s = 0.574, p = 0.012).

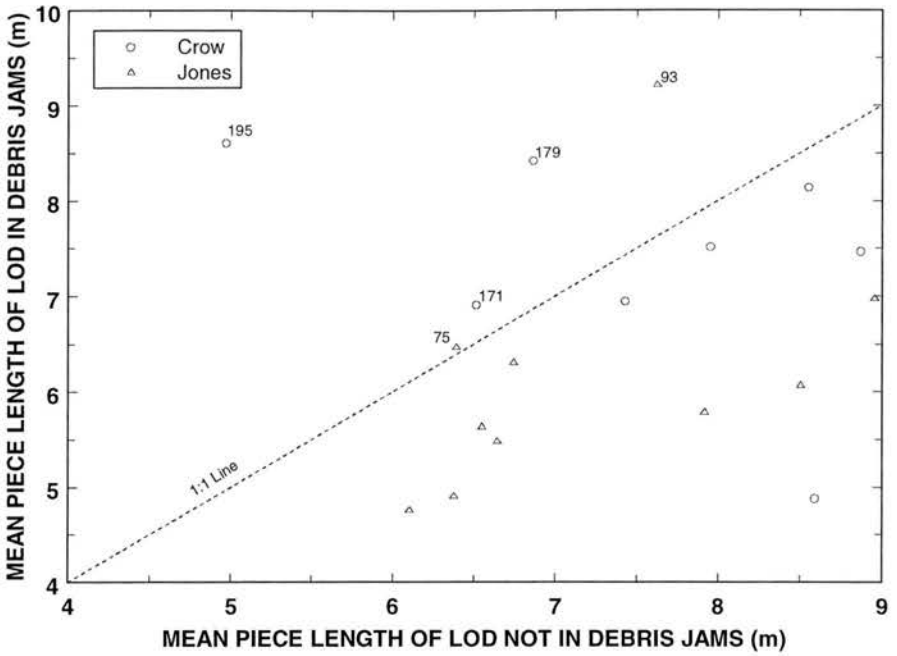

Figure 5.7. Scatter plot of reach-mean total piece length for LOD in debris jams versus all other pieces.

Further insight is gained by summarizing the ratio of L_t to channel width (L_t:W_{bf}). The ratio varied from 0.47 for reach 71 to 1.01 for reach 197. Values of L_t:W_{bf} for Crow Creek are significantly different (W = 142, p = 0.0039) from those for Jones Creek (table 5.1). The combination of larger average piece size in Crow Creek with wider channels in Jones Creek results in the very significantly different L_t:W_{bf} averages for the two streams, and is presumed (cf. Braudrick and Grant, 2000) to be an important factor underlying the greater LOD mobility reported for Jones Creek (Young, 1994). LOD pieces that are longer than the channel is wide are prone to become wedged against the channel margins. For example, Berg et al. (1998) reported that a majority of LOD pieces that were loose in

the channel or braced only by other debris had moved during a single year, compared with only 36 percent of pieces that were longer than bankfull width.

Average piece length within the active channel (L_a) was almost equal for Crow (5.06 m) and Jones (5.02 m) Creeks. Variance of L_a among the reaches of both streams is inflated by an outlier datum, site 189 for Crow Creek and site 93 for Jones Creek. Reach 189 appeared to have widened in response to flow deflection around three debris jams. But variability in L_a among Jones Creek reaches is greater than that among Crow Creek even when the outliers are excluded (CVs of 14.1 versus 7.5 percent, respectively). Jones Creek reaches 71, 106, and 107 each had L_a values less than the minimum value measured among Crow Creek's reaches.

Active-channel piece length is significantly correlated with reach gradient (R_s = -0.600, p = 0.0088) and mean bankfull width both of pools (R_s = 0.531, p = 0.0209) and riffles (R_s = 0.454, p = 0.0481). The inverse correlation between L_a and gradient may reflect the increased stream power of high flows in steeper reaches to break pieces of LOD that protrude into the active channel, thus decreasing the average length of pieces remaining in the reach.

The effect of longer pieces could be to deflect more flow against banks, widening the channel. If this were the cause of the correlations with channel width, then mean piece diameter and frequency of large, influential pieces might also be correlated with channel width. However, no channel width variable is rank correlated significantly with D_{LD} ($p > 0.4$), LDF_{inf} ($p > 0.3$), or the frequency of pieces with diameter > 30 cm ($p > 0.5$). Even after accounting for relations with drainage area, channel width variables are not significantly correlated with mean piece diameter (smallest $p > 0.18$ for W_p). Obviously, a wider channel can include a longer piece of debris within its banks than can

a narrow reach, and by elimination this appears to be the reason for the correlations between L_a and channel width variables.

5.2.2 Mean Piece Volume

Reach-mean piece volume within the active channel (V_a) ranged from 0.096 m^3 for site 107 to 0.47 m^3 for site 93 (fig. 5.8). Greater average V_a for Crow Creek (median = 0.23 m^3) versus that for Jones Creek (0.20 m^3) is a significant difference between streams (one-sided $p = 0.032$). V_a is more strongly correlated with mean diameter ($R_s = 0.877$, $p = 0.0001$) than with mean active-channel piece length ($R_s = 0.301$), because cylindrical volume is proportional to the square of diameter.

V_a is highly correlated with LDF_{inf} ($R_s = 0.826$, $p = 0.0003$) and percentage of drainage area underlain by talus (Qt%; $R_s = -0.626$, $p = 0.0063$). The inverse correlation with Qt% appears to reflect the difference between watersheds: median Qt% among Crow Creek study sites (2.3 percent) is significantly less ($W = 57$, $p < 0.0001$) than that for Jones Creek sites (5.6 percent). The correlation of influential-LOD frequency with V_a is an artifact of their mutual high correlation with mean piece diameter.

Reach-mean piece volume (V_t; fig. 5.8) shows a similar pattern as that seen for V_a. Average piece size ranged from 0.16 m^3 for reach 107 to 0.51 m^3 for reach 93. The difference between streams is more significant (one-sided $p = 0.026$), showing Crow Creek (median $V_t = 0.33$ m^3) to have larger LOD volume per piece, on average, than Jones Creek (median = 0.26 m^3). V_t is even more strongly correlated with D_{LD} ($R_s = 0.917$, $p < 0.0001$) than is V_a.

In the downstream reaches, 1990 mean piece volume was not significantly different between streams (Young, 1994). In 1999, mean piece volume in Crow Creek

was 0.56 m^3 (versus 0.48 m^3 in 1990), and was 0.65 m^3 in Jones Creek (essentially unchanged from 0.63 m^3 in 1990). The unchanged rank order of mean piece volume for these reaches masks the opposing changes noted for mean diameter and length of LOD.

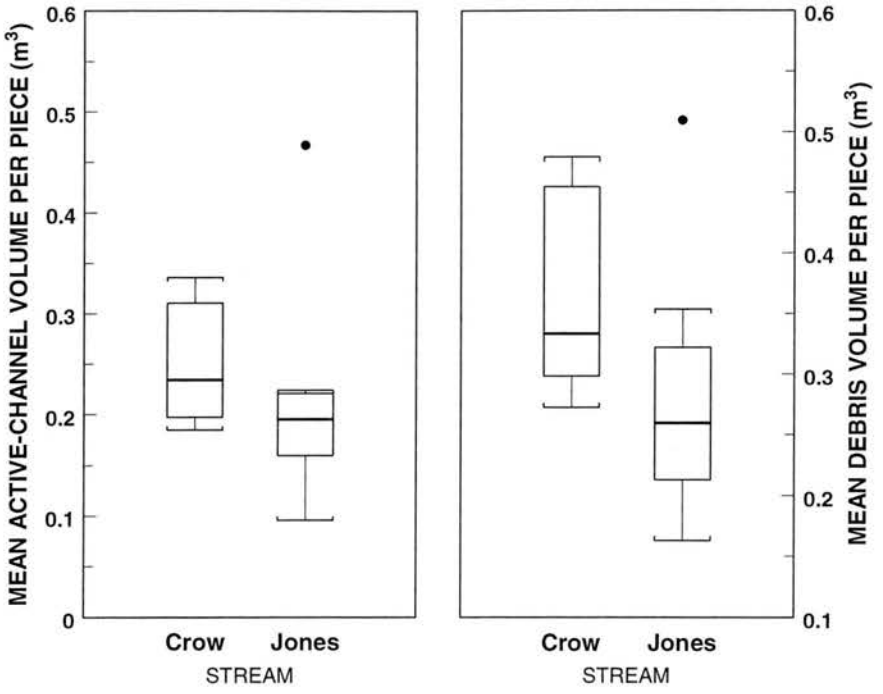

Figure 5.8. Boxplot diagrams by stream of frequency distribution of reach-mean active-channel and total LOD volume per piece.

The average size of LOD is presumed to be related strongly to the size of debris delivered to the channels and to the age structure of riparian timber stands along these streams. Riparian trees adjacent to Crow Creek have continued growing for another decade since the fire that killed nearly all such trees along Jones Creek, so the average size of standing trees is presumably greater along Crow Creek. Additionally, greater duration of high streamflows in Jones Creek provided capability for greater transport of LOD (cf. Young, 1994), whereas in Crow Creek same-size debris may have been immobile or less mobile. Given this *a priori* knowledge, the rank-sum tests of differences between streams in average LOD size per piece (table 5.1) were conducted

for one-sided hypotheses of larger LOD in the reference stream than in the burned stream.

However, Young (1994) reported that although riparian trees were smaller along Jones Creek than along Crow Creek, mean diameter of LOD was greater in Jones Creek in 1990. Note that Young's study sites were the downstream reaches of each creek, and in 1999 Jones Creek's terminal reach had the largest mean volume per piece (0.51 m^3) among all study reaches.

The greater reach-mean diameters and volumes per piece of LOD for Crow Creek reaches are interpreted as a fire-related difference. The fire killed trees of all ages along the banks of Jones Creek, and younger trees would have thinner roots that would decay more rapidly than the thick roots of older trees. Therefore, the rate at which younger trees would be expected to fall into Jones Creek is greater than that expected for an undisturbed stream such as Crow Creek. The greater mean piece length for Crow Creek, though not significantly different from Jones Creek, also lends support for this interpretation.

5.2.3 Summary

Reach-mean LOD diameter is about 10 percent smaller in Jones Creek than Crow Creek. Mean piece length for pieces composing debris jams was shorter (median difference of 0.70 m) than that for other pieces, a marginally significant difference. This difference indicates that short, highly mobile pieces of LOD are detained in and comprise a sizable component of most debris jams. The ratio of piece length to channel width is significantly different between streams. This difference results from the combination of larger average piece size in Crow Creek with wider channels in Jones Creek, and is

presumed to be an important factor underlying the greater LOD mobility reported for Jones Creek by Young (1994).

On average, Crow Creek has larger pieces of debris than Jones Creek. Two factors may contribute to this difference. Riparian trees along Crow Creek have continued to grow since the fire that killed nearly all riparian trees along Jones Creek. Also, the fire killed trees of all ages along Jones Creek, and smaller trees would fall at a faster rate because their smaller roots would decay more rapidly.

5.3 LOD Loading

Given that LOD loading units used for this study were volume per channel length, it was expected that active-channel LOD loading might be related to channel width, whereas total loading might be independent of channel width and related to unmeasured characteristics of riparian stands. Total LOD loading per 100 m (VL_t) ranged from 4.8 m^3 in reach 106 to 51 m^3 in reach 93, both in Jones Creek (fig. 5.9). Berg et al. (1998) reported LOD loadings of 3.9 and 8.7 m^3 per 100 m for two central Sierra Nevada eastern-slope streams draining smaller watersheds burned within the previous 75 years. These loadings are similar to those found in some Jones Creek reaches.

Total LOD loading per 100 m of channel in Crow Creek reaches (median VL_t = 21.6 m^3) tended to be greater than for Jones Creek (median VL_t = 13.8 m^3), but the difference was not significant ($p = 0.105$). Variability among the reaches of Jones Creek was much greater than that among Crow Creek reaches (fig. 5.9), as indicated by the CV (table 5.1), but the influence of site 93 (VL_t = 51 m^3) is very strong on the parametric statistics. Substantial lateral migration of this reach was reported by Young (1994), and the extent of recent bank erosion and undercutting of streamside trees along this downstream reach are atypical of Jones Creek as a whole.

Active-channel LOD loading (VL_a) ranged from 3.3 m^3 per 100 m in reach 106 to 47 m^3 per 100 m in reach 93. On average, VL_a is slightly greater among Crow Creek reaches (median VL_a = 14.6 m^3 per 100 m) than for Jones Creek (median VL_a = 8.9 m^3), but the difference is not significant (p = 0.22). Site 93 again is a positive outlier among the Jones Creek data (fig. 5.9). VL_a is highly correlated with nearly all computed measures of LOD accumulations, including frequency of pieces in contact groups (R_s = 0.889, p = 0.0001), frequency of contact groups (R_s = 0.702, p = 0.0022), percentage of pieces occurring in contact accumulations (R_s = 0.700, p = 0.0023), frequency of influential pieces (R_s = 0.697, p = 0.0024), frequency of pieces in debris jams (R_s = 0.640, p = 0.0053), and frequency of pieces in small accumulations (R_s = 0.630, p = 0.0061). Also, VL_a is significantly correlated with frequency of debris jams (R_s = 0.538, p = 0.019) but not with any of the three channel-width variables (W_{bf}, W_r, and W_p).

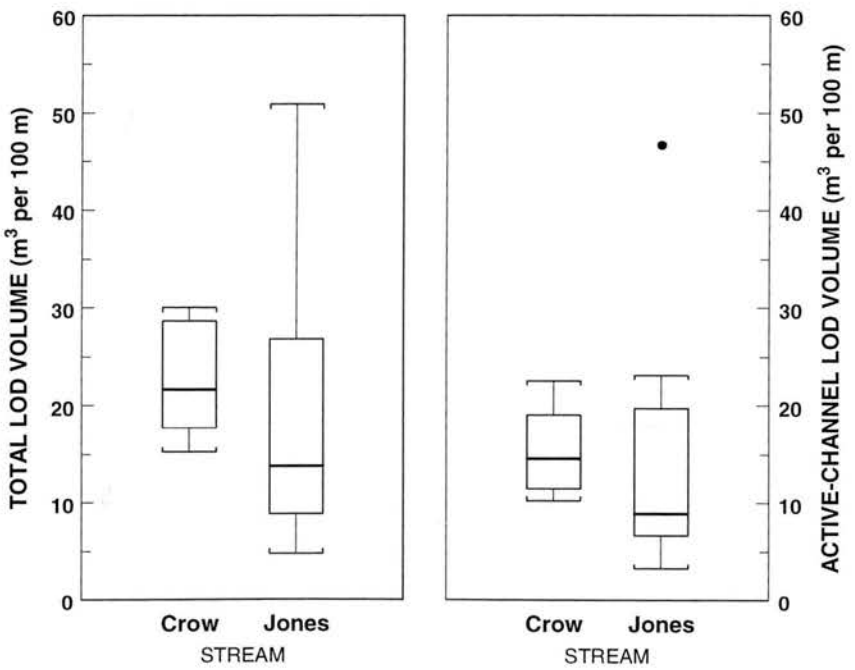

Figure 5.9. Boxplot diagrams by stream of frequency distribution of reach-mean total and active-channel LOD loading.

Although the anticipated relation with channel width did not surface as a rank correlation, development of a multiple linear regression model for active-channel loading was explored to see whether it or other factors might be significant after accounting for the strong influence of LOD accumulations. Normality of residuals was achieved by using the logarithm of VL_a as the dependent variable. The model chosen by stepwise selection uses debris jam frequency (DJF), frequency of influential LOD pieces (LDF_{inf}), the dummy variable for stream identity (WS), and the interaction between drainage area (A_d) and WS as independent variables. The model,

$$\log(VL_a) = 1.03 + 0.118\ DJF + 0.032\ LDF_{inf} - 0.57\ WS - 0.0069\ A_d + 0.013\ A_d{:}WS \quad (5.2)$$

fitted using all 20 study reaches (fig. 5.10), explains 86.9 percent of the variability in VL_a with a RSE of 0.12 log units. However, with so many independent variables included in

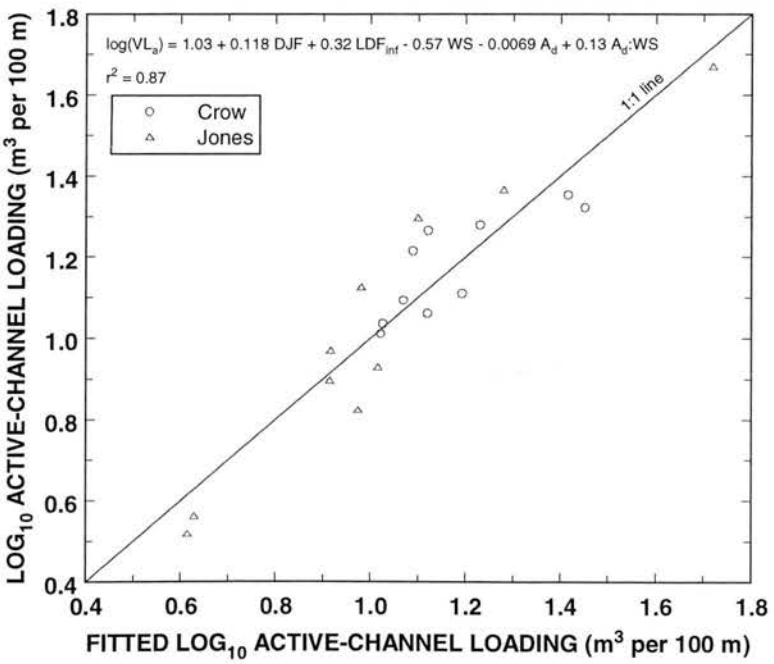

Figure 5.10. Fit of multiple linear regression model for reach-mean active-channel LOD loading.

the model, its applicability beyond the calibration data set is less likely. Both LOD independent variables are highly significant ($p < 0.0015$ for each) and the interaction term is significant ($p = 0.014$). The difference between streams also is highly significant ($t = -3.47$, $p = 0.0038$) and indicates that LOD loading in Crow Creek reaches is 0.57 log units greater (with 0.16 SE) than that in Jones Creek when A_d approaches zero, after accounting for the relations with the independent LOD variables. The coefficient for drainage area, quite small in magnitude, is not significantly different than zero ($t = -1.72$, $p = 0.108$) but is included in the model for completeness.

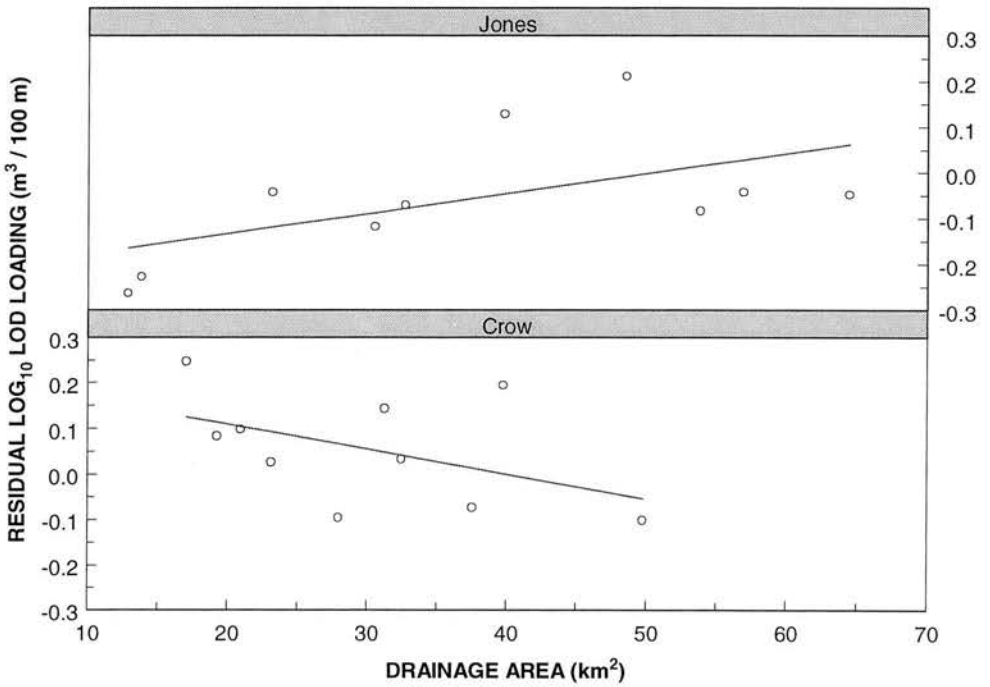

Figure 5.11. Interaction between drainage area and stream in multiple-regression model for reach-mean active-channel LOD loading (eq. 5.2). Ordinate is residual $\log(VL_a)$ from linear regression with DJF and LDF_{inf}.

The positive coefficient of the interaction in equation 5.2 indicates that LOD loading is more responsive to downstream increases in drainage area in Jones Creek than in Crow Creek. To illustrate this result, residuals from multiple linear regression of $\log(VL_a)$ with DJF and LDF_{inf} were plotted versus drainage area, by stream (fig. 5.11). It

is also noteworthy that this contracted model explained 73.6 percent of the variability in $\log(VL_a)$ using only two terms rather than the five terms used in model 5.2. The importance of debris jams and influential individual pieces in retaining highly mobile LOD in specific reaches is reflected by the regression results. The differences between streams are consistent with continued greater mobility of LOD in Jones Creek, which would lead to more rapid delivery of LOD to downstream segments (interaction term) and export out of the watershed (dummy variable).

5.4 LOD Orientation

Piece counts by category of orientation were converted to percentages of the total piece count within each study reach. Streamwise-average percentages by orientation category (table 5.2) show the least common orientation is angled upstream (fig. 5.12). This orientation has been reported as unstable (Bilby and Ward, 1989) and is the least likely orientation of a piece (having attached rootwad or nonfloating end) that has been moved by the flow (cf. Braudrick and Grant, 2000). Also, because prevailing winds in this region are westerly and both streams trend east-northeast, windthrow would not be expected to deposit LOD with an angled-upstream orientation.

Table 5.2 – *Summary of large organic debris orientation in study reaches.*

[CV, coefficient of variation; p-value, probability value; sample size is 10 reaches for each stream]

		Crow Creek			Jones Creek			
LOD orientation	Variable name	Mean	Median	CV (%)	Mean	Median	CV (%)	p-value for rank-sum test of different medians
Parallel to streamflow	$O\%_{par}$	32	30	21	37	35	31	0.143
Angled downstream	$O\%_{ds}$	31	31	23	25	22	52	.089
Transverse to streamflow	$O\%_{tr}$	31	30	25	32	29	28	> .5
Angled upstream	$O\%_{us}$	5.9	5.9	45	6.3	6.2	76	> .5

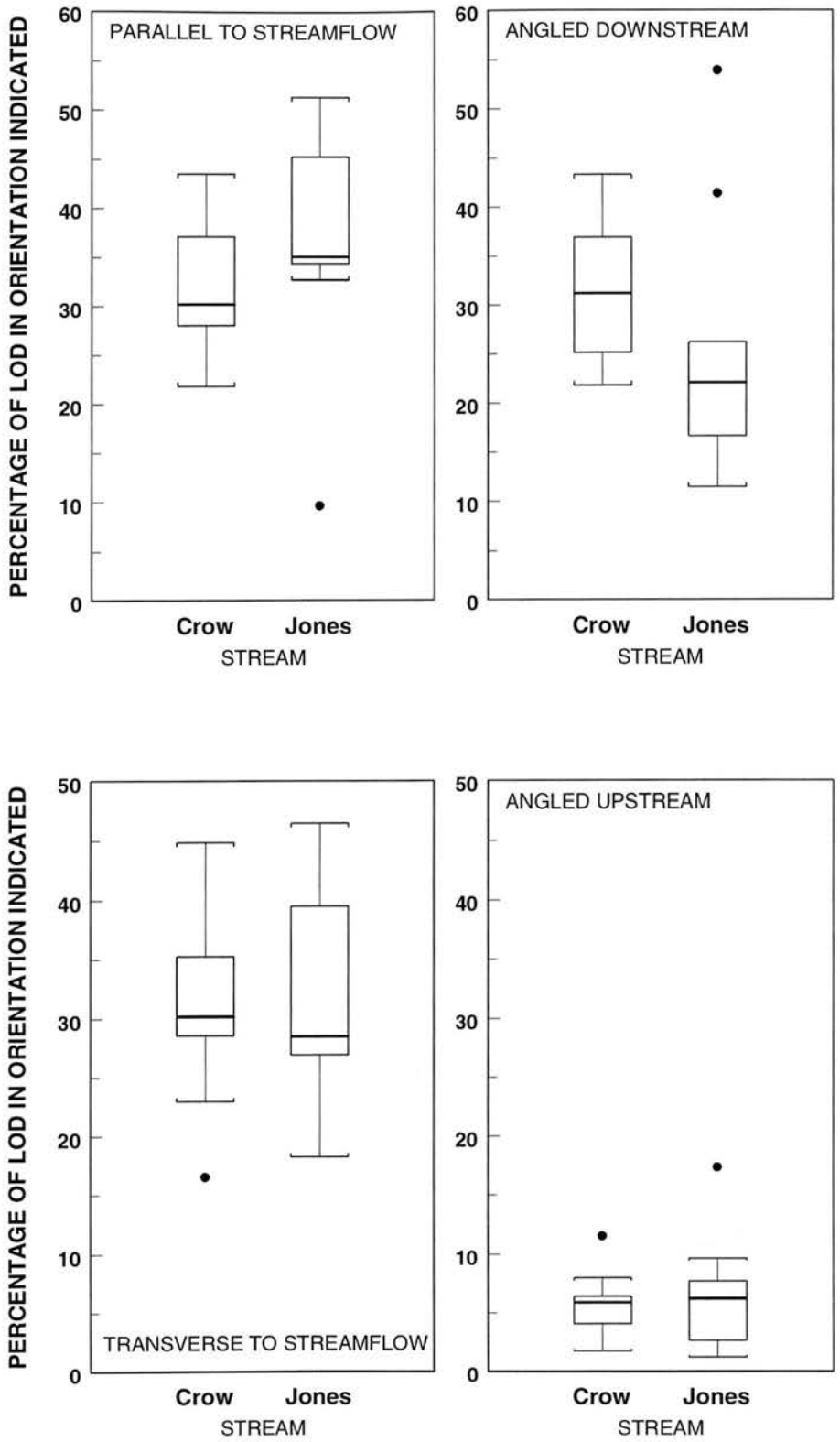

Figure 5.12. Boxplot diagrams of frequency distribution of reach-mean LOD orientation, by stream and orientation category.

Overall, about two-thirds of pieces were oriented either transverse or parallel to flow (table 5.2), with at least 52 percent of pieces so oriented in all study reaches except site 107 (36.5 percent). The reaches of Jones Creek contained LOD with more variable orientation than those of Crow Creek (i.e., larger CV for Jones Creek reaches for all four categories), though graphic summaries (fig. 5.12) show that IQRs for Jones Creek are noticeably larger only for the "transverse" and "angled upstream" categories. No reach characteristics were found to be correlated significantly with $O\%_{tr}$ or $O\%_{us}$.

There was only one LOD-orientation difference between streams that was even marginally significant: the percentage of LOD angled downstream to flow ($O\%_{ds}$) was marginally greater among Crow Creek reaches ($W = 128$; $p = 0.089$). The only site with a majority of its LOD oriented as "angled downstream" was reach 107 of Jones Creek. This reach also had the smallest mean piece diameter among study reaches (17.2 cm), and its finer LOD loading may have been more readily rotated by streamflow. However, there was no correlation between reach-average values of $O\%_{ds}$ and D_{LD} overall ($R_s = 0.009$). Rather, $O\%_{ds}$ was significantly rank correlated with the ratio of mean total piece length to bankfull channel width (L_t:W_{bf}; $R_s = 0.511$, $p = 0.026$), but not correlated with L_t itself. Meanwhile, $O\%_{par}$ is significantly inversely correlated with L_t:W_{bf} ($R_s = -0.635$, $p = 0.0056$) and positively correlated with all three channel-width variables (W_r, W_p, and W_{bf}) at significant levels ($p = 0.0051$, 0.018, and 0.0048, respectively).

In wider reaches more of the LOD is subject to rotation by streamflow into parallel orientation, whereas pieces with greater length relative to channel width are less likely to be rotated into parallel orientation but rather to be angled downstream. In the reference stream, nearly equal proportions of inventoried pieces were oriented parallel, angled downstream, and transverse to streamflow. Typically stable LOD delivered

chiefly by windthrow and bank erosion probably produces this uniformity of orientation distribution (excluding the angled upstream category). In Jones Creek a shift in the orientation distribution from angled-downstream to parallel to flow may reflect greater LOD mobility resulting from increased streamflow and smaller average piece size.

5.5 LOD Anchoring

Prior to presenting results for the reach-level variables, one notable relation found for the data set of individual pieces of debris is presented. Figure 5.13 illustrates that pieces having a greater number of anchors have greater midpoint diameter, on average, and that this pattern exists for both study streams.

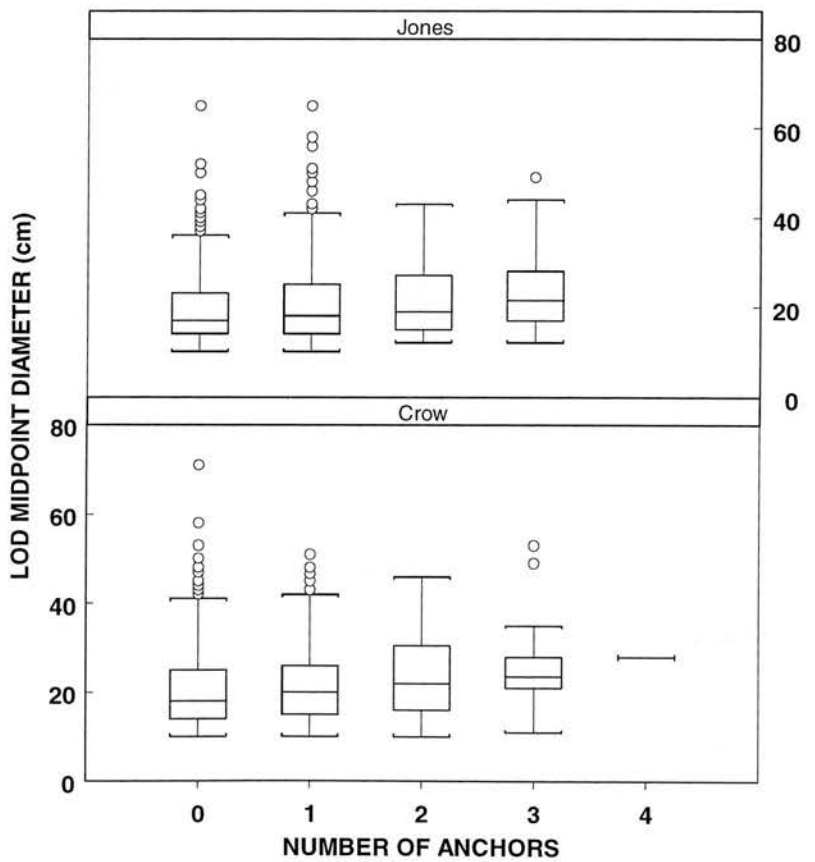

Figure 5.13. Boxplot diagrams of frequency distribution of LOD diameter per piece, by stream and by number of anchor points.

In addition to summarizing the reach-mean number of anchors per piece (N_a) directly (table 5.1), the piece counts by category of anchoring were converted to percentages of the total piece count within each study reach. Crow Creek reaches averaged 0.76 anchors per piece and Jones Creek reaches averaged 0.59 anchors per piece (fig. 5.14), a significant difference (W = 131, one-sided p = 0.026). Results for reach-total percentage of pieces anchored (a%) and percentage of pieces well anchored (a_W%) indicate with marginal significance (W = 126; one-sided p = 0.062 for each variable) that more debris was better anchored in Crow Creek than in Jones Creek.

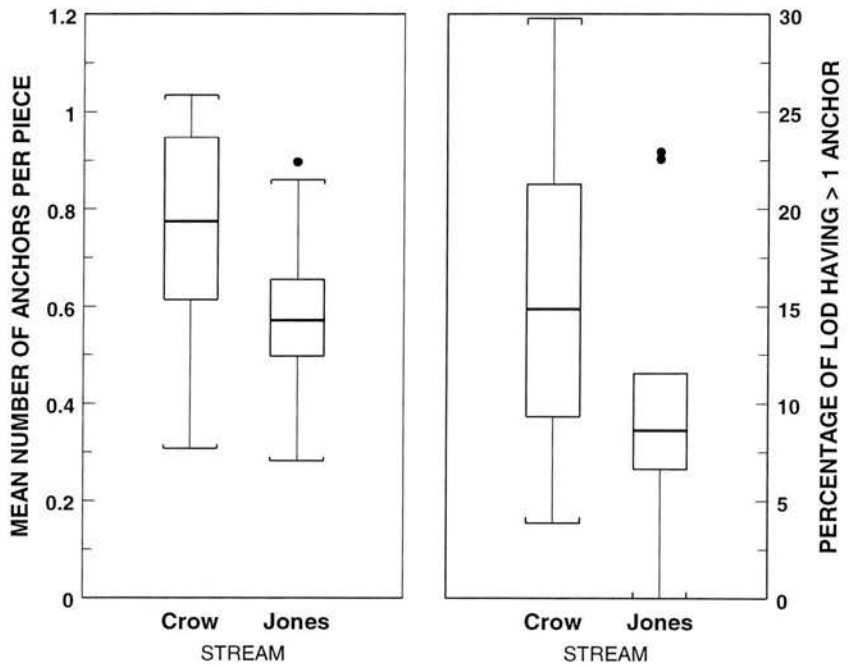

Figure 5.14. Boxplot diagrams by stream of frequency distribution of reach-mean number of anchor points per piece and percentage of LOD having more than one anchor.

In six Jones Creek reaches and four Crow Creek reaches, at least half of inventoried LOD was not anchored. As expected, the frequency of occurrence of anchoring decreased with increasing number of anchors, from streamwise means of 38 and 35 percent of LOD having exactly one anchor in Crow and Jones Creeks,

respectively, to 5.6 and 3.0 percent having more than two anchors, respectively. The most common type of anchoring observed in these watersheds was attachment by roots, so the root decay of fire-killed trees may have contributed to less frequent anchoring of LOD in Jones Creek. Also, the smaller average piece size in Jones Creek is another factor that would tend to result in less tensile strength in roots. The larger percentage of pieces occurring in debris jams in Jones Creek also contributes to a smaller number of anchors and anchored pieces, as compared with Crow Creek.

The several variables computed for LOD anchoring are mutually correlated and show very similar patterns of correlation with only a pair of reach characteristics. For example, a% is inversely rank correlated with drainage area (R_s = -0.531, p = 0.020) and downstream sequence (R_s = -0.486, p = 0.034), and a_W% is more strongly correlated with the same two characteristics (R_s = -0.668, p = 0.0036; and R_s = -0.640, p = 0.0052, respectively). Reach-mean N_a also is correlated with A_d and downstream sequence, at significance levels intermediate to those of the other anchoring variables.

Being most highly correlated with A_d, a_W% was selected for further analysis of possible differences between streams. A plot of a_W% versus A_d by stream (fig. 5.15) indicated the probable presence of an interaction effect between A_d and stream. Linear regression models fitted using least-squares estimation violated underlying assumptions about residuals. A robust least-trimmed-squares regression fit for a_W% among the Crow Creek reaches (fig. 5.15) used 9 of the 10 sites to estimate the linear model,

$$a_W\% = 39.0 - 0.0071\ A_d \qquad (5.3).$$

The robust estimate of the coefficient of determination is 73.5 percent, with estimated residual scale of 3.9 percent of reach LOD. For comparison, the LSE fit using the same 9 reaches explains 81 percent of the variability in a_W% (among 9 values instead of 10) with

RSE of 3.9 percent, is highly significant ($p = 0.0010$), and has very similar coefficients ($\beta_0 = 38.3$ and $\beta_1 = -0.0070$). No significant linear model was found for the Jones Creek reaches ($p > 0.14$).

The fitted simple model for $a_W\%$ in Crow Creek (eq. 5.3) indicates that the relative abundance of well-anchored LOD decreases as drainage area (presumed to represent streamflow discharge) increases. Among Crow Creek reaches only, $a_W\%$ also is highly correlated with the frequency of isolated pieces of LOD (LDF_{iso}; $R_s = 0.794$, $p = 0.018$). As reaches are subjected to increasing magnitudes of discharge and stream power, relatively fewer pieces of LOD are able to remain immobile (Berg et al., 1998), and consequently fewer isolated pieces are found per unit channel length.

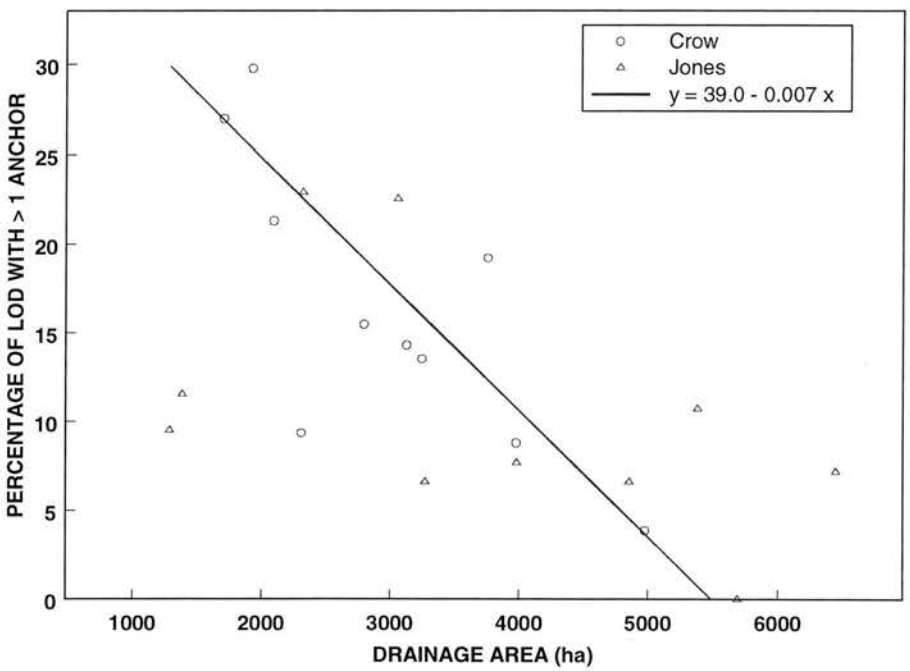

Figure 5.15. Scatter plot of percentage of well-anchored LOD versus drainage area, and robust least-trimmed-squares estimate of linear model for Crow Creek reaches only.

The lack of significance for those correlations in Jones Creek, and the presence of significant inverse correlations with mean piece diameter ($R_s = -0.855$, $p = 0.0098$) and

mean total piece volume (V_t; R_s = -0.709, p = 0.032), indicates that certain factors associated with smaller average piece size may be influential. Within Jones Creek, mean piece diameter is highly rank-correlated with LDF_{inf} (R_s = 0.900), L_t:W_{bf} ratio (R_s = -0.685), LOD loading (R_s = 0.661), and LOD loading in debris jams (R_s = 0.588). The L_t:W_{bf} ratio also is marginally correlated with a_W% among Jones Creek reaches (R_s = 0.648, p = 0.054). Although figure 5.13 indicates that pieces having a greater number of anchors tend to have a greater midpoint diameter, on the reach-average level the relation between these variables becomes inverse (fig. 5.16) as stout, well-anchored pieces frequently collect accumulations of smaller, non-anchored LOD. The residual root strength of thicker pieces also is probably much greater than that of finer pieces a decade after wildfire in this burned stream, increasing their ability to remain anchored and snag smaller, mobile LOD.

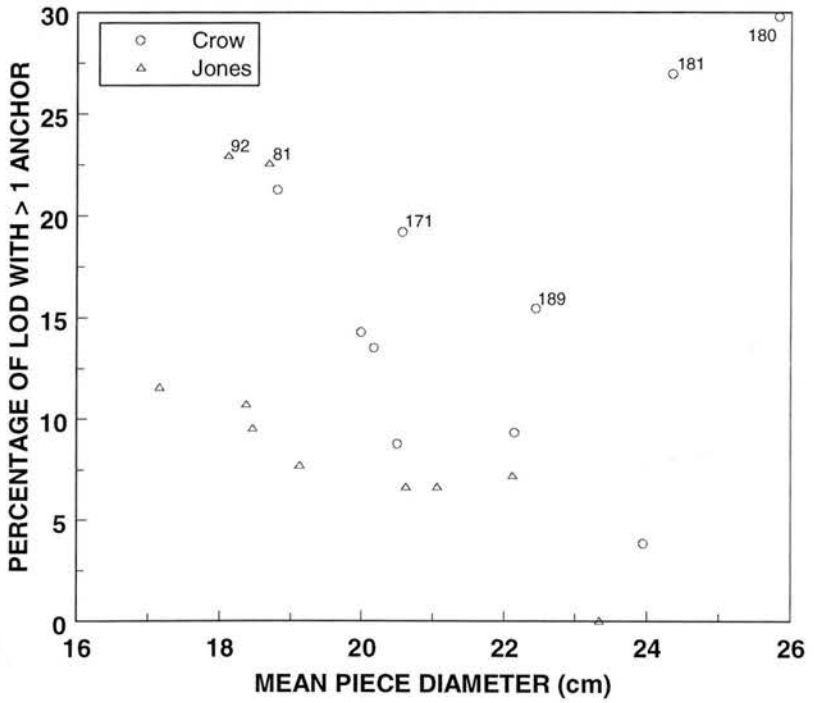

Figure 5.16. Scatter plot of reach-mean piece diameter versus percentage of well-anchored LOD.

Several reaches (sites 81, 92, 171, and 189, see fig. 5.16) have relatively greater percentages of well-anchored LOD and together seem to suggest a second population of reaches also showing an inverse relation with mean piece size. These four sites all feature low bank heights along at least one side of the stream where a number of well-buried pieces of LOD are partially exposed where they extend from flood-plain alluvium. Two reaches (sites 180 and 181, see fig. 5.16) have large average values of both a_W% and D_{LD}. Each of these reaches is just downstream from a very large debris jam (not inventoried) that may be detaining the upstream supply of smaller LOD to these sites. Without abundant fine LOD, the buried or attached larger debris forms a greater proportion of the total LOD loading.

5.6 LOD Piece Position

Pieces are most commonly positioned as drift in the study streams, and slightly more than one third of LOD is positioned as ramps. The least common piece position is collapsed bridge, accounting for 1 percent of Crow Creek LOD and 0.6 percent of Jones Creek debris. Fallen logs bridging these streams are not especially abundant (42 were included in the inventory of 20 reaches, or 2.1 percent of pieces overall), and once broken, powerful high flows would tend to separate the two ends within a few years.

Summaries of the reach-average percentages (table 5.3) show that on average, 96 percent of pieces are positioned as either drift or ramps. Only three reaches (sites 106, 107, and 173) have less than 94 percent of pieces in these categories. Fraction of LOD as drift (Π $\%_{dr}$) ranged from 33 percent for site 107 to 78 percent for site 93. Streamwise averages (table 5.3) and IQRs (11.5 and 11.0 percent for Crow and Jones Creeks, respectively) for Π $\%_{dr}$ are quite similar. Rank correlations with Π $\%_{dr}$ are significant for

the L_t:W_{bf} ratio (R_s = -0.598, p = 0.0090), mean channel width (R_s = 0.564, p = 0.014), and percentage of LOD occurring in debris jams (DJ%; R_s = 0.520, p = 0.024). Drift pieces on average are significantly shorter than ramps or steps (fig. 5.17; $p < 0.0001$ each for rank-sum test of all pieces of each position category). Where channels are wider, especially relative to mean piece length, typically loose, short pieces of LOD drift are probably more likely to be deposited on shallow riffles during waning flows or to be retained in LOD accumulations.

Table 5.3 – *Summary of large organic debris position in study reaches.*

[CV, coefficient of variation; p-value, probability value; sample size is 10 reaches for each stream]

		Crow Creek			Jones Creek			p-value for rank-sum test of different medians
LOD position	Variable name	Mean	Median	CV (%)	Mean	Median	CV (%)	
Bridge (collapsed or whole)	$\Pi\%_{br}$	3.0	3.2	97	2.3	1.2	146	> 0.5
Drift	$\Pi\ \%_{dr}$	60	62	12	62	64	21	.44
Ramp	$\Pi\ \%_{ra}$	36	33	24	35	33	33	> .5
Step	$\Pi\ \%_{st}$	.9	.5	127	1.1	0	167	> .5

Relative abundance of ramp pieces ($\Pi\ \%_{ra}$) ranged from 22 percent for sites 80 and 93 to 58 percent for site 107. Streamwise average $\Pi\ \%_{ra}$ is very similar for both streams, and IQR is 15 percent among reaches of each creek. There is a significant inverse correlation between $\Pi\%_{ra}$ and reach-mean active-channel volume per piece (R_s = -0.510, p = 0.026), but no correlation with total volume per piece. On average, active-channel volume composed only 53 percent of a ramp piece's total volume, versus medians of 100 percent for drift and step pieces. Thus, where ramp pieces dominate the LOD inventory, drift and steps consequently compose a smaller proportion, so more LOD volume occurs outside the active channel.

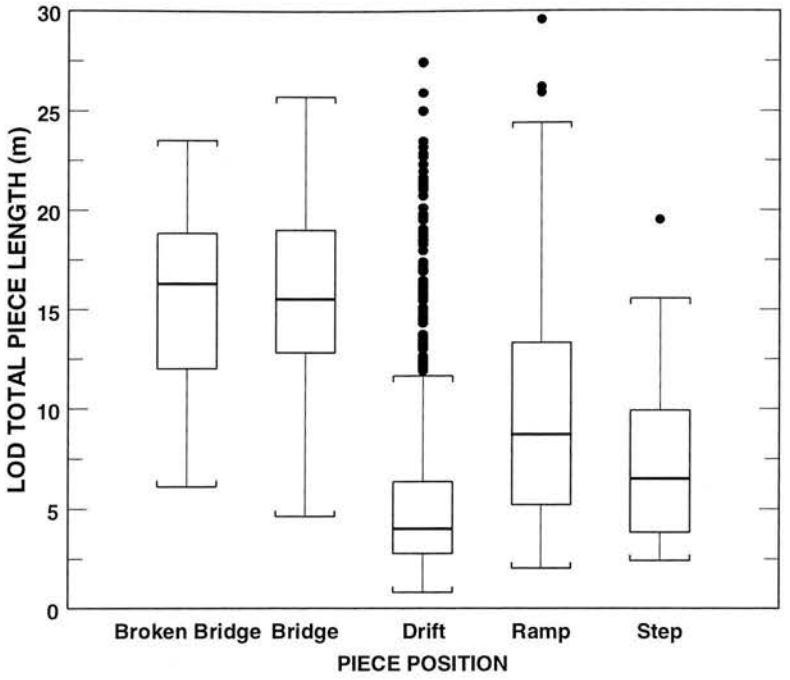

Figure 5.17. Boxplot diagrams by piece-position category of frequency distribution of reach-mean total piece length.

Combined occurrence of bridges and collapsed bridges is summarized in table 5.3. The range of $\Pi\%_{br}$ was from none in reaches 73, 81, 103, 171, 179, and 197 to 9.6 percent for site 107. In Jones Creek, only the two upstream-most reaches had more than 2 percent of their debris positioned as bridges. Crow Creek's two upstream-most reaches also had $\Pi\%_{br} > 2$ percent, in addition to three other reaches scattered along its length. There is no difference between streams in $\Pi\%_{br}$, but occurrence of log bridges is most highly and inversely correlated with reach-mean pool width ($R_s = -0.604$, $p = 0.0084$). Other reach characteristics significantly correlated with $\Pi\%_{br}$ include gradient ($R_s = 0.600$, $p = 0.0090$) and mean bankfull width ($R_s = -0.469$, $p = 0.040$). Except where channels are narrow enough for wind-thrown trees to bridge beyond the opposite stream bank, bridges are rare in the study streams.

Log steps account for 0.9 percent of Crow Creek debris and 1.1 percent of Jones Creek LOD. Percentage of LOD being well-anchored ($R_s = 0.583$, $p = 0.011$) and reach-average water depth in riffle crests ($R_s = -0.466$, $p = 0.042$) are significantly correlated with $\Pi\%_{st}$. In addition to possessing sufficient girth and strength to resist being snapped by the current, log steps must additionally be anchored sufficiently on both banks to resist being rotated into an angled drift position. The inverse relation with riffle-crest depth parallels marginally significant inverse correlations with A_d and downstream sequence, suggesting that stream size may be an underlying factor. Richmond and Fausch (1995) found that stream size was inversely related to both the percentage of pieces spanning the channel and the percentage of pieces lying perpendicular to flow. Most log steps clearly possess those characteristics. Bilby and Ward (1989) found LOD-associated plunge pools were most common in streams less than 7 m wide but decreased in frequency as stream size increased, and were significantly associated with pieces of debris oriented perpendicular to flow.

5.7 LOD Contact Accumulations

5.7.1 All Contact Groups

The number of contact groups, or accumulations of LOD pieces in physical contact with each other, was totaled for each reach and divided by reach length to derive average frequency. The mean number of contact groups per 100 meters (DAF) ranged from 3.3 for site 106 to 12.7 for site 180. Streamwise median DAF (table 5.1) was 8.9 for Crow Creek and 4.5 for Jones Creek. Average values of DAF (fig. 5.18) are significantly different between streams ($W = 72$, $p = 0.0115$).

Reach variables highly correlated with DAF include overall LOD frequency ($p = 0.704$) and both total and active-channel LOD loading ($R_s = 0.722$, $p = 0.0017$; and $R_s = 0.702$, $p = 0.0022$, respectively). Other significant rank correlations include those with total and active-channel volume per piece ($R_s = 0.508$, $p = 0.027$; and $R_s = 0.482$, $p = 0.036$, respectively) and mean piece diameter ($R_s = 0.476$, $p = 0.038$). Although the length of a young tree may exceed channel width, it is piece mass that most importantly determines whether a piece can maintain the stability of a debris accumulation during high flows (Likens and Bilby, 1982). Thus, the correlation between DAF and total volume per piece (presumed to represent mass) is stronger than correlations with either mean piece diameter or length.

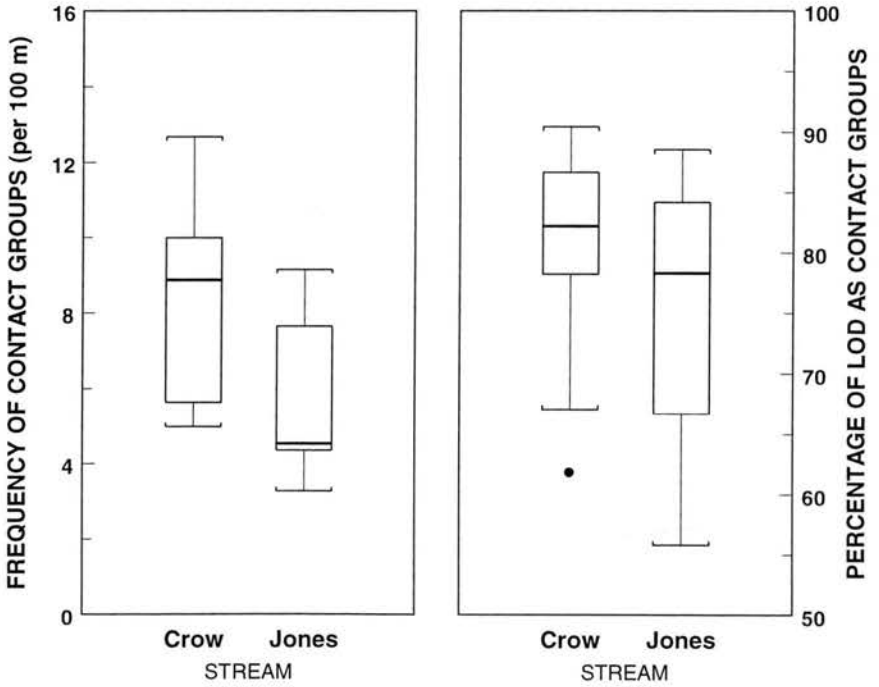

Figure 5.18. Boxplot diagrams by stream of frequency distribution of reach-mean frequency of LOD contact groups and percentage of LOD as contact groups.

The mean number of pieces per contact group (P_{acc}) ranged from 3.7 for site 181 to 11.8 for site 93. Results from the rank-sum test ($W = 88$, $p = 0.109$) indicate that

median size of contact groups in Jones Creek (7.4 pieces) was not significantly larger than that in Crow Creek (6.5 pieces).

The percentage of inventoried pieces occurring in contact groups (DA%) was somewhat greater for reaches of Crow Creek than for Jones Creek (fig. 5.18), but streamwise averages differed by less than 6 percent of total piece count. The difference between streams was not significant ($p = 0.31$). Variability in DA% among Jones Creek reaches was greater than for Crow Creek (for example, IQR was twice as large), as shown in figure 5.18.

The pattern of results for LOD contact groups indicates that the frequency of these accumulations is significantly greater in the reference stream compared with the burned stream, and is greater where debris loading and debris size are large. The larger average piece size and less competent streamflows in Crow Creek probably are chief factors, and would contribute also to greater stability of LOD in that stream as compared with the burned watershed. Reaches where large trees fall into the channel and remain largely immobile are more likely to have numerous small debris accumulations rather than fewer, larger debris jams.

5.7.2 Small Contact Groups

The frequency of small contact groups (SAF; contact groups of < 10 pieces) ranged from 2.6 per 100 m for site 106 to 12.7 per 100 m for site 180 (fig. 5.19). Rank-sum test results ($W = 74$, $p = 0.0185$) indicate that small contact groups are significantly more frequent along Crow Creek (median 7.0 per 100 m) than along Jones Creek (median 3.6 per 100 m). The greater frequency of all contact groups (DAF) along Crow Creek (see section 5.7.1) is caused by the greater frequency of small accumulations of LOD.

The reach-average size of small contact groups (P_{scg}) ranged from 1 piece for sites 180 and 181 to 7.2 pieces for site 93. Streamwise median P_{scg} values were 2.6 and 3.1 pieces for Crow and Jones Creeks, respectively, and the difference was not significant ($W = 84$, $p = 0.123$).

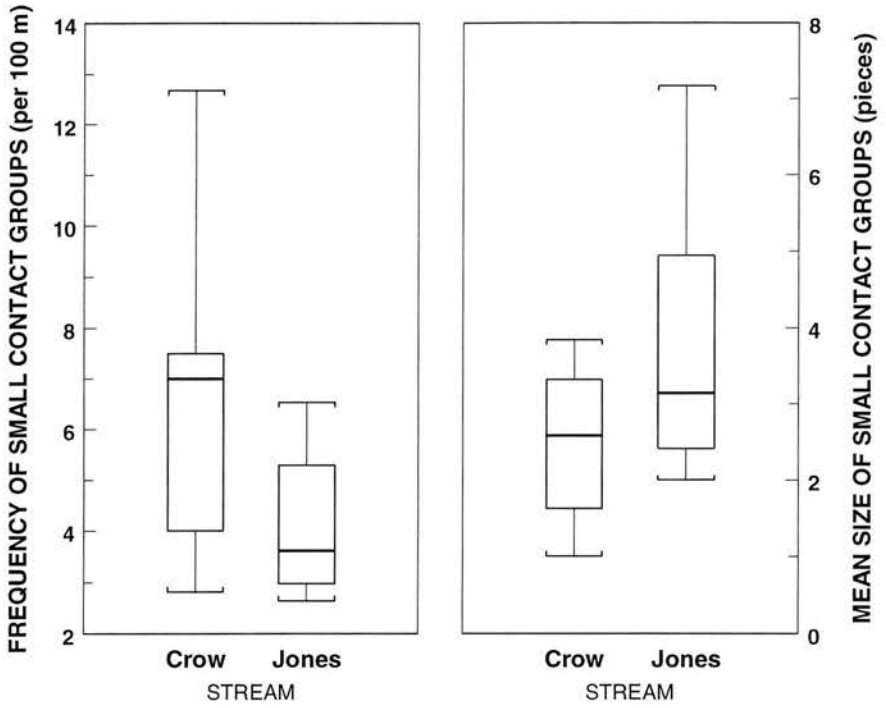

Figure 5.19. Boxplot diagrams of frequency distribution by stream of reach-mean frequency and size of small contact groups of LOD.

5.7.3 Debris Jams

In this section, results for the average frequency and size of debris jams are presented, followed by results pertaining to LOD loading in debris jams. A total of 28 jams were inventoried in Jones Creek study reaches, versus 24 in Crow Creek reaches.

5.7.3.1 Frequency of Debris Jams

The frequency of debris jams (DJF) in study reaches ranged from none to 3.6 per 100 m of channel length, and was insignificantly greater in Jones Creek than in Crow

Creek (W = 103; $p > 0.5$). Two Crow Creek reaches (sites 180 and 181) had no LOD jams, whereas every study reach in Jones Creek had at least one jam. Maximum debris jam frequencies were found in reaches 93 (3.6 per 100 m) and 171 (3.3 per 100 m).

Among the 15 reaches classified as forced-pool-riffle channels, the average DJF is twice as great in Crow Creek (median 2.2 per 100 m) than in Jones Creek (median 1.1 per 100 m). The difference between streams is insignificant (W = 63, p = 0.46) because the variability among reaches within each stream is large.

Frequency of LOD jams is highly correlated with mean size of small accumulations of LOD ($R_s = 0.786$, $p = 0.0006$), mean piece length of LOD (L_t; $R_s = 0.754$, $p = 0.0010$), and active-channel length per piece ($R_s = 0.750$, $p = 0.0011$). DJF also is significantly correlated with LOD loading ($R_s = 0.538$, $p = 0.019$), channel width (all three variables, most significantly with W_r: $R_s = 0.538$, $p = 0.019$), and reach gradient ($R_s = -0.487$, $p = 0.034$). The correlation with L_t could represent a tendency for longer pieces of mobile debris to accumulate in debris jams. This possibility is not supported by the data, as total length per piece is actually less for pieces in LOD jams than for remaining pieces (signed rank test V = 165, p = 0.024). Alternatively, the correlation shown may reflect a causal relation in which debris jams are more likely to occur where LOD pieces long enough to span the channel occur frequently. If so, a positive correlation would be expected between DJF and the frequency of pieces having total length greater than mean channel width ($LDF_{L>W}$). In fact, these two variables are significantly correlated ($R_s = 0.517$, $p = 0.024$) in these streams. Braudrick and Grant (2000) noted that longer pieces are often the key pieces in jam formation.

Scatter plots of DJF versus L_t and $LDF_{L>W}$ suggested that a linear model including the dummy variable for difference between streams might be significant in

explaining observed debris jam frequency. A multiple linear regression model for DJF using reach-mean piece length (L_t) and WS as the independent variables provided a better fit, after excluding anomalous reach 171. This model,

$$DJF = -5.49 + 0.96\ L_t + 0.70\ WS \qquad (5.4),$$

explains 73 percent of the variability in debris jam frequency (fig. 5.20) with a RSE of 0.57 jams per 100 m of channel length. The coefficient for difference between streams (0.70 jams per 100 m with SE = 0.27) is significant (t = 2.58, p = 0.020), indicating that, on average, debris jams occur more frequently along Jones Creek after accounting for

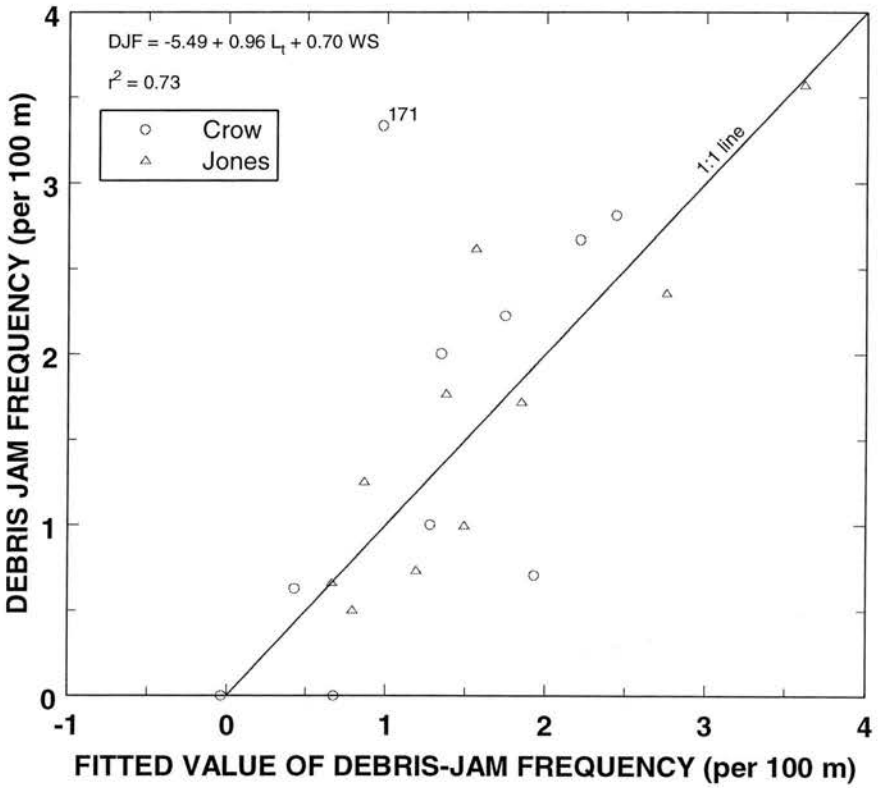

Figure 5.20. Fit of multiple linear regression model for reach-mean frequency of debris jams. Model was estimated excluding the data from reach 171.

the relation with mean piece length. For comparison, the best linear model for DJF using $LDF_{L>W}$ and WS as predictors (fig. 5.21) achieved a robust coefficient of determination

of 62 percent, robust estimate of residual scale of 0.71 jams per 100 m, and had a larger coefficient for difference between streams (1.23 jams per 100 m). Residuals from a robust fit of DJF with $LDF_{L>W}$ alone were significantly larger for Jones Creek than for Crow Creek (medians differed by 0.86 jams per 100 m; W = 77, p = 0.036), indicating a greater frequency of debris jams along Jones Creek after accounting for the relation with $LDF_{L>W}$.

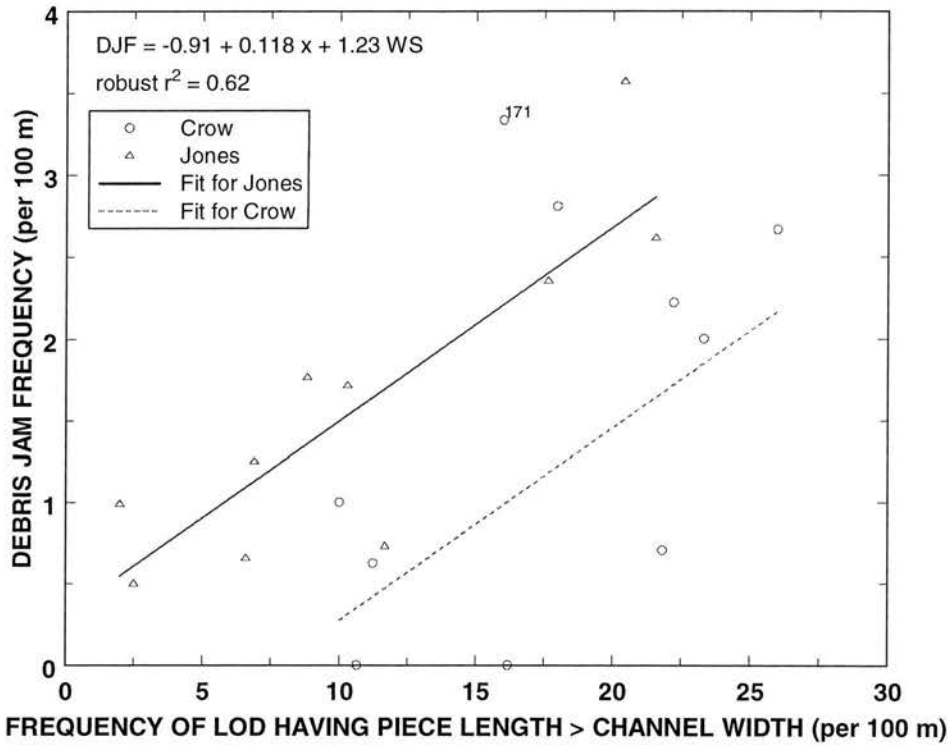

Figure 5.21. Fit of robust least-trimmed squares estimate of linear model for reach-mean frequency of debris jams. Regression lines are least-trimmed-squares estimate of linear model having the equation shown.

The reach-average frequencies of incidence for each category of LOD accumulation (i.e., LDF_{iso}, SAF, and DJF) have been presented. Comparison of their relative frequencies (fig. 5.22) shows that isolated pieces occur more frequently than either type of contact group. Only in reaches 195 and 199 did isolated pieces comprise less than 50 percent of LOD accumulations. The ratio of DJF to SAF ranged from 0

(sites 180 and 181 had no debris jams) to 1 (sites 93 and 189), but did not differ between streams ($W = 92$, $p > 0.35$). Neither was the rank correlation between DJF and SAF significant.

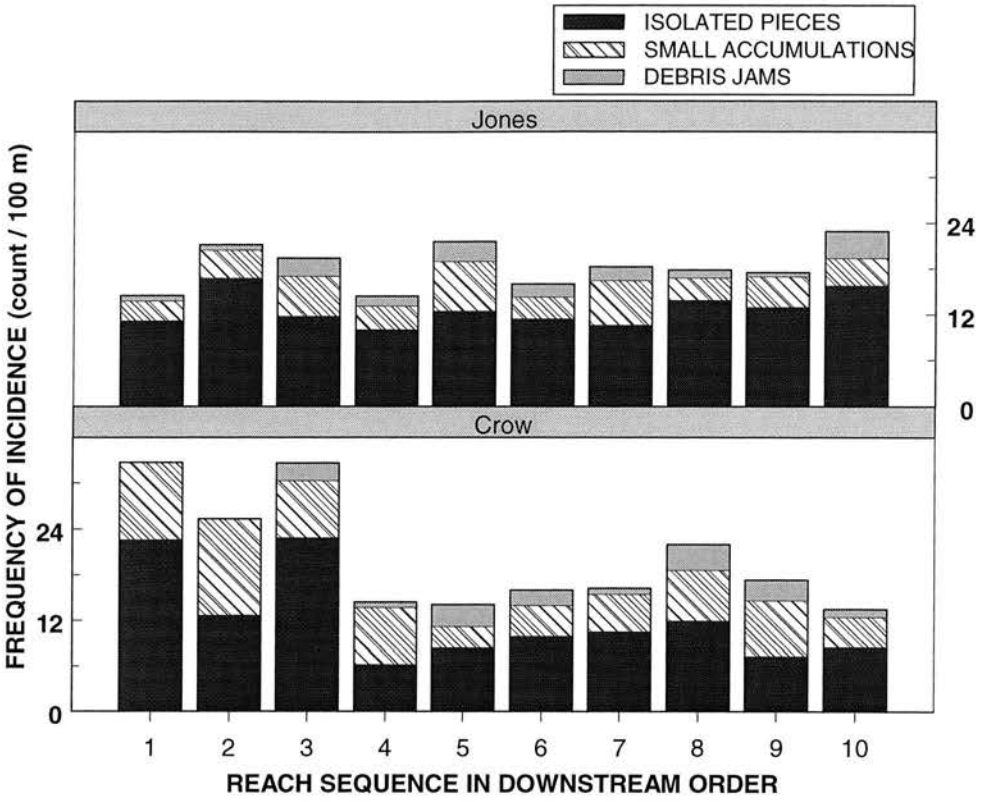

Figure 5.22. Reach-mean frequency of LOD-accumulation incidence by type of accumulation, in downstream order.

5.7.3.2 Size of Debris Jams

Debris jam size was analyzed in terms both of piece counts and estimated piece volumes. Piece counts per jam (P_{jam}) ranged from 13 in reach 92 to 34.7 in reach 75 (among reaches having at least one jam). Average size of jams is slightly larger in Jones Creek reaches (median 21.3 pieces) than in Crow Creek (median 17.7 pieces), but the difference is not significant. The large P_{jam} value for site 197 (34 pieces) appears as an outlier among Crow Creek reaches (fig. 5.23). Sites 195 and 197 are the only two Crow

Creek reaches that had exactly one debris jam present. They also have the largest P_{jam} values among Crow Creek reaches, illustrating the hazards of using averages based on one observational unit. When only reaches having three or more debris jams were retained for the analysis, five reaches from each stream yielded median P_{jam} values of 16.8 and 22.3 pieces per jam for Crow and Jones Creeks, respectively. The difference between streams is marginally significant (W = 20, one-sided p = 0.075).

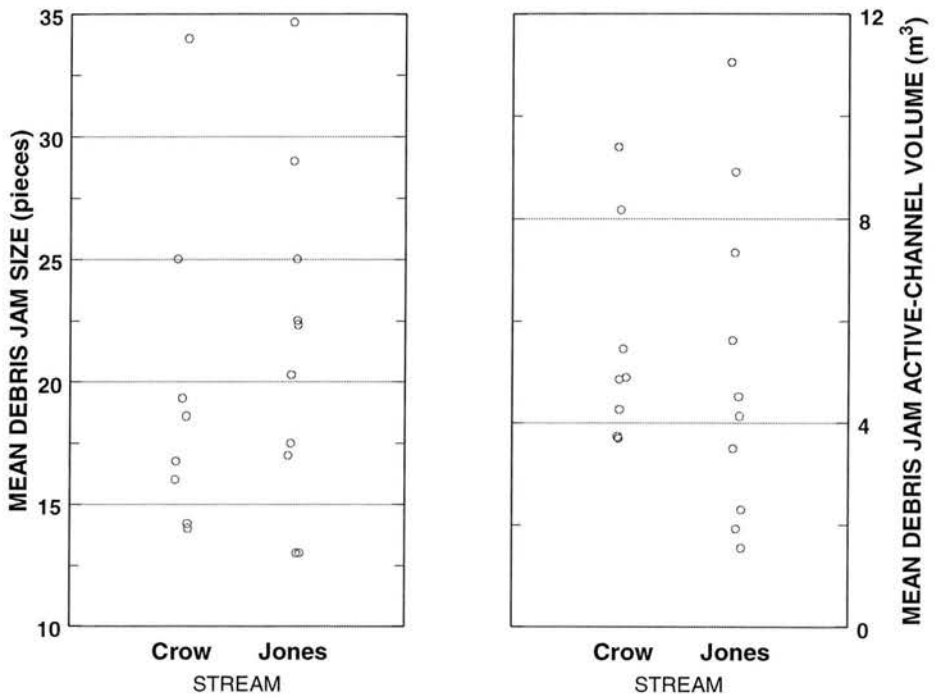

Figure 5.23. Plots by stream of reach-mean debris-jam size and estimated volume.

Among the 10 reaches with at least three jams, P_{jam} is significantly inversely correlated with LOD anchoring variables, including A_W% (τ = -0.822, p = 0.0009), N_a (τ = -0.778, p = 0.0017), and a% (τ = -0.689, p = 0.0056). Two additional but weaker correlations noted are those with drainage area (τ = 0.556, p = 0.025), and piece length L_t (τ = -0.467, p = 0.060). The inverse correlations with piece anchoring and piece length simply reflect the observation that relatively few of the pieces in a large debris jam are

anchored and many short, highly mobile pieces are found in storage mode most commonly in jams. The positive correlation with A_d seems to be caused by the three reaches with smallest drainage area having small P_{jam} values, which may be coincidence.

It is perhaps noteworthy that of four extremely large debris jams observed in Jones Creek, only one was included in a study reach. A more extensive LOD inventory might have produced a larger value for average number of pieces per jam for Jones Creek. However, there were very large debris jams in Crow Creek also (e.g., downstream of site 197) that were not included in any study reach.

Reach-mean active-channel LOD volume per jam (V_{jam}) ranged from 1.54 in reach 106 to 11.0 in reach 93 (among the 18 reaches where debris jams occurred). The average estimated volume of debris jams is slightly larger among Crow Creek reaches than in Jones Creek (table 5.1), but the difference is not significant. When only reaches having three or more debris jams were retained for the analysis, the median of V_{jam} values is larger among Jones Creek reaches (5.6 m^3) than for Crow Creek sites (4.3 m^3), but the difference is not significant ($W = 22$, $p = 0.155$). Among these 10 reaches, V_{jam} is significantly correlated with LDF_{inf} ($\tau = -0.711$, $p = 0.0041$), size of small contact groups (P_{scg}; $\tau = -0.556$, $p = 0.025$), and average piece size (e.g., D_{LD}; $\tau = -0.644$, $p = 0.0095$). Because debris jams comprise at least 57 percent of LOD loading in each of these reaches, the correlation with reach-mean piece size (and possibly with LDF_{inf}) is probably spurious. The positive correlation with P_{scg} likely results from the overall abundance of LOD in many reaches producing increased size of all accumulations, small or large.

5.7.4 Summary

The mean frequency of LOD contact groups of all types is significantly greater in Crow Creek than in Jones Creek. The larger average piece size and less competent

streamflows in Crow Creek probably are the main causes of this difference. Small contact groups (less than 10 pieces) are significantly more frequent along Crow Creek than along Jones Creek. Debris jams are more frequent where there are more LOD pieces long enough to span the channel. The frequency of debris jams is significantly greater in Jones Creek after accounting either for differences in mean piece length, or differences in the frequency of pieces with length greater than channel width. Among reaches having three or more debris jams, the mean size of debris jams is marginally significantly larger in Jones Creek than Crow Creek.

5.8 LOD-Related Sediment Storage

The frequency, thickness, and volume of fine-sediment deposits associated with LOD pieces or accumulations may be an indicator of increased supplies of mobile sediment from upstream sources. Flow deflection around LOD creates zones of locally increased and decreased boundary shear stress that produces areas that favor scour and deposition, respectively.

5.8.1 Frequency of Fine-Sediment Deposits

The reach-mean frequency of LOD-associated fine-sediment deposits per 100 meters of channel length (FDF) ranged from 0 for site 071 to 6.1 for site 93. The median frequency per 100 meters is 3.4 for Crow Creek versus 1.6 for Jones Creek (table 5.4), a marginally significant difference between streams ($W = 81$, $p = 0.075$). Moreover, the set of study reaches in Jones Creek included three sites with large mean FDF values (sites 80, 93, and 103; fig. 5.24) that cause a much larger CV for that stream as compared with Crow Creek (table 5.4). Site 80 has a very low gradient that promotes sediment deposition. Site 103 is adjacent to and immediately downstream from lobes of the large

slope failure that delivered fine sediment and LOD directly to Jones Creek and continues to be a source area for wash load. Site 93 at the mouth of Jones Creek has the largest channel width, LOD loading, and mean piece size. The widened channel includes many large pieces of LOD in this reach that appeared to effectively create pockets of lower streamflow velocity that coincide with sediment deposition.

Table 5.4 – *Summary of reach-average characteristics of fine-sediment deposits associated with large organic debris.*

[CV, coefficient of variation; p-value, probability value; sample size is 9 reaches for each stream, except that for variables FDF sample size is 10 reaches for each stream, and for variables FDT and FDV sample size is 9 for Crow Creek and 8 for Jones Creek]

Characteristic	Variable name	Crow Creek			Jones Creek			p-value for rank-sum test of different medians
		Mean	Median	CV (%)	Mean	Median	CV (%)	
Frequency of fine-sediment deposits (per 100 m)	FDF	3.6	3.4	39.1	2.4	1.6	88.9	0.075
Mean deposit thickness (cm)	FDT	15.7	15.0	28.5	20.1	17.5	43.0	.046
Total volume of fine-sediment deposits (m^3)	FDV_t	8.1	6.2	76.3	10.7	7.0	106	> .5
Volume of fine-sediment deposits per 100 m (m^3)	FDV_l	5.2	4.3	69.9	6.0	3.6	96.2	> .5
Volume of fine-sediment per deposit (m^3)	FDV	1.4	.88	67.6	4.0	1.6	149	.138
Percentage of LOD with fine-sediment deposits	FS%	12.3	11.6	40.1	10.1	7.5	97.0	.25

Excepting these three reaches, the distributions of reach-average FDF values for the two streams do not even overlap (fig. 5.24). Similarly, Hogan (1987) reported frequencies of LOD-related sediment-storage sites for reference streams that were 3 to 4 times greater than those in logged or torrented streams.

Rank correlations with FDF are significant for active-channel LOD loading (VL_a, $R_s = 0.848$, $p = 0.0002$), LOD frequency (LDF, $R_s = 0.803$, $p = 0.0005$), frequency of

LOD in contact groups (LDF_{acc}, $R_s = 0.772$, $p = 0.0008$), debris-jam loading (DJL_a, $R_s = 0.624$, $p = 0.0066$), frequency of contact groups (DAF, $R_s = 0.616$, $p = 0.0073$), and frequency of LOD in jams (LDF_{jam}, $R_s = 0.593$, $p = 0.0098$). Additional significant rank correlations include those with debris-jam frequency (DJF, $R_s = 0.581$, $p = 0.012$) and active-channel volume per piece (V_a, $R_s = 0.577$, $p = 0.012$). LOD abundance, and secondly the frequency and size of debris accumulations, are most positively associated with the frequency of LOD-associated fines deposits.

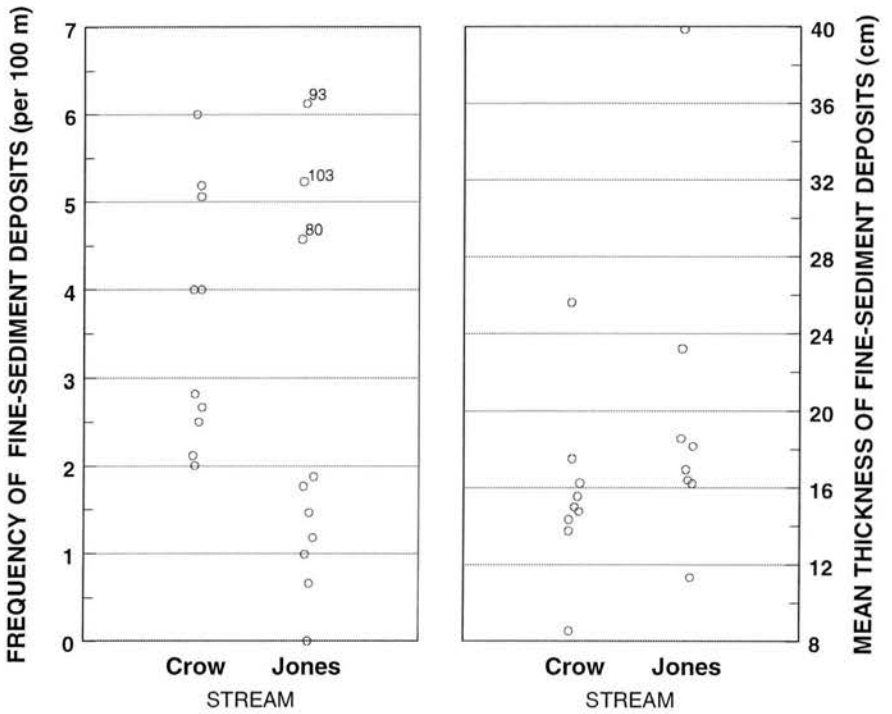

Figure 5.24. Plots by stream of reach-mean frequency and mean thickness of LOD-associated fine-sediment deposits.

A multiple-regression model for FDF that uses debris-jam frequency and the dummy variable, WS, for difference between streams explains 59.5 percent of the variability in the frequency of LOD-associated fine-sediment deposits:

$$FDF = 1.80 + 1.19\ DJF - 1.34\ WS \qquad (5.5).$$

This model has a RSE of 1.26 deposits per 100 m, and indicates that Jones Creek reaches

average 1.34 fewer deposits per 100 m (with SE = 0.56) than do Crow Creek reaches (t = -2.386, p = 0.029), after accounting for debris-jam frequency. The model (F = 12.49, p = 0.0005) and the debris-jam term (t = 4.477, p = 0.0003) also are very significant. When an interaction term was included in this model (fig. 5.25), the results suggested that FDF is more sensitive to debris-jam frequency in Jones Creek than in Crow Creek, but the significance of the interaction term was only marginal (t = 1.830, p = 0.086). A similar finding was reported by Hogan (1987), who found in logged streams that large volumes of sediment were stored upstream of log jams that occurred less frequently than did storage sites in the paired reference streams.

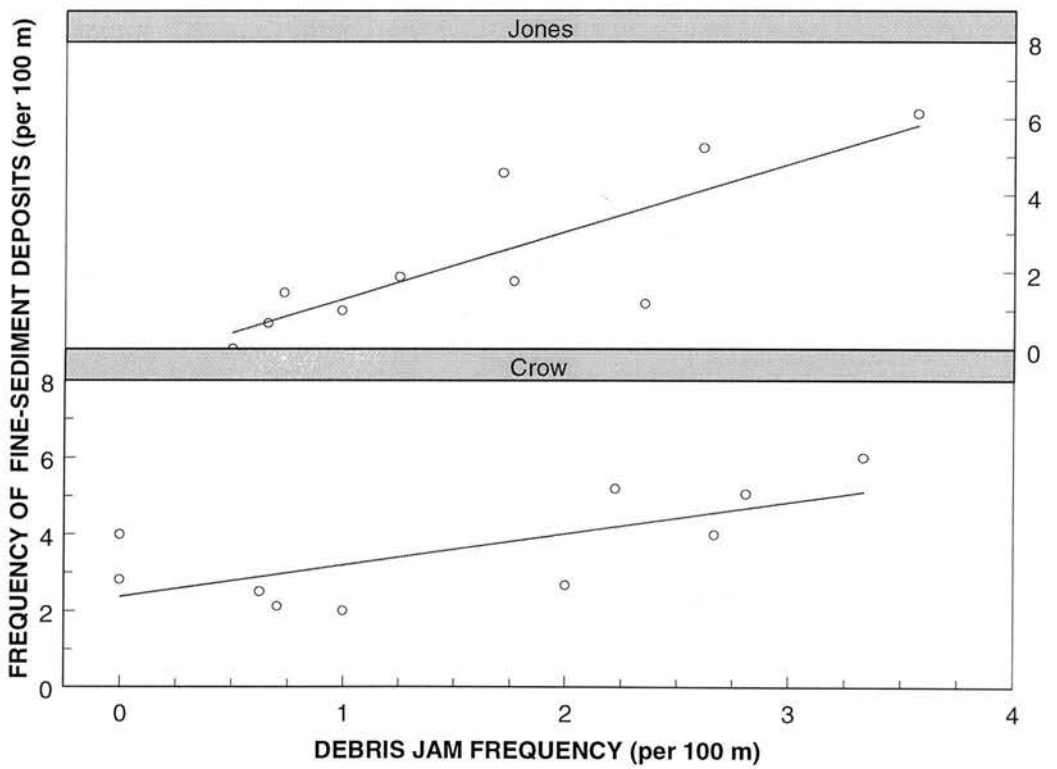

Figure 5.25. Multiple linear regression model of reach-mean frequency of LOD-associated fine-sediment deposits, showing marginally significant interaction between debris-jam frequency and stream. Equation of regression line is FDF = 2.37 + 0.82 DJF – 2.82 WS + 0.93 DJF:WS.

5.8.2 Thickness of Fine-Sediment Deposits

Reach-average mean thickness of LOD-related fine-sediment deposits (FDT) ranged from 8.5 cm for site 197 to 40 cm for site 73 (fig. 5.24). Three reaches lack data for FDT: no thickness measurements were made for sites 106 and 195, and no such deposits were observed for reach 71. Stream median FDT is significantly greater ($W = 63$, one-sided $p = 0.046$) for Jones Creek (17.5 cm) than for Crow Creek (15.0 cm).

Rank correlations with FDT were significant for percentage of reach length in pools (P%; $R_s = 0.843$, $p = 0.0008$), V^*_w ($R_s = 0.811$, $p = 0.0012$), pool residual depth (D_r; $R_s = 0.716$, $p = 0.0043$), and median particle size of pool fines ($[d_{50}]_p$, $R_s = -0.661$, $p = 0.0083$). Positive association with percent pools parallels the results for pool fines (V_{rf}), indicating P% as a good predictor of areas where better depositional sites are likely. Similarly, the positive correlations with D_r (not shown) and V^*_w (fig. 5.26) and the inverse relation with $(d_{50})_p$ suggest that the same hydraulic factors characterizing a particular reach that favor deposition of fine sediment in deep pools contribute to thicker fines deposits in slackwater habitats associated with LOD.

5.8.3 Volume of Fine-Sediment Deposits

Total volume of LOD-associated fine-sediment deposits within each reach (FDV_t) ranged from 0 m^3 for site 71 to 37 m^3 for site 73. Although average FDV_t values for Jones Creek are slightly larger than those for Crow Creek (table 5.2), the difference is not significant ($p > 0.5$). After normalizing per 100 m of channel length, LOD-associated fines volume (FDV_l) still shows no difference between streams ($p > 0.5$), though Crow Creeks reaches have a slightly larger median value of FDV_l (4.3 versus 3.6 m^3 per 100 m). Similarly, Hogan (1987) found little difference in LOD-associated sediment volumes per unit area of channel for three pairs of logged and non-logged reaches.

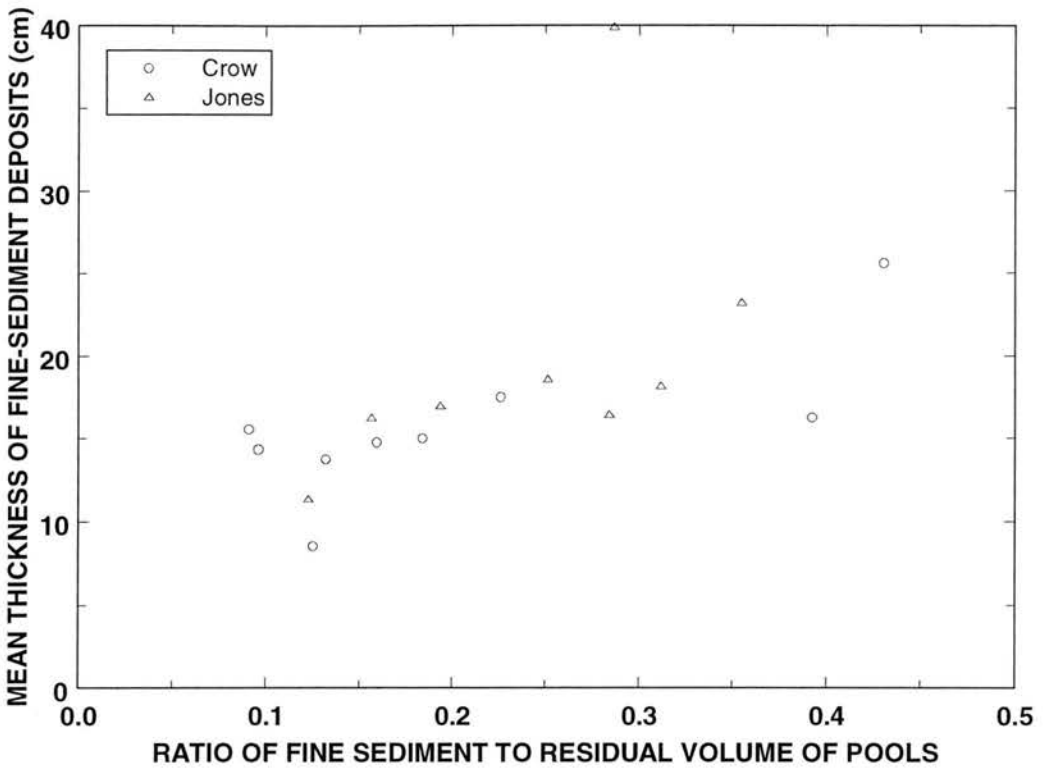

Figure 5.26. Scatter plot of mean thickness of LOD-associated fine-sediment deposits versus reach-mean ratio, V^*_w, of fine-sediment volume to residual-pool volume.

When the LOD-associated fine-sediment volumes are expressed per deposit or storage site (FDV), however, the average for Jones Creek reaches is nearly double that for Crow Creek (median 1.6 versus 0.88 m^3). Overall, values of FDV ranged from 0.58 m^3 for site 93 to 18.3 m^3 for site 73. But only 17 study reaches have reach-mean values of FDV, contributing to diminished statistical power, and the difference between streams is non-significant ($W = 69$, $p = 0.138$). Hogan's (1987) data for three pairs of logged and non-logged stream reaches show a similar pattern in which there is a greater total volume of LOD-associated sediment stored in fewer locations in the logged channels compared to the non-logged. Two of his logged channels had sediment volume per storage site about four times as large as their non-logged counterparts, whereas the third pair showed a 50 percent larger volume per deposit in the logged channel.

5.8.4 Percentage of LOD Storing Fine-Sediment Deposits

The percentage of LOD in each reach that was storing fine-sediment deposits (FS%) ranged from 0 for site 71 to 32 for site 80. Although average FS% is somewhat greater for Crow Creek than for Jones Creek, the difference is not significant ($W = 121$, $p = 0.25$). The maximum value of FS% causes an inflated CV for the Jones Creek reaches; the IQR among reaches is about 7 to 8 percent of reach LOD for both streams.

The finding that an average of only 7 to 12 percent of LOD is associated with fine-sediment deposits is not surprising. Berg et al. (1998) reported that 2.7 percent of pieces surveyed along 60 stream reaches in the central Sierra Nevada trapped measurable sediment deposits. In the Pacific Northwest, Montgomery et al. (1995) found that the proportion of LOD influencing pool formation ranged up to 40 percent but appeared independent of LOD loading. Similarly, FS% is only marginally rank-correlated with LOD loading (VL_a) in the present study ($R_s = 0.409$, $p = 0.075$). Moreover, only three reach characteristics are significantly correlated with FS%. These are the D_r:D_{rc} ratio ($R_s = 0.577$, $p = 0.0119$), frequency of LOD in contact groups (LDF_{acc}; $R_s = 0.468$, $p = 0.042$), and median size of riffle armor (d_{50R}; $R_s = -0.468$, $p = 0.042$). The correlation between FS% and LDF_{acc} suggests that contact accumulations of LOD may create depositional areas with regularity. However, the correlation of FS% with D_r:D_{rc} ratio may simply reflect the coincidence of both pool- and LOD-assocated fines deposits in reaches with deeper pools. Alternatively, the pools may be formed by flow convergence forced around pieces of LOD that also create zones favorable for deposition along pool margins.

5.8.5 Summary

The reach-mean frequency of LOD-associated fine-sediment deposits is greater for Crow Creek than Jones Creek. After accounting for differences in debris-jam

frequency, multiple-linear regression indicates that the reaches in Jones Creek average 1.34 fewer such deposits per 100 m than in Crow Creek. Reach-average mean thickness of LOD-related fine-sediment deposits is significantly greater in Jones Creek than Crow Creek. Correlation results suggest that the same hydraulic characteristics that favor deposition of fine sediment in deep pools contribute to the thicker fine deposits in slackwater habitats associated with LOD. An average of only 7 to 12 percent of LOD is associated with fine-sediment deposits in the study streams.

5.9 Chapter Summary

Reach-mean LOD diameter is about 10 percent smaller for Jones Creek than for Crow Creek. On average, Crow Creek has larger pieces of debris than does Jones Creek. The combination of larger average piece size in Crow Creek with wider channels in Jones Creek results in a greater average ratio of piece length to channel width in the reference stream. This difference presumably contributes to greater mobility of LOD in the burned stream, as reflected in significant correlations between this ratio and the percentages of LOD oriented in the angled-downstream and parallel-to-flow directions. The ratio of average piece length to channel width appears to control the likelihood of many pieces to be rotated into an orientation parallel to streamflow. In the burned stream, a shift in the orientation distribution from angled-downstream to parallel may reflect greater LOD mobility resulting from increased streamflow and smaller average piece size.

Pieces of LOD in the burned stream were less well anchored, as evidenced by a smaller average number of anchors per piece and smaller percentage of pieces being anchored. The larger percentage of pieces occurring in debris jams in Jones Creek contributes to fewer anchors and anchored pieces, as compared with Crow Creek.

LOD position did not differ significantly between the study streams. Neither can it be concluded that LOD-associated fine-sediment volume (either per unit length of channel or per deposit) is different between streams. However, LOD-associated fine-sediment deposits are thicker but occur less frequently in the burned stream than in the reference stream. Correlation results suggest that the same hydraulic characteristics that favor deposition of fine sediment in deep pools contribute to thicker fines deposits in slackwater habitats associated with LOD.

Contact accumulations of LOD occur more frequently along the reference stream than the burned stream. However, the frequency of debris jams is greater in Jones Creek after accounting either for differences in mean piece length or differences in the frequency of pieces with length greater than channel width. Also, among reaches having three or more debris jams, mean debris-jam size (in pieces) is marginally greater in the burned stream.

Comparison of LOD loadings in the study streams showed that neither total nor active-channel volumetric loading of LOD is significantly different between streams when tested using rank-sum procedures. However, a regression model (eq. 5.2) indicates that active-channel LOD loading was significantly greater in Crow Creek than in Jones Creek, after accounting for the relations with the other independent variables.

The frequency of LOD pieces is another measure of LOD loading. LOD frequency in forced-pool-riffle channels is greater in Crow Creek than in the burned stream. Also, a multiple linear regression model (eq. 5.1) indicates that LOD frequency in the burned stream is less than that in Crow Creek on average, after accounting for the effect of debris-jam frequency. This difference is found chiefly in the frequency of LOD in small contact groups, which is greater in Crow Creek than in Jones Creek.

The differences between streams in LOD loading are consistent with continued greater mobility of LOD in the burned stream, leading to rapid delivery of LOD to downstream segments and export out of the watershed. The importance of debris jams and influential individual pieces in detaining highly mobile LOD in specific reaches also is reflected by the regression results.

Chapter 6

CONCLUSIONS AND RECOMMENDATIONS

This chapter presents the principal findings of this study. First are presented the specific conclusions of this study in relation to its objectives. Second, a conceptual framework of general conclusions is presented and implications for resource management are discussed. Finally, future research and methodological recommendations are discussed.

6.1 Specific Conclusions of the Case Study

(1) Objective: *Measure and compare channel characteristics of Crow and Jones Creeks, with particular focus on fine-sediment deposits in pools.*

After accounting for differences in drainage area and other factors, bankfull width is greater in Jones Creek than Crow Creek a decade after the wildfire, and the width difference is significant for both pools and riffles. Average bankfull channel width in Jones Creek was 1.2 m greater, or 14 percent wider, than in Crow Creek, after accounting for differences in drainage area and number of LOD jams. Mean width of pools was 2.2-m greater for the burned stream than for the reference stream after accounting for relations with drainage area and mean active-channel LOD piece length.

Fine-sediment deposits in pools of both streams were predominantly coarse sand to very fine gravel, and typically very poorly sorted. The fraction, V^*_w, of residual pool volume occupied by fine sediment was not significantly different between streams.

There were no significant differences between streams in percent pools, pool spacing, residual-pool mean depth, or pool length. Graphic mean size of riffle armor is about 0.80 phi-units coarser on average in Jones Creek than in Crow Creek, after accounting for differences in reach gradient. The riffle armor for both streams was poorly sorted in nearly all reaches.

(2) Objective: *Evaluate and compare channel stability in Crow and Jones Creeks.*

Stream-type-specific classification of overall channel-stability ratings (Rosgen, 1996) indicates that 20 percent of Crow Creek reaches and 50 percent of Jones Creek reaches were rated as having "fair" stability, and the remainder were rated as "poor" stability. Bank-stability ratings were not different between streams. The marginally significant difference between streams in streambed stability appears to reflect geologic differences rather than fire-related effects. The difference between streams in channel width implies that decreased channel stability followed the burning of Jones Creek.

(3) Objective: *Measure and compare LOD loading and the characteristics of the LOD present in the two streams.*

Differences in average volumetric LOD loadings between the study streams are not significant. LOD loadings in Jones Creek reaches varied over one order of magnitude and were more responsive to downstream increases in drainage area than were loadings in Crow Creek. Frequencies of debris jams and influential individual pieces accounted for most of the variation in volumetric LOD loading. This suggests the important function of jams and influential pieces in retaining highly mobile LOD in specific reaches.

LOD loading measured as frequency of pieces was greater in forced-pool-riffle channels of Crow Creek than in those of Jones Creek. Linear regression results also indicate that LOD frequency was greater in Crow Creek than in the burned stream, after accounting for debris-jam frequency. This difference between streams is found chiefly in the frequency of LOD in small contact groups.

Average piece size of LOD was smaller in Jones Creek than in Crow Creek. The combination of larger average piece size and narrower channels in Crow Creek resulted in a greater average ratio of piece length to channel width in the reference stream than in Jones Creek. Pieces of LOD were less well anchored in Jones Creek. The larger percentage of pieces occurring in debris jams in Jones Creek contributes to fewer anchors and anchored pieces. These differences between streams in LOD anchoring, piece size, and channel width would be expected to contribute to greater mobility of LOD in the burned stream. LOD mobility is suggested by the correlations between the piece-length-to-channel-width ratio and the percentages of LOD oriented in the angled-downstream and parallel-to-flow directions. Relative to Crow Creek, the Jones Creek LOD exhibited a shift in the orientation distribution from angled-downstream to parallel to streamflow.

(4) Objective: *Measure and compare accumulations of LOD and fine-sediment deposits associated with LOD in the two creeks.*

Both the overall frequency of contact accumulations of LOD and the frequency of contact groups of less than 10 pieces were greater along Crow Creek than Jones Creek. However, the frequency of debris jams was greater in Jones Creek after accounting either for differences in mean piece length or differences in the frequency of pieces with length greater than channel width. Also, among reaches having three or more debris jams, mean debris-jam size (in pieces) was marginally greater in the burned stream.

LOD-associated fine-sediment deposits were thicker but less frequent along Jones Creek than Crow Creek. Correlation results suggest that the same hydraulic characteristics that favor deposition of fine sediment in deep pools contribute to thicker fines deposits in slackwater areas associated with LOD.

(5) Objective: *Identify the fire-related or other hydro-geomorphic processes that could explain any significant differences between the two streams.*

Bank erosion by increased streamflow in Jones Creek during the early post-fire period (Troendle and Bevenger, 1996) may be responsible for the larger channel width of Jones Creek. The direction and magnitude of channel-width differences are consistent with typical hydraulic-geometry relations applied to the increased duration of near-bankfull discharge in Jones Creek as compared to Crow Creek. The similarity of mean pool length for both streams implies that Jones Creek pool geometry, like channel width, has responded to the post-fire increase in flow through a proportional increase in size.

Widths of pools and riffles were significantly correlated with the frequency and size of LOD accumulations, suggesting that flow deflection against banks also increased channel width. The importance of LOD in deflecting flow appears to have a greater influence on pool widths than riffle widths. Riffle-armor coarsening in Jones Creek was probably caused by increased duration of near-bankfull streamflow.

Larger average piece size of LOD in Crow Creek may be caused partly by presumed slight differences in age of riparian stands, but a more probable chief cause is the greater rate at which small fire-killed trees would have fallen relative to larger trees. Smaller piece size tends to provide capability for greater transport of LOD (cf. Young, 1994). The results for volumetric LOD loading suggest that piece mobility continues to

be greater in Jones Creek, with consequently more rapid delivery of LOD to downstream segments and export out of the watershed.

6.2 General Conclusions and Implications

6.2.1 Conceptual Framework

Severe burning of nearly all of a third-order forested watershed in steep volcanic terrain of the Middle Rocky Mountains may be expected to produce a series of hydrologic and geomorphic changes (fig. 6.1). A number of these changes remain evident or appear sometime after the first years following the fire. Based on the previously available data and the results from this case study, the following framework organizes what is known about channel characteristics and LOD in the study streams.

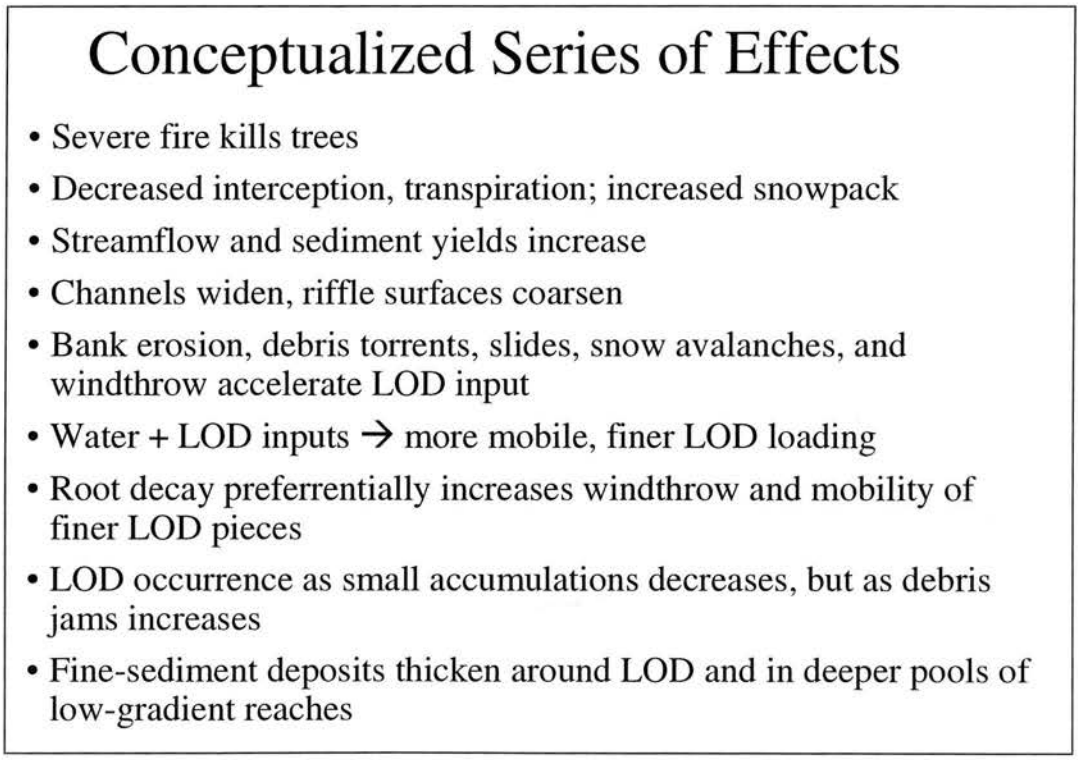

Figure 6.1. Conceptualized series of fire effects on channel and LOD characteristics.

1) Severe burning removed forest canopy cover from at least 60 percent of the Jones Creek watershed. Loss of forest canopy coincides with decreased interception and

transpiration, and increased exposure of land and water surfaces to solar radiation. These changes endured for at least 11 years, but patches of lodgepole pine saplings are now beginning to form a low canopy in many areas. The regenerating forest community lacks the spruces and firs that were abundant prior to the fire.

2) Decreases in forest cover, interception, and transpiration over such a large fraction of the burned watershed causes increases in snow accumulation, soil moisture, and streamflow. Snowmelt runoff is temporally advanced, magnitude of runoff volume increased, duration and magnitude of summer low flows increased, and duration of near-bankfull flows increased by about 16 percent (U.S. Geological Survey, 1990-1994). There was no evidence of increased magnitude of the largest, most infrequent peak flows, however. Available data document the streamflow alteration for 5 years, but the persistence of the deforested condition suggests that these changes probably will endure much longer than 11 years (cf. Troendle and King, 1985), but with decreasing magnitude in recent years.

3) Sediment yield from the burned watershed increased about fourfold compared to the reference stream (Troendle and Bevenger, 1996). Within-channel sources are suspected, as evidenced by a wider channel for the burned stream. Available data (U.S. Geological Survey, 1990-1994) document the sediment yield differences only for 5 years. However, the presence of post-1995 landslide and debris-torrent deposits adjacent to and within the channel of Jones Creek indicate the likelihood that sediment yields in some years, particularly in years with an above-average snowpack, continue to be elevated relative to Crow Creek.

No evidence for surface erosion on vegetated hillslopes was observed in either watershed. A few gullies were noted in one section of the burned watershed, and

torrented channels, debris fans, and slope-failure scars in several locations indicate that bank erosion is not the only post-fire source contributing to sediment yield from Jones Creek.

4) Despite increased sediment inputs following the fire, the increased runoff appears to have been competent to transport most delivered sediment out of the watershed. Also, a coarser riffle armor in the burned streams is presumed to be a post-fire change effected by the runoff increases.

5) Input of LOD has been accelerated to the burned stream through a combination of bank erosion, windthrow, snow avalanches, debris torrents, and at least one landslide. Because several of these processes are not selective with respect to size of LOD piece, the LOD load delivered to the burned stream includes a larger percentage of fine LOD than does the load into the reference stream.

6) The combination of increased streamflow and finer LOD loading in Jones Creek results in reduced anchoring and greater mobility of LOD. This mobility produces a decrease in LOD occurrence as small accumulations and, in reaches where the ratio of piece length to channel width is large, an increase in debris jams. LOD mobility is reflected by increased orientation of pieces parallel to streamflow in wide reaches relative to reaches where the ratio of piece length to channel width is large. Increased mobility probably is also related to the lower frequency of plunge pools in Jones Creek relative to Crow Creek. Greater mobility of LOD in the burned stream implies that the energy-dissipation benefit of heavy LOD loading is concentrated chiefly at debris jam sites rather than being more homogeneously distributed along the channel.

7) Pool spacing is inversely associated with LOD frequency. In Jones Creek pool spacing differs by channel type and is inversely related to the frequency of debris-jam

pieces. Pool spacing in the burned stream may have adjusted to post-fire changes in channel width. Pool size is associated with average piece length of LOD, frequency of debris jams, and, in the burned stream, with drainage area and stream size. Although pool-forming elements were not directly assessed, the data suggest that pool frequency in the burned stream is related to debris jams, whereas in the reference stream pools are associated more with influential pieces and small contact groups of LOD than debris jams.

8) Reach gradient accounts for most of the variation in fine-sediment volume in residual pools. The fraction of pool volume filled by fine-sediment deposits was inversely related to pool spacing, and positively associated with pool depth and percentage of reach length in pools. Fine-sediment deposits associated with LOD occurred more frequently along Crow Creek, where both fine deposits and pieces of LOD in contact groups were more evenly distributed than in Jones Creek. On average, fine-sediment deposits associated with LOD were thicker in the burned stream than in Crow Creek.

6.2.2 Implications for Future Channel Conditions

This case study represents a single point in time along the temporally continuous pattern of stream conditions following wildfire. In the near absence of data for pre-fire or earlier post-fire condition of the study reaches, little can be stated conclusively concerning channel recovery from the findings of this study. This section addresses some probable future conditions that are implied by the findings.

Given the patchy character and slow growth of the regenerating forest, it is probable that there will be a discontinuity of LOD inputs to Jones Creek as the supply of fire-killed trees along the channel becomes exhausted. Declines in LOD input and small

LOD accumulations in Jones Creek may correspond to a decrease in habitat complexity and fish cover along that stream. Reduction of LOD loading or its concentration in fewer locations deprives a channel of much of the energy-dissipation benefit of LOD loading. This may contribute to bank erosion and prolong the duration of widened channels in Jones Creek. One feature in this steep watershed that may partially offset the exhaustion of LOD input from riparian stands is the likelihood of delivery of LOD by snow avalanche or mass erosional events. During two of the winters between field visits to Jones Creek, snow avalanches delivered large accumulations of LOD to the lower third of Jones Creek where chutes extend uninterrupted from the upper ridge slopes to the stream.

LOD conditions in Jones Creek are likely to remain strongly influenced by the large existing debris jams. A gradual but steady decrease in the duration of near-bankfull streamflow is expected to accompany the regrowth of forest over much of the burned area. Thus in the absence of rare floods the streamflows will become incapable of mobilizing large jams, but will probably continue to deliver additional pieces to those accumulations.

Gradual increase in the size of riparian trees along the burned stream will over the next several decades restore the stream shading conditions that typify the reference stream. Consequently cooler water temperatures and low overhanging branches would improve the physical habitat for native fish. Increased root density in streambanks also will accompany riparian regrowth and resist further channel widening.

6.2.3 Implications for Non-wilderness Areas

One of the advantages of the wilderness study area was the absence of potentially confounding influences of human land- and water-use practices. The implications of the

findings from this study for managing watersheds outside the wilderness depend largely on the types of human modifications made to slopes and channels prior to a severe fire. However, it would be much less likely to see a developed third-order watershed experience a near-complete burn. Forest access roads and typical fire-management policies would usually result in effective fire suppression over much of the watershed. In watersheds that are only partially burned, the magnitude and duration of effects would tend to be moderated.

Many of the factors controlling post-fire channel conditions are either natural characteristics of soils and channels or fire-affected processes over which managers could exert little influence. Decreases in interception and transpiration and increases in snow accumulation cannot be practically mitigated, so increased duration of near-bankfull flows will likely occur in proportion to the deforested area of the watershed. If streambank materials are erodible and the instream LOD loading either is consumed by the fire or mobilized by subsequent high flows, bank erosion and channel widening would be difficult to avoid in coarse-bed streams, short of impractical installation of bank-stabilization measures along the entire length of the channel. If, however, water-management options such as controlling reservoir releases, flow diversions, or flow augmentations were available that could decrease streamflows through burned watersheds, those actions could minimize post-fire channel erosion. Also, the LOD surviving the fire could be stabilized, and actions taken to increase LOD loading during the early post-fire years. In addition to its stabilizing influence on stream channels, such debris could detain sediment and organic matter, and provide shading and fish cover (Minshall and Brock, 1991).

A second area for management action relates to mitigating hillslope erosion. Except for mass erosion events, there was little evidence observed that hillslope erosion contributed largely to sediment yields from Jones Creek. If massive hillslope erosion is not inevitable in wilderness areas, it seems likely that measures intended to control surface erosion until revegetation occurs could be effective in highly susceptible areas. Minshall and Brock (1991) suggested that post-fire management actions often should be restricted to controlling runoff and erosion during the first few years.

6.3 Recommendations

6.3.1 Future Research

A principal recommendation, given the number of differences between streams that are significant after a decade of post-fire recovery, is to periodically monitor these streams at 5- or 10-year intervals to better define the pattern and duration long-term recovery from fire disturbance. The area has experienced a relatively dry period in recent years, but when a period of above-normal precipitation returns the potential for differential responses in the two watersheds continues to exist. Unfortunately, some of the study reaches of Crow Creek can no longer serve as undisturbed reference conditions because they are downstream of the area burned in 2000.

A second recommendation for additional study stems from the high degree of correlation between the volume and median particle size of fine sediment deposits in residual pools, and between V^*_w and the mean thickness of LOD-associated fine-sediment deposits. These results suggest potential for development of indicators of fine-sediment enrichment as alternatives to the labor-intensive methods for measuring V^*.

Hilton and Lisle (1993) do not recommend measuring V* in small pools; i.e., those with maximum depth less than twice the riffle-crest depth. Although maximum pool depth was not measured for the present study, many of the pools measured did not satisfy this suggested criterion. By measuring pools of many sizes, an interesting interaction was documented between LOD piece size and residual-pool for pools less than about 9 m^3 in volume. There may be value in further study of relations between LOD characteristics and the V^*_w ratio, particularly if the V* methodology becomes widely used.

Partial burning of the Crow Creek watershed in 2000 presents a rare opportunity to study fire effects on channels for which some pre-fire baseline data exist. Monitoring of all Crow Creek study reaches in or downstream from the 2000 burn is recommended.

6.2.2 Methodological Recommendations

Several recommendations relate to data collection methods and might be classified as lessons learned by hindsight. Other recommendations represent insights gained from field observations and data analysis.

A more sensitive analysis of relations between channel characteristics and LOD could be achieved if the data were segregated by geomorphic unit. For example, in this study only channel width and bed material size were measured separately for pools and riffles. If gradient and LOD inventory had been similarly stratified, greater insight into channel processes and possibly stronger correlations with controlling variables or differences between streams may have resulted. Future studies might also benefit from records linking individual pieces or accumulations of LOD to channel features at or adjacent to the debris. For example, Lisle (1986) recorded channel data for a series of

unit reaches one bed-width in length. Hydraulic and sedimentation-related effects may be more easily identified at that scale than by using reach-average characteristics.

The results for key pool characteristics such as mean depth and volume of the residual pool lend support to the applicability of stream classification systems that feature gradient as a prominent classification variable. For example, Frissel et al. (1986) noted that reach slope is one of the primary controls of potential pool-riffle morphology, and reaches with similar gradient may be expected to have a predictable spatial association of pool-riffle classes. Although they may not introduce bias, the lower precision of hand-level estimates of reach gradient probably is best avoided. Recent developments in light-weight laser levels may allow much more precise leveling in remote locations.

Stratification of study reaches with respect to gradient could be improved. Reaches with gradients less than 3 percent were randomly selected using GIS-calculated slopes, but a better approach might have been to randomly select from segments stratified by gradient in 1-percent intervals, e.g., 0-1 percent, 1-2 percent, and 2-3 percent. This should have produced sets of reaches that did not differ in gradient between streams.

In this study, pool-selection bias was avoided by measuring all qualifying pools sequentially. However, the guidance from Hilton and Lisle (1993) concerning sample sizes and pool types to which the V* methodology is applicable does warrant repetition in light of the significance level of results obtained in this study for a simple difference between streams in the V^*_w ratio. A reach should include a minimum of 10 to 15 pools, and a measurable pool's maximum depth should be at least twice as deep as the water depth at the downstream riffle crest and pool width should include at least half of the low-flow channel (Hilton and Lisle, 1993).

Future inventories of LOD in streams would benefit from including an assessment of the functional characteristics of each piece or grouping. For example, the observer could visualize a range of streamflow levels and record at which stream stages the piece appears to deflect flow against either channel banks or bed. Other functions that might be included are effect on pool morphology, anchoring other pieces of debris, causing a vertical scour hole, and anchoring a "pioneer island" (cf. Montgomery et al., 1995; Gurnell et al., 2000).

Information about the vertical position of each piece of LOD would have improved this study, and should be acquired in future studies of LOD in streams. For example, Platts et al. (1987) and Peck et al. (2000) describe LOD inventory methods that distinguish pieces that extend at least partially below the bankfull stage from those that are only suspended over the channel. Some studies also have noted whether a piece was in contact with the water surface at the time of inventory (Young, 1994). A quantitative survey of piece position within the channel cross-section, although beyond the scope of this and many studies, was made in a large Italian stream by Gurnell et al. (2000), who found that the majority of debris was preferentially stored within distinct elevation zones corresponding to bar crests, island margins, and island surfaces.

REFERENCES

Albin, D.P., 1979, Fire and stream ecology in some Yellowstone Lake tributaries: *California Fish and Game*, v. 65, p. 216-238.

Anderson, H.W., Hoover, M.D., and Reinhart, K.G., 1976, Forests and water—Effects of forest management on floods, sedimentation, and water supply: U.S. Department of Agriculture Forest Service General Technical Report PSW-18, 115 p.

Andrews, E., 1983, Entrainment of gravel from naturally sorted riverbed material: *Geol. Soc. of America Bulletin*, v. 94, p. 1225-1231.

Bagnold, R.A., 1977, Bed load transport by natural rivers: *Water Resources Research*, v. 13, no. 2, p. 303-312.

Barrett, S.W., 1994, Fire regimes on andesitic mountain terrain in northeastern Yellowstone National Park, Wyoming: *International Journal of Wildland Fire*, v. 4, p. 65-76.

Benda, Lee, and Dunne, T., 1987, Sediment routing by debris flow, *in* Erosion and sedimentation in the Pacific Rim: IAHS Publ. 165, p. 213-223.

Berg, N.[H.], Carlson, A., and Azuma, D., 1998, Function and dynamics of woody debris in stream reaches in the central Sierra Nevada, California: *Canadian Journal of Fisheries and Aquatic Sciences*, v. 55, p. 1807-1820.

Berg, N.H., Roby, K.B., McGurk, B.J., 1996, Cumulative watershed effects—Applicability of available methodologies to the Sierra Nevada, in Sierra Nevada Ecosystem Project--Final report to Congress, v. III: Davis, Univ. of Calif., Centers for Water and Wildland Resources, p. 39-78.

Bilby, R.E., and Ward, J.W., 1989, Changes in characteristics and function of woody debris with increasing size of streams in western Washington: *Transactions of the American Fisheries Society*, 118:368-378.

Billings Gazette, 1995, *Yellowstone on Fire!* (2d ed.): The Billings Gazette, 128 p.

Booker, F.A., Dietrich, W.E., and Collins, L.M., 1993, Runoff and erosion after the Oakland firestorm: *California Geology*, v. 46, p. 159-173.

Bozek, M.A., and Young, M.K., 1994, Fish mortality resulting from delayed effects of fire in the Greater Yellowstone ecosystem: *Great Basin Naturalist*, v. 54, p. 91-95.

Braudrick, C.A., and Grant, G.E., 2000, When do logs move in rivers?: *Water Resources Research*, v. 36, p. 571-583.

Bull, W.B., 1979, Threshold of critical power in streams: *Geological Soc. of America Bulletin*, v. 90, p. 453-464.

Bunte, K. [I], 1996, Analyses of the temporal variation of coarse bedload transport and its grain size distribution, Squaw Creek, Montana, USA: U.S. Department of Agriculture, Forest Service General Technical Report RM-GTR-288, 124 p.

Bunte, K.I., 2001, Portable bedload traps with high sampling intensity for representative sampling of gravel transport in wadable mountain streams: Proceedings of 7th Federal Interagency Sedimentation Conf., 2001, Reno, Nev., sect. III, p. 24-31.

Bunte, K. [I.], and Abt, S.R., 2001, Sampling surface and subsurface particle-size distributions in wadable gravel- and cobble-bed streams for analyses in sediment transport, hydraulics, and streambed monitoring: U.S. Department of Agriculture, Forest Service General Technical Report RMRS-GTR-74, 428 p.

Bunte, K. [I], and MacDonald, L.H., 1996, Scale considerations and the detectability of sedimentary cumulative watershed effects: Final report submitted to U.S. Forest Service and National Council for Air and Stream Improvement, 326 p.

Burroughs, E.R., Jr., and Thomas, B.R., 1977, Declining root strength in Douglas-fir after felling as a factor in slope stability: U.S. Department of Agriculture, Forest Service Research Paper INT-190, 27 p.

Cannon, S.H., Ellis, W.L., and Godt, J.W., 1998a, Evaluation of the landslide potential in Capulin Canyon following the Dome Fire, Bandelier National Monument, New Mexico: U.S. Geological Survey Open-File Report 98-42, 21 p.

Cannon, S.H., Powers, P.S., Pihl, R.A., and Rogers, W.P., 1995, Preliminary evaluation of the fire-related debris flows on Storm King Mountain, Glenwood Springs, Colorado: U.S. Geological Survey Open-File Report 95-508, online URL <http://gldage.cr.usgs.gov/html_files/ofr95-508/skrep.html> [accessed 9/29/97].

Cannon, S.H., Powers, P.S., and Savage, W.Z., 1998b, Fire-related hyperconcentrated and debris flows on Storm King Mountain, Glenwood Springs, Colorado, USA: *Environmental Geology*, v. 35, p. 210-218.

Cannon, S.H., and Reneau, S.L., 2000, Conditions for generation of fire-related debris flows, Capulin Canyon, New Mexico: *Earth Surface Processes and Landforms*, v. 25, p. 1103-1121.

Carling, P.A., and Reader, N.A., 1982, Structure, composition and bulk properties of upland stream gravels: *Earth Surface Processes and Landforms*, v. 7, p. 349-365.

Costa, J.E., 1983, Paleohydraulic reconstruction of flash-flood peaks from boulder deposits in the Colorado Front Range: *Geological Society of America Bulletin*, v. 94, p. 986-1004.

Costa, J.E., 1988, Reologic, geomorphic, and sedimentologic differentiation of water floods, hyperconcentrated flows, and debris flows, *in* Baker, V.R., Kochel, R.C., and Patton, P.C., eds., *Flood geomorphology*: New York, John Wiley, p. 113-122.

Costa, J.E., and Jarrett, R.D., 1981, Debris flows in small mountain stream channels of Colorado, and their hydrologic implications: *Bull. Assoc. Eng. Geol.*, v. 18, p. 309-322.

Craighead, J.J., 1991, Yellowstone in transition, *in* Keiter, R.B., and Boyce, M.S., eds., *The Greater Yellowstone ecosystem--Redefining America's wilderness heritage*: New Haven, Conn., Yale Univ. Press, p. 27-39.

DeBano, L.F., 1981, Water repellant soils--A state-of-the-art: U.S. Department of Agriculture, Forest Service General Technical Report PSW-46, 21 p.

DeBano, L.F., Neary, D.G., and Ffolliott, P.F., 1998, *Fire's effects on ecosystems*: New York, John Wiley and Sons, 333 p.

Dendy, F.E., and Champion, W.A., 1978, Sediment deposition in U.S. reservoirs--Summary of data reported through 1975: U.S. Department of Agriculture, Miscellaneous Publication 1362, 82 p.

De Ronde, C., 1990, Impact of prescribed fire on soil properties--comparison with wildfire effects, *in* Goldammer, J.G., and Jenkins, M.J., eds., Fire in ecosystem dynamics: Proceedings of International Symposium on Fire Ecology, 3rd, Freiburg, FRG, 1989, SPB Academic Publishing, p. 127-136.

Despain, D.G., 1987, The two climates of Yellowstone National Park: Proceedings of the Montana Academy of Science, v. 47, p. 11-20.

Despain, D.G., 1990, *Yellowstone vegetation--Consequences of environment and history in natural setting*: New York, Roberts Rinehart.

Dietrich, W.E., Kirchner, J.W., Ikeda, H., and Iseya, F., 1989, Sediment supply and development of coarse surface layer in gravel bedded rivers: *Nature*, v. 340, p. 215-217.

Diplas, P., and Fripp, J.B., 1992, Properties of various sediment sampling procedures: *J. Hydraulic Engineering*, v. 118, p. 955-970.

Dunne, T., and Leopold, L.B., 1978, *Water in environmental planning*: New York, W.H. Freeman, 818 p.

Dyrness, C.T., 1976, Effect of wildfire on soil wettability in the high Cascades of Oregon: U.S. Department of Agriculture, Forest Service Research Paper PNW-202, 18 p.

Edwards, T.K., and Glysson, G.D., 1999, Field methods for measurement of fluvial sediment: U.S. Geological Survey Techniques of Water-Resources Investigations, Book 3, Chap. C2, 89 p.

Einstein, H.A., Anderson, A.G., and Johnson, J.W., 1940, A distinction between bedload and suspended load in natural streams: *Am. Geophys. Union Trans.*, v. 21, p. 628-633.

ESRI, 1990, *Understanding GIS--The Arc/Info method*: Redlands, Calif., Environmental Systems Research Institute [variously paged].

Ewing, R., 1996, Postfire suspended sediment from Yellowstone National Park, Wyoming: *Water Resources Bulletin*, v. 32, p. 605-627.

Fitzpatrick, F.A., Waite, I.R., D'Arconte, P.J., Meador, M.R., Maupin, M.A., and Gurtz, M.E., 1998, Revised methods for characterizing stream habitat in the National Water-Quality Assessment Program: U.S. Geological Survey Water-Resources Investigations Report 98-4052, 67 p.

Folk, R.L., 1974, *Petrology of sedimentary rocks*: Austin, Tex., Hemphill Publishing, 182 p.

Folk, R.L., and Ward, W.C., 1957, Brazos River bar—A study in the significance of grain size parameters: *J. Sedimentary Petrology*, v. 27, p. 3-26.

Fripp, J.B., and Diplas, P., 1993, Surface sampling in gravel streams: ASCE *J. of Hydraulic Engineering*, v. 119, p. 473-490.

Frissell, C.A., Liss, W.J., Warren, C.E., and Hurley, M.D., 1986, A hierarchical framework for stream habitat classification—Viewing streams in a watershed context: *Environmental Management*, v. 10, p. 199-214.

Gilliom, R.J., Alley, W.M., and Gurtz, M.E., 1995, Design of the National Water-Quality Assessment Program: occurrence and distribution of water-quality conditions: U.S. Geological Survey Circular 1112, 33 p.

Gordon, N.D., McMahon, T.A., and Finlayson, B.L., 1992, *Stream hydrology, an introduction for ecologists*: New York, John Wiley, 526 p.

Grant, G., 1987, Assessing effects of peak flow increases on stream channels--A rational approach: Proceedings of the California Watershed Management Conference, November 18-20, 1986, West Sacramento, Calif., p. 142-149.

Gray, D.H., and Megahan, W.F., 1981, Forest vegetation removal and slope stability in the Idaho Batholith: USDA Forest Service Research Paper INT-271, 23 p.

Greater Yellowstone Coordinating Committee, 1988, Greater Yellowstone area fire situation, 1988: Greater Yellowstone Coordinating Committee, 207 p.

Greater Yellowstone Coordinating Committee, 1989, The Greater Yellowstone postfire assessment: Greater Yellowstone Coordinating Committee, Postfire Assessment Committee, 147 p.

Greater Yellowstone Postfire Ecological Assessment Workshop, 1989, Ecological consequences of the 1988 fires in the Greater Yellowstone Area: Greater Yellowstone Coordinating Committee, Postfire Ecological Assessment Workshop, 58 p.

Gurnell, A.M., Petts, G.E., Hannah, D.M., Smith, B.P.G, Edward, P.J., Kollmann, J., Ward, J.V., Tockner, K., 2000, Wood storage within the active zone of a large European gravel-bed river: *Geomorphology*, v. 34, p. 55-72.

Heede, B.H., Harvey, M.D., and Laird, J.R., 1988, Sediment delivery linkages in a chaparral watershed following a wildfire: *Environmental Management*, v. 12, p. 349-358.

Helley, E.J., and Smith, W., 1973, Development and calibration of a pressure-difference bedload sampler: U.S. Geological Survey Open-File Report 73-108, 38 p.

Helsel, D.R., and Hirsch, R.M., 1992, *Statistical methods in water resources*: New York, Elsevier Science Publ., 522 p.

Helvey, J.D., 1980, Effects of a north central Washington wildfire on runoff and sediment production: *Water Resources Bulletin*, v. 16, p. 627-634.

Hewlett, J.D., 1982, *Principles of forest hydrology*: Athens, Univ. of Georgia Press, 183 p.

Hilton, S., and Lisle, T.E., 1993, Measuring the fraction of pool volume filled with fine sediment: U.S. Dept. of Agriculture, Forest Service Research Note PSW-RN-414, 11 p.

Hogan, D.L., 1987, The influence of large organic debris on channel recovery in the Queen Charlotte Islands, British Columbia, Canada, *in* Beschta, R.L., and others, eds., Erosion and sedimentation in the Pacific rim: IAHS Publication 165, p. 343-353.

Horowitz, A.J., Rinella, F.A., Lamothe, P., Miller, T.L., Edwards, T.K., Roche, R.L., and Rickert, D.A., 1989, Cross-sectional variability in suspended sediment and associated trace element concentrations in selected rivers in the U.S., *in* Hadley, R.F., and Ongley, E.D., eds., Sediment and the environment: IAHS Publication 184, p. 57-66.

Inman, D.L., 1952, Measures for describing the size distribution of sediments: *J. Sedimentary Petrology*, v. 22, p. 125-145.

Isaak, D.J., Hubert, W.A., and Krueger, K.L., 1999, Accuracy and precision of stream reach water surface slopes estimated in the field and from maps: *North Amer. J. of Fisheries Management*, v. 19, p. 141-148.

Iverson, R.M., 1997, The physics of debris flows: *Reviews of Geophysics*, v. 35, p. 245-296.

Iverson, R.M., and Denlinger, R.P., 1987, The physics of debris flows – A conceptual assessment, *in* Erosion and Sedimentation in the Pacific Rim: IAHS Publication 165, p. 155-165.

Jarrett, R.D., 1990, Hydrologic and hydraulic research in mountain rivers, *in* Hydrology of mountainous areas: IAHS Publication 190, p. 107-117.

Jones, J.A., and Grant, G.E., 1996, Peak flow responses to clear-cutting and roads in small and large basins, western Cascades, Oregon: *Water Resources Research*, v. 32, p. 959-974.

Julien, P.Y., 1995, *Erosion and sedimentation*: New York, Cambridge University Press, 280 p.

Keller, E.A., MacDonald, A., Tally, T., and Merrit, N.J., 1995, Effects of large organic debris on channel morphology and sediment storage in selected tributaries of Redwood Creek, northwestern California: U.S. Geological Survey Professional Paper 1454-P, 29 p.

Keller, E.A., and Melhorn, W.N., 1978, Rhythmic spacing and origin of pools and riffles: *Geol. Soc. of America Bulletin*, v. 89, p. 723-730.

Keller, E.A., and Swanson, F.J., 1979, Effects of large organic material on channel form and fluvial processes: *Earth Surface Processes*, v. 4, p. 361-380.

Kendall, M.G., 1962, *Rank correlation methods*, 3rd ed.: New York, Hafner Publ., 199 p.

Kennedy, R.C., 1895, Prevention of silting in irrigation canals: *Institute of Civil Engineers Proceedings*, v. 119, p. 281-290.

Kelsey, H.M., 1980, A sediment budget and an analysis of geomorphic processes in the Van Duzen River basin, northcoastal California, 1941-1975: *Geological Society of America Bulletin*, v. 91, p. 1119-1216.

King, K.W., 1995, Silvertip Monitoring Project--Stream macroinvertebrate bioassessments to assess effects due to wildfires of 1988: Cheyenne, Wyoming Department of Environmental Quality, 23 p.

Klock, G.O., and Helvey, J.D., 1976, Debris flows following wildfire in north central Washington, *in* Proceedings of the Third Federal Inter-Agency Sedimentation Conference, Denver, 1976: Water Resources Council, p. 91-98.

Knighton, D., 1984, *Fluvial forms and processes*: London, Edward Arnold, 218 p.

Kondolf, G.M., 1997, Hungry water; effects of dams and gravel mining on river channels: *Environmental Management*, v. 21, no. 4, p. 533-551.

Kondolf, G.M., 1997, Application of the pebble count--Notes on purpose, method, and variants: *Journal of American Water Resources Assoc.*, v. 33, no. 1, p. 79-87.

Lacey, G., 1930, Stable channels in alluvium: *Institute of Civil Engineers Proceedings*, v. 229, p. 259-384.

Laird, J.R., and Harvey, M.D., 1986, Complex-response of a chaparral drainage basin to fire, *in* Hadley, R.F., ed., Drainage basin sediment delivery: IAHS Publication 159, p. 165-183.

Lambert, C.P., and Walling, D.E., 1988, Measurement of channel storage of suspended sediment in a gravel-bed river: *Catena*, v. 15, p. 65-80.

Lane, L.J., Nichols, M.H., Hernandez, M., Manetsch, C., and Osterkamp, W.R., 1994, Variability in discharge, stream power, and particle-size distributions in ephemeral-stream channel systems, *in* Variability in stream erosion and sediment transport: IAHS Publication 224, p. 335-342.

Lathrop, R.G., Jr., 1994, Impacts of the 1988 wildfires on the water quality of Yellowstone and Lewis Lakes, Wyoming: *International Journal of Wildland Fire*, v. 4, p. 169-175.

Leopold, L.B., and Maddock, T.M., Jr., 1953, The hydraulic geometry of stream channels and some physiographic implications: U.S. Geological Survey Professional Paper 252, 57 p.

Leopold, L.B., Wolman, M.G., and Miller, J.P., 1964, *Fluvial processes in geomorphology*: San Francisco, W.H. Freeman, 522 p.

Lisle, T.E., 1986, Stabilization of a gravel channel by large streamside obstructions and bedrock bends, Jacoby Creek, northwestern California: *Geological Society of America Bulletin*, v. 97, p. 999-1011.

Lisle, T.E., 1995, Particle size variations between bed load and bed material in natural gravel bed channels: *Water Resources Research*, v. 31, p. 1107-1118.

Lisle, T.E., and Hilton, S., 1992, The volume of fine sediment in pools—An index of sediment supply in gravel-bed streams: *Water Resources Bulletin*, v. 28, no. 2, p. 371-383.

Lisle, T.E., and Hilton, S., 1999, Fine bed material in pools of natural gravel bed channels: *Water Resources Research*, v. 35, p. 1291-1304.

Lowry, M.E., and Smalley, M.L., 1993, Hydrology of Park County, Wyoming, exclusive of Yellowstone National Park: U.S. Geological Survey Water-Resources Investigations Report 93-4183, 67 p.

Lyon, L.J., 1984, The Sleeping Child burn--21 years of postfire change: U.S. Department of Agriculture, Forest Service Research Paper INT-330, 17 p.

MacDonald, A., and Keller, E.A., 1987, Stream channel response to the removal of large woody debris, Larry Damm Creek, northwestern California, *in* Beschta, R.L., and others, eds., Erosion and sedimentation in the Pacific Rim: IAHS Publication no. 165, p. 405-406.

MacDonald, L.H., Smart, A., and Wissmar, R.C., 1991, Monitoring guidelines to evaluate effects of forestry activities on streams in the Pacific Northwest and Alaska: Seattle, Wash., U.S. Environmental Protection Agency, EPA/910/9-91-001, 166 p.

Madej, M.A., and Ozaki, V., 1996, Channel response to sediment wave propagation and movement, Redwood Creek, California, USA: *Earth Surface Processes and Landforms*, v. 21, p. 911-927.

Madsen, S.W., 1995, Channel response associated with predicted water and sediment yield increases in northwest Montana: Fort Collins, Colorado State Univ., Dept. of Earth Resources, unpub. M.S. thesis, 230 p.

Marcus, W.A., Ladd, S.C., Stoughton, J.A., and Stock, J.W., 1995, Pebble counts and the role of user-dependent bias in documenting sediment size distributions: *Water Resources Research*, v. 31, no. 10, p. 2625-2631.

Marston, R.A., 1982, The geomorphic significance of log steps in forest streams: *Annals of the Assoc. Amer. Geog.*, v. 72, p. 99-108.

Marston, R.A., and Anderson, J.E., 1991, Watersheds and vegetation of the Greater Yellowstone ecosystem: *Conservation Biology*, v. 5, p. 338-346.

Martin, D.A., and Moody, J.A., 2001, The flux and particle size distribution of sediment collected in hillslope traps after a Colorado wildfire: Proceedings of 7th Federal Interagency Sedimentation Conf., 2001, Reno, Nev., sect. III, p. 40-47.

Martner, B.E., 1986, *Wyoming climate atlas*: Lincoln, University of Nebraska Press, 432 p.

Massey, A.J., 2000, Large woody debris loading in forest streams due to 1997 Routt Divide blowdown: Laramie, Univ. of Wyoming, Dept. of Geography and Recreation, unpub. M.A. thesis, 99 p.

McCord, V.A.S., 1996, Flood history reconstruction in Frijoles Canyon using flood-scarred trees, in Fire effects in southwestern forests--Proceedings of the second La Mesa fire symposium: U.S. Department of Agriculture, Forest Service General Technical Report RM-GTR-286, p. 114-122.

McIntyre, M.J., and Minshall, G.W., 1996, Changes in transport and retention of coarse particulate organic matter in streams subjected to fire, *in* Greenlee, Jason, ed., The ecological implications of fire in Greater Yellowstone--Conference on the Greater Yellowstone ecosystem, 2d, Yellowstone National Park, 1993: Fairfield, Wash., International Association of Wildland Fire, p. 59-75.

Megahan, W.F., Day, N.F., and Bliss, T.M., 1978, Landslide occurrence in the western and central Northern Rocky Mountain physiographic province in Idaho, in North American Forest Soils Conference, 5th [Proceedings]: Fort Collins, Colorado State Univ., p. 116-139.

Meyer, G.A., and Wells, S.G., 1997, Fire-related sedimentation events on alluvial fans, Yellowstone National Park, U.S.A.: *Journal of Sedimentary Research*, v. 67, no. 5, p. 776-791.

Meyer, G.A., Wells, S.G., and Jull, A.J.T., 1995, Fire and alluvial chronology in Yellowstone National Park--Climatic and intrinsic controls on Holocene geomorphic processes: *Geol. Society of America Bulletin*, v. 107, p. 1211-1230.

Mihuc, T.B., and Minshall, G.W., 1995, Trophic generalists vs. trophic specialists—Implications for food web dynamics in post-fire streams: *Ecology*, v. 76, p. 2361-2372.

Mihuc, T.B., Minshall, G.W., and Robinson, C.T., 1996, Response of benthic macroinvertebrate populations in Cache Creek, Yellowstone National Park to the 1988 wildfires, *in* Greenlee, Jason, ed., The ecological implications of fire in Greater Yellowstone--Conference on the Greater Yellowstone ecosystem, 2d, Yellowstone National Park, 1993: Fairfield, Wash., International Association of Wildland Fire, p. 83-94.

Miller, J.F., Frederick, R.H., and Tracey, R.J., 1973, Precipitation-frequency atlas of the Western United States--Vol. 2, Wyoming: U.S. Department of Commerce, NOAA Atlas No. 2, 43 p.

Minshall, G.W., and Brock, J.T., 1991, Observed and anticipated effects of forest fire on Yellowstone stream ecosystems, *in* Keiter, R.B., and Boyce, M.S., eds., *The Greater Yellowstone ecosystem--Redefining America's wilderness heritage*: New Haven, Conn., Yale University Press, p. 123-135.

Minshall, G.W., Brock, J.T., and Varley, J.D., 1989, Wildfires and Yellowstone's stream ecosystems: *Bioscience*, v. 39, no. 10, p. 707-715.

Montgomery, D.R., and Buffington, J.M., 1993, Channel classification, prediction of channel response, and assessment of channel condition: Washington State Timber/Fish/Wildlife Agreement, Report TFW-SH10-93-002, 84 p.

Montgomery, D.R., Buffington, J.M., Smith, R.D., Schmidt, K.M., and Pess, G., 1995, Pool spacing in forest channels: *Water Resources Research*, v. 31, p. 1097-1105.

Moody, J.A., 2001, Sediment transport regimes after a wildfire in steep mountainous terrain: Proceedings of 7th Federal Interagency Sedimentation Conf., 2001, Reno, Nev., sect. X, p. 41-48.

Myers, T.J., and Swanson, S., 1992, Variation of stream stability with stream type and livestock bank damage in northern Nevada: *Water Resources Bulletin*, v. 28, p. 743-754.

Nelson, W.H., and Pierce, W.G., 1968, Wapiti Formation and Trout Peak Trachyandesite, northwestern Wyoming: U.S. Geological Survey Bulletin 1254-H, 11 p.

Newson, M.D., 1980, The geomorphological effectiveness of floods—A contribution stimulated by two recent events in Mid-Wales: *Earth Surface Processes*, v. 5, p. 1-16.

Nissen, T.C., and Case, J.C., 1998, Preliminary map of landslides on the Pelican Cone quadrangle: Laramie, Geological Survey of Wyoming, scale 1:62,500.

Olive, L.J., Olley, J.M., Murray, A.S., and Wallbrink, P.J., 1994, Spatial variation in suspended sediment transport in the Murrumbidgee River, New South Wales, Australia, *in* Variability in stream erosion and sediment transport: IAHS Publication 224, p. 241-249.

O'Loughlin, C.L., 1974, The effect of timber removal on the stability of forest soils: *Journal of Hydrology* (N.Z.), v. 13, p. 121-134.

O'Loughlin, E.M., Cheney, N.P., and Burns, J., 1982, The Bushrangers experiment--Hydrological response of a eucalypt catchment to fire: Proceedings of Symposia on Forest Hydrology, Melbourne, May 11-13, 1982, p. 132-138.

Osterkamp, W.R., and Costa, J.E., 1987, Changes accompanying an extraordinary flood on a sand-bed stream, *in* Mayer, L., and Nash, D., eds., *Catastrophic flooding*: Boston, Allen and Unwin, p. 201-224.

Osterkamp, W.R., and Hedman, E.R., 1977, Variation of width and discharge for natural high-gradient stream channels: *Water Resource Research*, v. 13, p. 256-258.

Osterkamp, W.R., and Hedman, E.R., 1982, Perennial-streamflow characteristics related to channel geometry and sediment in Missouri River Basin: U.S. Geological Survey Professional Paper 1242, 37 p.

Ott, R.L., 1992, *An introduction to statistical methods and data analysis*, 4th ed.: Belmont, Calif., Duxbury Press, 1051 p.

Parker, G., Dhamotharan, S., and Stefan, H., 1982, Model experiments on mobile, paved gravel bed streams: *Water Resources Research*, v. 18, 1395-1408.

Parks, D.S., and Cundy, T.W., 1989, Soil hydraulic characteristics of a small southwest Oregon watershed following high-intensity wildfire, *in* Proceedings of the symposium on fire and watershed management: U.S. Department of Agriculture, Forest Service General Technical Report PSW-109, p. 63-67.

Peck, D.V., Lazorchak, J.M., and Klemm, D.J., eds., 2000 [unpublished draft], Environmental Monitoring and Assessment Program—Surface waters—Western Pilot Study field operations manual for wadeable streams: U.S. Washington, D.C., U.S. Environmental Protection Agency, 230 p.

Petrie, J., and Diplas, P., 2000, Statistical approach to sediment sampling accuracy: *Water Resources Research*, v. 36, 597-605.

Pfankuch, D.J., 1975, Stream reach inventory and channel stability evaluation: U.S. Dept. of Agriculture, Forest Service, Northern Region, R1-75-002, 26 p.

Phillips, P.J., and Harlin, J.M., 1984, Spatial dependency of hydraulic geometry exponents in a subalpine stream: *Journal of Hydrology*, v. 71, p. 277-283.

Platts, W.S., Megahan, W.F., and Minshall, G.W., 1983, Methods for evaluating stream, riparian, and biotic conditions: U.S. Department of Agriculture, Forest Service General Technical Report INT-138, 70 p.

Platts, W.S., Armour, C., Booth, G.D., Bryant, M., Bufford, J.L., Cupin, P., Jensen, S., Lienkaemper, G.W., Minshall, G.W., Monsen, S.B., Nelson, R.L., Sedell, J.R., and Tuhy, J.S., 1987, Methods for evaluating riparian habitats with applications to management: U.S. Department of Agriculture, Forest Service General Technical Report INT-221, 177 p.

Pierson, T.C., and Costa, J.E., 1987, A rheologic classification of subaerial sediment-water flows, *in* Costa, J.E., and Wieczorek, G.F., eds., Debris flows/avalanches: *Geological Society of America Reviews in Engineering Geology*, v. 7, p. 1-12.

Pierson, T.C., and Scott, K.M., 1985, Downstream dilution of a lahar—Transition from debris flow to hyperconcentrated stream flow: *Water Resources Research*, v. 21, p. 1511-1524.

Pitlick, J., 1993, Response and recovery of a subalpine stream following a catastrophic flood: *Geological Society of America Bulletin*, v. 105, p. 657-670.

Potyondy, J.P., and Hardy, T., 1994, Use of pebble counts to evaluate fine sediment increase in stream channels: *Water Resources Bulletin*, v. 30, no. 3, p. 509-520.

Reid, L.M., 1991, Research and cumulative watershed effects: U.S. Dept. of Agric., Forest Service General Technical Report PSW-GTR-141, 118 p.

Rich, L.R., 1962, Erosion and sediment movement following a wildfire in a Ponderosa pine forest of central Arizona: U.S. Department of Agriculture, Forest Service Research Paper RM-76, 12 p.

Richmond, A.D., and Fausch, K.D., 1995, Characteristics and function of large woody debris in Rocky Mountain subalpine streams in northern Colorado: *Canadian Journal of Fisheries and Aquatic Sciences*, vol. 52, p. 1789-1802.

Robichaud, P.R., Beyers, J.L., and Neary, D.G., 2000, Evaluating the effectiveness of postfire rehabilitation treaments: U.S. Department of Agriculture, Forest Service General Technical Report RMRS-GTR-63, 85 p.

Robichaud, P.R., and Waldrop, T.A., 1994, A comparison of surface runoff and sediment yields from low- and high-severity site preparation burns: *Water Resources Bulletin*, v. 30, no. 1.

Robinson, C.T., and Minshall, G.W., 1996, Physical and chemical responses of streams in Yellowstone National Park following the 1988 wildfires, *in* Greenlee, J., ed., The ecological implications of fire in Greater Yellowstone--Proceedings of the Second Biennial Conference on the Greater Yellowstone Ecosystem, September 19-21, 1993, Yellowstone National Park, Wyo.: Fairfield, Wash., International Association of Wildland Fire, p. 217-221.

Roby, K.B., 1989, Watershed response and recovery from the Will Fire--Ten years of observation, *in* Proceedings of the symposium on fire and watershed management: U.S. Department of Agriculture, Forest Service General Technical Report PSW-109, p. 131-136.

Romme, W.H., and Knight, D.H., 1982, Landscape diversity--The concept applied to Yellowstone National Park: *Bioscience*, v. 32, p. 664-670.

Rosgen, D.L., 1994, A classification of natural rivers: Catena, v. 22, p. 169-199.

Rosgen, D.[L.], 1996, *Applied river morphology*: Pagosa Springs, Colo., Wildland Hydrology [variously paged].

Rousseeuw, P.J., and Leroy, A.M., 1987, *Robust regression and outlier detection*: New York, John Wiley, 329 p.

Schumm, S.A., 1963, A tentative classification of alluvial river channels: U.S. Geological Survey Circular 477, 10 p.

Schumm, S.A., 1977, *The fluvial system*: New York, Wiley-Interscience, 338 p.

Schumm, S.A., 1980, Some applications of the concept of geomorphic thresholds, *in* Coates, D.R., and Vitek, J.D., eds., *Thresholds in geomorphology*: London, George Allen and Unwin, p. 473-485.

Schumm, S.A., and Rea, D.K., 1995, Sediment yield from disturbed earth systems: *Geology*, v. 23, no. 5, p. 391-394.

Shakesby, R.A., Coelho, C.O.A., Ferreira, A.D., Terry, J.P., and Walsh, R.P.D., 1993, Wildfire impacts on soil erosion and hydrology in wet Mediterranean forest, Portugal: *International Journal of Wildland Fire*, v. 3, 95-110.

Shields, A., 1936, Anwendung der Aehnlichkeitsmechanik und der turbulenzforshung auf die geschiebebewegung: Mitteilung der Preussischen versuchsanstalt fuer Wasserbau und Schiffbau, Heft 26, Berlin [cited in Grant, 1987].

Simonson, T.D., Lyons, John, and Kanehl, P.D., 1994, Quantifying fish habitat in streams—Transect spacing, sample size, and a proposed framework: *North American Journal of Fisheries Management*, v. 14, p. 607-615.

Smedes, H.W., and Prostka, H.J., 1972, Stratigraphic framework of the Absaroka Volcanic Supergroup in the Yellowstone National Park region: U.S. Geological Survey Professional Paper 729-C, 33 p.

Strahler, A.N., 1957, Quantitative analysis of watershed geomorphology: *Transactions of the American Geophysical Union*, v. 38, p. 913-920.

Swanson, F.J., 1981, Fire and geomorphic processes, *in* Fire regimes and ecosystem properties: USDA Forest Service General Technical Report WO-26, p. 401-420.

Thilenius, J.F., and Smith, D.R., 1985, Vegetation and soils of an alpine range in the Absaroka Mountains, Wyoming: U.S. Department of Agriculture, Forest Service General Technical Report RM-121, 18 p.

Thompson, D.M., 1995, The effects of large organic debris on sediment processes and stream morphology in Vermont: *Geomorphology*, v. 11, p. 235-244.

Tiedemann, A.R., Conrad, C.E., Dieterich, J.H., Hornbeck, J.W., Megahan, W.F., Viereck, L.A., and Wade, D.D., 1979, Effects of fire on water--A state-of-knowledge review: U.S. Department of Agriculture, Forest Service General Technical Report WO-10, 28 p.

Todd, M., and Elmore, W., 1997, Historical changes in western riparian ecosystems, *in* Wadsworth, K.G., ed., Transactions of the 62d North American Wildlife and Natural Resources Conference, March 14-18, 1997, Washington, D.C.: Washington, D.C., Wildlife Management Institute, p. 454-468.

Trimble, S.W., 1975, Denudation studies--Can we assume stream steady state?: *Science*, v. 188, p. 1207-1208.

Troendle, C.A., and Bevenger, G.S., 1996, Effect of fire on streamflow and sediment transport, Shoshone National Forest, Wyoming, *in* Greenlee, Jason, ed., The ecological implications of fire in Greater Yellowstone--Conference on the Greater Yellowstone ecosystem, 2d, Yellowstone National Park, 1993: Fairfield, Wash., International Association of Wildland Fire, p. 43-52.

Troendle, C.A., and King, R.M., 1985, The effect of timber harvest on the Fool Creek watershed, 30 years later: *Water Resources Research*, v. 21, p. 1915-1922.

Troendle, C.A., and Olsen, W.K., 1994, Potential effects of timber harvest and water management on streamflow dynamics and sediment transport, *in* Sustainable ecological systems--Implementing an ecological approach to land management: U.S. Department of Agriculture, Forest Service General Technical Report RM-247, p. 34-41.

U.S. Geological Survey, 1990-1994, Water Resources Data – Wyoming – Water Year [year]: U.S. Geological Survey Water-Data Reports.

Varley, J.D., 1991, Testimony before the U.S. Congressional Subcommittee, in Recovery of forest resources from the Greater Yellowstone wildfires, Exxon Valdez oilspill, and the Mount St. Helens eruption: Hearing before the Subcommittee on Forests, Family Farms, and Energy of the House Committee on Agriculture, 102nd Congress, April 10, 1991, serial no. 102-8.

Venables, W.N., and Ripley, B.D., 1994, *Modern applied statistics with S-PLUS*: New York, Springer-Verlag, 462 p.

Wells, C.G., Campbell, R.E., DeBano, L.F., Lewis, C.E., Fredriksen, R.L., Franklin, E.C., Froelich, R.C., and Dunn, P.H., 1979, Effects of fire on soil--A state-of-knowledge review: U.S. Department of Agriculture, Forest Service General Technical Report WO-7, 34 p.

Wiberg, P.L., and Smith, J.D., 1987a, Initial motion of coarse sediment in streams of high gradient, *in* Erosion and sedimentation in the Pacific Rim: IAHS Publ. 165, p. 299-308.

Wiberg, P.L., and Smith, J.D., 1987b, Calculations of the critical shear stress for motion of uniform and heterogeneous sediments: *Water Resources Research*, v. 23, p. 1471-1480.

Williams, H., Turner, F.J., and Gilbert, C.M., 1955, *Petrography*: San Francisco, W.H. Freeman, 406 p.

Wohl, E.E., 2000, *Mountain rivers*: Amer. Geophys. Union Water Resources Monograph 14, 320 p.

Wohl, E.E., Anthony, D.J., Madsen, S.W., and Thompson, D.M., 1996, A comparison of surface sampling methods for coarse fluvial sediments: *Water Resources Research*, v. 32, p. 3219-3226.

Wohl, E.E., and Pearthree, P.A., 1991, Debris flows as geomorphic agents in the Huachuca Mountains of southeastern Arizona: *Geomorphology*, v. 4, p. 273-292.

Wohlgemuth, P.M., 2001, Prescribed fire as a sediment management tool in southern California chaparral watersheds: Proceedings of 7th Federal Interagency Sedimentation Conf., 2001, Reno, Nev., sect. X, p. 49-56.

Wolman, M.G., 1954, A method of sampling coarse river-bed material: *Trans. of American Geophysical Union*, v. 35, no. 6, p. 951-956.

Wright, R.F., 1976, The impact of forest fire on the nutrient influxes to small lakes in northeastern Minnesota: *Ecology*, v. 57, p. 649-663.

Young, M.K., 1994, Movement and characteristics of stream-borne coarse woody debris in adjacent burned and undisturbed watersheds in Wyoming: *Can. J. For. Res.*, v. 24, p. 1933-1938.

Young, M.K., and Bozek, M.A., 1996, Post-fire effects on coarse woody debris and adult trout in northwestern Wyoming streams, *in* Greenlee, Jason, ed., The ecological implications of fire in Greater Yellowstone--Conference on the Greater Yellowstone ecosystem, 2d, Yellowstone National Park, 1993: Fairfield, Wash., International Association of Wildland Fire, p. 137-143.

Ziemer, R.R., and Swanston, D.N., 1977, Root strength changes after logging in southeast Alaska: U.S. Department of Agriculture, Forest Service Research Note PNW-306, 10 p.

Appendix A

DATA TABLES

Table A.1 – *Reach index location data.*

[UTM, Universal Transverse Mercator projection, zone 12, horizontal datum is NAD83; --, not measured; DOQ, digital orthophoto quadrangle (1-meter pixels)]

Site number	Stream name	Date measured	UTM coordinates		Estimated horizontal error (m)	Remarks
			Easting (m)	Northing (m)		
071	Jones	7-01-00	578,210	4,934,182	19	upstream end of reach
073	Jones	7-01-00	577,996	4,934,156	20	downstream end of reach
075	Jones	7-01-00	576,243	4,933,775	21	at pool 5, upstream of LOD reach
080	Jones	6-09-98	575,086	4,933,531	5	upstream end of reach
081	Jones	--	573,090	4,932,770	DOQ	near mid-reach
092	Jones	6-10-98	572,135	4,932,400	7	about 60 m downstream of reach
093	Jones	--	580,830	4,934,150	DOQ	near mid-reach
103	Jones	6-30-00	573,455	4,932,940	21	near mid-reach
106	Jones	--	570,000	4,931,960	DOQ	near mid-reach
107	Jones	--	570,380	4,931,997	DOQ	near mid-reach
171	Crow	6-19-98	577,367	4,929,605	7	in left-bank meadow near mid-reach
173	Crow	7-20-99	581,846	4,929,407	10	high on left bank near mid-reach
174	Crow	7-26-99	575,803	4,929,299	10	near downstream end of reach
179	Crow	8-03-99	573,113	4,928,833	10	on bar, about 50 m upstream of reach
180	Crow	7-22-99	572,719	4,928,661	10	near downstream end of reach
181	Crow	7-21-99	572,121	4,928,498	10	near mid-reach
189	Crow	8-08-99	574,870	4,929,084	10	near upstream end of reach
195	Crow	7-24-99	573,438	4,928,952	10	near upstream end of reach
197	Crow	9-17-99	576,189	4,929,322	10	near downstream end of reach
199	Crow	9-18-99	578,084	4,929,557	8	in left-bank meadow near downstream end of reach

Table A.2 – *Drainage-area characteristics data.*

[DA, drainage area; DGU, dominant geologic unit; SDGU, subdominant geologic unit; Qg, glacial till; Tlv, Langford Fm, vent facies; Tlp, Langford Fm, Promontory Mbr; Tt, Trout Peak Trachyandesite]

Site number	Stream name	Drainage area (ha)	Average slope (percent)	Percentage burned in 1988	Dominant geologic unit	Percentage of DA as DGU	Sub-dominant geologic unit	Percentage of DA as SDGU
071	Jones	5690	41.3	98.3	Tlv	25.8	Tt	24.7
073	Jones	5382	41.0	98.2	Tlv	27.3	Tt	24.3
075	Jones	4854	41.1	98.1	Tlv	30.2	Tt	22.5
080	Jones	3981	41.6	97.7	Tlv	36.4	Tt	19.7
081	Jones	3055	43.5	97.0	Tlv	45.1	Tlp	14.6
092	Jones	2318	44.6	96.0	Tlv	53.1	Tlp	15.3
093	Jones	6446	41.4	98.5	Tt	24.5	Tlv	22.8
103	Jones	3270	43.0	97.2	Tlv	42.5	Qg	15.0
106	Jones	1288	42.8	94.0	Tlv	65.2	Tlp	14.9
107	Jones	1383	43.3	94.2	Tlv	64.4	Tlp	14.8
171	Crow	3758	42.3	6.8	Tlv	33.9	Tt	23.5
173	Crow	4977	42.1	7.8	Tt	27.0	Tlv	25.6
174	Crow	3126	41.7	3.5	Tlv	38.1	Tlp	23.2
179	Crow	2094	42.2	1.2	Tlv	42.3	Tlp	28.5
180	Crow	1924	41.6	1.1	Tlv	42.6	Tlp	29.7
181	Crow	1704	41.8	1.3	Tlv	43.5	Tlp	33.1
189	Crow	2797	42.0	1.9	Tlv	39.4	Tlp	25.1
195	Crow	2314	42.6	1.6	Tlv	40.9	Tlp	28.1
197	Crow	3248	41.7	3.4	Tlv	37.5	Tlp	22.7
199	Crow	3978	42.4	7.7	Tlv	32.1	Tt	24.1

Table A.3 – *Segment characteristics data.*

[MSL, mean sea level datum; Geologic units: Qa, alluvium; Qs, landslide deposits; Qt, talus, colluvium; Tw, Wapiti Fm]

Site number	Stream name	Segment length (m)	Minimum elevation (m MSL)	Segment gradient (m/m)	Adjacent geologic unit
071	Jones	434	2190	0.029	Tw
073	Jones	695	2203	.016	Tw
075	Jones	719	2227	.019	Tw
080	Jones	1,589	2265	.018	Qt
081	Jones	757	2322	.010	Qt
092	Jones	780	2342	.024	Qt
093	Jones	608	2079	.029	Qs
103	Jones	745	2302	.027	Qt
106	Jones	327	2409	.026	Qt
107	Jones	372	2398	.028	Qt
171	Crow	730	2275	.018	Qt
173	Crow	532	2033	.044	Qs
174	Crow	731	2326	.016	Qt
179	Crow	201	2399	.008	Qa
180	Crow	1,018	2401	.028	Qa
181	Crow	344	2430	.033	Qt
189	Crow	63	2338	.010	Qt
195	Crow	281	2387	.002	Qa
197	Crow	313	2326	.001	Qt
199	Crow	640	2252	.026	Qt

Table A.4 – *Reach-average characteristics data.*

[m, meter; Channel types: FPR, forced pool-riffle; PB, plane bed]

Site number	Date sampled	Primary reach length (m)	Water-surface gradient (m/m)	Bankfull riffle width (m)	Bankfull pool width (m)	Weighted-average bankfull width (m)	Pool-reach length (m)	Pool spacing (m)	Channel type
071	8/11/99	200	0.029	12.3	12.2	12.3	209	41.4	FPR
073	8/25/99	202	.009	12.5	14.1	12.9	228	58.2	FPR
075	8/24/99	170	.018	13.1	12.3	13.0	324	65.3	PB
080	8/12/99	175	.007	9.5	13.0	11.4	126	24.9	FPR
081	8/20/99	160	.011	8.8	13.0	10.1	125	26.1	FPR
092	8/22/99	170	.008	9.8	14.4	11.1	137	27.9	FPR
093	9/05/99	196	.014	15.1	17.5	15.4	324	80.0	PB
103	8/18/99	153	.015	8.9	11.2	9.9	109	21.3	FPR
106	8/13/99	152	.025	8.4	8.5	8.4	177	34.8	FPR
107	8/14/99	137	.028	7.2	7.8	7.3	131	26.7	FPR
171	9/16/99	150	.015	11.4	12.7	12.0	139	28.8	FPR
173	9/20/99	200	.033	7.1	8.8	7.6	143	28.4	FPR
174	8/09/99	150	.019	7.7	8.0	7.8	238	47.2	PB
179	8/03/99	135	.019	8.6	10.7	9.1	140	28.3	FPR
180	8/04/99	142	.023	7.6	8.4	7.8	106	21.1	FPR
181	8/05/99	150	.023	7.5	9.1	7.7	221	44.1	PB
189	8/08/99	178	.016	9.9	10.3	10.0	187	37.5	FPR
195	8/06/99	160	.025	8.2	9.8	8.6	126	25.2	FPR
197	9/17/99	142	.023	7.3	9.9	7.7	168	33.9	PB
199	9/18/99	150	.029	9.6	8.9	9.5	182	36.4	FPR

Table A.4 – *Reach-average characteristics data — Continued*

[m, meter; vol., volume; V^*_w, volume-weighted average of V* ratios for individual pools; mm, millimeter; GSD, grain-size distribution; d_{16}, 16th percentile; d_{50}, 50th percentile; d_{84}, 84th percentile]

Site number	Mean pool length (m)	Percentage of pool-reach length in pools	Mean residual pool depth (m)	Mean residual pool vol. (m^3)	Mean residual-pool fine-sediment vol. (m^3)	Ratio, V^*_w, of vol. of pool fines to residual pool vol.	Size of GSD percentile for pool fines (mm)		
							d_{16}	d_{50}	d_{84}
071	4.6	12.0	0.11	1.26	0.19	0.15	0.68	4.1	11.5
073	15.7	27.2	.22	16.65	4.77	.29	.29	1.8	9.5
075	10.3	19.0	.18	6.34	.99	.16	.48	2.4	9.8
080	11.4	53.9	.25	14.32	5.08	.35	.18	.50	4.5
081	9.0	31.1	.19	5.99	1.70	.28	.36	1.1	11
092	6.7	28.1	.24	3.90	.75	.19	.33	1.2	9.2
093	10.4	13.5	.14	5.52	.68	.12	.31	1.9	10
103	8.4	41.6	.21	7.08	1.78	.25	.34	1.2	13
106	6.2	19.1	.15	2.09	.45	.22	.58	2.4	11
107	5.4	17.3	.10	.95	.30	.31	1.8	5.5	16
171	13.4	45.8	.27	12.53	5.40	.43	.32	.70	3.6
173	7.3	26.0	.12	2.48	.23	.09	.56	6.1	18
174	7.5	16.7	.15	3.51	.46	.13	.65	2.8	11.5
179	6.4	19.9	.17	3.54	1.39	.39	.32	2.3	10
180	4.4	20.5	.14	2.82	.52	.18	.58	2.9	9.8
181	6.0	15.0	.16	3.19	.31	.10	.32	3.2	11
189	9.6	26.4	.19	7.59	1.72	.23	.26	.80	2.7
195	6.4	26.3	.16	4.29	.78	.18	.51	5.3	17
197	4.9	14.1	.11	.97	.12	.13	.88	7.0	15
199	5.4	15.4	.12	1.03	.16	.16	.52	4.2	12

Table A.4 – *Reach-average characteristics data — Continued*

[mm, millimeter; GSD, grain-size distribution; d_{10}, 10th percentile; d_{16}, 16th percentile; d_{25}, 25th percentile; d_{50}, 50th percentile; d_{75}, 75th percentile; d_{84}, 84th percentile; d_{90}, 90th percentile]

Site number	Pool fines, graphic mean size (ϕ units)	Pool fines, graphic standard deviation (ϕ units)	Riffle armor, graphic mean size (ϕ units)	Riffle armor, graphic standard deviation (ϕ units)	Size, in mm, of indicated percentile of mean GSD on riffles				
					d_{10}	d_{16}	d_{50}	d_{84}	d_{90}
071	1.97	-1.67	-6.61	2.08	11.9	22	118	362	519
073	2.42	-0.77	-5.29	1.43	9.6	13.3	46	99	119
075	2.10	-1.17	-5.46	2.07	6.4	10.1	48	177	252
080	2.27	0.43	-4.82	1.45	5.5	10.7	31	69	89
081	2.39	-0.69	-5.32	1.31	10.3	16.2	41	96	113
092	2.32	-0.62	-4.74	1.28	7.1	10.3	31	60	70
093	2.43	-0.85	-5.83	1.67	10.1	15.3	75	161	190
103	2.47	-0.80	-5.59	1.36	12.6	18.6	53	114	158
106	2.08	-1.31	-5.94	1.40	14.1	23	67	151	180
107	1.55	-2.44	-5.83	1.97	8.6	12.7	71	206	269
171	1.91	0.10	-4.58	1.39	6.1	9.1	25	60	75
173	2.37	-1.98	-6.02	1.57	12.7	21	75	172	226
174	2.05	-1.46	-5.29	1.69	6.3	11.6	45	113	139
179	2.38	-0.96	-4.54	1.24	6.9	9.7	24	53	64
180	1.98	-1.35	-4.79	1.47	7.5	9.7	28	78	95
181	2.45	-1.16	-5.51	1.47	10.1	15.1	53	117	135
189	1.84	0.28	-5.08	1.39	6.6	12.7	39	78	89
195	2.36	-1.84	-4.57	1.74	4.4	6.4	27	76	90
197	1.96	-2.18	-4.99	1.93	5.0	7.7	36	115	149
199	2.17	-1.57	-5.52	1.90	6.6	10.2	63	150	181

Table A.4 – *Reach-average characteristics data — Continued*

[Three pools were sampled at each site; approximately 1 liter of pool fines composed each sample, with no more than 300 milliliters from any single point on the pool streambed; mm, millimeters; --, not analyzed]

Site number	Mean percentage of pool-fines sample finer than indicated size in mm										
	25	19	12.5	9.5	4.75	2.36	1.18	0.6	0.3	0.15	0.075
071	100.0	100.0	88.3	75.7	53.0	38.7	26.0	13.7	4.7	1.7	0.9
073	100.0	97.3	91.5	84.0	66.3	55.1	43.6	28.5	16.5	7.3	2.8
075	100.0	96.0	89.0	83.6	65.8	49.6	35.8	20.7	6.3	1.7	0.8
080	100.0	97.7	94.7	92.1	84.6	79.0	68.6	56.0	32.1	10.0	3.5
081	100.0	93.0	85.3	82.4	74.0	66.5	53.5	30.6	10.9	3.8	1.7
092	100.0	96.0	88.7	84.3	71.9	59.5	49.3	38.9	13.1	4.6	2.1
093	100.0	98.3	90.0	--	65.3	53.3	42.7	31.3	15.7	6.7	3.3
103	100.0	95.3	83.8	80.3	69.5	61.3	49.7	32.1	12.2	3.5	1.4
106	100.0	99.3	88.0	79.7	64.0	49.7	34.0	16.7	7.3	3.0	1.4
107	100.0	91.3	79.2	70.1	44.5	20.5	9.7	5.0	2.7	1.4	0.7
171	100.0	98.3	96.7	90.0	85.7	81.3	70.3	44.0	13.3	3.7	1.9
173	100.0	87.3	73.2	61.1	44.0	35.9	28.6	17.0	6.4	2.5	1.2
174	100.0	95.8	85.8	80.2	62.9	45.9	28.5	14.3	4.4	1.2	0.4
179	100.0	96.1	89.9	--	62.5	50.5	43.3	32.8	14.0	4.4	1.8
180	100.0	96.9	92.5	--	61.4	45.3	30.4	16.5	6.4	2.0	0.9
181	100.0	96.7	89.7	--	55.7	46.0	40.0	29.0	15.0	6.3	2.7
189	100.0	100.0	96.7	94.5	88.1	83.0	61.4	41.2	18.2	8.0	4.4
195	100.0	89.2	75.8	--	46.6	37.3	28.7	18.6	6.1	1.7	0.7
197	100.0	94.9	78.3	59.9	37.4	29.1	20.7	10.1	3.8	2.3	1.0
199	100.0	100.0	85.0	74.3	52.3	38.0	27.0	18.0	7.0	2.0	1.2

Table A.4 – *Reach-average characteristics data — Continued*

[mm, millimeters]

Site number	Number of riffle samples	Total number of particles	Mean percentage of riffle armor finer than indicated size in mm									
			2	4	8	16	32	64	128	256	512	1024
071	2	200	2.5	4.5	7.0	12.5	20.0	34.5	52.5	75.0	89.5	100.0
073	2	225	1.8	2.7	6.7	19.1	37.6	66.6	92.1	97.0	100.0	100.0
075	2	233	3.1	5.3	12.6	26.8	39.9	57.9	74.1	90.4	100.0	100.0
080	2	216	7.4	8.4	10.7	24.1	51.7	82.7	96.7	100.0	100.0	100.0
081	2	207	4.3	5.7	8.6	15.4	40.5	69.0	94.2	100.0	100.0	100.0
092	2	217	3.6	5.8	11.0	28.5	52.2	87.4	99.6	100.0	100.0	100.0
093	3	364	4.5	5.3	7.6	16.7	27.5	44.7	74.8	96.3	100.0	100.0
103	3	353	2.8	3.0	6.4	13.2	31.2	59.9	87.7	94.5	100.0	100.0
106	2	206	1.0	2.0	4.9	11.1	24.7	48.5	78.4	95.6	100.0	100.0
107	2	205	2.9	5.4	8.8	17.6	29.3	47.3	70.8	89.3	100.0	100.0
171	2	216	3.7	6.0	13.5	29.7	62.5	86.5	98.1	100.0	100.0	100.0
173	3	304	4.7	4.7	6.4	11.6	23.8	43.8	71.8	92.2	99.5	100.0
174	2	206	3.9	5.3	11.7	20.4	36.9	64.1	87.9	98.5	99.5	100.0
179	3	445	1.5	4.3	12.5	30.2	60.2	90.1	98.2	100.0	100.0	100.0
180	2	214	2.3	2.3	10.8	34.1	54.2	77.6	97.2	99.1	100.0	100.0
181	2	200	6.0	7.0	9.0	17.0	32.5	60.5	89.5	99.5	100.0	100.0
189	3	308	6.6	9.0	10.7	19.6	40.8	76.2	97.3	100.0	100.0	100.0
195	2	204	4.4	8.3	19.2	34.9	54.0	78.9	97.0	100.0	100.0	100.0
197	2	218	5.2	8.0	16.7	29.0	47.9	65.3	87.0	94.8	99.1	100.0
199	2	221	4.1	5.4	12.6	21.5	29.2	50.6	79.1	94.5	100.0	100.0

Table A.4 – *Reach-average characteristics data — Continued*

[LOD, large organic debris; cm, centimeter; m^3, cubic meters; $L_t > W_{bf}$, total piece length greater than mean bankfull width of channel; --, not applicable]

Site number	LOD piece count	Mean piece diameter (cm)	Mean piece length (cm)	Mean active-channel piece length (cm)	Mean piece volume (m^3)	Mean active-channel piece volume (m^3)	Total LOD loading per unit channel length (m^3/m)	Active-channel LOD loading per unit channel length (m^3/m)	Frequency of pieces with $L_t > W_{bf}$ $(100\ m)^{-1}$	Frequency of influential pieces $(100\ m)^{-1}$
071	78	23.3	583	426	0.35	0.22	0.138	0.085	2.5	0.045
073	84	18.4	656	469	.21	.16	.089	.066	2.0	.020
075	152	20.6	644	503	.30	.22	.268	.197	8.8	.041
080	104	19.1	693	586	.27	.22	.163	.133	10.3	.023
081	71	18.7	591	481	.23	.18	.100	.079	6.9	.038
092	96	18.1	788	544	.24	.16	.138	.093	17.6	.012
093	196	22.1	878	770	.51	.47	.509	.466	20.4	.138
103	166	21.1	663	463	.32	.21	.349	.231	21.6	.098
106	43	18.5	570	411	.17	.12	.048	.033	6.6	0
107	52	17.2	625	370	.16	.10	.062	.036	11.7	0
171	151	20.6	675	523	.30	.22	.300	.225	16.0	.080
173	78	23.9	707	465	.45	.28	.177	.109	10.0	.070
174	98	20.0	714	519	.27	.19	.178	.124	23.3	.007
179	94	18.8	756	534	.28	.18	.196	.129	22.2	.015
180	85	25.8	644	437	.48	.32	.287	.190	16.2	.106
181	89	24.3	570	438	.40	.31	.236	.184	10.7	.067
189	111	22.4	828	636	.46	.34	.289	.209	18.0	.090
195	75	22.1	618	484	.33	.25	.153	.115	11.2	.056
197	74	20.2	775	508	.32	.20	.167	.103	21.8	.042
199	115	20.5	805	514	.34	.21	.261	.164	26.0	.007

Table A.4 – *Reach-average characteristics data — Continued*

[LOD, large organic debris; m, meter; m^3, cubic meters; --, not applicable]

Site number	Frequency of LOD $(100\ m)^{-1}$	Frequency of isolated pieces $(100\ m)^{-1}$	Number of LOD contact groups	Mean number of pieces per contact group	Frequency of pieces in contact groups $(100\ m)^{-1}$	Frequency of LOD contact groups $(100\ m)^{-1}$	Frequency of small contact groups (<10 pieces) $(100\ m)^{-1}$	Number of debris jams (10 or more pieces)	Mean number of pieces per debris jam
071	39	13.0	9	5.8	26	4.5	4.0	1	29
073	42	13.9	8	7.0	28	4.0	3.0	2	17.5
075	89	10.6	13	10.3	79	7.6	5.9	3	35
080	59	11.4	8	10.5	48	4.6	2.9	3	22
081	44	10.0	7	7.9	34	4.4	3.1	2	22
092	56	11.8	13	5.8	45	7.6	5.3	4	13.0
093	100	15.8	14	11.8	84	7.1	3.6	7	20
103	108	12.4	14	10.5	96	9.2	6.5	4	25
106	28	11.2	5	5.2	17	3.3	2.6	1	13.0
107	38	16.8	6	4.8	21	4.4	3.6	1	17.0
171	101	12.0	15	8.9	89	10.0	6.7	5	18.6
173	39	8.5	10	6.1	31	5.0	4.0	2	16.0
174	65	10.0	9	9.2	55	6.0	4.0	3	19.3
179	70	23	13	4.8	47	9.6	7.4	3	14.0
180	60	12.7	18	3.7	47	12.7	12.7	0	--
181	59	23	15	3.7	37	10.0	10.0	0	--
189	62	8.4	10	9.6	54	5.6	2.8	5	14.2
195	47	6.3	13	5.0	41	8.1	7.5	1	25
197	52	10.6	8	7.4	42	5.6	4.9	1	34
199	77	7.3	15	6.9	69	10.0	7.3	4	16.8

Table A.4 – *Reach-average characteristics data — Continued*

[LOD, large organic debris; FSD, fine sediment deposits; m, meters; cm, centimeters; m^3, cubic meters; --, not applicable]

Site number	Frequency of pieces in debris jams $(100\ m)^{-1}$	Frequency of debris jams $(100\ m)^{-1}$	Number of LOD-related FSD	Frequency of LOD-related FSD $(100\ m)^{-1}$	Mean thickness of LOD-related FSD (cm)	Mean volume of LOD-related FSD (m^3)	Number of LOD pieces storing FSD	Mean number of anchor points per LOD piece	Percentage of LOD pieces with anchors
071	14.5	0.50	0	0	--	--	0	0.28	28
073	17.3	.99	2	.99	40	18.3	4	.63	52
075	61	1.76	3	1.76	16.2	1.0	3	.50	40
080	38	1.71	8	4.6	23	2.1	33	.55	44
081	28	1.25	3	1.88	16.4	1.4	3	.86	58
092	31	2.4	2	1.18	16.9	5.9	11	.90	54
093	72	3.6	12	6.1	11.3	.6	20	.59	50
103	65	2.6	8	5.2	18.6	1.8	35	.41	31
106	8.6	.66	1	.66	--	--	5	.55	45
107	12.4	.73	2	1.46	18.2	1.0	2	.65	54
171	62	3.3	9	6.0	26	1.6	30	.83	57
173	16.0	1.00	4	2.0	15.5	.9	4	.31	27
174	39	2.0	4	2.7	13.7	.8	15	.71	52
179	31	2.2	7	5.2	16.2	.9	8	.95	67
180	0	0	4	2.8	15.0	.7	8	1.00	62
181	0	0	6	4.0	14.3	.8	10	1.03	66
189	40	2.8	9	5.1	17.5	2.3	20	.95	73
195	15.6	.63	4	2.5	--	--	9	.61	45
197	24	.70	3	2.1	8.5	3.5	12	.64	46
199	45	2.7	6	4.0	14.8	1.1	8	.61	50

Table A.4 – *Reach-average characteristics data — Continued*

[LOD, large organic debris]

Site number	Percentage of pieces with 2 or more anchors	Percentage of LOD oriented to streamflow as indicated				Percentage of LOD positioned as indicated			
		Parallel	Angled downstream	Transverse	Angled upstream	Bridge (broken or whole)	Drift	Ramp	Step
071	0	46	17	29	7.7	1.3	59	40	0
073	10.7	45	26	27	1.2	0	64	36	0
075	6.6	51	22	24	2.6	1.3	69	29	.7
080	7.7	35	41	18	5.8	1.9	76	22	0
081	22	35	15	46	2.8	0	69	30	1.4
092	23	45	11	42	2.1	1.0	51	44	4.2
093	7.2	33	22	28	17.3	.5	78	22	0
103	6.6	34	23	36	6.6	0	58	42	0
106	9.5	35	19	40	7.0	7.0	63	26	4.7
107	11.5	10	54	27	9.6	9.6	33	58	0
171	19.2	37	25	30	7.9	0	68	28	3.3
173	3.8	22	22	45	11.5	9.0	63	28	0
174	14.3	31	35	29	6.1	1.0	60	38	1.0
179	21	41	22	30	6.4	0	54	46	0
180	30	29	32	35	3.5	2.4	56	39	2.4
181	27	36	26	33	5.6	4.5	65	29	1.1
189	15.5	26	37	31	6.3	4.5	67	29	0
195	9.3	28	31	36	5.3	4.0	68	28	0
197	13.5	30	43	23	4.1	0	50	49	1.4
199	8.8	43	38	17	1.7	4.3	48	48	0

Table A.5 – *Bankfull width data.*

[m, meters; downstream distance, measured from one end of study reach, is negative in upstream direction; --, not measured]

Site number	Stream name	Date measured	Channel unit	Downstream distance (m)	Bankfull width (m)
071	Jones	8/11/99	riffle	--	11.6
071	Jones	8/11/99	riffle	--	13.2
071	Jones	8/11/99	riffle	--	12.2
071	Jones	8/11/99	pool	188	11.0
071	Jones	8/11/99	pool	120	11.7
071	Jones	8/11/99	pool	95	11.7
071	Jones	8/11/99	pool	84	12.8
071	Jones	8/11/99	pool	40	16.8
071	Jones	8/11/99	pool	-19	9.1
073	Jones	8/25/99	riffle	0	14.0
073	Jones	8/25/99	riffle	-81	11.3
073	Jones	8/25/99	riffle	-125	12.5
073	Jones	8/25/99	riffle	-155	12.2
073	Jones	8/25/99	pool	13	9.5
073	Jones	8/25/99	pool	-99	13.9
073	Jones	8/25/99	pool	-51	8.5
073	Jones	8/25/99	pool	-188	14.9
073	Jones	8/25/99	pool	-221	23.8
075	Jones	8/23/99	riffle	-68	13.4
075	Jones	8/23/99	riffle	-84	13.6
075	Jones	8/23/99	riffle	-108	12.5
075	Jones	8/23/99	pool	-29	8.7
075	Jones	8/23/99	pool	-144	13.7
075	Jones	8/23/99	pool	-166	15.2
075	Jones	7/1/00	pool	-287	12.8
075	Jones	7/1/00	pool	-347	10.9
080	Jones	8/12/99	riffle	-70	9.1
080	Jones	8/12/99	riffle	9	9.6
080	Jones	8/12/99	riffle	-150	9.8
080	Jones	8/12/99	pool	0	15.8
080	Jones	8/12/99	pool	-14	16.4
080	Jones	8/12/99	pool	-42	14.3
080	Jones	8/12/99	pool	-58	14.9
080	Jones	8/12/99	pool	-114	8.0
080	Jones	8/12/99	pool	-124	8.5
081	Jones	8/20/99	riffle	-2	8.7
081	Jones	8/20/99	riffle	-98	10.7
081	Jones	8/20/99	riffle	-130	7.6
081	Jones	8/20/99	riffle	-150	7.9
081	Jones	8/20/99	pool	-29	13.4
081	Jones	8/20/99	pool	-63	19.7
081	Jones	8/20/99	pool	-84	12.2

Site number	Stream name	Date measured	Channel unit	Downstream distance (m)	Bankfull width (m)
081	Jones	8/20/99	pool	-74	13.4
081	Jones	8/20/99	pool	-111	9.9
081	Jones	8/20/99	pool	-160	9.4
092	Jones	8/22/99	riffle	0	13.4
092	Jones	8/22/99	riffle	-13	9.7
092	Jones	8/22/99	riffle	-59	8.2
092	Jones	8/22/99	riffle	-96	8.1
092	Jones	8/22/99	pool	-7	15.5
092	Jones	8/22/99	pool	-28	13.0
092	Jones	8/22/99	pool	-44	18.3
092	Jones	8/22/99	pool	-75	10.7
093	Jones	8/10/99	riffle	-196	18.6
093	Jones	8/10/99	riffle	-150	21.9
093	Jones	8/10/99	riffle	-4	10.2
093	Jones	8/10/99	riffle	20	9.5
093	Jones	9/5/99	pool	-238	22.9
093	Jones	9/5/99	pool	-331	14.3
093	Jones	8/10/99	pool	-13	13.0
093	Jones	8/10/99	pool	-100	19.8
103	Jones	8/20/99	pool	103	12.5
103	Jones	8/20/99	pool	134	6.6
103	Jones	8/20/99	pool	94	11.1
103	Jones	8/20/99	pool	70	14.6
103	Jones	8/20/99	pool	27	11.3
103	Jones	8/20/99	pool	38	10.9
103	Jones	8/20/99	riffle	113	11.3
103	Jones	8/20/99	riffle	44	8.5
103	Jones	8/20/99	riffle	54	8.8
103	Jones	8/20/99	riffle	-2	7.0
106	Jones	8/13/99	riffle	0	9.0
106	Jones	8/13/99	riffle	-43	5.4
106	Jones	8/13/99	riffle	-110	9.0
106	Jones	8/13/99	riffle	-134	9.1
106	Jones	8/13/99	riffle	-156	9.3
106	Jones	8/13/99	pool	-18	5.9
106	Jones	8/13/99	pool	-64	10.5
106	Jones	8/13/99	pool	-147	6.0
106	Jones	8/13/99	pool	-192	11.5
107	Jones	8/14/99	riffle	0	7.8
107	Jones	8/14/99	riffle	17	5.9
107	Jones	8/14/99	riffle	96	6.1
107	Jones	8/14/99	riffle	76	7.5
107	Jones	8/14/99	riffle	139	8.5
107	Jones	8/14/99	riffle	108	7.7
107	Jones	8/14/99	pool	44	7.9
107	Jones	8/14/99	pool	89	7.2
107	Jones	8/14/99	pool	-14	6.8

Site number	Stream name	Date measured	Channel unit	Downstream distance (m)	Bankfull width (m)
107	Jones	8/14/99	pool	-44	9.4
171	Crow	9/16/99	riffle	20	11.3
171	Crow	9/16/99	riffle	35	12.5
171	Crow	9/16/99	riffle	134	10.4
171	Crow	9/16/99	riffle	71	11.6
171	Crow	9/16/99	pool	-2	14.6
171	Crow	9/16/99	pool	52	11.3
171	Crow	9/16/99	pool	102	12.2
173	Crow	7/20/99	riffle	-2	7.6
173	Crow	9/20/99	riffle	-49	7.0
173	Crow	7/20/99	riffle	-125	7.5
173	Crow	9/20/99	riffle	-138	6.0
173	Crow	9/20/99	riffle	-175	7.3
173	Crow	9/20/99	pool	-16	10.1
173	Crow	9/20/99	pool	-30	8.4
173	Crow	9/20/99	pool	-42	10.1
173	Crow	9/20/99	pool	-53	8.7
173	Crow	9/20/99	pool	-68	8.0
173	Crow	9/20/99	pool	-157	7.8
174	Crow	8/9/99	riffle	0	9.0
174	Crow	8/9/99	riffle	-100	6.6
174	Crow	8/9/99	riffle	-222	7.6
174	Crow	8/9/99	riffle	-150	7.0
174	Crow	8/9/99	riffle	-2	8.8
174	Crow	8/9/99	riffle	-75	7.3
174	Crow	8/9/99	pool	-24	8.0
179	Crow	8/3/99	riffle	3	11.3
179	Crow	8/3/99	riffle	32	7.6
179	Crow	8/3/99	riffle	88	6.6
179	Crow	8/3/99	riffle	135	6.7
179	Crow	7/23/99	riffle	131	8.1
179	Crow	8/3/99	riffle	-25	9.9
179	Crow	8/3/99	riffle	1	10.3
179	Crow	8/3/99	pool	66	10.4
179	Crow	8/3/99	pool	82	9.8
179	Crow	8/3/99	pool	-32	12.0
180	Crow	7/22/99	riffle	--	8.3
180	Crow	7/22/99	riffle	--	8.1
180	Crow	7/22/99	riffle	--	5.0
180	Crow	7/22/99	riffle	--	6.4
180	Crow	8/4/99	riffle	-30	9.1
180	Crow	8/4/99	riffle	-49	7.3
180	Crow	8/4/99	riffle	-77	8.5
180	Crow	8/4/99	riffle	-118	7.9
180	Crow	8/4/99	pool	-18	7.9
180	Crow	8/4/99	pool	-34	8.5
180	Crow	8/4/99	pool	-62	9.8

Site number	Stream name	Date measured	Channel unit	Downstream distance (m)	Bankfull width (m)
180	Crow	8/4/99	pool	-86	8.1
180	Crow	8/4/99	pool	-123	7.6
181	Crow	8/5/99	riffle	140	7.8
181	Crow	8/5/99	riffle	131	6.5
181	Crow	8/5/99	riffle	108	8.2
181	Crow	8/5/99	riffle	125	6.7
181	Crow	8/5/99	riffle	82	8.2
181	Crow	8/5/99	pool	120	8.2
181	Crow	8/5/99	pool	8	10.5
181	Crow	8/5/99	pool	-38	7.6
181	Crow	8/5/99	pool	-78	10.1
189	Crow	8/8/99	riffle	-12	9.1
189	Crow	8/8/99	riffle	-43	11.9
189	Crow	8/8/99	riffle	-40	9.1
189	Crow	8/8/99	riffle	-176	9.6
189	Crow	8/8/99	pool	0	16.0
189	Crow	8/8/99	pool	-180	6.8
189	Crow	8/8/99	pool	-190	8.0
195	Crow	8/5/99	riffle	86	5.5
195	Crow	8/5/99	riffle	49	7.6
195	Crow	8/5/99	riffle	16	9.1
195	Crow	8/5/99	riffle	115	10.4
195	Crow	8/5/99	pool	62	9.1
195	Crow	8/5/99	pool	72	7.9
195	Crow	8/5/99	pool	102	8.5
195	Crow	8/5/99	pool	41	8.8
195	Crow	8/5/99	pool	26	8.4
195	Crow	8/5/99	pool	2	9.9
195	Crow	8/5/99	pool	-24	15.5
197	Crow	7/26/99	riffle	--	7.2
197	Crow	7/27/99	riffle	-104	7.4
197	Crow	9/17/99	riffle	-6	8.5
197	Crow	9/17/99	riffle	-39	5.8
197	Crow	9/17/99	riffle	-110	7.8
197	Crow	9/17/99	riffle	-134	7.2
197	Crow	9/17/99	pool	-22	7.6
197	Crow	9/17/99	pool	-33	7.0
197	Crow	9/17/99	pool	-88	15.8
197	Crow	9/17/99	pool	-144	8.2
197	Crow	9/17/99	pool	-193	11.0
199	Crow	9/18/99	riffle	25	12.2
199	Crow	9/18/99	riffle	18	9.1
199	Crow	9/18/99	riffle	74	9.0
199	Crow	9/18/99	riffle	158	7.2
199	Crow	9/18/99	riffle	80	10.7
199	Crow	9/18/99	pool	6	9.6
199	Crow	9/18/99	pool	14	9.1

Site number	Stream name	Date measured	Channel unit	Downstream distance (m)	Bankfull width (m)
199	Crow	9/18/99	pool	98	7.6
199	Crow	9/18/99	pool	121	8.4
199	Crow	9/18/99	pool	172	9.5
199	Crow	9/18/99	pool	187	9.1

Table A.6 – *Pebble count data for individual riffle-substrate samples.*

[m, meters; downstream distance, measured from one end of study reach, is negative in upstream direction; --, not a within-riffle replicate sample]

Site number	Stream name	Replicate pair ID	Date sampled	Downstream distance (m)	Number of particles	Percentage of sample finer than indicated size in mm									
						2	4	8	16	32	64	128	256	512	1024
71	Jones	--	08/24/99	5	100	2.0	4.0	8.0	13.0	21.0	39.0	54.0	75.0	89.0	100.0
71	Jones	--	08/24/99	85	100	3.0	5.0	6.0	12.0	19.0	30.0	51.0	75.0	90.0	100.0
73	Jones	--	08/25/99	0	110	1.8	3.6	7.3	16.4	29.1	64.5	95.5	100.0	100.0	100.0
73	Jones	--	08/25/99	-81	115	1.7	1.7	6.1	21.7	46.1	68.7	88.7	93.9	100.0	100.0
75	Jones	--	08/23/99	-67.5	123	1.6	3.3	10.6	22.8	32.5	50.4	69.1	85.4	100.0	100.0
75	Jones	--	08/23/99	-100	110	4.5	7.3	14.5	30.9	47.3	65.5	79.1	95.5	100.0	100.0
80	Jones	--	06/12/98	-150	106	9.4	11.3	15.1	23.6	45.3	71.7	93.4	100.0	100.0	100.0
80	Jones	--	08/23/99	-66	110	5.5	5.5	6.4	24.5	58.2	93.6	100.0	100.0	100.0	100.0
81	Jones	--	08/20/99	-5	102	1.0	2.0	4.9	12.7	34.3	66.7	93.1	100.0	100.0	100.0
81	Jones	--	08/21/99	-99	105	7.6	9.5	12.4	18.1	46.7	71.4	95.2	100.0	100.0	100.0
92	Jones	--	06/11/98	19	115	5.2	8.7	11.3	29.6	50.4	89.6	99.1	100.0	100.0	100.0
92	Jones	--	08/22/99	-50	102	2.0	2.9	10.8	27.5	53.9	85.3	100.0	100.0	100.0	100.0
93	Jones	--	08/10/99	0	120	0.8	2.5	4.2	16.7	28.3	50.0	80.0	97.5	100.0	100.0
93	Jones	f	09/05/99	-195	127	7.9	7.9	13.4	18.9	29.1	42.5	67.7	93.7	100.0	100.0
93	Jones	f	09/05/99	-196	117	8.5	8.5	8.5	14.5	23.9	35.9	71.8	96.6	100.0	100.0
103	Jones	--	06/30/00	52	118	1.7	1.7	5.9	14.4	33.1	57.6	82.2	90.7	100.0	100.0
103	Jones	g	08/20/99	-4	135	3.0	3.0	5.9	12.6	30.4	62.2	92.6	97.0	100.0	100.0
103	Jones	g	08/16/99	-7	100	5.0	6.0	8.0	11.0	28.0	62.0	94.0	100.0	100.0	100.0
106	Jones	--	08/13/99	-56	100	1.0	3.0	6.0	10.0	22.0	46.0	71.0	95.0	100.0	100.0
106	Jones	--	08/13/99	-130	106	0.9	0.9	3.8	12.3	27.4	50.9	85.8	96.2	100.0	100.0
107	Jones	--	08/14/99	21	103	1.9	3.9	7.8	15.5	25.2	45.6	67.0	90.3	100.0	100.0
107	Jones	--	08/14/99	105	102	3.9	6.9	9.8	19.6	33.3	49.0	74.5	88.2	100.0	100.0
171	Crow	b	10/19/98	30	101	5.9	5.9	7.9	21.8	43.6	65.3	96.0	100.0	100.0	100.0
171	Crow	a	10/19/98	150	167	9.6	13.2	18.6	40.1	75.4	95.8	100.0	100.0	100.0	100.0
171	Crow	b	07/27/99	22	106	2.8	4.7	17.0	35.8	65.1	82.1	96.2	100.0	100.0	100.0
171	Crow	a	09/16/99	151	110	4.5	7.3	10.0	23.6	60.0	90.9	100.0	100.0	100.0	100.0

Site number	Stream name	Replicate pair ID	Date sampled	Downstream distance (m)	Number of particles	Percentage of sample finer than indicated size in mm									
						2	4	8	16	32	64	128	256	512	1024
173	Crow	c	07/20/99	-125	99	9.1	9.1	10.1	12.1	26.3	56.6	78.8	97.0	100.0	100.0
173	Crow	--	07/20/99	-300	103	1.0	1.0	1.9	9.7	24.3	39.8	70.9	88.3	99.0	100.0
173	Crow	c	09/20/99	-138	102	7.8	7.8	11.8	14.7	20.6	39.2	66.7	95.1	100.0	100.0
174	Crow	--	07/26/99	-75	103	3.9	6.8	16.5	29.1	44.7	68.0	89.3	99.0	99.0	100.0
174	Crow	--	07/26/99	-2	103	3.9	3.9	6.8	11.7	29.1	60.2	86.4	98.1	100.0	100.0
179	Crow	d	07/23/99	-125	201	2.5	5.5	13.9	36.3	68.7	93.0	100.0	100.0	100.0	100.0
179	Crow	--	07/24/99	-15	137	0.7	1.5	9.5	26.3	55.5	89.1	96.4	100.0	100.0	100.0
179	Crow	d	08/04/99	-134	107	1.9	10.3	18.7	29.9	57.9	87.9	100.0	100.0	100.0	100.0
180	Crow	--	07/22/99	-15	109	2.8	2.8	8.3	34.9	54.1	77.1	96.3	98.2	100.0	100.0
180	Crow	--	07/23/99	-118	105	1.9	1.9	13.3	33.3	54.3	78.1	98.1	100.0	100.0	100.0
181	Crow	--	06/23/98	45	100	5.0	6.0	7.0	12.0	27.0	58.0	86.0	99.0	100.0	100.0
181	Crow	--	07/22/99	87	100	7.0	8.0	11.0	22.0	38.0	63.0	93.0	100.0	100.0	100.0
189	Crow	--	07/25/99	-178	100	5.0	7.0	8.0	17.0	33.0	63.0	95.0	100.0	100.0	100.0
189	Crow	e	07/25/99	-33	105	11.4	15.2	19.0	26.7	52.4	87.6	99.0	100.0	100.0	100.0
189	Crow	e	08/08/99	-32	103	4.9	6.8	7.8	17.5	44.7	91.3	100.0	100.0	100.0	100.0
195	Crow	--	07/24/99	110	101	5.9	9.9	22.8	42.6	59.4	78.2	96.0	100.0	100.0	100.0
195	Crow	--	06/26/00	12	103	2.9	6.8	15.5	27.2	48.5	79.6	98.1	100.0	100.0	100.0
197	Crow	--	07/26/99	-5	115	2.6	4.3	13.0	27.8	44.3	62.6	90.4	97.4	98.3	100.0
197	Crow	--	07/27/99	-103	103	7.8	11.7	20.4	30.1	51.5	68.0	83.5	92.2	100.0	100.0
199	Crow	--	07/28/99	-70	113	3.5	5.3	15.0	29.2	38.1	54.9	84.1	95.6	100.0	100.0
199	Crow	--	09/17/99	-125	108	4.6	5.6	10.2	13.9	20.4	46.3	74.1	93.5	100.0	100.0

Table A.7 – *Pool characteristics data.*

[Pool type codes: T, pool is of type indicated; F, pool not of type indicated.]

Site number	Stream name	Date sampled	Pool number	Pool type					Pool length (meters)
				Vertical scour	Plunge	Lateral scour / bend	Fluvial (freely formed)	Channel constric -tion	
071	Jones	8/11/99	1	T	F	F	F	F	2.4
071	Jones	8/11/99	2	T	F	F	F	F	8.5
071	Jones	8/11/99	3	T	F	F	F	F	5.4
071	Jones	8/11/99	4	F	T	F	F	F	3.0
071	Jones	8/11/99	5	F	T	F	F	F	2.5
071	Jones	8/11/99	6	F	F	F	F	T	5.7
073	Jones	8/25/99	1	T	F	F	F	T	6.8
073	Jones	8/25/99	2	T	F	F	F	F	13.7
073	Jones	8/25/99	3	F	F	F	F	T	27
073	Jones	8/25/99	4	F	F	F	F	T	14.5
073	Jones	8/25/99	5	T	F	T	F	F	16.5
075	Jones	8/24/99	1	T	F	F	T	F	8.0
075	Jones	8/24/99	2	T	F	F	F	T	5.6
075	Jones	8/24/99	3	F	F	T	F	T	8.4
075	Jones	8/24/99	4	F	T	F	F	F	16.8
075	Jones	7/1/00	5	T	F	T	F	F	10.7
075	Jones	7/1/00	6	T	F	T	F	F	12.2
080	Jones	8/12/99	1	F	F	T	F	F	9.0
080	Jones	8/12/99	2	F	F	T	F	F	9.8
080	Jones	8/12/99	3	F	F	T	F	F	9.0
080	Jones	8/12/99	4	T	F	T	F	F	23.8
080	Jones	8/12/99	5	F	F	F	F	T	3.9
080	Jones	8/12/99	6	T	F	F	F	T	12.6
081	Jones	8/20/99	1	F	F	T	F	T	3.5
081	Jones	8/20/99	2	T	F	F	T	F	12.8
081	Jones	8/20/99	3	T	T	F	F	F	3.3
081	Jones	8/20/99	4	T	F	F	F	F	6.1
081	Jones	8/20/99	5	F	F	F	T	F	13.1
081	Jones	8/20/99	6	F	F	T	T	F	15.1
092	Jones	8/22/99	1	T	T	F	F	F	2.6
092	Jones	8/22/99	2	T	F	T	F	F	9.5
092	Jones	8/22/99	3	F	F	T	F	F	10
092	Jones	8/22/99	4	T	F	F	F	F	5.2
092	Jones	8/22/99	5	T	F	F	F	F	5.2
092	Jones	8/22/99	6	T	F	F	F	T	7.6
093	Jones	8/10/99	1	F	F	T	F	T	15.5
093	Jones	8/10/99	2	T	F	F	F	F	4.5
093	Jones	8/10/99	3	F	F	F	F	T	14
093	Jones	9/5/99	4	T	F	T	F	F	9.6
093	Jones	9/5/99	5	F	F	F	F	T	8.3

Site number	Stream name	Date sampled	Pool number	Pool type					Pool length (meters)
				Vertical scour	Plunge	Lateral scour / bend	Fluvial (freely formed)	Channel constric -tion	
103	Jones	8/18/99	1	F	F	F	F	T	10.7
103	Jones	8/18/99	2	T	F	F	F	T	11
103	Jones	8/18/99	3	F	F	F	F	T	6
103	Jones	8/18/99	4	T	F	T	F	F	11
103	Jones	8/18/99	5	T	F	F	F	T	6.7
103	Jones	8/18/99	6	F	F	T	F	T	4.8
106	Jones	8/13/99	1	T	F	F	F	F	3.2
106	Jones	8/13/99	2	F	F	F	F	T	8.6
106	Jones	8/13/99	3	T	F	F	F	T	5.5
106	Jones	8/13/99	4	F	T	F	F	F	3.9
106	Jones	8/13/99	5	F	T	F	F	F	6.2
106	Jones	8/13/99	6	F	F	F	F	T	9.7
107	Jones	8/14/99	1	T	F	F	F	F	6.7
107	Jones	8/14/99	2	F	T	F	F	F	4.3
107	Jones	8/14/99	3	F	F	F	F	T	2.4
107	Jones	8/14/99	4	T	T	F	F	F	4.7
107	Jones	8/14/99	5	F	T	F	F	F	4.6
107	Jones	8/14/99	6	F	F	F	F	T	9.7
171	Crow	9/16/99	1	T	F	T	F	F	16.5
171	Crow	9/16/99	2	T	T	F	F	F	12.2
171	Crow	9/16/99	3	T	F	T	F	F	19.8
171	Crow	9/16/99	4	F	F	T	F	T	14.9
171	Crow	9/16/99	5	T	F	F	F	F	10.7
171	Crow	9/16/99	6	F	F	F	T	F	6.1
173	Crow	9/20/99	1	F	F	F	F	T	8.1
173	Crow	9/20/99	2	T	T	F	F	T	10.0
173	Crow	9/20/99	3	F	T	F	F	T	8.0
173	Crow	9/20/99	4	F	T	F	F	F	3.0
173	Crow	9/20/99	5	F	F	T	F	T	8.0
173	Crow	9/20/99	6	F	F	F	F	T	6.5
174	Crow	8/9/99	1	T	F	F	F	F	8.6
174	Crow	8/9/99	2	F	F	F	F	T	9.1
174	Crow	8/9/99	3	F	T	F	F	F	6.0
174	Crow	8/9/99	4	F	T	F	F	F	7.5
174	Crow	8/9/99	5	F	F	F	F	T	8.5
174	Crow	8/9/99	6	F	T	F	F	T	5.5
179	Crow	8/3/99	1	F	T	F	F	F	5.6
179	Crow	8/3/99	2	T	F	T	F	F	3.5
179	Crow	8/3/99	3	T	F	T	F	F	6.2
179	Crow	8/3/99	4	T	F	F	F	F	5.2
179	Crow	8/3/99	5	F	T	F	F	F	7.3
179	Crow	8/3/99	6	T	F	T	F	F	10.5
180	Crow	8/4/99	1	F	T	F	F	F	6.0
180	Crow	8/4/99	2	F	T	F	F	F	3.5

Site number	Stream name	Date sampled	Pool number	Pool type					Pool length (meters)
				Vertical scour	Plunge	Lateral scour / bend	Fluvial (freely formed)	Channel constric -tion	
180	Crow	8/4/99	3	F	T	F	F	F	4.0
180	Crow	8/4/99	4	F	T	F	F	F	3.2
180	Crow	8/4/99	5	T	F	F	F	F	5.2
180	Crow	8/4/99	6	T	F	F	F	T	4.3
181	Crow	8/5/99	1	F	T	F	F	F	4.0
181	Crow	8/5/99	2	T	F	T	F	F	12.0
181	Crow	8/5/99	3	T	F	F	F	F	6.0
181	Crow	8/5/99	4	T	F	F	F	T	6.0
181	Crow	8/5/99	5	F	F	F	F	T	5.2
181	Crow	8/5/99	6	F	T	F	F	F	2.6
189	Crow	8/8/99	1	T	F	F	F	F	8.3
189	Crow	8/8/99	2	T	F	F	F	F	5.0
189	Crow	8/8/99	3	F	F	F	F	T	4.2
189	Crow	8/8/99	4	T	F	F	F	T	22.4
189	Crow	8/8/99	5	T	F	F	F	F	9.5
189	Crow	8/8/99	6	F	F	F	F	T	8.3
195	Crow	8/5/99	1	F	F	F	F	T	4.4
195	Crow	8/5/99	2	F	T	F	F	T	7.0
195	Crow	8/6/99	3	F	F	F	F	T	10.0
195	Crow	8/6/99	4	T	T	F	F	F	5.0
195	Crow	8/6/99	5	F	F	T	F	T	6.6
195	Crow	8/6/99	6	T	F	F	F	T	5.2
197	Crow	9/17/99	1	F	T	F	F	F	3.5
197	Crow	9/17/99	2	T	F	T	F	F	4.5
197	Crow	9/17/99	3	F	T	F	F	F	4.5
197	Crow	9/17/99	4	T	F	F	F	T	6.2
197	Crow	9/17/99	5	F	F	F	F	T	5.0
197	Crow	9/17/99	6	F	T	F	F	F	5.5
199	Crow	9/17/99	1	F	T	F	F	F	4.0
199	Crow	9/17/99	2	T	T	F	F	F	6.0
199	Crow	9/18/99	3	F	F	F	F	T	9.5
199	Crow	9/18/99	4	T	F	F	F	T	4.8
199	Crow	9/18/99	5	T	T	F	F	F	3.5
199	Crow	9/18/99	6	F	T	F	F	T	4.3

Table A.7 – *Pool characteristics data – Continued*

Site number	Pool number	Depth at riffle crest (cm)	Step height (cm)	Pool spacing (m)	Residual pool volume (m^3)	Residual-pool fine-sediment volume (m^3)	Residual-pool fines volume ratio (V*)	Residual-pool mean depth (m)	Mean top width (m)
071	1	40.3	--	--	0.508	0.162	0.319	0.077	7.7
071	2	36.2	--	59.2	3.209	0.428	0.133	0.179	4.1
071	3	37.7	--	43.8	0.810	0.196	0.242	0.095	4.4
071	4	34.8	--	11.0	0.492	0.043	0.087	0.086	3.7
071	5	42.0	--	25.5	0.564	0.055	0.098	0.141	4.0
071	6	41.0	--	67.7	1.984	0.250	0.126	0.112	7.9
073	1	38.0	--	--	2.946	1.336	0.453	0.176	5.2
073	2	25.3	--	66.55	10.859	1.805	0.166	0.165	8.7
073	3	24.8	--	47.55	25.359	7.062	0.278	0.225	7.3
073	4	22.1	--	85.75	16.364	5.373	0.328	0.172	8.4
073	5	33.7	--	33	27.734	8.277	0.298	0.343	9.0
075	1	35.2	--	--	1.088	0.447	0.411	0.058	7.1
075	2	36.9	--	115.9	1.647	0.357	0.217	0.119	5.7
075	3	36.0	--	25.3	5.261	1.315	0.250	0.182	6.2
075	4	33.1	--	96.9	11.944	1.650	0.138	0.269	5.4
075	5	57.8	--	22.5	8.183	1.290	0.158	0.219	9.1
075	6	52.8	--	66.0	9.888	0.886	0.090	0.244	6.0
080	1	27.3	--	22.1	11.407	3.362	0.295	0.297	6.9
080	2	43.3	--	10.4	2.300	0.280	0.122	0.135	5.7
080	3	39.8	--	55.7	14.790	6.487	0.439	0.367	7.9
080	4	31.4	--	16.5	45.591	18.529	0.406	0.275	10.4
080	5	38.0	--	27.9	0.655	0.255	0.389	0.107	4.9
080	6	32.6	--	14.1	11.207	1.589	0.142	0.304	6.0
081	1	41.2	--	--	1.861	0.582	0.313	0.241	3.7
081	2	22.5	--	34.0	9.503	1.807	0.190	0.172	5.6
081	3	30.2	--	11.4	1.242	0.332	0.268	0.197	3.7
081	4	25.7	--	9.9	7.263	2.278	0.314	0.199	12.3
081	5	24.4	--	26.6	4.471	2.837	0.635	0.077	8.3
081	6	25.1	--	48.9	11.581	2.370	0.205	0.236	5.9
092	1	19.2	--	--	1.078	0.283	0.262	0.124	5.0
092	2	34.5	--	21.8	4.155	0.423	0.102	0.229	5.4
092	3	22.7	--	13.1	6.936	1.488	0.215	0.278	3.8
092	4	15.2	--	10.1	4.988	0.399	0.080	0.317	4.2
092	5	63.5	--	23.8	1.422	0.283	0.199	0.144	4.4
092	6	27.7	--	70.8	4.816	1.655	0.344	0.323	3.2
093	1	31.4	--	--	9.415	1.162	0.123	0.188	7.0
093	2	41.2	--	39.5	1.097	0.044	0.040	0.114	6.4
093	3	43.4	--	49.3	13.273	1.687	0.127	0.198	9.9
093	4	36.0	--	137.7	2.343	0.300	0.128	0.103	6.2
093	5	37.7	--	93.7	1.464	0.194	0.132	0.089	8.0
103	1	25.2	--	--	6.382	0.759	0.119	0.249	5.6

Site number	Pool number	Depth at riffle crest (cm)	Step height (cm)	Pool spacing (m)	Residual pool volume (m^3)	Residual-pool fine-sediment volume (m^3)	Residual-pool fines volume ratio (V*)	Residual-pool mean depth (m)	Mean top width (m)
103	2	24.5	--	31.5	12.345	1.965	0.159	0.262	6.6
103	3	51.4	--	9.4	2.330	1.507	0.647	0.149	9.1
103	4	29.0	--	23.5	4.912	2.686	0.547	0.178	5.9
103	5	23.2	--	32.2	15.037	3.570	0.237	0.235	8.8
103	6	42.5	--	9.8	1.503	0.190	0.126	0.201	4.4
106	1	24.2	--	--	0.599	0.089	0.149	0.113	2.3
106	2	17.1	--	33.7	7.475	1.849	0.247	0.304	4.8
106	3	38.3	--	10.6	1.533	0.110	0.072	0.157	3.1
106	4	17.7	--	29.7	1.103	0.464	0.421	0.139	3.0
106	5	35.4	104	53.7	0.671	0.040	0.060	0.069	5.6
106	6	29.8	--	46.3	1.172	0.154	0.132	0.093	4.7
107	1	27.9	--	5.880	0.565	0.087	0.154	0.061	3.1
107	2	34.2	--	51.270	0.358	0.027	0.076	0.115	4.2
107	3	22.0	--	6.250	0.312	0.034	0.109	0.105	2.9
107	4	28.0	--	39.450	0.595	0.090	0.151	0.103	4.8
107	5	34.0	--	30.850	0.511	0.110	0.215	0.084	3.9
107	6	19.2	--	--	3.356	1.427	0.425	0.108	6.1
171	1	24.0	--	--	6.051	2.306	0.381	0.110	6.0
171	2	15.0	--	53.6	21.742	6.050	0.278	0.359	6.7
171	3	4.0	--	44.3	15.953	9.141	0.573	0.284	3.9
171	4	26.8	--	5.8	12.497	7.082	0.567	0.345	3.9
171	5	15.2	--	21.9	13.972	5.885	0.421	0.287	6.2
171	6	29.5	--	18.4	4.991	1.925	0.386	0.232	5.6
173	1	33.0	--	--	0.971	0.115	0.118	0.084	4.7
173	2	22.9	55	14.05	3.358	0.381	0.113	0.123	5.6
173	3	28.4	55	12.5	6.273	0.378	0.060	0.246	6.1
173	4	31.3	55	10.7	0.273	0.042	0.154	0.047	4.7
173	5	31.3	--	15.3	3.436	0.343	0.100	0.168	5.0
173	6	30.8	--	89.25	0.550	0.095	0.172	0.065	4.3
174	1	21.5	--	--	1.585	0.149	0.094	0.093	4.2
174	2	20.3	--	17.1	4.314	0.277	0.064	0.146	5.6
174	3	17.3	70	21.7	4.565	0.243	0.053	0.241	4.9
174	4	23.3	--	21.5	1.765	0.735	0.417	0.092	4.6
174	5	25.0	--	95.0	4.823	0.363	0.075	0.184	5.9
174	6	27.6	--	81.0	4.009	1.014	0.253	0.163	5.9
179	1	21.2	--	77.55	3.969	1.470	0.370	0.199	5.1
179	2	27.1	--	21.95	1.291	0.810	0.627	0.160	4.3
179	3	34.9	--	14.85	2.174	0.646	0.297	0.136	4.9
179	4	35.8	--	20	1.985	0.360	0.181	0.195	2.8
179	5	21.0	--	7.0	3.045	1.325	0.435	0.167	4.5
179	6	30.6	--	--	8.749	3.719	0.425	0.158	8.4
180	1	19.1	75	--	4.986	0.888	0.178	0.191	6.5
180	2	22.5	95	16.3	3.704	0.334	0.090	0.187	7.5
180	3	25.5	--	28.7	1.991	0.308	0.155	0.113	8.3

Site number	Pool number	Depth at riffle crest (cm)	Step height (cm)	Pool spacing (m)	Residual pool volume (m^3)	Residual-pool fine-sediment volume (m^3)	Residual-pool fines volume ratio (V*)	Residual-pool mean depth (m)	Mean top width (m)
180	4	25.2	57.5	23.7	0.808	0.323	0.400	0.071	5.7
180	5	22.0	--	16.4	4.907	1.135	0.231	0.206	7.0
180	6	31.2	--	20.7	0.542	0.129	0.237	0.078	5.5
181	1	24.5	57.5	--	4.492	0.431	0.096	0.267	6.0
181	2	32.2	--	23	10.249	0.877	0.086	0.296	6.0
181	3	24.2	--	102	1.585	0.122	0.077	0.154	3.7
181	4	13.2	--	10	1.295	0.270	0.208	0.105	3.5
181	5	20.2	--	46.4	1.288	0.088	0.068	0.109	4.5
181	6	35.8	60	39.2	0.231	0.052	0.226	0.056	8.3
189	1	25.5	--	--	5.626	0.536	0.095	0.188	6.5
189	2	24.7	--	34.9	2.508	0.400	0.159	0.136	7.0
189	3	36.3	--	22.6	1.303	0.564	0.433	0.168	7.0
189	4	23.5	--	49.7	29.420	7.203	0.245	0.340	5.8
189	5	21.2	--	69.9	3.908	1.218	0.312	0.127	7.3
189	6	37.8	--	10.3	2.803	0.381	0.136	0.164	5.0
195	1	32.7	--	--	2.771	0.440	0.159	0.172	7.1
195	2	24.3	57.5	30	7.203	1.659	0.230	0.224	6.6
195	3	27.1	--	31.5	11.306	1.687	0.149	0.271	6.0
195	4	23.6	47.5	15.5	1.397	0.447	0.320	0.093	5.0
195	5	32.8	--	23.0	1.733	0.222	0.128	0.113	4.4
195	6	15.4	--	26.1	1.337	0.219	0.164	0.109	4.3
197	1	34.0	40	--	0.601	0.050	0.083	0.142	5.8
197	2	29.6	--	9.5	0.721	0.062	0.086	0.115	4.4
197	3	23.8	45	29.0	0.783	0.045	0.057	0.125	3.4
197	4	25.8	--	26.6	1.778	0.253	0.142	0.123	6.6
197	5	29.8	--	56.2	0.744	0.117	0.158	0.089	4.4
197	6	23.4	45	48.3	1.181	0.200	0.170	0.081	6.8
199	1	28.8	70	--	0.846	0.057	0.067	0.127	3.5
199	2	23.2	40	9	0.872	0.162	0.186	0.084	4.3
199	3	33.8	--	83.25	1.551	0.398	0.257	0.106	4.5
199	4	28.5	--	23.15	1.115	0.303	0.272	0.103	7.5
199	5	26.2	60	50.4	1.267	0.036	0.028	0.232	2.6
199	6	31.0	50	16.2	0.500	0.025	0.050	0.080	6.0

Table A.8 – *Channel stability index data.*

[Values for channel stability factors are scores on scales varying by factor (Pfankuch, 1975)]

Site number	Stream name	Date visited	Upper Banks				Lower Banks				
			Bank slope	Mass-wasting potential	Float-able objects	Vegeta-tion density	Chan-nel capa-city	Rock content	Flow deflec-tors	Bank cutting	Bar depo-sition
071	Jones	7/01/00	8.0	8.0	6.0	7.0	2.0	3.0	3.0	7.0	5.0
073	Jones	8/25/99	8.0	8.0	6.0	6.0	2.0	5.0	5.0	13.0	11.0
075	Jones	8/24/99	8.0	7.0	7.0	5.0	2.0	3.0	4.0	11.0	7.0
080	Jones	8/12/99	8.0	9.0	7.0	5.0	2.0	8.0	5.0	10.0	9.0
081	Jones	8/21/99	8.0	5.0	6.0	4.0	2.0	4.0	4.0	10.0	7.0
092	Jones	8/22/99	6.0	5.0	6.0	3.0	2.0	5.0	4.0	8.0	5.0
093	Jones	9/06/99	8.0	6.0	8.0	7.0	2.0	4.0	5.0	15.0	8.0
103	Jones	8/20/99	8.0	8.0	8.0	9.0	2.0	3.0	5.0	6.0	9.0
106	Jones	8/13/99	8.0	10.0	5.0	6.0	2.0	3.0	3.0	14.0	6.0
107	Jones	8/14/99	8.0	9.0	5.0	8.0	2.0	2.0	3.0	13.0	6.0
171	Crow	7/27/99	6.0	10.0	7.0	6.0	4.0	2.0	6.0	13.0	11.0
173	Crow	7/20/99	8.0	8.0	7.0	4.0	2.0	4.0	5.0	10.0	5.0
173	Crow	9/20/99	8.0	8.0	6.0	6.0	2.0	2.0	2.0	8.0	5.0
173	Crow	mean	8.0	8.0	6.5	5.0	2.0	3.0	3.5	9.0	5.0
174	Crow	8/09/99	8.0	8.0	7.0	9.0	2.0	2.0	3.0	13.0	8.0
179	Crow	8/04/99	8.0	10.0	7.0	5.0	2.0	3.0	5.0	11.0	11.0
180	Crow	8/04/99	8.0	10.0	5.0	7.0	2.0	4.0	4.0	14.0	8.0
181	Crow	8/05/99	8.0	7.0	6.0	5.0	2.0	4.0	4.0	10.0	8.0
189	Crow	8/08/99	8.0	6.0	8.0	6.0	3.0	4.0	6.0	8.0	8.0
195	Crow	8/06/99	8.0	11.0	8.0	7.0	3.0	3.0	5.0	15.0	10.0
197	Crow	9/17/99	8.0	6.0	6.0	7.0	2.0	4.0	4.0	13.0	6.0
199	Crow	9/18/99	8.0	6.0	5.0	7.0	2.0	2.0	3.0	11.0	6.0

Table A.8 – *Channel stability index data – Continued*

Site number	Streambed						Subtotal for upper banks	Subtotal for lower banks	Subtotal for streambed	Total score for channel stability
	Clast angularity	Brightness	Packing	Size distribution shift	Scour and fill	Clinging aquatic vegetation				
071	2.0	3.0	4.0	9.0	7.0	2.0	29.0	20.0	27.0	76.0
073	2.0	2.0	5.0	11.0	8.0	3.0	28.0	36.0	31.0	95.0
075	2.0	2.0	3.0	8.0	7.0	2.0	27.0	27.0	24.0	78.0
080	3.0	3.0	7.0	13.0	11.0	3.0	29.0	34.0	40.0	103.0
081	2.0	1.0	4.0	11.0	11.0	1.0	23.0	27.0	30.0	80.0
092	2.0	1.0	6.0	11.0	12.0	1.0	20.0	24.0	33.0	77.0
093	2.0	2.0	4.0	8.0	9.0	2.0	29.0	34.0	27.0	90.0
103	2.0	2.0	5.0	13.0	13.0	1.0	33.0	25.0	36.0	94.0
106	2.0	2.0	5.0	7.0	6.0	1.0	29.0	28.0	23.0	80.0
107	2.0	1.0	3.0	5.0	6.0	1.0	30.0	26.0	18.0	74.0
171	3.0	3.0	6.0	13.0	19.0	4.0	29.0	36.0	48.0	113.0
173	3.0	2.0	4.0	6.0	8.0	3.0	27.0	26.0	26.0	79.0
173	2.0	2.0	3.0	6.0	7.0	3.0	28.0	19.0	23.0	70.0
173	2.5	2.0	3.5	6.0	7.5	3.0	27.5	22.5	24.5	74.5
174	1.5	3.0	6.0	12.0	13.0	2.0	32.0	28.0	37.5	97.5
179	2.0	3.0	5.0	13.0	12.0	3.0	30.0	32.0	38.0	100.0
180	2.0	3.0	4.0	9.0	12.0	3.0	30.0	32.0	33.0	95.0
181	2.0	3.0	5.0	10.0	12.0	3.0	26.0	28.0	35.0	89.0
189	1.0	3.0	6.0	12.0	12.0	3.0	28.0	29.0	37.0	94.0
195	2.0	3.0	5.0	11.0	15.0	2.0	34.0	36.0	38.0	108.0
197	2.0	2.0	4.0	11.0	10.0	3.0	27.0	29.0	32.0	88.0
199	2.0	2.0	4.0	9.0	8.0	2.0	26.0	24.0	27.0	77.0

Appendix B

CORRELATION MATRIX

Table B.1 – *Matrix of Spearman's rho coefficient of rank correlation between variables.*

[sample size, n, is 20 sites for all variables except as footnoted; underscored values of rho are significant at the 0.05 significance level]

Variable	A_d	B%	S_{basin}	Tw%	Tt%	Tl%	Qg%	Qt%	Z_{seg}	S_{seg}
B%	0.672									
S_{basin}	-0.572	-0.227								
Tw%	0.806	0.686	-0.657							
Tt%	0.889	0.328	-0.645	0.722						
Tl%	-0.983	-0.567	0.594	-0.797	-0.947					
Qg%	0.895	0.770	-0.459	0.723	0.692	-0.854				
Qt%	0.132	0.720	0.370	0.146	-0.226	-0.021	0.424			
Z_{seg}	-0.973	-0.701	0.428	-0.795	-0.859	0.965	-0.908	-0.254		
S_{seg}	0.156	0.257	-0.105	0.395	0.114	-0.131	0.134	0.098	-0.168	
S_w	-0.212	-0.341	0.062	-0.047	0.068	0.108	-0.244	-0.257	0.140	0.388
W_{bf}[1]	0.791	0.735	-0.389	0.749	0.602	-0.739	0.732	0.312	-0.812	0.067
W_p[1]	0.644	0.637	-0.203	0.592	0.388	-0.560	0.561	0.342	-0.646	-0.082
W_r[1]	0.772	0.672	-0.390	0.698	0.640	-0.739	0.698	0.253	-0.796	0.116
F%	-0.058	-0.215	-0.301	0.090	0.170	-0.028	-0.208	-0.417	0.079	0.228
PL_m	0.460	0.444	-0.176	0.354	0.283	-0.420	0.495	0.218	-0.465	-0.245
PL	0.185	0.102	-0.097	0.123	0.128	-0.186	0.307	0.045	-0.211	-0.262
SP_m	0.420	0.290	-0.560	0.438	0.493	-0.459	0.301	-0.132	-0.371	0.117
SP	0.114	-0.002	-0.479	0.258	0.287	-0.198	0.021	-0.281	-0.080	0.117
P%	-0.051	0.032	0.352	-0.178	-0.229	0.120	0.117	0.298	0.006	-0.310
D_r	0.059	0.110	0.082	-0.095	-0.150	0.030	0.150	0.162	-0.018	-0.329
V_r	0.328	0.280	-0.189	0.192	0.135	-0.259	0.350	0.068	-0.274	-0.322
V_{rf}	0.110	0.164	-0.001	-0.006	-0.074	-0.035	0.168	0.110	-0.078	-0.385
V^*_w	-0.230	0.029	0.318	-0.318	-0.350	0.298	-0.068	0.296	0.195	-0.403
$(d_{10})_R$	0.029	0.362	0.148	0.281	-0.114	0.024	0.044	0.373	-0.113	0.654
$(d_{16})_R$	0.171	0.516	0.040	0.382	-0.022	-0.118	0.252	0.443	-0.248	0.555

Variable	A_d	B%	S_{basin}	Tw%	Tt%	Tl%	Qg%	Qt%	Z_{seg}	S_{seg}
$(d_{25})_R$	0.262	0.521	0.003	0.427	0.121	-0.238	0.311	0.386	-0.343	0.642
$(d_{50})_R$	0.328	0.529	-0.141	0.510	0.250	-0.328	0.371	0.328	-0.400	0.699
$(d_{75})_R$	0.271	0.431	-0.216	0.459	0.253	-0.295	0.321	0.238	-0.336	0.608
$(d_{84})_R$	0.269	0.429	-0.241	0.453	0.250	-0.290	0.323	0.232	-0.326	0.600
$(d_{90})_R$	0.328	0.463	-0.220	0.452	0.298	-0.347	0.377	0.262	-0.391	0.561
$(M_\phi)_R$	-0.272	-0.522	0.068	-0.446	-0.170	0.263	-0.359	-0.392	0.361	-0.689
$(s_\phi)_R$	0.287	0.164	-0.435	0.344	0.411	-0.347	0.280	-0.120	-0.265	0.253
$(\alpha_\phi)_R$	-0.173	-0.147	0.013	-0.163	-0.206	0.192	-0.083	0.018	0.165	-0.262
$(D_r)_{sp}$	0.256	0.203	-0.005	0.109	0.035	-0.180	0.311	0.186	-0.232	-0.089
$(L)_{sp}$	0.558	0.356	-0.276	0.391	0.402	-0.523	0.561	0.044	-0.525	-0.056
$(V_r)_{sp}$	0.468	0.317	-0.298	0.337	0.275	-0.409	0.495	0.044	-0.418	-0.069
$(V_{rf})_{sp}$	0.280	0.230	-0.138	0.133	0.074	-0.198	0.311	0.101	-0.227	-0.256
$(V^*_w)_{sp}$	-0.134	0.035	0.160	-0.207	-0.254	0.214	-0.020	0.244	0.141	-0.417
$(d_{10})_p$	-0.190	-0.174	0.138	-0.179	-0.041	0.138	-0.170	0.014	0.134	0.103
$(d_{16})_p$	-0.231	-0.143	0.153	-0.187	-0.102	0.185	-0.183	0.079	0.169	0.157
$(d_{25})_p$	-0.062	-0.084	-0.040	-0.013	0.105	-0.004	-0.053	-0.033	0.017	0.190
$(d_{50})_p$	-0.129	-0.283	-0.050	0.017	0.123	0.030	-0.213	-0.272	0.098	0.242
$(d_{75})_p$	-0.148	-0.266	0.044	0.018	0.088	0.048	-0.235	-0.236	0.098	0.238
$(d_{84})_p$	-0.078	-0.093	0.274	-0.050	0.015	0.016	-0.114	-0.008	-0.011	0.170
$(d_{90})_p$	-0.191	-0.095	0.482	-0.180	-0.149	0.140	-0.167	0.167	0.060	-0.014
$(M_\phi)_p$	0.126	0.212	0.010	-0.006	-0.104	-0.033	0.182	0.176	-0.077	-0.209
$(s_\phi)_p$	0.186	0.221	0.033	0.239	0.008	-0.135	0.081	0.042	-0.171	0.144
$(\alpha_\phi)_p$	0.009	0.346	0.221	-0.130	-0.283	0.099	0.200	0.492	-0.021	-0.189
CS_1	0.029	0.000	-0.347	0.214	0.087	-0.087	0.058	-0.202	-0.029	0.029
CS_2	-0.298	-0.313	-0.023	-0.103	-0.127	0.266	-0.273	-0.245	0.301	-0.022
CS_3	0.331	0.076	-0.144	0.194	0.285	-0.344	0.165	-0.259	-0.287	-0.291
CS_4	0.028	-0.038	-0.088	-0.131	0.120	-0.052	-0.055	-0.184	0.015	0.091
CS_5	-0.094	-0.343	0.159	-0.269	0.074	0.048	-0.167	-0.343	0.094	-0.362
CS_6	0.095	0.177	-0.266	0.233	-0.084	-0.020	0.100	0.068	-0.002	-0.115
CS_7	0.152	-0.065	-0.112	0.016	0.111	-0.128	0.025	-0.277	-0.077	-0.390
CS_8	-0.195	-0.207	-0.156	-0.070	0.022	0.131	-0.274	-0.266	0.221	-0.197
CS_9	-0.012	-0.208	-0.189	-0.126	0.023	0.020	-0.109	-0.415	0.109	-0.413
CS_{10}	0.287	0.202	0.017	0.325	0.229	-0.266	0.362	0.199	-0.331	0.244
CS_{11}	-0.038	-0.478	-0.425	-0.054	0.187	-0.016	-0.181	-0.747	0.172	-0.105
CS_{12}	-0.154	-0.191	0.111	-0.315	-0.204	0.195	-0.133	-0.097	0.233	-0.379

Variable	A_d	B%	S_{basin}	Tw%	Tt%	Tl%	Qg%	Qt%	Z_{seg}	S_{seg}
CS_{13}	0.008	-0.212	0.074	-0.350	-0.066	0.031	-0.037	-0.201	0.078	-0.599
CS_{14}	-0.208	-0.506	0.209	-0.497	-0.156	0.214	-0.373	-0.482	0.303	-0.367
CS_{15}	0.200	-0.411	-0.533	0.156	0.459	-0.277	0.052	-0.685	-0.103	-0.114
CS_{ub}	-0.170	-0.169	-0.030	-0.105	-0.082	0.153	-0.248	-0.256	0.204	-0.069
CS_{lb}	-0.046	-0.233	-0.310	-0.041	0.080	0.023	-0.150	-0.437	0.149	-0.488
CS_{sb}	-0.109	-0.440	0.018	-0.358	-0.058	0.113	-0.221	-0.477	0.222	-0.481
CS_{tot}	-0.059	-0.343	-0.192	-0.212	0.025	0.052	-0.163	-0.491	0.177	-0.515
D_r:D_{rc}	-0.119	-0.066	0.210	-0.323	-0.268	0.195	-0.017	0.116	0.161	-0.317
DS	0.939	0.486	-0.473	0.689	0.954	-0.972	0.794	0.009	-0.942	0.112
LDF	0.253	-0.068	-0.138	-0.099	0.220	-0.247	0.117	-0.296	-0.164	-0.077
LDF_{iso}	-0.090	0.148	-0.206	0.150	-0.169	0.162	-0.205	-0.048	0.176	0.369
LDF_{inf}	0.294	-0.071	-0.289	0.241	0.324	-0.297	0.067	-0.458	-0.211	0.253
LDF_{acc}	0.314	-0.012	-0.123	-0.067	0.263	-0.310	0.215	-0.217	-0.238	-0.098
LDF_{scg}	-0.098	-0.547	-0.078	-0.311	0.068	0.060	-0.256	-0.623	0.200	0.108
LDF_{jam}	0.526	0.329	-0.046	0.132	0.387	-0.511	0.461	0.117	-0.520	-0.216
D_{LD}	0.185	-0.283	-0.373	0.210	0.353	-0.242	-0.011	-0.641	-0.107	0.418
L_t	0.350	-0.024	-0.076	0.083	0.408	-0.397	0.176	-0.149	-0.331	-0.202
L_t:W_{bf}	-0.445	-0.674	0.291	-0.446	-0.177	0.328	-0.487	-0.361	0.398	-0.090
L_a	0.314	0.008	-0.114	0.068	0.310	-0.335	0.173	-0.167	-0.262	-0.441
V_t	0.281	-0.223	-0.363	0.258	0.445	-0.343	0.020	-0.621	-0.202	0.388
V_a	0.266	-0.217	-0.400	0.273	0.414	-0.325	0.066	-0.626	-0.179	0.281
VL_t	0.248	-0.189	-0.223	0.006	0.311	-0.278	0.050	-0.490	-0.164	0.161
VL_a	0.251	-0.128	-0.242	0.035	0.268	-0.265	0.093	-0.450	-0.155	0.138
N_a	-0.597	-0.659	0.195	-0.621	-0.451	0.582	-0.696	-0.454	0.668	-0.272
a%	-0.531	-0.553	0.190	-0.555	-0.397	0.519	-0.632	-0.395	0.582	-0.272
a_W%	-0.668	-0.630	0.294	-0.683	-0.564	0.674	-0.714	-0.316	0.725	-0.283
DAF	-0.142	-0.535	0.035	-0.352	0.002	0.115	-0.333	-0.583	0.239	0.111
P_{acc}	0.645	0.539	-0.240	0.343	0.425	-0.611	0.681	0.264	-0.632	-0.206
DA%	0.366	-0.007	-0.018	-0.079	0.345	-0.384	0.329	-0.126	-0.338	-0.238
SAF	-0.223	-0.551	0.076	-0.345	-0.060	0.196	-0.405	-0.547	0.300	0.108
P_{scg}	0.432	0.486	-0.039	0.196	0.201	-0.386	0.461	0.332	-0.443	-0.297
DJF	0.363	0.229	0.152	0.029	0.270	-0.357	0.288	0.150	-0.395	-0.157
P_{jam}^2	0.435	0.318	-0.389	0.244	0.282	-0.401	0.431	-0.087	-0.379	-0.136
V_{jam}^2	0.482	0.086	-0.454	0.381	0.494	-0.521	0.284	-0.484	-0.449	-0.053
DJ%	0.557	0.451	-0.140	0.252	0.357	-0.530	0.566	0.226	-0.554	-0.296
$O\%_{par}$	0.325	0.395	-0.223	0.201	0.156	-0.241	0.349	0.265	-0.274	0.006

Variable	A_d	B%	S_{basin}	Tw%	Tt%	Tl%	Qg%	Qt%	Z_{seg}	S_{seg}
$O\%_{ds}$	-0.129	-0.352	-0.157	-0.256	0.042	0.063	-0.081	-0.365	0.186	-0.217
$O\%_{tr}$	-0.374	-0.214	0.533	-0.229	-0.405	0.397	-0.408	0.077	0.295	0.116
$O\%_{us}$	0.053	0.089	0.071	0.232	0.119	-0.090	-0.056	-0.051	-0.113	0.395
$\Pi\%_{br}$	-0.346	-0.210	0.132	-0.004	-0.198	0.277	-0.191	-0.019	0.265	0.451
$\Pi\%_{dr}$	0.374	0.319	-0.341	0.445	0.275	-0.362	0.376	-0.039	-0.347	-0.083
$\Pi\%_{ra}$	-0.226	-0.186	0.235	-0.418	-0.217	0.244	-0.244	0.048	0.232	-0.074
$\Pi\%_{st}$	-0.430	-0.240	0.246	-0.444	-0.441	0.463	-0.329	0.125	0.439	-0.077
FDF	0.076	-0.296	-0.012	-0.159	0.141	-0.110	-0.103	-0.496	-0.009	-0.063
FDT^4	0.054	0.328	0.212	0.021	-0.169	0.054	0.233	0.471	-0.096	-0.145
FDV_t^3	0.174	0.069	0.055	-0.066	0.067	-0.137	0.181	0.055	-0.117	-0.420
FDV_l^3	0.061	-0.049	0.036	-0.200	-0.022	-0.022	0.082	-0.028	0.020	-0.536
FDV^4	0.118	0.252	0.204	-0.131	-0.076	-0.051	0.255	0.475	-0.118	-0.532
FS%	-0.162	-0.299	0.170	-0.391	-0.177	0.167	-0.137	-0.179	0.226	-0.328
DJV%	0.439	0.257	-0.091	0.114	0.345	-0.443	0.353	0.037	-0.437	-0.392
DJL_a	0.464	0.185	-0.074	0.100	0.419	-0.484	0.357	-0.056	-0.454	-0.296

Variable	S_w	W_{bf}^1	W_p^1	W_r^1	F%	PL_m	PL	SP_m	SP	P%
W_{bf}^1	-0.553									
W_p^1	-0.775	0.856								
W_r^1	-0.440	0.967	0.761							
F%	0.634	-0.325	-0.537	-0.170						
PL_m	-0.756	0.686	0.679	0.621	-0.420					
PL	-0.456	0.233	0.228	0.158	-0.304	0.788				
SP_m	0.012	0.368	0.156	0.470	0.387	0.229	0.062			
SP	0.259	-0.112	-0.260	-0.018	0.606	-0.065	-0.023	0.839		
P%	-0.582	0.235	0.363	0.140	-0.653	0.574	0.608	-0.577	-0.726	
D_r	-0.802	0.486	0.591	0.414	-0.619	0.735	0.617	-0.149	-0.444	0.817
V_r	-0.811	0.670	0.677	0.596	-0.445	0.887	0.693	0.017	-0.289	0.708
V_{rf}	-0.776	0.539	0.575	0.451	-0.506	0.803	0.653	-0.202	-0.478	0.811
V^*_w	-0.436	0.130	0.186	0.072	-0.481	0.361	0.322	-0.451	-0.636	0.683
$(d_{10})_R$	0.227	0.104	0.072	0.114	0.197	-0.114	-0.123	0.054	0.051	-0.116
$(d_{16})_R$	0.116	0.195	0.120	0.192	0.107	0.071	0.102	0.208	0.145	-0.102
$(d_{25})_R$	0.297	0.116	0.001	0.146	0.238	-0.057	-0.037	0.323	0.292	-0.344
$(d_{50})_R$	0.448	0.093	-0.112	0.158	0.417	-0.162	-0.165	0.439	0.457	-0.534
$(d_{75})_R$	0.569	-0.014	-0.255	0.051	0.528	-0.285	-0.241	0.453	0.541	-0.660
$(d_{84})_R$	0.567	-0.030	-0.258	0.030	0.528	-0.305	-0.272	0.442	0.532	-0.672

Variable	S_w	W_{bf}^1	W_p^1	W_r^1	F%	PL_m	PL	SP_m	SP	P%
$(d_{90})_R$	0.561	-0.002	-0.253	0.054	0.527	-0.283	-0.263	0.389	0.471	-0.632
$(M_\phi)_R$	-0.453	-0.063	0.140	-0.118	-0.371	0.171	0.138	-0.340	-0.358	0.451
$(s_\phi)_R$	0.561	-0.114	-0.347	-0.084	0.459	-0.385	-0.307	0.362	0.489	-0.693
$(\alpha_\phi)_R$	-0.039	-0.068	-0.037	-0.186	-0.184	-0.038	0.059	-0.474	-0.429	0.308
$(D_r)_{sp}$	-0.725	0.523	0.640	0.461	-0.614	0.698	0.570	-0.062	-0.371	0.686
$(L)_{sp}$	-0.671	0.684	0.682	0.653	-0.401	0.887	0.695	0.256	-0.077	0.501
$(V_r)_{sp}$	-0.723	0.633	0.644	0.575	-0.431	0.844	0.705	0.087	-0.212	0.618
$(V_{rf})_{sp}$	-0.845	0.630	0.689	0.547	-0.592	0.820	0.632	-0.081	-0.405	0.756
$(V^*_w)_{sp}$	-0.543	0.360	0.402	0.300	-0.555	0.398	0.254	-0.347	-0.612	0.710
$(d_{10})_p$	0.707	-0.535	-0.639	-0.519	0.363	-0.703	-0.426	-0.156	0.114	-0.459
$(d_{16})_p$	0.720	-0.556	-0.657	-0.530	0.383	-0.737	-0.470	-0.106	0.173	-0.515
$(d_{25})_p$	0.769	-0.511	-0.644	-0.471	0.541	-0.697	-0.426	0.085	0.388	-0.645
$(d_{50})_p$	0.840	-0.598	-0.657	-0.536	0.644	-0.742	-0.483	0.081	0.438	-0.691
$(d_{75})_p$	0.851	-0.617	-0.643	-0.563	0.636	-0.717	-0.457	0.034	0.391	-0.655
$(d_{84})_p$	0.691	-0.551	-0.538	-0.554	0.466	-0.542	-0.271	-0.155	0.170	-0.418
$(d_{90})_p$	0.520	-0.526	-0.443	-0.563	0.251	-0.413	-0.161	-0.225	0.096	-0.228
$(M_\phi)_p$	-0.848	0.568	0.682	0.519	-0.631	0.719	0.460	-0.032	-0.376	0.663
$(s_\phi)_p$	-0.302	0.258	0.428	0.175	-0.020	0.292	0.147	0.008	0.027	0.156
$(\alpha_\phi)_p$	-0.738	0.439	0.453	0.363	-0.671	0.665	0.504	-0.149	-0.448	0.677
CS_1	0.376	-0.250	-0.376	-0.250	0.579	-0.231	-0.058	0.116	0.405	-0.405
CS_2	0.298	-0.243	-0.371	-0.280	0.146	-0.102	0.152	-0.366	-0.261	0.189
CS_3	-0.402	0.408	0.404	0.378	-0.029	0.600	0.425	0.080	-0.110	0.276
CS_4	0.354	-0.340	-0.520	-0.265	0.545	-0.312	-0.207	0.010	0.143	-0.373
CS_5	-0.074	0.095	0.017	0.145	-0.135	0.272	0.318	-0.082	-0.269	0.364
CS_6	-0.590	0.258	0.562	0.168	-0.339	0.235	0.064	-0.069	-0.099	0.264
CS_7	-0.636	0.405	0.536	0.376	-0.265	0.633	0.432	-0.126	-0.357	0.567
CS_8	0.103	-0.212	-0.274	-0.213	0.236	-0.055	-0.068	0.117	0.338	-0.244
CS_9	-0.469	0.163	0.190	0.108	-0.080	0.521	0.517	-0.095	-0.176	0.439
CS_{10}	-0.060	0.265	0.389	0.135	-0.495	0.205	0.205	-0.339	-0.436	0.371
CS_{11}	0.111	-0.069	-0.206	-0.055	0.124	-0.040	0.140	0.031	-0.020	-0.028
CS_{12}	-0.544	0.087	0.197	0.074	-0.429	0.393	0.422	-0.106	-0.282	0.515
CS_{13}	-0.594	0.100	0.278	0.041	-0.422	0.403	0.412	-0.269	-0.459	0.565
CS_{14}	-0.373	-0.117	0.021	-0.149	-0.254	0.197	0.263	-0.329	-0.371	0.439
CS_{15}	-0.048	0.046	0.076	0.066	0.007	0.175	0.317	0.126	0.080	0.084
CS_{ub}	0.169	-0.245	-0.378	-0.270	0.313	-0.052	0.080	-0.308	-0.204	0.057

Variable	S_w	W_{bf}^{1}	W_p^{1}	W_r^{1}	F%	PL_m	PL	SP_m	SP	P%
CS_{lb}	-0.429	0.109	0.187	0.051	-0.110	0.421	0.376	0.007	-0.001	0.266
CS_{sb}	-0.442	-0.030	0.118	-0.087	-0.358	0.285	0.360	-0.309	-0.411	0.488
CS_{tot}	-0.452	0.047	0.098	-0.018	-0.186	0.413	0.450	-0.169	-0.220	0.430
D_r:D_{rc}	-0.684	0.193	0.328	0.153	-0.519	0.574	0.621	-0.162	-0.341	0.756
DS	-0.018	0.654	0.471	0.686	0.043	0.344	0.133	0.435	0.181	-0.148
LDF	-0.387	0.298	0.202	0.353	-0.046	0.365	0.085	0.102	-0.086	0.121
LDF_{iso}	-0.137	0.034	0.145	0.002	0.087	-0.032	-0.160	0.080	0.013	-0.175
LDF_{inf}	-0.099	0.250	0.276	0.243	0.096	0.158	0.060	-0.060	-0.159	0.091
LDF_{acc}	-0.412	0.342	0.233	0.389	-0.115	0.403	0.129	0.053	-0.132	0.185
LDF_{scg}	0.180	-0.235	-0.260	-0.168	0.279	-0.232	-0.125	-0.107	-0.018	-0.059
LDF_{jam}	-0.515	0.564	0.462	0.601	-0.206	0.630	0.251	0.217	-0.091	0.220
D_{LD}	0.373	0.028	-0.130	0.082	0.366	-0.218	-0.126	0.068	0.093	-0.241
L_t	-0.302	0.235	0.296	0.328	-0.026	0.266	-0.038	0.176	0.068	0.002
L_t:W_{bf}	0.457	-0.854	-0.721	-0.774	0.324	-0.504	-0.176	-0.232	0.186	-0.238
L_a	-0.600	0.421	0.505	0.435	-0.365	0.534	0.176	0.185	-0.039	0.208
V_t	0.277	0.089	-0.009	0.175	0.369	-0.192	-0.284	0.128	0.122	-0.313
V_a	0.060	0.209	0.107	0.239	0.121	0.087	0.018	0.101	0.056	-0.084
VL_t	-0.155	0.209	0.121	0.288	0.151	0.224	0.027	0.122	0.003	-0.006
VL_a	-0.247	0.279	0.188	0.335	0.052	0.308	0.093	0.086	-0.062	0.078
N_a	-0.232	-0.418	-0.204	-0.396	-0.165	-0.113	-0.033	-0.122	-0.014	0.095
a%	-0.260	-0.279	-0.128	-0.233	-0.143	0.000	0.009	-0.038	-0.015	0.119
a_W%	-0.256	-0.456	-0.198	-0.465	-0.268	-0.143	-0.024	-0.226	-0.101	0.182
DAF	0.060	-0.150	-0.156	-0.092	0.097	-0.194	-0.261	-0.151	-0.133	-0.032
P_{acc}	-0.597	0.613	0.547	0.585	-0.274	0.720	0.439	0.235	-0.025	0.263
DA%	-0.229	0.306	0.154	0.362	-0.074	0.314	0.123	-0.008	-0.163	0.223
SAF	0.279	-0.301	-0.272	-0.282	0.194	-0.420	-0.358	-0.238	-0.125	-0.128
P_{scg}	-0.720	0.633	0.617	0.577	-0.514	0.730	0.344	0.180	-0.127	0.311
DJF	-0.487	0.484	0.427	0.559	-0.253	0.601	0.223	0.178	-0.130	0.275
P_{jam}^{2}	-0.040	0.216	0.124	0.083	0.024	0.036	-0.006	0.025	0.022	-0.157
V_{jam}^{2}	0.038	0.341	0.221	0.304	0.218	0.119	-0.057	0.179	0.098	-0.214
DJ%	-0.649	0.654	0.599	0.624	-0.407	0.714	0.335	0.217	-0.086	0.272
$O\%_{par}$	-0.271	0.589	0.496	0.586	-0.215	0.173	-0.107	0.377	0.032	-0.023
$O\%_{ds}$	0.107	-0.491	-0.491	-0.442	0.200	-0.132	0.101	-0.107	0.123	-0.095
$O\%_{tr}$	0.039	-0.111	0.023	-0.151	-0.159	-0.048	0.077	-0.380	-0.332	0.371
$O\%_{us}$	0.286	-0.039	-0.114	-0.032	0.156	0.033	0.065	0.009	-0.041	-0.156
$\Pi\%_{br}$	0.600	-0.380	-0.569	-0.284	0.290	-0.372	-0.143	-0.026	0.195	-0.216

Variable	S_w	W_{bf}[1]	W_p[1]	W_r[1]	F%	PL_m	PL	SP_m	SP	P%
$\Pi\%_{dr}$	-0.468	0.604	0.526	0.496	-0.338	0.713	0.559	0.247	0.051	0.287
$\Pi\%_{ra}$	0.223	-0.449	-0.342	-0.388	0.202	-0.543	-0.475	-0.168	-0.071	-0.248
$\Pi\%_{st}$	-0.153	-0.212	-0.083	-0.241	-0.353	-0.137	-0.069	-0.074	-0.026	0.094
FDF	-0.279	0.072	0.118	0.094	-0.071	0.304	0.174	-0.109	-0.173	0.175
FDT[4]	-0.505	0.350	0.338	0.288	-0.450	0.559	0.571	-0.353	-0.650	0.843
FDV_t[3]	-0.684	0.297	0.493	0.326	-0.330	0.620	0.470	0.009	-0.234	0.540
FDV_l[3]	-0.672	0.191	0.404	0.221	-0.308	0.546	0.432	-0.042	-0.259	0.531
FDV[4]	-0.512	0.194	0.368	0.194	-0.384	0.284	0.262	-0.145	-0.414	0.527
FS%	-0.379	-0.151	0.018	-0.158	-0.263	0.250	0.328	-0.281	-0.292	0.417
DJV%	-0.553	0.570	0.466	0.585	-0.230	0.670	0.305	0.312	0.020	0.180
DJL_a	-0.384	0.515	0.373	0.566	-0.116	0.554	0.205	0.234	-0.053	0.136

Variable	D_r	V_r	V_{rf}	V^*_w	$(d_{50})_R$	$(M_\phi)_R$	$(s_\phi)_R$	$(\alpha_\phi)_R$	$(d_{50})_p$	$(M_\phi)_p$
V_r	0.889									
V_{rf}	0.902	0.943								
V^*_w	0.565	0.459	0.699							
$(d_{10})_R$	-0.202	-0.198	-0.198	-0.155						
$(d_{16})_R$	-0.124	-0.067	-0.134	-0.186						
$(d_{25})_R$	-0.358	-0.273	-0.369	-0.353						
$(d_{50})_R$	-0.553	-0.406	-0.538	-0.504						
$(d_{75})_R$	-0.691	-0.526	-0.646	-0.575	0.940					
$(d_{84})_R$	-0.700	-0.532	-0.646	-0.565	0.915					
$(d_{90})_R$	-0.699	-0.511	-0.617	-0.529	0.895					
$(M_\phi)_R$	0.520	0.397	0.493	0.421	-0.982					
$(s_\phi)_R$	-0.699	-0.508	-0.632	-0.558	0.489	-0.417				
$(\alpha_\phi)_R$	0.164	0.107	0.283	0.352	-0.435	0.302	-0.162			
$(D_r)_{sp}$	0.847	0.753	0.699	0.278	-0.331	0.301	-0.585	0.113		
$(L)_{sp}$	0.720	0.847	0.695	0.176	-0.099	0.125	-0.326	-0.180		
$(V_r)_{sp}$	0.782	0.902	0.788	0.265	-0.191	0.182	-0.427	0.011		
$(V_{rf})_{sp}$	0.916	0.940	0.922	0.525	-0.459	0.430	-0.644	0.173		
$(V^*_w)_{sp}$	0.725	0.577	0.752	0.859	-0.630	0.558	-0.672	0.402		
$(d_{10})_p$	-0.741	-0.774	-0.702	-0.333	0.240	-0.270	0.608	0.227		
$(d_{16})_p$	-0.772	-0.830	-0.758	-0.359	0.321	-0.356	0.587	0.194		
$(d_{25})_p$	-0.860	-0.813	-0.820	-0.477	0.459	-0.447	0.751	-0.023		
$(d_{50})_p$	-0.869	-0.836	-0.870	-0.617	0.382	-0.333	0.712	-0.105		

Variable	D_r	V_r	V_{rf}	V^*_w	$(d_{50})_R$	$(M_\phi)_R$	$(s_\phi)_R$	$(\alpha_\phi)_R$	$(d_{50})_p$	$(M_\phi)_p$
$(d_{75})_p$	-0.850	-0.824	-0.846	-0.589	0.418	-0.373	0.623	-0.148	0.966	
$(d_{84})_p$	-0.709	-0.662	-0.660	-0.452	0.444	-0.444	0.492	-0.047	0.803	
$(d_{90})_p$	-0.535	-0.566	-0.534	-0.337	0.291	-0.310	0.309	0.054	0.669	
$(M_\phi)_p$	0.890	0.838	0.832	0.525	-0.398	0.371	-0.732	0.003	-0.971	
$(s_\phi)_p$	0.286	0.335	0.236	-0.138	0.104	-0.078	-0.358	-0.099	-0.177	0.259
$(\alpha_\phi)_p$	0.767	0.680	0.764	0.639	-0.265	0.185	-0.592	0.182	-0.908	0.812
CS_1	-0.491	-0.231	-0.289	-0.289	0.405	-0.405	0.376	0.000	0.390	-0.405
CS_2	0.011	-0.004	0.183	0.374	-0.266	0.219	0.010	0.443	0.103	-0.194
CS_3	0.432	0.635	0.550	0.025	-0.248	0.280	-0.182	0.001	-0.400	0.381
CS_4	-0.493	-0.318	-0.294	-0.143	0.240	-0.229	0.470	-0.125	0.379	-0.491
CS_5	0.345	0.384	0.414	0.276	-0.456	0.453	-0.143	-0.015	-0.250	0.246
CS_6	0.377	0.398	0.290	0.008	-0.214	0.239	-0.353	-0.081	-0.380	0.506
CS_7	0.686	0.804	0.800	0.434	-0.579	0.582	-0.513	0.123	-0.633	0.679
CS_8	-0.280	-0.135	-0.092	-0.027	-0.169	0.206	0.259	0.090	0.256	-0.304
CS_9	0.578	0.688	0.747	0.509	-0.575	0.577	-0.387	0.221	-0.483	0.475
CS_{10}	0.195	0.137	0.177	0.212	-0.057	0.023	-0.046	0.297	-0.094	0.105
CS_{11}	0.147	0.182	0.178	0.001	-0.364	0.387	0.028	0.104	-0.082	0.110
CS_{12}	0.706	0.538	0.561	0.389	-0.539	0.547	-0.578	-0.158	-0.637	0.660
CS_{13}	0.695	0.603	0.664	0.508	-0.704	0.680	-0.568	0.194	-0.613	0.609
CS_{14}	0.528	0.434	0.477	0.190	-0.710	0.710	-0.465	0.120	-0.364	0.388
CS_{15}	0.179	0.241	0.185	0.018	-0.377	0.413	-0.043	0.075	-0.054	0.164
CS_{ub}	-0.090	0.037	0.184	0.251	-0.150	0.126	0.064	0.267	0.057	-0.201
CS_{lb}	0.373	0.522	0.546	0.349	-0.593	0.623	-0.206	0.149	-0.330	0.344
CS_{sb}	0.608	0.523	0.574	0.358	-0.774	0.782	-0.454	0.139	-0.463	0.492
CS_{tot}	0.552	0.609	0.659	0.397	-0.719	0.721	-0.370	0.256	-0.460	0.447
D_r:D_{rc}	0.899	0.710	0.734	0.483	-0.528	0.496	-0.698	0.023	-0.727	0.749
DS	-0.112	0.151	-0.051	-0.293	0.320	-0.257	0.365	-0.245	0.042	-0.048
LDF	0.372	0.435	0.402	0.079	-0.314	0.332	-0.182	0.082	-0.416	0.414
LDF_{iso}	0.022	-0.004	0.091	0.224	0.090	-0.078	-0.135	0.081	-0.111	0.123
LDF_{inf}	0.114	0.324	0.220	-0.251	-0.054	0.045	-0.064	0.111	-0.141	0.195
LDF_{acc}	0.371	0.453	0.400	0.047	-0.304	0.320	-0.131	0.056	-0.423	0.406
LDF_{scg}	0.039	-0.023	-0.050	-0.271	-0.319	0.335	0.090	0.168	0.216	-0.141
LDF_{jam}	0.396	0.524	0.452	0.155	-0.117	0.137	-0.172	-0.080	-0.520	0.470
D_{LD}	-0.198	-0.047	-0.182	-0.556	0.140	-0.125	0.265	0.000	0.243	-0.164
L_t	0.069	0.143	0.056	-0.072	-0.180	0.266	-0.146	-0.388	-0.176	0.221

Variable	D_r	V_r	V_{rf}	V^*_w	$(d_{50})_R$	$(M_\phi)_R$	$(s_\phi)_R$	$(\alpha_\phi)_R$	$(d_{50})_p$	$(M_\phi)_p$
L_t:W_{bf}	-0.489	-0.595	-0.534	-0.260	-0.075	0.099	0.092	-0.158	0.564	-0.523
L_a	0.432	0.490	0.403	0.104	-0.448	0.529	-0.293	-0.245	-0.507	0.552
V_t	-0.254	-0.065	-0.221	-0.570	0.143	-0.093	0.220	-0.186	0.205	-0.105
V_a	0.006	0.206	0.054	-0.412	-0.027	0.075	0.147	-0.123	-0.023	0.116
VL_t	0.170	0.296	0.223	-0.164	-0.146	0.164	-0.086	0.011	-0.231	0.266
VL_a	0.281	0.414	0.337	-0.093	-0.185	0.206	-0.090	0.012	-0.330	0.365
N_a	0.215	0.035	0.140	0.230	-0.579	0.595	-0.436	-0.020	-0.182	0.271
a%	0.250	0.123	0.236	0.347	-0.508	0.520	-0.486	-0.077	-0.291	0.362
a_W%	0.256	0.014	0.144	0.265	-0.605	0.589	-0.508	0.099	-0.206	0.275
DAF	0.106	0.006	0.027	-0.113	-0.414	0.444	-0.067	0.113	0.045	0.031
P_{acc}	0.384	0.598	0.459	0.050	0.041	-0.043	-0.070	-0.055	-0.547	0.484
DA%	0.278	0.375	0.284	-0.048	-0.270	0.287	0.051	0.006	-0.227	0.206
SAF	-0.072	-0.202	-0.154	-0.173	-0.355	0.378	0.090	0.253	0.333	-0.264
P_{scg}	0.474	0.595	0.550	0.305	-0.125	0.131	-0.259	-0.033	-0.699	0.633
DJF	0.399	0.454	0.428	0.254	-0.123	0.147	-0.354	-0.238	-0.561	0.526
P_{jam}^2	-0.104	0.113	0.007	-0.254	0.072	-0.056	0.536	0.396	0.136	-0.184
V_{jam}^2	-0.092	0.181	-0.003	-0.486	0.040	0.024	0.364	0.146	0.110	-0.100
DJ%	0.439	0.602	0.500	0.150	-0.111	0.123	-0.151	-0.033	-0.614	0.569
$O\%_{par}$	0.353	0.233	0.179	0.132	-0.014	0.026	-0.089	0.075	-0.302	0.334
$O\%_{ds}$	-0.227	-0.128	-0.108	0.084	-0.152	0.198	0.337	-0.221	0.237	-0.224
$O\%_{tr}$	0.209	0.059	0.120	-0.027	-0.090	0.011	-0.543	0.182	-0.122	0.128
$O\%_{us}$	-0.269	-0.162	-0.095	-0.036	0.374	-0.400	0.063	-0.030	0.062	-0.152
$\Pi\%_{br}$	-0.402	-0.434	-0.440	-0.274	0.409	-0.389	0.342	-0.346	0.415	-0.377
$\Pi\%_{dr}$	0.475	0.698	0.559	-0.002	-0.048	0.056	-0.092	0.060	-0.509	0.516
$\Pi\%_{ra}$	-0.322	-0.495	-0.377	0.098	-0.048	0.044	0.098	0.044	0.352	-0.359
$\Pi\%_{st}$	0.173	-0.105	-0.040	-0.008	-0.298	0.227	-0.257	0.337	-0.133	0.133
FDF	0.269	0.362	0.373	0.129	-0.329	0.344	-0.299	-0.026	-0.357	0.383
FDT^4	0.716	0.667	0.784	0.811	-0.265	0.203	-0.495	0.174	-0.661	0.608
FDV_t^3	0.678	0.690	0.622	0.375	-0.393	0.430	-0.569	-0.286	-0.634	0.725
FDV_l^3	0.680	0.676	0.639	0.461	-0.525	0.554	-0.591	-0.181	-0.637	0.717
FDV^4	0.510	0.426	0.402	0.453	-0.326	0.316	-0.336	-0.086	-0.410	0.444
FS%	0.439	0.353	0.373	0.183	-0.468	0.445	-0.379	-0.015	-0.396	0.403
DJV%	0.396	0.554	0.485	0.156	-0.205	0.226	-0.192	-0.012	-0.545	0.490
DJL_a	0.311	0.469	0.399	0.093	-0.190	0.221	-0.056	-0.053	-0.409	0.359

Variable	$(s_\phi)_p$	$(\alpha_\phi)_p$	CS_{ub}	CS_{lb}	CS_{sb}	CS_{tot}	D_r:D_{rc}	DS	LDF	LDF_{iso}
$(\alpha_\phi)_p$	-0.002									
CS_1	0.173	-0.434								
CS_2	-0.173	-0.044								
CS_3	0.262	0.263								
CS_4	-0.277	-0.241								
CS_5	-0.338	0.184								
CS_6	0.342	0.153								
CS_7	0.239	0.377								
CS_8	-0.147	-0.223								
CS_9	0.285	0.308								
CS_{10}	0.131	0.084								
CS_{11}	-0.165	-0.083								
CS_{12}	0.040	0.553								
CS_{13}	0.118	0.486								
CS_{14}	0.155	0.263								
CS_{15}	-0.132	-0.192								
CS_{ub}	-0.107	0.021								
CS_{lb}	0.036	0.153	0.341							
CS_{sb}	0.074	0.306	0.324	0.557						
CS_{tot}	0.115	0.303	0.503	0.846	0.857					
D_r:D_{rc}	0.223	0.698	-0.029	0.332	0.636	0.559				
DS	0.021	-0.142	-0.148	-0.055	-0.121	-0.086	-0.223			
LDF	0.165	0.299	0.134	0.225	0.462	0.453	0.277	0.243		
LDF_{iso}	0.214	0.055	0.177	0.132	-0.030	0.035	-0.046	-0.239	0.041	
LDF_{inf}	0.187	-0.054	0.126	0.237	0.261	0.274	-0.018	0.263	0.411	0.056
LDF_{acc}	0.081	0.341	0.131	0.204	0.451	0.431	0.289	0.317	0.972	-0.120
LDF_{scg}	0.084	-0.296	0.164	0.107	0.404	0.327	0.122	-0.030	0.579	-0.032
LDF_{jam}	0.126	0.462	-0.006	0.096	0.260	0.247	0.256	0.527	0.805	-0.177
D_{LD}	0.060	-0.403	0.107	-0.022	0.129	0.088	-0.256	0.214	0.249	-0.106
L_t	-0.039	0.020	-0.144	0.079	0.222	0.102	0.048	0.465	0.520	-0.194
L_t:W_{bf}	-0.224	-0.502	0.074	-0.166	0.021	-0.126	-0.244	-0.214	-0.131	-0.253
L_a	0.051	0.307	-0.158	0.369	0.509	0.417	0.304	0.341	0.581	-0.211
V_t	0.095	-0.438	0.009	-0.006	0.090	0.035	-0.340	0.338	0.364	-0.093
V_a	0.057	-0.197	0.045	0.247	0.278	0.268	-0.125	0.293	0.417	-0.132
VL_t	0.113	0.075	0.119	0.173	0.347	0.336	0.083	0.284	0.891	0.022

Variable	$(s_\phi)_p$	$(\alpha_\phi)_p$	CS_{ub}	CS_{lb}	CS_{sb}	CS_{tot}	D_r:D_{rc}	DS	LDF	LDF_{iso}
VL_a	0.149	0.167	0.147	0.249	0.420	0.414	0.155	0.242	0.899	0.030
N_a	-0.092	0.081	-0.153	0.311	0.415	0.303	0.316	-0.552	0.141	0.221
a%	-0.098	0.167	-0.141	0.340	0.356	0.292	0.304	-0.486	0.159	0.253
a_W%	-0.092	0.162	-0.163	0.286	0.387	0.288	0.398	-0.640	0.031	0.196
DAF	0.118	-0.173	0.105	0.132	0.452	0.339	0.119	-0.079	0.704	0.086
P_{acc}	0.102	0.530	-0.044	0.122	0.148	0.205	0.250	0.572	0.541	-0.278
DA%	-0.008	0.180	0.079	0.101	0.366	0.324	0.222	0.427	0.769	-0.534
SAF	0.146	-0.410	0.130	0.011	0.310	0.193	-0.042	-0.166	0.399	0.130
P_{scg}	0.065	0.680	-0.168	0.111	0.160	0.153	0.266	0.349	0.512	-0.098
DJF	0.068	0.499	-0.073	0.053	0.228	0.165	0.306	0.415	0.698	-0.132
P_{jam}^2	0.046	-0.104	0.116	0.070	0.048	0.116	-0.238	0.329	0.208	-0.076
V_{jam}^2	0.108	-0.245	0.159	0.169	0.170	0.213	-0.296	0.498	0.401	-0.196
DJ%	0.077	0.557	-0.179	0.115	0.192	0.183	0.223	0.497	0.618	-0.250
$O\%_{par}$	0.238	0.215	-0.410	-0.124	-0.046	-0.066	0.220	0.169	0.181	0.255
$O\%_{ds}$	-0.389	-0.226	0.278	0.342	0.237	0.272	-0.081	-0.003	0.097	-0.117
$O\%_{tr}$	0.290	0.146	-0.013	-0.175	0.054	-0.043	0.269	-0.389	-0.263	-0.131
$O\%_{us}$	-0.144	0.029	0.460	-0.054	-0.078	-0.054	-0.296	0.139	-0.026	0.266
$\Pi\%_{br}$	-0.295	-0.315	-0.020	-0.304	-0.391	-0.425	-0.337	-0.252	-0.422	-0.227
$\Pi\%_{dr}$	0.284	0.394	-0.058	0.456	0.203	0.386	0.244	0.245	0.205	-0.126
$\Pi\%_{ra}$	-0.214	-0.266	-0.068	-0.428	-0.128	-0.341	-0.194	-0.166	-0.028	0.211
$\Pi\%_{st}$	-0.204	0.277	-0.312	0.017	0.005	0.003	0.314	-0.426	-0.069	-0.035
FDF	0.201	0.180	0.267	0.415	0.602	0.580	0.211	0.130	0.803	0.081
FDT^4	-0.034	0.664	0.176	0.203	0.270	0.276	0.613	-0.091	-0.059	0.146
FDV_t^3	0.224	0.441	-0.136	0.515	0.537	0.513	0.670	0.138	0.310	-0.131
FDV_l^3	0.162	0.443	-0.058	0.586	0.635	0.619	0.697	0.020	0.346	-0.085
FDV^4	-0.132	0.375	-0.278	0.044	0.184	0.032	0.500	0.078	-0.216	-0.255
FS%	-0.039	0.370	0.275	0.422	0.708	0.628	0.577	-0.130	0.389	-0.216
DJV%	0.050	0.477	-0.063	0.181	0.251	0.272	0.214	0.442	0.701	-0.220
DJL_a	0.001	0.337	0.091	0.187	0.322	0.318	0.151	0.515	0.792	-0.266

Variable	LDF_{inf}	LDF_{acc}	LDF_{scg}	LDF_{jam}	D_{LD}	L_t	L_t:W_{bf}	L_a	V_t	V_a
LDF_{acc}	0.424									
LDF_{scg}	0.474	0.537								
LDF_{jam}	0.202	0.848	0.108							
D_{LD}	0.797	0.247	0.600	-0.073						
L_t	0.120	0.577	0.080	0.667	-0.053					

Variable	LDF_{inf}	LDF_{acc}	LDF_{scg}	LDF_{jam}	D_{LD}	L_t	$L_t:W_{bf}$	L_a	V_t	V_a
$L_t:W_{bf}$	-0.200	-0.108	0.215	-0.242	0.018	0.316				
L_a	0.129	0.626	0.005	0.718	-0.090	0.812	-0.026			
V_t	0.800	0.367	0.529	0.109	0.917	0.277	0.089	0.159		
V_a	0.826	0.447	0.486	0.174	0.877	0.221	-0.044	0.301	0.902	
VL_t	0.700	0.874	0.665	0.630	0.591	0.493	-0.006	0.447	0.693	0.710
VL_a	0.697	0.889	0.630	0.640	0.577	0.427	-0.122	0.481	0.659	0.743
N_a	-0.010	0.047	0.230	-0.180	-0.074	0.116	0.317	0.209	-0.030	0.030
a%	-0.006	0.051	0.101	-0.090	-0.117	0.138	0.194	0.241	-0.044	0.018
a_W%	-0.066	-0.047	0.185	-0.273	-0.159	-0.018	0.275	0.096	-0.162	-0.096
DAF	0.400	0.634	0.903	0.231	0.476	0.233	0.173	0.220	0.508	0.482
P_{acc}	0.254	0.651	-0.138	0.847	-0.050	0.493	-0.347	0.588	0.062	0.188
DA%	0.331	0.863	0.512	0.774	0.260	0.511	-0.057	0.544	0.346	0.402
SAF	0.261	0.306	0.875	-0.082	0.431	-0.063	0.209	-0.102	0.372	0.282
P_{scg}	0.025	0.566	-0.332	0.818	-0.315	0.497	-0.373	0.706	-0.154	0.013
DJF	0.102	0.730	-0.013	0.922	-0.187	0.754	-0.113	0.750	0.047	0.102
P_{jam}^2	0.413	0.225	0.271	0.171	0.365	-0.292	-0.340	-0.147	0.243	0.274
V_{jam}^2	0.815	0.434	0.457	0.379	0.802	0.143	-0.195	0.234	0.763	0.783
DJ%	0.178	0.694	-0.153	0.901	-0.121	0.574	-0.344	0.748	0.041	0.187
$O\%_{par}$	-0.252	0.081	-0.020	0.194	-0.218	-0.116	-0.635	0.081	-0.227	-0.266
$O\%_{ds}$	-0.054	0.149	0.189	-0.010	0.009	0.254	0.511	0.096	0.068	0.126
$O\%_{tr}$	0.240	-0.263	0.014	-0.303	0.170	-0.326	-0.006	-0.251	0.039	0.032
$O\%_{us}$	0.272	-0.024	-0.165	0.062	0.211	-0.005	0.053	-0.090	0.192	0.218
$\Pi\%_{br}$	-0.145	-0.371	-0.083	-0.466	0.237	-0.213	0.347	-0.340	0.178	0.200
$\Pi\%_{dr}$	0.412	0.242	-0.141	0.306	0.241	-0.099	-0.598	0.344	0.168	0.487
$\Pi\%_{ra}$	-0.359	-0.093	0.153	-0.119	-0.290	0.110	0.402	-0.235	-0.218	-0.510
$\Pi\%_{st}$	-0.119	-0.061	0.117	-0.221	-0.165	-0.255	-0.021	-0.115	-0.273	-0.198
FDF	0.535	0.772	0.469	0.593	0.345	0.504	0.114	0.566	0.475	0.577
FDT^4	-0.103	-0.051	-0.319	0.091	-0.395	-0.265	-0.495	-0.017	-0.500	-0.319
FDV_t^3	0.138	0.346	-0.053	0.454	-0.224	0.494	-0.156	0.606	-0.090	0.044
FDV_l^3	0.092	0.358	0.013	0.417	-0.255	0.449	-0.127	0.579	-0.135	-0.009
FDV^4	-0.234	-0.135	-0.311	0.080	-0.520	0.159	-0.181	0.206	-0.471	-0.461
FS%	0.239	0.468	0.284	0.323	0.054	0.310	0.165	0.436	0.068	0.232
DJV%	0.163	0.730	-0.032	0.920	-0.108	0.605	-0.256	0.765	0.052	0.163
DJL_a	0.261	0.839	0.181	0.953	0.052	0.648	-0.190	0.748	0.214	0.305

Variable	VL_t	VL_a	N_a	a%	a_W%	DAF	P_{acc}	DA%	SAF	P_{scg}
VL_a	0.974									
N_a	0.128	0.096								
a%	0.141	0.113	0.961							
a_W%	-0.003	-0.036	0.961	0.895						
DAF	0.722	0.702	0.390	0.300	0.313					
P_{acc}	0.428	0.472	-0.378	-0.308	-0.415	-0.146				
DA%	0.678	0.700	-0.177	-0.182	-0.247	0.510	0.630			
SAF	0.417	0.384	0.313	0.182	0.276	0.891	-0.433	0.275		
P_{scg}	0.299	0.353	-0.040	0.068	-0.102	-0.136	0.824	0.439	-0.417	
DJF	0.553	0.538	-0.001	0.121	-0.097	0.194	0.694	0.621	-0.156	0.786
P_{jam}^2	0.167	0.209	-0.431	-0.460	-0.434	0.057	0.402	0.322	0.201	0.135
V_{jam}^2	0.575	0.583	-0.375	-0.406	-0.478	0.315	0.478	0.507	0.262	0.158
DJ%	0.454	0.503	-0.171	-0.083	-0.247	-0.026	0.920	0.638	-0.326	0.950
$O\%_{par}$	-0.071	-0.038	-0.083	-0.036	-0.060	0.082	0.061	0.022	0.116	0.199
$O\%_{ds}$	0.123	0.140	0.198	0.161	0.087	0.119	0.023	0.183	0.035	-0.109
$O\%_{tr}$	-0.120	-0.150	0.143	0.117	0.283	-0.018	-0.284	-0.213	0.066	-0.237
$O\%_{us}$	0.165	0.143	-0.296	-0.224	-0.322	-0.147	0.069	-0.178	-0.215	0.013
$\Pi\%_{br}$	-0.188	-0.160	-0.095	-0.098	-0.139	-0.114	-0.407	-0.224	-0.098	-0.431
$\Pi\%_{dr}$	0.226	0.356	-0.170	-0.099	-0.191	-0.133	0.517	0.214	-0.288	0.482
$\Pi\%_{ra}$	-0.140	-0.253	0.272	0.220	0.253	0.169	-0.342	-0.115	0.334	-0.211
$\Pi\%_{st}$	-0.114	-0.150	0.385	0.272	0.583	0.111	-0.188	-0.140	0.110	-0.096
FDF	0.830	0.848	0.263	0.289	0.134	0.616	0.384	0.544	0.301	0.357
FDT^4	-0.211	-0.110	-0.093	0.088	-0.061	-0.304	0.134	-0.051	-0.311	0.208
FDV_t^3	0.205	0.269	0.075	0.162	0.088	-0.023	0.478	0.347	-0.297	0.376
FDV_l^3	0.203	0.261	0.187	0.265	0.197	0.042	0.420	0.337	-0.212	0.339
FDV^4	-0.382	-0.331	-0.115	-0.051	-0.037	-0.409	0.185	0.108	-0.413	0.134
FS%	0.352	0.409	0.132	0.062	0.176	0.243	0.366	0.432	-0.012	0.150
DJV%	0.530	0.538	-0.020	0.086	-0.123	0.108	0.803	0.652	-0.177	0.892
DJL_a	0.660	0.678	-0.171	-0.085	-0.288	0.292	0.774	0.819	-0.004	0.740

Variable	DJF	P_{jam}^2	V_{jam}^2	DJ%	$O\%_{par}$	$O\%_{ds}$	$O\%_{tr}$	$O\%_{us}$	$\Pi\%_{br}$	$\Pi\%_{dr}$
P_{jam}^2	-0.255									
V_{jam}^2	0.075	0.718								
DJ%	0.801	0.291	0.408							
$O\%_{par}$	0.116	0.091	-0.150	0.173						

Variable	DJF	P_{jam}^2	V_{jam}^2	DJ%	O%$_{par}$	O%$_{ds}$	O%$_{tr}$	O%$_{us}$	Π%$_{br}$	Π%$_{dr}$
O%$_{ds}$	-0.038	0.106	0.036	-0.049	-0.513					
O%$_{tr}$	-0.166	-0.317	-0.094	-0.291	-0.189	-0.611				
O%$_{us}$	0.142	-0.110	0.195	-0.016	-0.430	-0.060	0.138			
Π%$_{br}$	-0.328	-0.334	-0.170	-0.420	-0.419	0.214	0.085	0.202		
Π%$_{dr}$	0.183	0.299	0.455	0.520	0.081	-0.227	0.090	0.107	-0.104	
Π%$_{ra}$	-0.081	-0.024	-0.329	-0.268	0.122	0.206	-0.236	-0.287	-0.192	-0.872
Π%$_{st}$	-0.175	-0.101	-0.278	-0.159	0.165	-0.309	0.369	-0.230	-0.124	-0.038
FDF	0.581	0.038	0.389	0.440	-0.231	0.311	-0.132	0.270	-0.236	0.255
FDT[4]	0.159	-0.136	-0.375	0.110	0.221	-0.037	0.098	-0.020	-0.137	0.145
FDV_t^3	0.508	-0.229	-0.068	0.432	0.088	0.191	-0.073	-0.183	-0.364	0.255
FDV_l^3	0.450	-0.185	-0.091	0.382	0.108	0.265	-0.119	-0.259	-0.426	0.181
FDV[4]	0.104	-0.036	-0.236	0.156	0.270	0.132	-0.123	-0.404	-0.309	-0.135
FS%	0.304	-0.051	0.141	0.247	-0.323	0.349	0.050	0.119	-0.151	0.146
DJV%	0.857	0.178	0.395	0.926	0.173	-0.085	-0.228	0.023	-0.479	0.437
DJL_a	0.862	0.231	0.554	0.853	0.096	0.046	-0.305	0.135	-0.370	0.356

Variable	Π%$_{ra}$	Π%$_{st}$	FDF	FDT[4]	FDV_t^3	FDV_l^3	FDV[4]	FS%	DJV%
Π%$_{st}$	-0.008								
FDF	-0.198	-0.219							
FDT[4]	-0.113	-0.159	-0.082						
FDV_t^3	-0.261	-0.078	0.412	0.488					
FDV_l^3	-0.150	-0.025	0.426	0.483	0.975				
FDV[4]	0.206	0.029	-0.294	0.593	0.716	0.721			
FS%	-0.269	0.160	0.572	0.113	0.664	0.686	0.277		
DJV%	-0.185	-0.137	0.500	0.005	0.326	0.304	-0.006	0.199	
DJL_a	-0.197	-0.253	0.624	0.007	0.390	0.357	0.045	0.351	0.919

[1]Reach 173 is excluded from analyses of channel width; n = 19.

[2]Only 18 study reaches had debris jams present; n = 18.

[3]LOD-related fine sediment deposits were not measured in 2 study reaches; n = 18.

[4]In 2 reaches LOD-related fine sediment deposits were not measured, and another reach had none present; n = 17.

Appendix C

SYMBOL DEFINITIONS

Table C.1 – *Variables measured or calculated.*

[LOD, large organic debris]

Variable	Definition
$(\alpha_\phi)_p$	graphic skewness of reach-mean grain-size distribution for fine sediment in pools
$(\alpha_\phi)_R$	graphic skewness of reach-mean grain-size distribution for surface layer on riffles
a%	percentage of LOD with one or more ends or sides buried in soil or sediment (i.e., anchored)
a_W%	percentage of LOD with two or more ends or sides buried in soil or sediment (i.e., well anchored)
A_d	drainage area, in square kilometers
B%	burned area as a percentage of A_d
CS_1	channel stability rating for upper-bank slope
CS_2	channel stability rating for upper-bank mass-wasting potential
CS_3	channel stability rating for upper-bank floatable objects
CS_4	channel stability rating for upper-bank vegetation density
CS_5	channel stability rating for lower-bank channel capacity
CS_6	channel stability rating for lower-bank rock content
CS_7	channel stability rating for lower-bank flow deflectors
CS_8	channel stability rating for lower-bank cut banks
CS_9	channel stability rating for lower-bank bar enlargement
CS_{10}	channel stability rating for streambed angularity
CS_{11}	channel stability rating for streambed brightness
CS_{12}	channel stability rating for streambed packing
CS_{13}	channel stability rating for streambed size distribution
CS_{14}	channel stability rating for streambed scour and deposition
CS_{15}	channel stability rating for streambed clinging flora
CS_{lb}	lower-bank subtotal of channel-stability index rating
CS_{sb}	streambed subtotal of channel-stability index rating
CS_{tot}	overall channel-stability index rating
CS_{ub}	upper-bank subtotal of channel-stability index rating
CT	dummy variable for channel type (CT = 0 for plane bed, 1 for forced-pool-riffle type)
$(d_{10})_p$	10th percentile of reach-mean grain-size distribution for fine sediment in pools
$(d_{10})_R$	10th percentile of reach-mean grain-size distribution for surface layer on riffles

Variable	Definition
$(d_{16})_L$	16th percentile of grain-size distribution for individual bedload sample
$(d_{16})_p$	16th percentile of reach-mean grain-size distribution for fine sediment in pools
$(d_{16})_R$	16th percentile of reach-mean grain-size distribution for surface layer on riffles
$(d_{25})_L$	25th percentile of grain-size distribution for individual bedload sample
$(d_{25})_p$	25th percentile of reach-mean grain-size distribution for fine sediment in pools
$(d_{25})_R$	25th percentile of reach-mean grain-size distribution for surface layer on riffles
$(d_{50})_L$	50th percentile of grain-size distribution for individual bedload sample
$(d_{50})_p$	50th percentile of reach-mean grain-size distribution for fine sediment in pools
$(d_{50})_R$	50th percentile of reach-mean grain-size distribution for surface layer on riffles
$(d_{75})_p$	75th percentile of reach-mean grain-size distribution for fine sediment in pools
$(d_{75})_R$	75th percentile of reach-mean grain-size distribution for surface layer on riffles
$(d_{84})_L$	84th percentile of grain-size distribution for individual bedload sample
$(d_{84})_p$	84th percentile of reach-mean grain-size distribution for fine sediment in pools
$(d_{84})_R$	84th percentile of reach-mean grain-size distribution for surface layer on riffles
$(d_{90})_L$	90th percentile of grain-size distribution for individual bedload sample
$(d_{90})_p$	90th percentile of reach-mean grain-size distribution for fine sediment in pools
$(d_{90})_R$	90th percentile of reach-mean grain-size distribution for surface layer on riffles
$(d_{95})_L$	95th percentile of grain-size distribution for individual bedload sample
$(d_{95})_R / D_m$	relative submergence of 95th-percentile size of bed material at time of bedload sampling
$(d_{95})_L / (d_{50})_R$	mobility ratio 1 at time of bedload sampling
$(d_{95})_L / (d_{50})_L$	mobility ratio 2 at time of bedload sampling
$(d_{95})_L / (d_{25})_R$	mobility ratio 3 at time of bedload sampling
D_L	mean depth of streamflow in thalweg zone of estimated maximum bedload transport
D_{LD}	reach-mean average diameter of LOD pieces
D_m	mean depth of streamflow cross-section
D_r	reach-mean average depth of residual pools
$(D_r)_{sp}$	reach-mean average depth of residual pools among pools where a bulk sample of fine sediment was collected
D_{rc}	water depth at downstream hydraulic control of residual pool (thalweg at riffle crest)
D_r:D_{rc}	reach-mean ratio of average depth of residual pool to average riffle-crest depth
DA%	percentage of reach LOD count occurring within contact groups
DAF	mean frequency of LOD contact groups along channel
DJ%	percentage of reach LOD count occurring within debris jams
DJF	mean frequency of debris jams along channel
DJL_a	partial volumetric loading of LOD occurring in debris jams, including only piece volume within active channel
DJV%	percentage of reach LOD volume occurring within debris jams
DS	rank of reach when ordered by downstream position along its respective stream
F%	percentage of pools that were forced by channel obstructions to flow, rather than free formed
FDF	mean frequency of fine-sediment deposits associated with LOD
FDT	reach-mean thickness of individual fine-sediment deposits associated with LOD
FDV	reach-mean volume of individual fine-sediment deposits associated with LOD
FDV_l	volume of fine-sediment deposits associated with LOD per 100 m of channel length
FDV_t	reach-total volume of fine-sediment deposits associated with LOD
FS%	percentage of LOD associated with fine-sediment deposits

Variable	Definition
GU	geologic unit containing stream segment
I_b	instantaneous bedload transport rate per unit channel width
L_a	reach-mean active-channel partial length of LOD per piece
L_{po}	pool length
L_{rch}	reach length
$(L)_{sp}$	reach-mean pool length for pools where a bulk sample of fine sediment was collected
L_t	reach-mean total length per piece of LOD
L_t:W_{bf}	ratio of reach-mean value of variable L_t to variable W_{bf}
LDF	mean frequency of LOD along channel
LDF_{acc}	mean frequency of LOD in contact groups along channel
LDF_{inf}	mean frequency of influential pieces of LOD along channel
LDF_{iso}	mean frequency of isolated pieces of LOD along channel
LDF_{jam}	mean frequency of LOD in debris jams along channel
$LDF_{L>W}$	mean frequency of LOD with total piece length greater than mean channel width
LDF_{scg}	mean frequency of LOD in small contact groups along channel
$(M_\phi)_p$	graphic mean size of reach-mean grain-size distribution for fine sediment in pools
$(M_\phi)_R$	graphic mean size of reach-mean grain-size distribution for surface layer on riffles
N_a	reach-mean number of ends or sides of each piece of LOD buried in soil or sediment
N_{jam}	number of LOD jams in reach
ω_L	stream power per unit width in thalweg zone of estimated maximum bedload transport
Ω	total stream power
$O\%_{ds}$	percentage of LOD oriented as angled downstream with streamflow
$O\%_{par}$	percentage of LOD oriented parallel to streamflow
$O\%_{tr}$	percentage of LOD oriented transverse to streamflow
$O\%_{us}$	percentage of LOD oriented as angled upstream against streamflow
$\Pi\%_{br}$	percentage of LOD positioned as bridges spanning the channel
$\Pi\%_{dr}$	percentage of LOD positioned as drift within the channel
$\Pi\%_{ra}$	percentage of LOD positioned as ramps extending beyond the channel
$\Pi\%_{st}$	percentage of LOD positioned as log steps within the channel
P%	percentage of reach length occupied by pools
P_{acc}	reach-mean size of LOD contact groups, in pieces
P_{jam}	reach-mean size of LOD debris jams, in pieces
P_{scg}	reach-mean size of LOD small contact groups, in pieces
PL	reach-mean pool length, in channel-width units
PL_m	reach-mean pool length, in meters
PT_{bend}	percentage of pools that are of the lateral scour type
PT_{const}	percentage of pools that are of the type formed by a channel constriction
PT_{plunge}	percentage of pools that are of the type formed by flow plunging over a step
PT_{vscour}	percentage of pools that are of the vertical scour type
PT_{fluv}	percentage of pools that are of the type freely formed by fluvial dynamics
PT_{forc}	percentage of pools that are of the type forced by a channel obstruction
Q	instantaneous streamflow discharge

Variable	Definition
Q_b	instantaneous bedload discharge
Q_{bn}	instantaneous bedload discharge normalized per unit drainage area
Q_n	instantaneous streamflow discharge normalized per unit drainage area
Qg%	area underlain by glacial till as a percentage of A_d
Qt%	area underlain by talus and colluvium as a percentage of A_d
$(s_\phi)_L$	graphic sorting statistic for grain-size distribution for individual bedload sample
$(s_\phi)_p$	graphic sorting statistic for reach-mean grain-size distribution for fine sediment in pools
$(s_\phi)_R$	graphic sorting statistic for reach-mean grain-size distribution for surface layer on riffles
S_{basin}	mean land-surface slope of drainage area, in percent
S_L	water-surface gradient for bedload samples, estimated from bankfull-stage indicators
S_{seg}	mean water-surface gradient of segment, in m/m
S_w	mean water-surface gradient of reach, in m/m
SAF	mean frequency of small contact groups of LOD
SP	reach-mean pool spacing, in channel-width units
SP_m	reach-mean pool spacing, in meters
τ_0	average boundary shear stress
τ_L	estimated boundary shear stress in thalweg zone of estimated maximum bedload transport
τ^*	Shields dimensionless shear stress parameter
τ^*_c	critical Shields dimensionless shear stress parameter for $(d_{95})_L$ particle size
τ^*_{cA}	predicted critical Shields dimensionless shear stress for $(d_{95})_L$ particle size
Tl%	area underlain by Langford Fm. as a percentage of A_d
Tt%	area underlain by Trout Peak Trachyandesite as a percentage of A_d
Tw%	area underlain by Wapiti Fm. as a percentage of A_d
V^*	fraction of residual-pool volume occupied by fine sediment (during period of low streamflow)
V^*_w	reach-mean fraction of residual-pool volume occupied by fine sediment (during period of low streamflow)
$(V^*_w)_{sp}$	mean fraction of residual-pool volume occupied by fine sediment (during period of low streamflow) among pools where a bulk sample of fine sediment was collected
V_a	estimated mean active-channel partial LOD volume per piece
V_{jam}	active-channel partial LOD volume per debris jam
V_m	mean streamflow velocity
V_r	reach-mean residual volume per pool
$(V_r)_{sp}$	reach-mean residual volume per pool where a bulk sample of fine sediment was collected
V_{rf}	reach-mean fine-sediment volume per residual pool
$(V_{rf})_{sp}$	reach-mean fine-sediment volume per residual pool where a bulk sample of fine sediment was collected
V_t	estimated mean total LOD volume per piece
VL_a	volumetric loading of LOD in reach, including only piece volume within active channel
VL_t	total volumetric loading of LOD in reach, including partial piece volume extending beyond active channel
W_{bf}	weighted mean bankfull width
W_p	mean bankfull pool width
W_r	mean bankfull riffle width
W_s	width of flow actually sampled by bedload sampler
W_w	wetted width across water surface

Variable	Definition
WS	dummy variable for stream identity (WS = 0 for Crow Cr., 1 for Jones Cr.)
Z_{seg}	mean channel elevation of segment

Table C.2 – *Acronyms and other symbols.*

Acronym or Symbol	Definition
α	the probability of rejecting the null hypothesis when it is true (Type I error)
β	the probability of accepting the null hypothesis when it is false (Type II error)
β_k	regression coefficient for the *k*th term in the linear model
χ^2	chi-square test score
cm	centimeter
°C	degrees centigrade
CV	coefficient of variation, calculated as the standard deviation divided by the mean value
d_i	size of some specific fraction, *i*, of bed particles in motion at time of sampling
$(d_{50})_S$	median particle size of subsurface bed material
DEMs	digital elevation models
ε	unexplained random variation
ϕ	phi scale of grain size : $\phi = -\log_2(d_s)$ where d_s is grain size in mm
ϕ_{10}	10th percentile of grain-size distribution, in phi units
ϕ_{16}	16th percentile of grain-size distribution, in phi units
ϕ_{50}	50th percentile of grain-size distribution, in phi units
ϕ_{84}	84th percentile of grain-size distribution, in phi units
ϕ_{90}	90th percentile of grain-size distribution, in phi units
F	ratio of the explained variation to unexplained variation divided by their respective degrees of freedom
FPR	forced-pool-riffle channel type
γ	specific weight of water
g	gram
GIS	geographic information system
GSD	grain-size distribution
GYA	Greater Yellowstone Area
ha	hectare
in.	inch
IAHS	International Association of Hydrological Sciences
IQR	interquartile range
kg	kilogram
km	kilometer
log(n)	base-10 logarithm of n
L	liter
LCL	lower limit of confidence interval for a specific significance level
LOD	large organic debris
LTS	least trimmed sum-of-squares estimation of regression model

Variable	Definition
WS	dummy variable for stream identity (WS = 0 for Crow Cr., 1 for Jones Cr.)
Z_{seg}	mean channel elevation of segment

Table C.2 – *Acronyms and other symbols.*

Acronym or Symbol	Definition
α	the probability of rejecting the null hypothesis when it is true (Type I error)
β	the probability of accepting the null hypothesis when it is false (Type II error)
β_k	regression coefficient for the *k*th term in the linear model
χ^2	chi-square test score
cm	centimeter
°C	degrees centigrade
CV	coefficient of variation, calculated as the standard deviation divided by the mean value
d_i	size of some specific fraction, *i*, of bed particles in motion at time of sampling
$(d_{50})_S$	median particle size of subsurface bed material
DEMs	digital elevation models
ε	unexplained random variation
ϕ	phi scale of grain size : $\phi = -\log_2(d_s)$ where d_s is grain size in mm
ϕ_{10}	10th percentile of grain-size distribution, in phi units
ϕ_{16}	16th percentile of grain-size distribution, in phi units
ϕ_{50}	50th percentile of grain-size distribution, in phi units
ϕ_{84}	84th percentile of grain-size distribution, in phi units
ϕ_{90}	90th percentile of grain-size distribution, in phi units
F	ratio of the explained variation to unexplained variation divided by their respective degrees of freedom
FPR	forced-pool-riffle channel type
γ	specific weight of water
g	gram
GIS	geographic information system
GSD	grain-size distribution
GYA	Greater Yellowstone Area
ha	hectare
in.	inch
IAHS	International Association of Hydrological Sciences
IQR	interquartile range
kg	kilogram
km	kilometer
log(n)	base-10 logarithm of n
L	liter
LCL	lower limit of confidence interval for a specific significance level
LOD	large organic debris
LTS	least trimmed sum-of-squares estimation of regression model

Acronym or Symbol	Definition
m	meter
mi	mile
mL	milliliter
Mg	megagram, or metric ton
MSL	mean sea level
n	sample size
p	probability of associated test statistic occurring when null hypothesis is true
q	unit discharge of streamflow
$Q_{1\%}$	daily mean discharge exceeded on 1 percent of the days in the period of record
$Q_{2\%}$	daily mean discharge exceeded on 2 percent of the days in the period of record
Q_s	sediment discharge
r^2	coefficient of determination
R	Pearson's linear-correlation coefficient
R_s	Spearman's rank-correlation coefficient
RMS	root-mean-square
RSE	residual standard error, or standard error of the estimate
SE	standard error of the mean value
τ	Kendall's tau, a rank-correlation coefficient
t	Student's t test score
twz	thalweg zone of maximum unit discharge and estimated maximum bedload transport
UCL	upper limit of confidence interval for a specific significance level
USDA	United States Department of Agriculture
USGS	United States Geological Survey
US SA-97	United States sediment analyzer approved in 1997 by the Federal Interagency Sedimentation Subcommittee
V	signed ranks test score
W	Wilcoxon's rank sum test score
YNP	Yellowstone National Park